Synthesis and structure-activity relationships of cyclic adenosine 5'-diphosphate ribose analogues

Ashamu, Gloria Abiodun

Award date:
1998

Awarding institution:
University of Bath

SYNTHESIS AND STRUCTURE-ACTIVITY RELATIONSHIPS OF CYCLIC ADENOSINE 5′-DIPHOSPHATE RIBOSE ANALOGUES

A thesis submitted by Gloria Abiodun Ashamu
for the degree of PhD of the University of Bath
1998

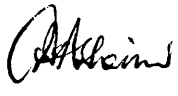

ProQuest LLC
789 East Eisenhower Parkway
P.O. Box 1346
Ann Arbor, MI 48106-1346

ABSTRACT

Cyclic adenosine 5′-diphosphate ribose (cADPR) is a naturally occuring metabolite of nicotinamide adenine dinucleotide $(NAD)^+$ and a potent Ca^{2+}-mobilising agent in a variety of cells. Structural analogues of cADPR have been synthesised, to probe the structure-activity profile for cADPR. The synthetic method employed in this work relies upon synthesis of chemically modified NAD^+ analogues from their mononucleotide subunits, followed by enzymatic cyclisation into cADPR analogues. Analogues were tested in two biological systems - sea urchin egg homogenates and in permeabilised Jurkat T-cells.

2′ And 3′-hydroxyl group deletion in the adenosine ribose moiety of cADPR were used to investigate the role of ribose hydroxyl group on the Ca^{2+} releasing potential of cADPR. In the sea urchin egg system, EC_{50} values of 32nM, 58nM and 5μM were obtained for cADPR, $2'_A$-deoxy-cADPR and $3'_A$-deoxy-cADPR respectively. This suggests that the 3′-hydroxyl group but not the 2′-hydroxyl is important for calcium releasing activity in this system. Interestingly, replacement of the 3′-OH with a methoxy group in $3'_A$-*O*-methyl-cADPR generated an antagonist with an approximate IC_{50} of 5μM. 3′-*O*-Methyl-cADPR is the first cADPR antagonist that is not modified at the 8-position of the purine ring in the sea urchin egg system. Replacement of the 2′-OH with a phosphate resulted in an inactive analogue. 3′-cADPRP and 2′,3′-cADPRP were both inactive in this system.

The data obtained from Jurkat T-cells showed some differences in the structural requirement for cADPR induced mechanism. cADPR mobilised Ca^{2+} with an EC_{50} of 2.5μM. 2′-Deoxy and 3′-deoxy-cADPR analogues were both inactive . 3′-*O*-Methyl-cADPR was a potent agonist suggesting that the hydrogen acceptor ability of the oxygen atom is important for Ca^{2+} releasing activity. 2′-cADPRP was a potent agonist, but both 2′-cADPRP and 2′,3′-cADPRP were inactive.

Substitution of the hydrogen atom at the 8-position of the purine ring with amino or bromo group are known to produce antagonists in the sea urchin system, hence these analogues and other substitutions at the 8-positions were synthesised to investigate whether substitution at this position resulted in antagonism of cADPR- induced response in Jurkat T-cells. All 8-substituted analogues were antagonists in the Jurkat T-cells, potency of which depended on the molecular volume and hydrophobicity of the substituent. In the sea urchin system antagonist activity depended on the size of the substituent.

DEDICATION

In the evergreen memory of my late father, Chief Emmanuel Oyedele Ashamu.

ACKNOWLEDGMENTS

I wish to expresss my gratitude to Professor B.V.L. Potter for his invaluable supervision and for arranging financial support for this work.

I would like to thank Dr. Antony Galione and Jazz Sethi of the Department of Pharmacology, University of Oxford; Dr Andreas Guse and Karin Weber (University of Hamburg, Germany), for biological testing of the compounds.

Dr. Simon Fortt, Victoria Bailey and Dr. Migaud for helpful discussion. All other members of my research group at Bath University, Soula Diogenous, Steve Mills, Andrew Riley, Dr. Changsheng Liu, Dave Jenkins, Dave Callis, Hartem Hejaz, Rachel Marwood and Shane Garrett for their friendship and help over the years. Thanks to others who made my time in Bath enjoyable particularly Joko, Aima and Peggy.

Kevin Smith for molecular modelling work, Dave Wood and Harry Hartell for running many NMR spectra. Richard Sadler, Gary Cooper, Charlotte Armah and Don for excellent technical support.

Thanks to the University of Bath for financial support.

I am indebted to Chief Olopoenia for financial assistance which helped me to start this work, my immediate family - Jade, Pate, Nike, Iyabo, Kemi, Yemi, Bimpe, Tola Oyetosho, and Akin for constant support. Thanks to Mum - for mother is Gold.

PUBLICATIONS

S. Rakovic, A. Galione, G.A. Ashamu, B.V.L.Potter and D.A. Terrar (1995), "Inhibition of excitation-contraction coupling in guinea-pig ventricular myocytes by 8-amino-cADPR, a specific competitive cADPR antagonist". *J. Physiol.* 483P p.P17.

G.A. Ashamu, A. Galione and B.V.L. Potter (1995), "Chemo-enzymatic synthesis of analogues of the second messenger candidate cyclic adenosine 5′-diphosphate ribose". *J. Chem. Soc. Chem. Commun.* 1359.

A.H. Guse, C.P. da Silva, F. Emmrich, G.A. Ashamu, B.V.L. Potter and G.W. Mayr (1995), "Characterisation of cyclic adenosine diphosphate ribose-induced Ca^{2+}-release in T-lymphocyte cell lines". *J. Immunol.* 155(7), 3353-3359.

S. Rakovic, A. Galione, G.A. Ashamu, B.V.L.Potter and D.A. Terrar (1996), "A specific cyclic ADP-ribose antagonist inhibits cardiac excitation-contraction coupling". *Current Biology* 6(8), 989-996.

A.H Guse, C.P. da Silva. K. Weber, G.A. Ashamu, B.V.L. Potter and G.W. Mayr (1996), "Regulation of cADPR-induced Ca^{2+}-release by Mg^{2+} and inorganic phosphate". *J. Biol. Chem.* 271(39), 23946-23953.

A.H. Guse, C.P. da Silva, K. Weber, C.N. Armah, G.A. Ashamu C. Schulze, B.V.L. Potter, G.W. Mayr, H. Hilz (1997), "1-(5-Phospho-β-D-ribosyl)2′-phosphoadenosine 5′-phosphate cyclic anhydride induced Ca^{2+} release in human T-cell lines". *Eur. J. Biochem.* (245) 411-417.

G. A. Ashamu, J. Sethi, A. Galione, B.V.L. Potter (1997), "Roles for ribose hydroxyl groups in cADPR-mediated Ca^{2+}-release". *Biochemistry* (36) 9509-9517.

ABBREVIATIONS

AMP	adenosine 5′-monophosphate
$Å^3$	cubic Ångstrom
ANP	atrial natruetic peptied
ATP	adenosine 5′-triphosphate
Ca^{2+}	calcium ions
cADPR	cyclic adenosine diphosphate ribose
cADPRP	cyclic adenosine-diphosphate ribose/ phosphate
cAMP	adenosine 3′,5′-cyclic monophosphate
COSY	correlated spectroscopy
CICR	calcium induced calcium release
DAG	diacylglycerol
DCC	N,N-dicyclohexylcarbodiimide
DCU	dicyclohexylurea
DMSO	dimethylsulfoxide
DMF	dimethylformamide
EC_{50}	concentration of drug required for half-maximal response
EDC	1-ethyl-3-(3-dimethylaminopropyl)-carbodiimide
ES	electrospray
FAB	fast atomic bombardment
cGMP	guanosine 3′,5′-cyclic monophosphate
G-protein	GTP-binding protein
G_s	stimulatory G-protein
GC	guanylate cyclase
GTP	guanosine 5′-triphosphate
HPLC	high perfomance liquid chromatograph
IC_{50}	concentration of drug required to inhibit a response by 50%
IP_3	*myo*-Inositol 1,4,5,-trisphosphate
IP_3R	IP_3 receptor

K_m	Michaelis constant
MS	mass spectroscopy
Mw	molecular weight
NAD^+	nicotinamide adenine dinucleotide
NAADP	nicotinic acid adenine dinucleotide phosphate
NMR	nuclear magnetic resonance
PtdIns	phosphatidyl-inositol
Pip	piperidyl group
RFU	relative fluorescence units
RT	room temperature
R_t	HPLC retention time
RyR	ryanodine receptor
SAR	structure activity relationship
SR	sarcoplasmic reticulum
TEAB	triethylammonium bicarbonate
TLC	thin layer chromatography
UV	Ultra-violet
V_{max}	maximum velocity

CONTENTS

CHAPTER 4: SYNTHESIS OF ANALOGUES OF cADPR

CHAPTER 5: BIOLOGICAL EVALUATION OF cADPR ANALOGUES

CHAPTER 6: EXPERIMENTAL

CHAPTER 1: GENERAL BACKGROUND

1.1 Cell Signalling

Communication between cells in multicellular organisms is essential for maintenance of life processes such as regulation of development and organisation into tissues, control of growth and division and co-ordination of cell functions. Communication can occur via gap junctions that directly join the cytoplasm of the interacting cells, by direct contact via plasma-membrane bound signalling molecules that influence other cells, and by secreting chemicals that signal to cells some distance away.

Chemical signalling can be achieved in three ways. First, endocrine signalling involving hormones which travel through the blood stream to influence target cells. Second, paracrine signalling where local chemical mediators are released to act on cells in the immediate environment, and third, synaptic signalling which is confined to the neurons in which neurotransmitters are released at specialised junctions called chemical synapses. The neurotransmitter diffuses across the synaptic cleft, typically a distance of about 50nm and acts only on the adjacent post-synaptic target cell. The signalling molecule known as the first messenger, binds to specific proteins called receptors on the target cells leading to a response. Small hydrophobic signalling molecules such as thyroid hormones and steroids, diffuse through the lipid bi-layer of the target cell, thereby eliciting a response. However, many messenger molecules (all neurotransmitters and majority of hormones and local mediators) are too hydrophilic to cross membranes in which case additional messengers are required to link surface receptor activation to internal response in the stimulated cell. These molecules are known as second messengers.

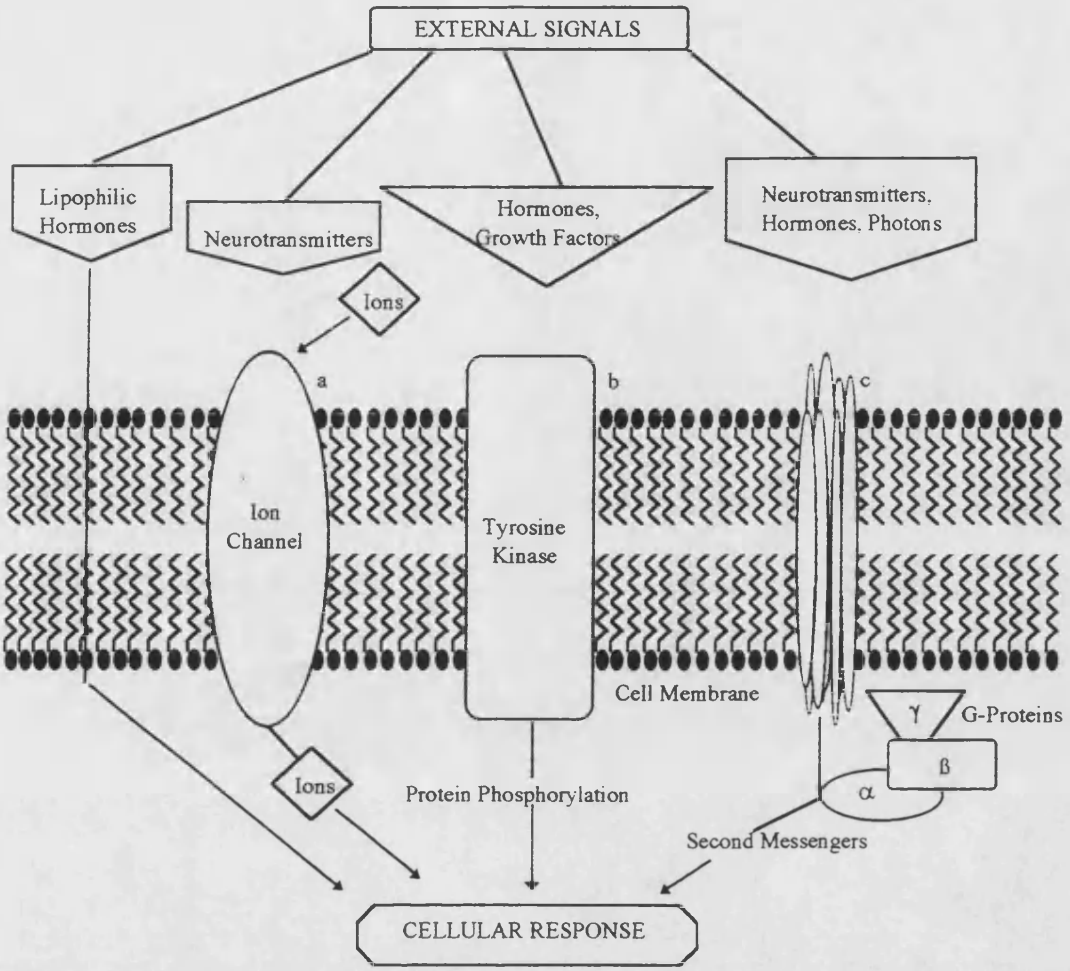

Figure 1.1: Mechanisms involved in signal transduction at cell surface receptors. Illustrating the three types of cell surface receptors, a) Ion-channel linked receptor, b) Tyrosine kinase receptors and c) G-protein linked receptors.

A single activated receptor protein can, in principle collide with and activate many molecules of G-protein thereby activating many molecules of enzyme. In some cases the extracellular ligand may not remain bound to its receptor long enough for this amplification to operate. However the Gs is thought to remain active for up to 10-15s. before hydrolysing its bound GTP hence can keep the enzyme, AC or GC active long after such extracellular ligand is dissociated. The intrinsic GTPase activity of the α-subunit hydrolyses GTP to bound GDP, the α-GDP subunit recombines with the βγ

subunit and the G-protein returns to its basal state. Receptors working through G-proteins include those for messenger molecules e.g. the β-adrenergic receptor and the muscarinic receptor and rhodopsin for light.

1.2 Calcium in Cell Signalling.

Elucidation of the role of Ca^{2+} as an intracellular messenger began over 100 years ago by Ringer 1883 [1]. Ringer observed that contraction of cardiac muscle was abolished when tap water in the medium was replaced with distilled water. The missing component in the distilled water required for muscle contraction was found to be calcium. It is well established today that transient elevation in cytosolic free Ca^{2+} plays a key role in diverse cellular processes. Agonists can raise $[Ca^{2+}]_i$ in two ways. a) by stimulating influx of Ca^{2+} through voltage gated or receptor gated Ca^{2+} channels in the plasma membrane. The large gradient of $[Ca^{2+}]_i$ between the extracellular fluid (1mM) and the cytoplasmic space (0.1μM) allows an influx of Ca^{2+} ions into the cell. b) Ca^{2+} can be released from intracellular pools. Ca^{2+} release from internal stores is important to cell signalling for a variety of cellular events. The cellular response observed depends on the type of cell targeted as well as the nature of the agonist.

1.3 Second Messengers.

The concept of a chemical second messenger was established with the identification of cyclic AMP as a mediator of the effects of epinephrine on glycogen metabolism about forty years ago [2]. A criterion for a second messenger role to be fulfilled was put forward in which the first messenger should increase the concentration of the second messenger in the target cell and an increase in the concentration of the second messenger inside the cell should transduce and amplify the effect of the first messenger.

The second messengers identified today include cyclic-adenosine 3′,5′-monophosphate (cAMP), cyclic-guanosine monophosphate (cGMP), Diacylglycerol (DAG) and D-myo-inositol 1,4,5-trisphosphate [D-Ins (1,4,5)P_3] in combination with Ca^{2+} ions. Other putative second messengers include cyclic ADP-ribose (cADPR), nicotinate adenine dinucleotide phosphate (NAADP). There appear to be few second messengers available compared to the large number of different hormones and neurotransmitters, indicating that internal signalling pathways are surprisingly similar in spite of the plenitude of biochemical and physiological processes to be regulated.

1.3.1 *Cyclic-AMP*

cAMP was discovered by Sutherland and Rall [2] during investigation of the mechanism by which adrenaline and glucagon increase the activity of glycogen phosphorylase in liver slices. Two forms of glycogen phosphorylase (a and b) had been previously isolated from skeletal muscle [3]. Sutherland and Rall later showed that ATP and Mg^{2+} were required for the conversion of isolated liver glycogen phosphorylase b (inactive in the absence of AMP) to phosphorylase a [4]. They were then able to develop a cell-free system in which addition of adrenaline or glucagon to a liver homogenate in the presence of ATP and Mg^{2+} caused an increase in phosphorylase activity. A heat stable factor was isolated from liver slices treated with hormone which was shown to activate glycogen phosphorylase in liver homogenates incubated in the absence of hormones. ATP was required both for the production of this factor in particulate fraction and for its activation of phosphorylase in the soluble fraction. At the time Sutherland and his colleagues were

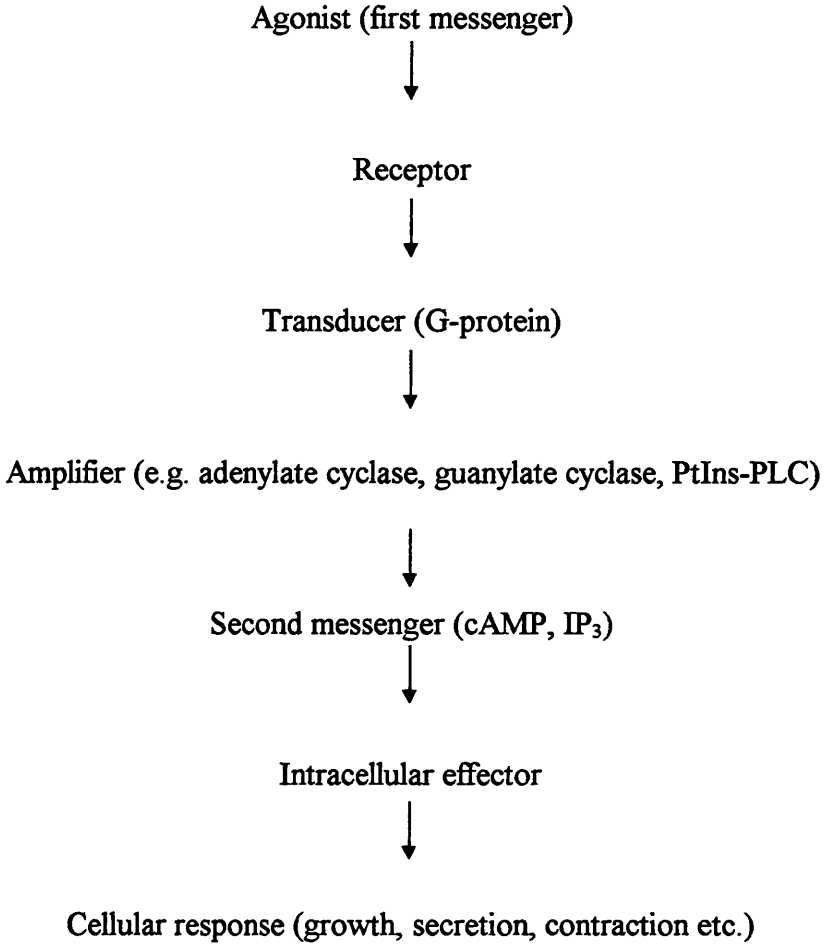

Figure 1.2: Sequence of events in Transmembrane signalling

studying the activation of glycogen phosphorylase, Lipkin was investigating the chemistry of compounds formed when ATP was treated with ($BaOH_2$) [5]. One of the products of this reaction was found to be similar in biological properties to the heat-stable activator or phosphorylase. The two groups collaborated in the elucidation of the structure of this factor which was subsequently identified to be an unusual nucleotide known as cyclic adenosine-3′,5′-monophosphate. The identification of cAMP established the concept of the second messenger. cAMP Is a ribonucleotide that possesses a diester involving phosphoric acid and the hydroxyl functions on the 3′ and 5′ carbons on the ribose ring. It is cyclic as it forms the ester with itself. cAMP is

synthesised from ATP by adenylate cyclase and it is degraded into AMP by cAMP phosphodiesterase (Fig 1.3). The activity of adenylate cyclase is principally controlled by extracellular agonists including corticotrophin, adrenaline, noradrenaline, glucagon and vasopressin. These act through a plasma-membrane bound receptor and either G_s (stimulatory G-protein) or G_i (inhibitory G-protein). The stimulatory part of G_s binds to AC and induces a conformational change in the enzyme. This allows the active site of AC to bind ATP.

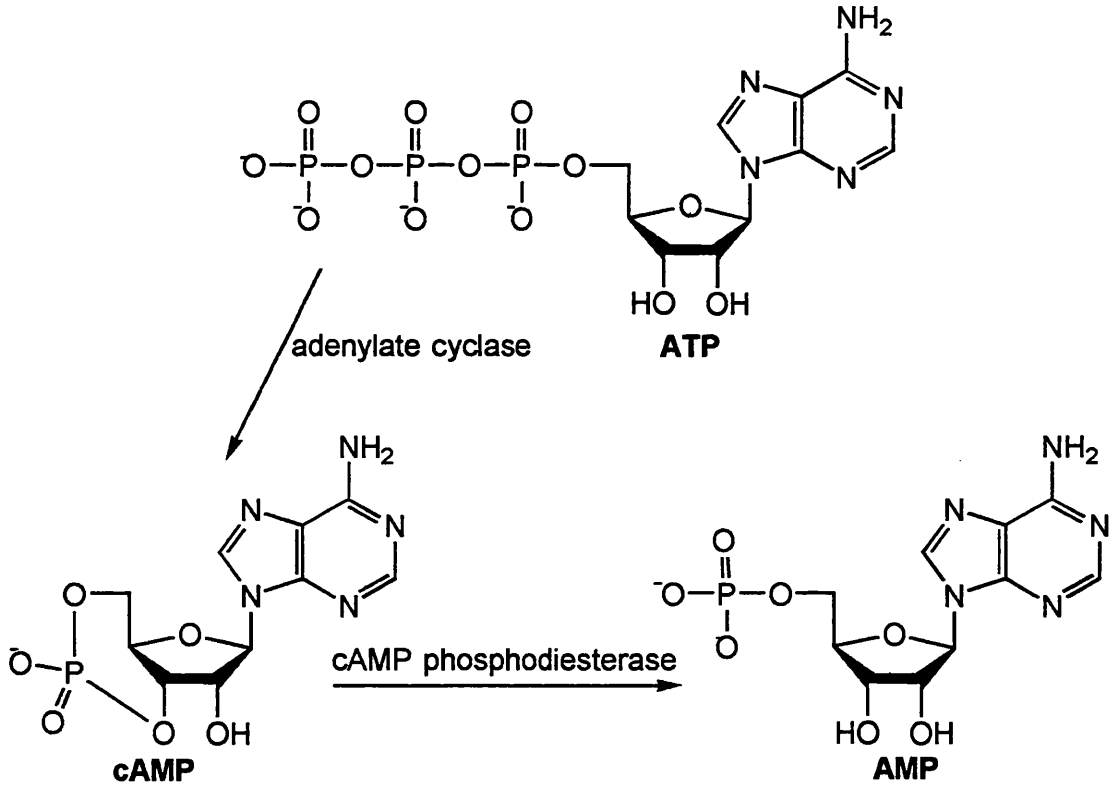

Figure 1.3: Metabolism of cAMP

The inhibition of AC through the action of G_i is mediated indirectly by the released $\beta\gamma$ subunits which bind to free α_s subunit, thereby preventing them from activating cyclase

molecules, and directly by interaction of α subunit with AC. cAMP exerts its effect in the cell mainly by activating an enzyme known as cyclic AMP-dependent protein kinase (A-kinase). This enzyme catalyses the transfer of terminal phosphate group from ATP to specific serine and threonine residues of selected proteins in the target cell, initiating a signalling cascade that results in long lasting alterations of cellular functions. A-kinase in its inactive state is tetrameric consisting of two regulatory (49kDa) and two catalytic (38kDa) subunits (R_2C_2). cAMP binding alters the conformation of the catalytic subunits causing them to dissociate from the complex. The dissociated C units known as active A-kinase phosphorylates substrate protein molecules. cAMP also inhibits protein phosphatase that would otherwise oppose the phosphorylation reactions stimulated by cAMP by activating A-kinase to phosphorylate a phosphatase inhibitor protein which can then bind to the protein phosphatase to inhibit it.

The response to cAMP varies with the type of cell concerned as different cells contain different enzymes serving as substrates for A-kinase. In liver cells for example, cAMP promotes glucose synthesis and glycogenolysis, in adrenal cortex, it produces an increase in glucocorticoid synthesis. Dissociation of the ligand is rapidly followed by disappearance of its effect, owing to degradation of cAMP by cAMP phosphodiesterase and dephosphorylation of kinase substrates by phosphatases.

1.3.2 *Cyclic-GMP*

The search for other cyclic nucleotides led to the discovery of guanosine 3′,5′-monophosphate (cGMP) in mammalian urine by Ashman *et al*[6]. The subsequent detection of cGMP in many cells, and all the enzymes analogous to those involved with cAMP metabolism and action i.e. guanylate cyclase, cGMP phosphodiesterase and

cGMP-dependent protein kinase, suggested that this cyclic nucleotide may have a role as an intracellular messenger.

Three forms of GC (enzyme which catalyses the production of cGMP from GTP-Fig. 1.4) have been identified so far. These are plasma-membrane GC, a cytoplasmic form which is activated by endothelium-derived relaxing factor (EDRF), and a Ca^{2+} activated form which is found associated with the cytoskeleton and plasma-membrane. The plasma-membrane form of GC composes of single polypeptide chain with molecular weight between 120 and 180kDa. It consists of an extracellular domain which binds ANP or a sperm-activating peptide, a single membrane-spanning sequence and a GC catalytic domain on the cytoplasmic side of the membrane. A region of the polypeptide chain in the cytoplasmic domain is phosphorylated at multiple sites. The binding of an agonist to the extracellular domain of the plasma-membrane GC induces a conformational change in the activity of GC. For sperm-cell GC, this change also induces dephosphorylation of the cytoplasmic domain and a subsequent decrease in GC activity even though the agonist remains bound to the extracellular domain of GC. The cytoplasmic form of GC which is activated by EDRF is composed of 2 subunits with Mw of 82 and 70kDa. One of these contains haem as a prosthetic group. Activation of the enzyme by EDRF involves combination of this molecule with the haem group resulting in a conformational change in GC. These actions of Ca^{2+} are probably exerted through an intermediary binding protein. The biological effects of cGMP appears to be more diverse. In addition to activation cGMP-dependent kinase, it also regulates cyclic nucleotide phosphodiesterase as well as having direct effects on Na^{+} channels [7,8].

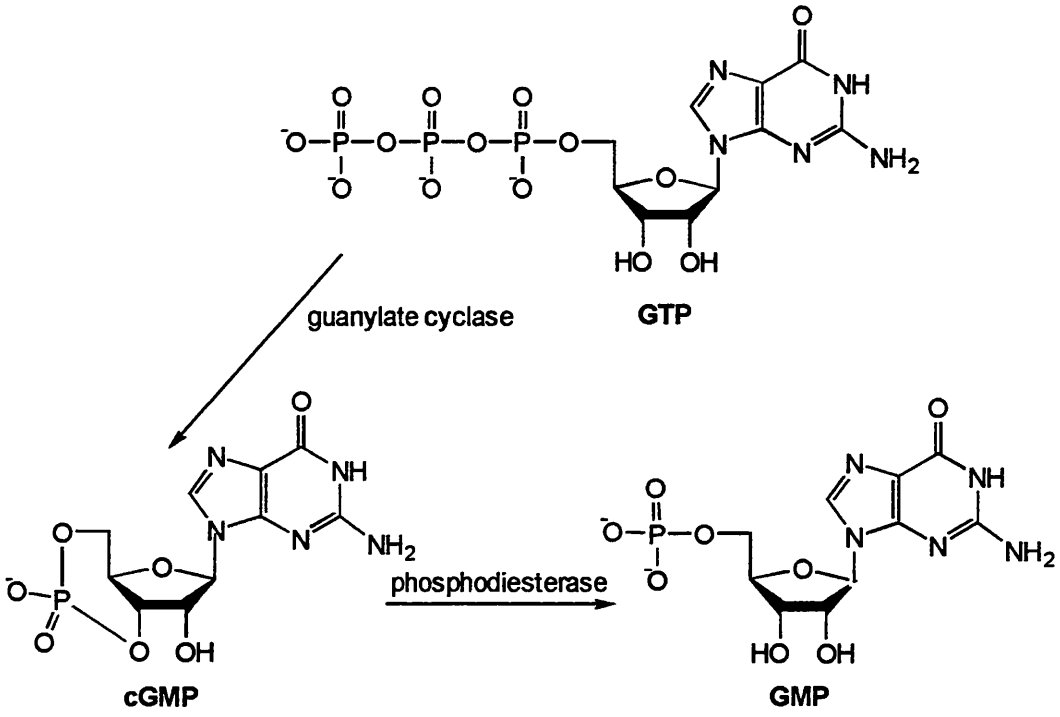

Figure 1.4: Formation and breakdown of cGMP.

1.3.3 *Inositol-1,4,5,-trisphosphate*

IP_3 (Fig 1.5) is employed as an intracellular messenger in a large number of cellular responses induced by agonists [9]. In 1953 Hokin and Hokin observed that in pancreatic cells, acetylcholine stimulated the incorporation of $[^{32}P]HPO_4^{=}$ into the minor phospholipid, phosphatidylinositol [10]. During the period of 1970 to 1975 it became apparent that for many agonists which bind to receptors on the plasma membrane, cyclic AMP is not responsible for conveying information from the plasma membrane to intracellular sites. It was not until 1975 that Michell pointed out that messengers that activate phosphoinositol response invariably also cause an increase in cytosolic Ca^{2+} concentration and proposed a link between the two events [11]. It was later discovered that the primary event by a number of agonists was the hydrolysis of a minor derivative PtdIns(4,5,)P_2. Berridge consequently discovered that in blow-fly salivary gland, 5-

hydroxytryptamine increases the intracellular concentration of inositol trisphosphates together with the concentration of bis and monophosphates [12].

Streb and co-workers showed that in permeabilised pancreatic acinar cells, IP_3 facilitates the outflow of Ca^{2+} from an intracellular store [13]. This observation has now been repeated in many other cell types and the site of Ca^{2+} release shown to be most likely a component of endoplasmic reticulum. IP_3 is a small water-soluble molecule which does not move through cellular membranes. It is synthesised from the polyphosphoinositide PtdIns(4,5)P_2. Various phosphoinositides have been identified in animal cells. These are PtdIns, PtdIns(4)P, PtdIns(4,5)P_2 and very small amounts of PtdIns(3)P, PtdIns(3,4,)P_2 and PtdIns(3,4,5)P_3 (Fig 1.6). PtdIns(3,4, P_2)and PtdIns(3,4,5)P_3 are only detected in cells stimulated by growth factor, for example PDGF, Insulin or CSF-1. Phosphoinositides are principally located in plasma membranes although they have been detected in other membranes such as nuclear membrane and the membranes of secretory vesicles. Formation of IP_3 from PtdIns(4,5 P_2) is catalysed by PtdIns(4,5 P_2) specific phospholipase C. This reaction occurs in the cytoplasmic face of the plasma membrane in the presence of ATP. This enzyme cleaves PIP_2 to generate two second messengers, IP_3 and DAG.

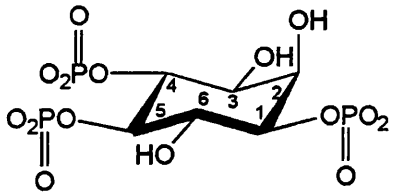

Figure 1.5: Structures of Inositol-1,4,5,-triphosphate (IP_3)

IP_3 interacts with specific intracellular Ca^{2+} release channel protein known as the IP_3 receptor. The receptor is a glycoprotein with a molecular weight of 260kDa. Opening of the Ca^{2+} channel which is part of the receptor protein allows Ca^{2+} to flow into the cytoplasmic space. IP_3 is rapidly de-phosphorylated by specific phosphatases, However not all IP_3 is de-phosphorylated some is phosphorylated to form Ins 1,3,4,5-tetrakisphosphate ($InsP_4$) which may mediate slower and more prolonged responses in the cell. At least two of the metabolites of IP_3, namely IP_4 and cyclic IP_3 have been suggested to have second messenger functions of their own [14,15]. Activation of the IP_3 receptor therefore results not only in the mobilisation of intracellular Ca^{2+} but also turns on a family of cellular processes. It thus appears that the IP_3 pathway is perhaps acting as a master switch for general activation of cell rather than a specific means of Ca^{2+} mobilisation. This raises the question of whether messenger molecules more specific for Ca^{2+} mobilisation other than IP_3 could exist.

Lithium has been found to inhibit two phosphatases which degrade inositol 1,4-bisphosphate and inositol-1-phosphate to free inositol thereby preventing the recycling of inositol into phosphoinositides. Since many peptide neurotransmitters activate phosphoinositide turnover, it is possible, that this explains the therapeutic effect of Lithium. There is substantial evidence that this pathway is involved in the control of smooth muscle, contractility, secretion, neuronal excitability, the activation of inflammatory cells and cell proliferation.

1.3.4 *Diacylglycerol*

In 1977 a protein kinase that requires Ca^{2+} and phospholipids for activity was discovered [16]. This was originally called Ca^{2+} and protein-dependent protein kinase, but is now

known as protein kinase C. They also found that DAG and tumour promoter phorbol esters such as 12-O-tetradecanoyl phorbol-13-acetate (TPA), are potent activators of this protein kinase. Stimulation of protein kinase C by DAG, results in phosphorylation of a variety of proteins and produces profound effects on cellular activities [17]. DAG is rapidly metabolised whereas, TPA is hardly metabolised which leads to distortion in cellular response. DAG is formed in the inner leaflet of the plasma membrane by the hydrolysis of phospholipids of which PIP_2 and phosphatidylcholine are the most common. DAG is lipophilic (Fig 1.7) and in contrast to cyclic nucleotides and IP_3, remains associated with the membrane. They function as intermediates in the synthesis of phospholipids and triacyglycerols as well as being second messengers.

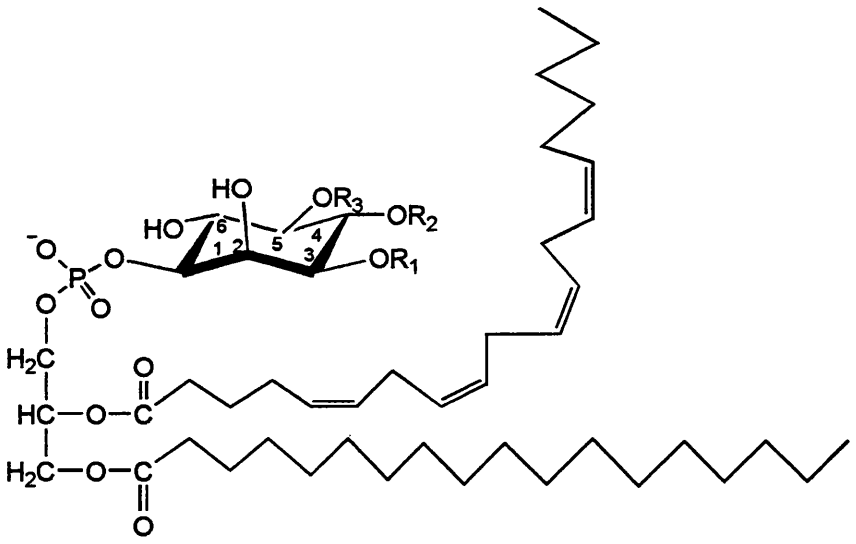

$R_1 = R_2 = R_3 = H$	PtdIns
$R_1 = R_2 = H$, $R_2 = PO_3^{2-}$	PtdIns(4)P
$R_2 = R_3 = PO_3^{2-}$, $R_1 = H$	PtdIns(4,5)P_2
$R_2 = R_3 = H$, $R_1 = PO_3^{2-}$	PtdIns(3)P
$R_1 = R_2 = PO_3^{2-}$, $R_3 = H$	PtdIns(3,4)P_2
$R_1 = R_2 = R_3 = PO_3^{2-}$	PtdIns(3,4,5)P_3

Figure 1.6 Phophatidyl-inositols

In contrast to IP_3, DAG and protein kinase C chiefly convey information for cell responses which are slow in onset and involve longer term changes in cell growth, proliferation, differentiation and in movement of the cytoskeleton.

DAG together with the phospholipid, phosphatidyl serine, in the cytoplasmic half of the plasma membrane, binds to C-kinase, increase affinity of the enzyme for Ca^{2+} so that C-kinase becomes active at low concentrations of Ca^{2+} in the cytosol. In many cells, it appears that protein kinase is activated by the co-operative effect of DAG and increase in cytosolic Ca^{2+} brought about by IP_3. Once activated, C-kinase transfers the terminal phosphate on target proteins that vary depending on the cell. The activation of C-kinase is transient because DAG is phosphorylated to form phosphatidate or further cleaved to arachidonic acid within seconds. The highest concentration of C-kinase is found in the brain where it phosphorylates ion channels in nerve cells, thereby changing their properties and altering the excitability of the nerve cells.

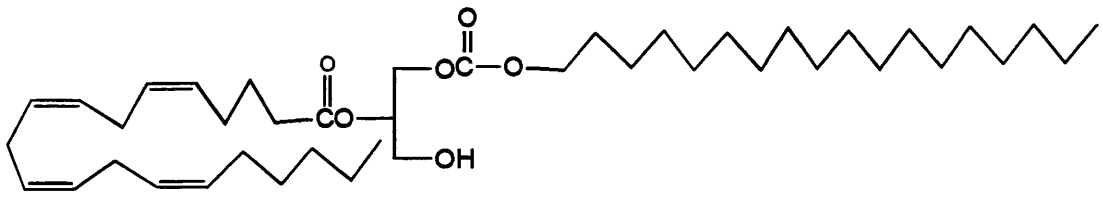

Figure 1.7: Structure of Diacylglycerol

1.4 Cyclic Adenosine Diphosphate Ribose

Advances in the technique for the measurement of the concentration and distribution of intracellular Ca^{2+} have revealed unsuspected complexity in the spatiotemporal dynamics of Ca^{2+} during cell signalling [9]. Ca^{2+} mobilising agonists do not generally produce simple elevations in intracellular free Ca^{2+} concentrations, but more often produce a series of recurring fluctuations or oscillations [20]. Furthermore, these Ca^{2+} oscillations are well organised spatially and often propagate as transcellular waves in either single cells or through networks of adjacent cells [21]. The fact that IP_3 may not be the only messenger for this process is supported by the findings of Ca^{2+} mobilisation with no or minimal change in endogenous IP_3 [22-25].

It was proposed that an initial release of Ca^{2+} from the IP_3 sensitive Ca^{2+} pool could act as a primer for further Ca^{2+} release from IP_3-insensitive pools producing a spike that could spread like a wave throughout a cell [9,20]. This mechanism known as Ca^{2+}-induced Ca^{2+} release (CICR), was first established in muscle cells [26,27] and later found in a variety of other cell types, has since been proposed to be involved in mechanisms of Ca^{2+} oscillations and Ca^{2+} wave propagation [28-31]. The ability of Ca^{2+} to activate its own release in Ca^{2+} signalling is the important feature of CICR. There is evidence that CICR may be under additional control from cell surface receptors. This release was previously thought to be from IP_3-insensitive stores [32]. The ryanodine receptor, a second intracellular Ca^{2+} release channel, also found widely in cells, was believed to solely mediate the CICR release mechanism [33], however recent findings have shown that two closely related Ca^{2+} channels with these properties are the IP_3 and ryanodine receptor [34]. IP_3Rs are well documented, where they appear to function as ubiquitous pathway for generating intracellular signals [35], RyR-mediated Ca^{2+} signalling is less well understood.

However, an awareness of the importance of this second pathway for Ca^{2+} mobilisation in an equally diverse set of cellular systems has increased [36-38]. Ryanodine and caffeine are known agonists for the RyR receptor [39]. Ruthenium red and procaine are commonly used antagonists for this receptor [40]. The physiological ligand for this receptor is however unknown. Experiments with classic RyR blockers indicated that cADPR acted via a RyR-like Ca^{2+} release channel [41]. These results led to the hypothesis that cADPR acts via a RyR-like mechanism, distinct from the IP_3R. Furthermore, agents that can activate RyRs, including divalent cations, caffeine, and ryanodine, can potentiate Ca^{2+} release by cADPR in sea urchin egg homogenates [42,43].

1.4.1 *Discovery of cADPR as a Ca^{2+}- Mobilising Agent.*

cADPR (Fig 1.9) a metabolite of NAD^+ was discovered in 1987 during investigations of the mechanism of Ca^{2+} mobilisation in sea urchin eggs [44]. The sea urchin egg has long been a favourite model system used to investigate the molecular mechanisms of fertilisation and also for understanding the basic mechanisms of intracellular Ca^{2+} signalling. Clapper and co-workers[44] developed an *in vitro* system that allows free access to internal Ca^{2+} stores by preparing homogenates from *Lytechinus pictus* eggs with a regular homogeniser equipped with a glass pestle [45]. A gentler technique of N_2 deactivation was needed for *Strongylocentrotus purpuratus* eggs [46]. In the presence of ATP, the endogenous Ca^{2+} pump in the homogenates sequesters the contaminating Ca^{2+} and lowers the ambient concentration of Ca^{2+} to the submicromolar range, allowing the convenient use of fluorescence Ca^{2+} indicators for monitoring the movement of Ca^{2+}. The preparation was found to be ideally suited for use as a bioassay for Ca^{2+} release activators as it is highly stable and very responsive to IP_3, which elicits a large and

immediate Ca^{2+} release. A large quantity of egg homogenates can be prepared for routine use and stored frozen without loss of responsiveness for long periods of time.

NAD^+ whose concentration is known to change dramatically during fertilisation was tested along with other possible candidates for Ca^{2+} release activators [47]. In contrast to the rapid release induced by IP_3 , there was a significant latency of 1-4min before calcium release was observed in response to NAD^+. Furthermore, pre-incubation of NAD^+ with egg extracts, produced an active metabolite that can release Ca^{2+} without a delay. This release was found to be stereospecific, requiring β-NAD^+, the α-form had no effect. These data suggested that an enzymatic conversion of β-NAD^+ to the active metabolite is likely to be involved, hence the product obtained by incubation with the egg extracts was purified by HPLC and called "enzyme-activated"-NAD^+ (E-NAD^+). Structural determination of E-NAD^+ led to the identification of a novel cyclised ADP-ribose cADPR is synthesized from NAD^+ by ADP-ribosyl cyclase and hydrolyzed to its inactive metabolite ADP-ribose by cADPR hydrolase. CD38, is a bi-functional enzyme that catalyses both the synthesis and degradation of cADPR

1.4.2 *Structure of cADPR*

Pure E-NAD^+ obtained from HPLC purification was subjected to structural analysis by Lee and co-workers [48]. The initial structural characterisation employed use of radioactive NAD^+ with labels at various positions of the molecule as precursors. The labels were lost only if they were on the nicotinamide group of NAD^+ prior to enzymatic conversion. This indicated that the nicotinamide group is lost during catalysis and this was confirmed by NMR studies, which showed that the only hydrogens that were

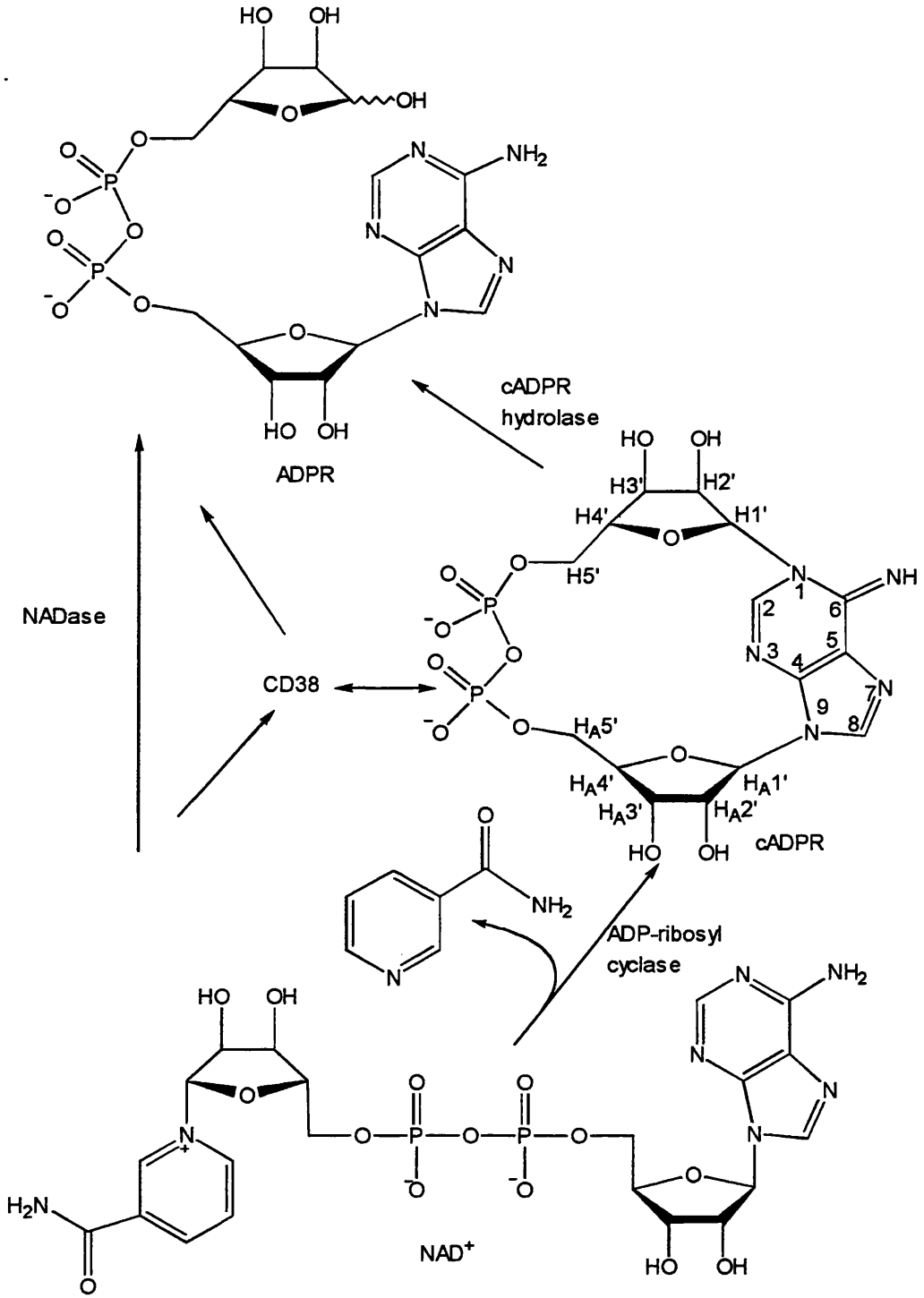

Figure 1.8: Formation and metabolism of cADPR (1).

missing are those on the nicotinamide and the rest of the hydrogens in NAD^+ remained intact. The exact mass of E-NAD^+ was determined by high resolution mass spectrometry, which together with total phosphate content determinations, uniquely specified the chemical formula of the molecule as $C_{15}H_{20}N_5O_{13}P_2$. The strongest evidence that it is a cyclised structure came from the analysis of its hydrolytic product which was shown to be ADP-ribose by NMR and mass spectrometry. The fact that ADP-ribose is exactly one molecule of water heavier than the molecular weight 541 of the active molecule is analogous to the hydrolysis of cAMP to AMP. Addition of a water molecule to the 3′-phosphate bond of cAMP breaks the cyclic linkage by exactly one water molecule larger than cAMP. From this analogy, E-NAD^+ was named cyclic ADP-ribose.

It was important to establish the exact site of cyclisation of cADPR. Two possible sites of cyclisation were identified; the terminal ribose can be linked to the adenine nitrogen at either position 1 or 6 (N1 or N6) of the adenine ring (see Fig 1.9). The N6-linkage was originally proposed [48], however analysis by pH titration and UV absorption spectroscopy favour the N1-linkage [49]. The ambiguity has now been unequivocally resolved by X-ray crystallography of crystals of cADPR from saturated aqueous solution of its free acid, stereoselective chemical synthesis of cADPR from β-NAD^+, and various NMR techniques [50-52]. Thus, cADPR is a cyclised ADP-ribose with an N-glycosyl bond between the anomeric carbon of the terminal ribose and the N1 of the adenine ring.

The shape of cADPR was demonstrated in a CPK view by Lee as more square than round with a little empty space in the centre [53]. The phosphate backbone of the molecule bulges out to one side of the adenine ring. The bonds between N1 and C1′ of

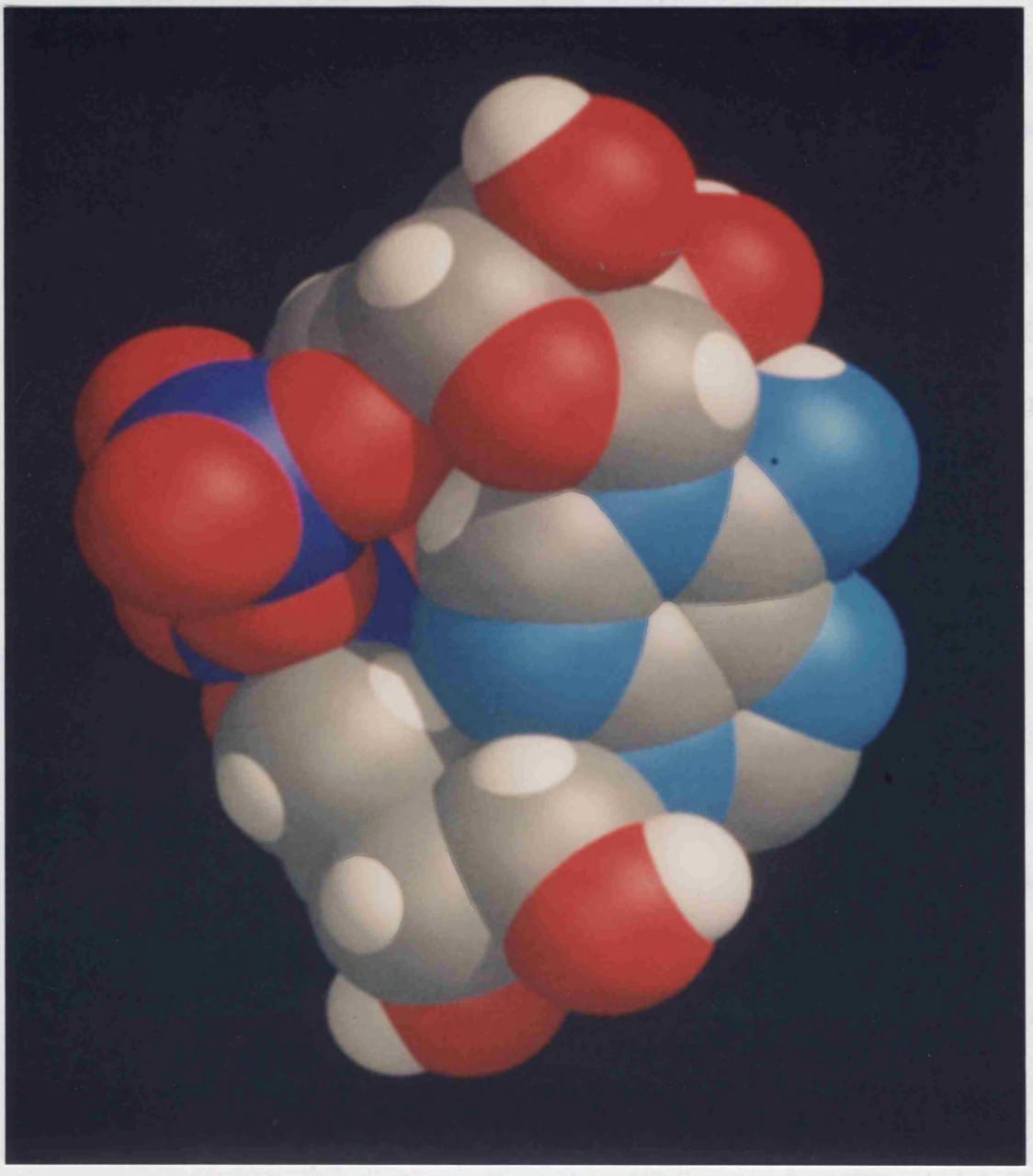

Figure 1.9: Computer modelling of cADPR[50]

the cyclising ribose and that between N9 and C1′ of the other ribose are both in the β configuration, being directed toward a position opposite from those of the ribosyl -OH groups. This configuration is similar to that of NAD^+ in which both glycosyl linkages are in the β configuration. The configuration of the adenine is *syn* with respect to the bond between N9 and the ribose, whereas the new cyclisation bond between N1 and the terminal ribose is in the *anti* configuration. In NAD^+ both the adenine ring and the nicotinamide group are in the *anti* configuration [54]. N6 is coplanar with the adenine and the three bond angles around C6 are all close to 120°, indicating N6-C6 being a sp^2 double bond. Only one hydrogen was found bonded to N6 indicating the imino tautomer.

1.4.3 *Enzymes Involved in the Metabolism of cADPR*

A) ADP-ribosyl cyclase

The identification of an activity in sea urchin egg homogenates that activates NAD^+ to release Ca^{2+} led to the discovery of ADP-ribosyl cyclase. This activity was latter demonstrated in a variety of mammalian cell extracts [55]. In contrast to other NAD^+ utilising enzymes, the enzymatic activity of ADP-ribosyl cyclase does not require exogenous cofactors and activity in sea urchin egg is found to be lowest, about a million fold lower than in *Aplysia* ovotestis and 200-fold lower than in mammalian brain extracts [56]. ADP-ribosyl cyclase exist both in soluble and membrane bound forms. The soluble form exists in dog testis, sea urchin egg and testis, and most abundantly, in the ovotestis of *Aplysia californica.* This soluble form was first purified and sequenced from the ovotestis of the marine mollusc, *Aplysia californica* [57-59]. It is a 29kDa protein, originally thought to be NADase because it was thought to convert NAD^+ to ADP-

ribose[58]. Use of HPLC and NMR techniques have demonstrated that the product from transformation of NAD^+ with this enzyme is cADPR, hence the name ADP-ribosyl cyclase. Purification of ADP-ribosyl cyclase by high resolution cation-exchange chromatography showed that the homogenous enzyme exists in multiple active forms differing in charge. The membrane bound form of ADP-ribosyl cyclase has been identified in sea urchin eggs and most mammalian tissues. Several membrane bound cyclases such as CD38, a 40kDa protein from lymphocytes, various homologous proteins such as CD38H [60] from rat islets of Langerhans, a 39-kDa protein from canine spleen [61] and a surface molecule on erythrocytes [62], have been characterised. These are bifunctional enzymes catalysing the synthesis and degradation of cADPR hence the overall reaction resembles that of NADase although the two reactions are different mechanistically in that the bifunctional reaction involves the formation of cADPR as intermediate, whereas the NADase reaction, does not involve cADPR. The *Aplysia* isoform has low cADPR hydrolase activity, and this makes it suitable for use commercially in the synthesis of cADPR from NAD^+.

B) cADPR hydrolase

For a second messenger role for cADPR to be established, there should be a pathway for switching off the message. The presence of an enzyme that degrades cADPR was noted by Rusinko and Lee 1989, during measurement of ADP-ribosyl activity in various tissue extracts [55]. Incubation of tissue extracts with NAD^+ resulted in the production of cADPR and progressive increase in Ca^{2+} release activity. These release was found to decline after reaching a peak, indicating that cADPR was destroyed by a degradation enzyme in the incubation mixture. The hydrolase from the dog brain extracts has been partially characterised [63]. The enzyme activity is associated with membranes and similar

to the cyclase is found to be equally widespread and does not appear to require any exogenous cofactors. cADPR hydrolase activities are often found associated with ADP-ribosyl cyclases, and both activities have been found on the same polypeptide [61]. also when the cyclase activity is high, as in brain extracts, the hydrolase activity is also high. The exception of this case is in *Aplysia* ovotestis in which the cyclase activity is so high that the hydrolase activity is insignificant in comparison. The product of cADPR hydrolase activity was identified as ADP-ribose indicating that this enzyme uniquely cleaves the N-glycosidic linkage between the adenine group and the terminal ribosyl moiety of cADPR by hydrolysis, hence the name, cADPR hydrolase. The enzyme has a K_m of 160μM for cADPR and a V_{max} of 1.2μmol/mg/hr. It displays a broad pH maximum near neutral and may be inhibited by millimolar ATP levels [64].

C) CD38 and homologous proteins.

CD38 is a multifunctional protein expressed primarily in on lymphoid cells. It appears to mediate several diverse activities, including signal transduction, cell adhesion and cADPR synthesis [65]. Human leukocyte antigen CD38 and its rodent homologues have been demonstrated to have both ADP-ribosyl and cADPR hydrolase activities [64,66]

Comparative studies revealed that the amino acid sequences of *Aplysia* cyclase which do not show cADPR hydrolase activity shows a high degree of amino acid sequence identity with that of CD38 and that 10 cysteine residues are conserved between *Aplysia* enzyme and human CD38 [66]. From recent results of cDNA cloning of rat [60,64] and mouse [68] homologous to human CD38, another 3 cysteine residues (Cys-16, Cys-116, Cys-209 in human CD38) are conserved among the mammalian CD38s, but that the amino acid residue corresponding to Cys-16 of CD38 is not in *Aplysia* enzymes and those

corresponding to Cys-119 and Cys-201 of CD38 are Lys-95 and Glu-176, respectively in *Aplysia* enzymes. Introduction of site-directed mutations into the CD38 cysteine residues 119 and 201 results in a CD38 protein that exhibited only ADP-ribosyl cyclase activity. Furthermore, *Aplysia* ADP-ribosyl cyclase into which mutations K95C and E176C (corresponding to residues 119 and 201 in CD38) to *Aplysia* ADP-ribosyl cyclase exhibited both cyclase and cADPR hydrolase activities. The fact that these enzymes are bi-functional in that they reside on the same protein has led to the suggestion that many common ecto-NAD^+ glycohydrolases, which convert NAD^+ to ADP-ribose, may do so via cADPR as an intermediate [61]. However, the development of the NGD^+/cGDPR technique to measure ADP-ribosyl activity *per se* has shown that in many cases NAD^+ glycohydrolases do not exhibit any ADP-ribosyl cyclase activity [69].

Three major differences were identified between the enzymatic reaction of CD38 antigen and *Aplysia* ADP-ribosyl cyclase [70]. First, an intact adenine moiety is required for the cleavage of the N-glycoside bond by ADP-ribosyl cyclase, but not by CD38 NADase. Second, the reaction by ADP-ribosyl cyclase was fully reversible, but CD38 did not catalyse the formation of β-NAD^+ from ADP-ribose and nicotinamide. CD38 NADase could produce β-NAD^+ from cADPR and nicotinamide, though it reaction rate was less than 4% of the hydrolysis rate of β-NAD^+. Third the NADase activity of CD38 was inhibited by DTT, but *Aplysia* ADP-ribosyl cyclase activity was not inhibited by DTT even though 10 out of 12 cysteine residues were conserved between the two enzymes. This suggests that the function of disulphide bond(s) if present, differed from each other with respect to catalytic activity. For CD38 to play a role in producing cADPR, a marked change in its enzyme property, such as conversion from NADase to cyclase

would be required. cGMP has been shown to stimulate the formation of cADPR [71] and ATP has been shown to inhibit the hydrolysis of cADPR catalysed by CD38 NADase [64], combination of these observations suggest that the enzyme property of CD38 antigen may be altered by post-translational modification, such as phosphorylation and dephosphorylation, or by interaction with an intracellular messenger(s). Interestingly, both CD38 and *Aplysia* cyclase have many consensus sites for cGMP-dependent kinase catalysed phosphorylation [56]. The best characterised example of bifunctional enzyme is 6-phosphofructokinase-2/fructose-2,6-bishosphatase from liver. These two activities are regulated by cAMP-dependent protein kinase; phosphorylation results in the activation of the bisphosphatase activity and inhibition of the kinase [72].

1.4.4 *Regulation of cADPR Synthesis by cGMP*

It is essential that intracellular levels of cADPR be under control of extracellular signals for it to be unambiguously assigned as a second messenger. Micro-injection of various Ca^{2+}-releasing molecules including IP_3 and cADPR into sea urchin eggs exhibited markedly different Ca^{2+} release pattern compared to that seen during fertilisation [73]. The only exception is cGMP whose pattern of Ca^{2+} release resembled that seen at fertilisation [74]. The effect of cGMP on Ca^{2+} release in sea urchin eggs have been examined at the level of the intact cell and of cell homogenates. The pattern is characterised by a latency of ca. 20sec before the Ca^{2+} transient is initiated and the time course is more protracted than that induced by IP_3 or cADPR and can last for as long as 10min. Ca^{2+} release induced by micro-injection of cGMP into intact eggs was not blocked by IP_3R antagonist heparin [74], but extracellular application of the membrane permeant analogue dibutyryl-cGMP in intact eggs was blocked by prior micro-injection of the ryanodine receptor antagonist ruthenium red, suggesting that the RyR receptor is

an essential element involved in the response to cGMP [71]. The fact that cADPR, like cGMP, releases Ca^{2+} by a mechanism sensitive to ryanodine and ruthenium red, suggested that cGMP may be releasing Ca^{2+} by the cADPR-sensitive mechanism. The pharmacology of the cGMP-induced Ca^{2+} release has been analysed in sea urchin egg homogenates [71].

In the presence of low concentrations of β-NAD^+, cGMP desensitised release by cADPR but not by IP_3; in cADPR-desensitised homogenates, cGMP failed to release Ca^{2+}, but IP_3 was still effective. This suggested that release by cGMP was via a cADPR-sensitive mechanism. That the effect of cGMP was indirect was revealed by the use cGMP-dependent protein kinase inhibitors (Rp-cAMPS and staurosporine) which blocked cGMP, but not cADPR induced release. This suggested that cGMP could be stimulating ADP-ribosyl cyclase, the enzyme that converts β-NAD^+ to cADPR. Analysis of [^{14}C]NAD^+ metabolism by TLC egg homogenates treated with cGMP suggested that cGMP stimulates the conversion of β-NAD^+ into cADPR and ADP-ribose (the hydrolytic product of cADPR). cGMP did not affect the rate of hydrolysis of ^{3}H-labeled cADPR to ADP-ribose, suggesting that it was not inhibiting cADPR hydrolases. These experiments support the idea that cGMP activates ADP-ribosyl cyclase, perhaps through cGMP-dependent protein phosphorylation, resulting in enhanced conversion of NAD^+ to cADPR.

By analogy to the phosphoinositide pathway, for cADPR to function as a second messenger, its synthetic enzyme, ADP-ribosyl cyclase would be expected to be regulated either directly or indirectly by cell-surface receptor activation like phophoinositidase C. cGMP itself has been established as a messenger for a number of different signalling

molecules [75] It is synthesised by intracellular guanylyl cyclases (see section.1.3.2) of which there are two isoforms. The first isoform is particulate and constitutes a family of cell-surface receptors possessing cytoplasmic domains that have intrinsic guanylate cyclase activity while the extracellular domains are capable of binding a variety of peptide hormones, including atrial natriuretic factor and a chemoattractant peptide secreted from eggs. The binding of these peptides to the receptor domain results in enhancement of the guanylate cyclase activity [76]. The second form of the GC is soluble; its enzymatic activity is stimulated by the gaseous transmitter nitric oxide and carbon monoxide [77]. NO, which elevates cGMP in sea urchin egg, probably by activating soluble GC, also leads to Ca^{2+} mobilisation in intact eggs and egg homogenates [78]. The pharmacology of this Ca^{2+} release suggests that NO activates a pathway which involves both cGMP and cADPR, but not IP_3, in that 8-amino-cADPR a selective competitive antagonist of cADPR, and nicotinamide, an inhibitor of ADP-ribosyl cyclase, inhibit the Ca^{2+} mobilising effects of NO, while heparin, a competitive antagonist of IP_3R, did not affect NO induce Ca^{2+} release. Rp-8-pCPT-cGMPS, a cGMP-dependent-protein kinase inhibitor blocked the Ca^{2+} mobilising effects of NO, also the effect was dependent on the GC substrate GTP. Since the activation of a number of cell-surface receptors leads to activation of GC, either directly or via the production of intermediate messengers such as NO [79], this pathway may be a way in which cell-surface events are linked to cADPR production. It will be interesting to see if such a pathway exists in mammalian cells too. Indeed, nitric oxide induced mobilisation of Ca^{2+} from ryanodine-sensitive stores has been observed in interstitial cells of the mammalian colon and has been proposed as a mechanism for the amplification of nitric oxide production in the mammalian gut [80].

1.4.5 *cADPR induced Ca^{2+} release*

A) Sea urchin egg as a model system

The sea urchin egg has been used as a model system for studying regulation of cellular functions by ionic mechanisms. Various preparations have been developed for biochemical analyses. Large quantities of homogeneous cells can be obtained readily and at the whole cell level, the eggs are large and sturdy enough for various micromanipulations, such as microinjection. Unfertilised eggs released into sea water are in a dormant state characterised by a depressed metabolism and a slightly acidic internal pH. The life span of the egg in this state is 1-2 days. Once fertilised, the eggs undergo dramatic transformations. This change is followed by resumption of protein and DNA synthesis, and the developmental program is set into motion. The fertilised eggs eventually develop into adults. All these changes that eventually immortalise a dying cell are triggered by two ionic changes: alkalinisation of internal pH as a result of activation of Na^+/H^+ exchanger in the plasma membrane, and transient elevation of internal Ca^{2+} due to mobilisation of intracellular stores.

The egg is a good model system for elucidating various mechanisms for Ca^{2+} mobilisation as multiple Ca^{2+}-regulation systems have been identified. Studies show that IP_3 and cADPR receptors are involved in mediating the Ca^{2+} mobilisation associated with fertilisation [63,71]. This process is analogous to other ligand-receptor mediated events as the external stimulus, the sperm, interacts with a surface receptor. Five other Ca^{2+} transients occur afterward which are different and so likely to involve other second messenger systems, in that the Ca^{2+} changes do not require an external stimuli and are temporally correlated with various developmental events such as pronucleus migration, nuclear membrane breakdown and metaphase [81]. The source of Ca^{2+} for these latter

transients appear to be internal stores, since the early development of the embryo, similar to the fertilisation process, can proceed normally for at least the first seven cleavages in the absence of external Ca^{2+} [79]. All the developmental events, in conjunction with the multiple Ca^{2+} transients associated with them , are likely to be controlled internally by mechanisms that are turned on at fertilisation as the fertilised egg is capable of surviving in total isolation.

The egg homogenate preparation was developed specifically for studying the mechanisms of Ca^{2+} mobilisation [44,45]. The prepation can be used without further fractionation. Detailed characterisation of this preparation led to the discovery of cADPR. In addition to the IP_3- and cADPR-dependent Ca^{2+} release systems, a third independent system sensitive to NAADP has been characterised [44,83] (section 1.5). The homogenate preparation has the simplicity and accessibility of a cell-free system, yet it contains a wealth of possibilities to be explored. Information obtained from the homogenate preparation has been applicable not only on the whole-egg level but also to other cell systems. Thus, cADPR was discovered in the in vitro preparation and has been shown to be active in intact eggs as well as in various mammalian systems [55,84]. Conversely, the Ca^{2+} mobilising effect of cGMP was first demonstrated in intact eggs [74] and later verified in the homogenate system. This preparation also allows identification and purification of various components of a complex pathway such as Ca^{2+} mobilisation. The plasma membrane and the associated cortical granules can be easily removed as large complexes by low speed centrifugation, since the gentle homogenisation largely preserves their association. The Ca^{2+} stores can be separated from mitochondria and yolk granules by Percoll density centrifugation [44,45].

B) Pharmacology of cADPR -induced Ca^{2+} release

The Ca^{2+} mobilising activity of cADPR was first demonstrated in sea urchin egg microsomes and since, then several mammalian cell systems have also been shown to be responsive. The sea urchin egg system remains the best characterised and much of what is known about the characteristics of the Ca^{2+} mobilising activity of cADPR come from investigations of this system.

Cyclic ADP-ribose is at least as effective as IP_3 in releasing Ca^{2+} in eggs homogenates [84]. Several lines of evidence indicate that cADPR-sensitive Ca^{2+} release mechanism is independent of the IP_3-receptor. First, the cADPR-sensitive Ca^{2+} release is insensitive to heparin, a competitive inhibitor of the IP_3-receptor. Second, high concentrations of IP_3 can desensitise the egg chromosomes to IP_3 but not to cADPR and vice versa . This cross-desensitisation has also been observed in several mammalian [86-89]. Third, ^{32}P-cADPR binding to egg chromosomes is insensitive to IP_3 or heparin, but can be competitively inhibited by nanomolar concentrations of unlabelled cADPR [58]. The close proximity observed between the mode of action of cADPR and that of the Ca^{2+} release mediated via RyRs has led to the hypothesis that cADPR is an endogenous regulator of RyRs, perhaps by an analogous mechanism by which IP_3R activated Ca^{2+} release via IP_3Rs [33].

C) cADPR as a modulator of CICR

The concept of Ca^{2+}-induced Ca^{2+}-release (CICR) originated from studies on excitation-contraction coupling in muscles. Investigators found that a small rapid increase in extravesicular Ca^{2+} could cause much larger release of stored Ca^{2+} from skinned muscle fibres or sarcoplasmic reticulum vesicles [40]. CICR has now been demonstrated in a

variety of other cell types [28,29]. The RyR was thought to solely mediate the CICR mechanism [33], however recent findings suggest that IP_3R, under appropriate conditions, can also be gated by Ca^{2+} and thus contribute to CICR [90]. Pertinent to this is the observation that the IP_3-sensitive Ca^{2+} release is strongly Ca^{2+} dependent and, in fact, IP_3 and Ca^{2+} are coagonists of the IP_3 receptor [91-93], but it is not known whether RyRs, in addition to being regulated by Ca^{2+} or mechanical activation, might also be regulated by small intracellular mediators. One candidate that might fulfil this role for RyRs is cADPR.

The pharmacology of the cADPR-sensitive Ca^{2+} release is very similar to the ryanodine sensitive CICR. Antagonists of CICR, such as procaine and ruthenium red, selectively inhibit the cADPR-sensitive Ca^{2+} release without affecting the IP_3-dependent component [41]. Selectivity of the CICR antagonists is also observed in other cell system [87,94]. Ruthenium red, but not procaine has been shown to inhibit cADPR-induced release in Jurkat T cells [95]. Furthermore, agonists of CICR, caffeine and divalent cations such as Sr^{+}, at low concentrations, can dramatically potentiate the Ca^{2+} releasing activity of cADPR. No such stimulation of the IP_3-independent Ca^{2+} is seen with similar concentrations of caffeine [42]. The converse is also true; low concentrations of cADPR that are sufficient to release Ca^{2+} by itself can similarly potentiate the Ca^{2+} releasing activities of caffeine and Sr^{+}. Indeed, nanomolar concentrations of cADPR increased the sensitivity of the Ca^{2+}-release mechanism to Sr^{2+} 10-20 fold. High concentrations of caffeine and ryanodine can release Ca^{2+} by themselves and selectively desensitise the response of the microsomes to cADPR but not to IP_3 [41]. These results indicated that cADPR may be a modulator of the ryanodine sensitive CICR. It appears that cADPR can function, in many respects as endogenous caffeine. Indeed, the structure of cADPR

has some similarities with caffeine. Both compounds have substituents at the N1 position. The N1 is linked with a methyl group in caffeine while it is the site of cyclisation in cADPR. The carbon atoms at the 6-position of both molecules are double bonded. It is an =NH group in cADPR, while it is an oxygen in caffeine. These structural similarities suggest that the two molecules could act on the same Ca^{2+}-release mechanism, while their differences explain why cADPR is five orders of magnitude more effective than caffeine.

D) IP_3 and ryanodine-sensitive Ca^{2+} stores

Cell fractionation studies measuring binding or functional parameters of exogenously applied pharmacological probes reveals that Ca^{2+}-release mechanisms are predominantly microsomal. Investigation of subcellular localisation of various Ca^{2+}-release channels have employed the use of single-cell Ca^{2+} imaging to examine spatial aspects of Ca^{2+} signals activated by pharmacological agonists of these channels [32] and use of electron microscopy in conjunction with specific immunocytochemical probes of the channels [96]. The results indicate that the IP_3 and ryanodine sensitive stores overlap to degrees, depending on the cell types. No overlapping principle governing their subcellular distribution seems to exist [97]. Certain cells such as *Xenopus* and hamster eggs and oocytes seem to contain only a single type of Ca^{2+}-release channel, the IP_3-sensitive channels [98,99], whereas cardiac and skeletal muscle mainly express the ryanodine receptors [40]. Most cells, including sea urchin eggs [71], neurons [96] and smooth muscle [100] contain both type of channels. In cells expressing dual Ca^{2+}-release channels, some appear to contain a single store with two release mechanisms whereas others appear to have different mechanisms distributed on separate Ca^{2+} pools [32]. In hippocampal

neurons, RyR are found in axons and dendritic spines wheres IP_3 receptors are found in cell bodies; both channels colocalise to dendritic shafts [96].

E) cADPR sensitive Ca^{2+} stores

The nature of the cADPR-sensitive Ca^{2+} pools has been investigated mainly in sea urchin eggs. Fractionation of egg homogenates by Percoll density centrifugation showed that cADPR-sensitive Ca^{2+} stores were well separated from mitochondria, but comigrated with a marker enzyme of the endoplasmic reticulum, glucose-6-phosphatase [44,59]. The nonmitochondrial nature is consistent with the fact that cADPR-sensitive Ca^{2+} release is not affected by mitochondrial inhibitors [44,84]. Several pieces of evidence suggest that IP_3 and cADPR-sensitive pools substantially overlap [84]. First, IP_3-and cADPR sensitive microsomes comigrate during fractionation using Percoll density centrifugation. Second, IP_3-and cADPR-induced Ca^{2+} releases are non-additive. Third, an inverse relationship between cADPR- and IP_3-induced Ca^{2+} release was detected. Sequential addition of the two agents to egg homogenates showed that, if one agent had released more Ca^{2+}, less was available for the other to release. The total releasable Ca^{2+} was similar in all cases. These results is consistent with two overlapping Ca^{2+} pools.

Interestingly, it has been observed in egg homogenates that high concentrations of cADPR can desensitise the microsomes so that subsequent additions of cADPR would not produce more Ca^{2+} release. This effect is not due to elevation of Ca^{2+} concentration since the effect persists even after the released Ca^{2+} is resequestered. The desensitised microsomes are fully responsive to other Ca^{2+} releasing agents such as IP_3. Similar results can be obtained with IP_3 [45]. Researchers have shown that the sensitivity of the refractory microsomes to IP_3 could be restored only if the vesicles were washed to

remove IP_3. A simple interpretation of these results would be that cADPR and IP_3 are releasing Ca^{2+} from two separate Ca^{2+} pools. This interpretation would be in contradiction with other results showing that the two pools overlap. Hence the mechanism involved may not be as simple as expected. It may be that the Ca^{2+}-release channels in sea urchin egg microsomes could potentially be desensitised by their own ligand in a Ca^{2+} independent manner. Irrespective of the exact mechanism, this property has proven very useful and has been used to demonstrate the presence of multiple Ca^{2+}-release mechanisms in egg microsomes. The apparent desensitisation has since been used to show the specificity of the bioassay for cADPR to identify a ryanodine receptor-like channel as mediator of the cADPR-dependent Ca^{2+} release [41], and to demonstrate the production of a cADPR-like metabolite in pancreatic β-cells following glucose treatments [87].

The question of Ca^{2+} pools has also been addressed at the intact egg level. IP_3 and cADPR injections into sea urchin eggs have been reported to induce similar Ca^{2+} waves [101]. However a different spatiotemporal pattern of Ca^{2+} release was observed for cADPR- and ryanodine-induced responses. The difference may reflect activation of different RyR receptors or differences in the mechanism of activation of the same channels by these two agents since, although cADPR and ryanodine appear to release Ca^{2+} by activating the same channels, the time course of release induced by these agents is very different [41]. These results indicate the definite existence of multiple Ca^{2+}-release mechanisms in the eggs.

1.4.6 *Identification of cADPR receptor*

A) Specific binding to sea urchin egg microsomes

In order to demonstrate specific binding, radioactive cADPR with high specific activity [^{31}P]cADPR was synthesised and the Ca^{2+} storing microsomes were purified [46]. The binding was not affected by either NAD^+ (the precursor) or ADP-ribose (the hydrolysis product), but was eliminated by 0.3μM of authentic cADPR. The unlabelled cADPR was an effective competitor of the binding, indicating that it was saturable. The specific binding was detected by filtration assay. Scatchard analysis inidicated a binding affinity of about 17nM and a capacity of about 25fmol/mg protein. The K_d for the receptor is identical to the EC_{50} of cADPR for activation Ca^{2+} release from egg homogenates. This suggests that the cADPR receptor in the Ca^{2+} storing microsomes may also be responsible for mediating Ca^{2+} release. An obvious possibility would be that the receptor itself is also the Ca^{2+} channel as has been shown for the IP_3 receptor. The binding is not affected by either IP_3 or the IP_3 antagonist heparin supporting the fact that the receptor for cADPR is different from the IP_3R The nature of the binding site remains unclear.

B) Ryanodine receptors as cADPR receptor

The RyR receptor-Ca^{2+} channel complex is a homotetramer, in which each monomer has a molecular weight of approximately 550kDa. The purified receptors can be visualised as quatrefoil or clover-leaf structures by electron microscopy [40]. Following the cloning and sequencing of the cDNA of the mammalian skeletal muscle ryanodine receptor (RY1 receptor), two other mammalian isoforms of the protein have been identified and their amino acid sequence deduced from their cloned cDNA. The ryanodine RY2 receptor which shows 66% identity with the RY1 receptor, is expressed in cardiac muscle and brain, while the RY3 receptor, which shows 67% identity with the RY1 receptor, is

expressed in the brain and at low levels in many other tissues. The fourth type reported is much smaller than the other three isoforms and is a brain specific transcript of the type 1 gene. This transcript encodes a protein of approximately 75kDa. The best characterised RYR isoforms are those expressed in mammalian cardiac and skeletal muscle (RyR1 & 2), where they constitute the pathway for the rapid release of Ca^{2+} from the sarcoplasmic reticulum which triggers muscle contraction. The cytoplasmic domain of the RyR is very large. For the RyR1, this domain is thought to interact with the dihydropyridine receptor in the sarcolemma, which is believed to confer voltage sensitivity onto Ca^{2+} release from the sarcoplasmic reticulum. This protein-protein interaction allows for rapid activation of the Ca^{2+} release, leading to a fast contractile response as demanded of skeletal muscle, without the apparent involvement of diffusable cytoplasmic messengers. Thus, the type 1 receptor may be atypical of ryanodine receptors because of this important specialisation in its regulation. The RyR2 of cardiac muscle is also opened by depolarisation of the sarcolemma but, in this case, the interaction is indirect in that it depends upon a small pulse of trigger calcium. In effect, calcium is functioning as a calcium-mobilising messenger.

Ryanodine receptors have been shown to be regulated by a variety of physiological ligands. For example, adenine nucleotides, Mg^{2+}, H^{+}, inorganic phosphate, sphingosine, acyl carnitines and calmodulin, as well as Ca^{2+}, regulate the opining and or closing of RYR channels in vitro. RyR activity is similarly modulated by a variety of non-physiological ligands including ryanodine, caffeine, ruthenium red, procaine halothane, perchlorate, and certain peptide toxins. cADPR induces the release of Ca^{2+} from ryanodine-sensitive, IP_3-insensitive, intracellular stores in sea urchin eggs and other cell types, and therefore it is not unreasonable to suggest that cADPR-induced release of

Ca^{2+} might be mediated by a ryanodine-sensitive channel. The hypothesis that cADPR may be an endogenous regulator of one or more isoforms of the RyR has been investigated by scientists. The first direct demonstration of the activation of RyR2 receptor but lack of effect on Ryl receptor by Meszaros and co-workers led to a general acceptance of the proposal that cADPR-induced Ca^{2+} release is mediated by the RyR receptor [93]. However there are significant discrepancies between the pharmacology profile of cADPR-induce Ca^{2+} release and that of the RyR2 receptor. Mezaros co-workers reported that cADPR had no effect on skeletal muscle SR Ca^{2+} efflux, yet showed ca. 70% inhibition of [^{3}H]ryanodine binding to skeletal muscle SR in the presence of 2μM cADPR. It was also concluded from this data that cADPR produced a conformational change in the skeletal muscle RyR that inhibits ryanodine binding without affecting SR Ca^{2+} release. In contrast, another group reported that Ca^{2+} efflux from skeletal muscle SR vesicles was activated by 1-17μM cADPR, however this efflux was insensitive to RyR channel inhibitors [102]. This group also demonstrated that cADPR had no effect on single skeletal muscle RyR channels in planar bilayers, hence concluded that skeletal muscle SR does exhibit a cADPR-activated Ca^{2+} release pathway, but that this pathway operates through non-RyR channels. Fruen and co-workers failed to reproduce the effects of cADPR on [^{3}H]ryanodine binding to cardiac and skeletal muscle [103]. They were also unable to confirm the reported stimulation by cADPR of cardiac RyR single-channel activity in lipid bilayers and in SR preparations. The possibility of cADPR being an endogenous regulator of the RyR therefore remains controversial.

C) Photoaffinity labelling of cADPR binding sites

8-azido-cADPR, an antagonist of cADPR was used as a photoaffinity probe for identifying the cADPR receptor as the azido group is photoactive. [^{32}P]8-Azido-cADPR

was used to specifically label two proteins having molecular masses of 140kDa and 100kDa from sea urchin egg preparations, and a 45kDa protein in cardiac muscle and a 75kDa protein from mammalian brain [104]. There molecular weights are much lower than known subunits of ryanodine receptors which are around four to five times as large [85]. Interestingly caffeine, an agonist of the ryanodine receptor, preferentially inhibits the photolabelling of the 100kDa protein relative to the 140kDa protein. This could account for the desensitising effect of caffeine on cADPR-dependent Ca^{2+} release. The relationship of these proteins to RyRs has yet to be determined. Further characterisation of these proteins is required to determine whether 100KDa and 140kDa represent smaller variants of the ryanodine receptor. A 75kDa variant of the ryanodine receptor has been described in brain [88]. It is possible that cADPR binds to an accessory protein which then interacts with the ryanodine receptor. The success of specifically labelling cADPR binding sites with ^{32}P-labeled 8-azido-cADPR represents a major step toward the eventual purification and identification of these proteins.

1.4.7 *Regulation of cADPR-induced release*

A) Calmodulin

Sea urchin egg microsomes purified by Percoll gradients were shown to loose sensitivity to cADPR, but the response can be restored by adding back cytosolic extracts whose active constituent was identified as an accessory protein known as calmodulin [105]. This was substantiated by the finding that addition of W7, a calmodulin antagonist, inhibited the cADPR-induced Ca^{2+} release. It is suggested that calmodulin may interact directly with and sensitise the Ca^{2+} release mechanism in a similar way to the potentiation of CICR in egg homogenates by low concentrations of caffeine and divalent cations as 1mM caffeine induced cADPR release without calmodulin as those treated with it.

Furthermore, increasing concentrations of Sr^{2+} (10-50μM) progressively sensitised the microsomes, resulting in cADPR releasing as much Ca^{2+} as microsomes treated with either calmodulin or caffeine. Therefore, Sr^{2+} and caffeine can substitute for calmodulin sensitising microsomes to cADPR, suggesting that cADPR is a modulator which can activate the Ca^{2+}-release mechanism when it is in a sensitised state. Indeed, calmodulin binding sites have been characterised on mammalian RyRs [106]. Lack of calmodulin or other accessory proteins may account for the reason why some workers have difficulties in seeing effects of cADPR on Ca^{2+} release from certain broken-cell mammalian systems.

B) Inorganic phosphate and magnesium ions

The effect of magnesium ions on cADPR-induced Ca^{2+} release has been investigated in sea urchin egg homogenates [107] and in Jurkat T-cells and HPB.ALL T-lymphocytes. Mg^{2+} is a known inhibitor of the RyR [37] and has also been shown to inhibit cADPR-dependent Ca^{2+} release. In sea urchin homogenates 1mM was the optimal concentration for cADPR-induced Ca^{2+}-release. Inhibition of cADPR response by Mg^{2+} was specific, as up to 10mM Mg^{2+} had no effect on the Ca^{2+} release induced by IP_3. The half maximal inhibitory concentration measured in sea urchin homogenates, 2.5mM Mg^{2+} is identical to the IC_{50} value observed for RyR. This further demonstrates the similarity of the two systems. In T-cells free [Mg^{2+}] at 0 and 8.58mM completely abolished cADPR-dependent mechanism, whereas maximal Ca^{2+}-release by cADPR was observed at 1.06mM. These data further substantiate the fact that RyR is one of the central players in cADPR-induced Ca^{2+}-release.

The dependency of cADPR-induced Ca^{2+}-release on [Pi] has only been investigated in permeabilised T-cell lines [108]. At low [Pi], very low Ca^{2+} release was observed in

response to cADPR, whereas at 4-5mM [Pi], cADPR-induced Ca^{2+} release was much more pronounced. Furthermore, stimulation of T cell receptor/CD3 complex with the anti-CD3 monoclonal antibody OKT3 in intact Jurkat T cells resulted in an increase in the intracellular [Pi] but there was no corresponding increase in [Mg^{2+}]. The TCR/CD3-mediated increase of [Pi] from 2.8mM to 4.5mM, where cADPR released considerably more Ca^{2+} in permeabilised cells. Therefore, increase in [Pi] may be a switch to turn on cADPR-induced release in the intact T cell. This explains the finding that high endogenous concentrations of cADPR remain unchanged during stimulation of the TCR/CD3 [95]. The catabolism of cADPR was shown to be reduced by high [Pi], compared to low [Pi] in permeabilised T-cells. Low [Mg^{2+}] appear to have little or no enhancing effect on the catabolism cADPR. Higher concentrations of magnesium ions did not show a significant difference in the catabolism of cADPR.

C) Polyamines

Spermine and related polyamines in physiological concentrations have recently been shown to inhibit the Ca^{2+} release induce by cADPR in sea urchin egg homogenate bioassays [109] with a half-maximal inhibitory concentration range from 0.25-1mM when Ca^{2+} release was triggered by addition of 60 to 200nM cADPR respectively.. Spermine did not affect Ca^{2+} release induced by IP_3 or NAADP (see section.1.5.). and was a more potent inhibitor of cADPR -induced mechanism compared to spermidine and putrescine. Addition of caffeine and divalent cations such as Ca^{2+} and Sr^{2+} to spermine-pretreated homogenates counteracted the inhibitory effect of spermine on cADPR-induced Ca^{2+} release. In contrast to 8-amino-cADPR (a known specific antagonist of cADPR), spermine was also able to inhibit Ca^{2+} release induced by caffeine and ryanodine. This is consistent with the view that cADPR acts on the RyR indirectly by first binding to a

specific receptor, whereas the polyamines probably bind directly to the RyR [81]. Addition of up to 2mM Spermine did not produce a significant release of Ca^{2+}.

A) Polyamines have been proposed as second messengers [110]. Levels of spermine and spermidine in sea urchin eggs increase just after fertilisation and reach a maximum concentration of 1-2mM after 30min [111]. These results indicate that polyamines may be endogenous regulators of the cADPR-induced Ca^{2+} release by inhibition the RyR during sea urchin egg fertilisation.

D) Palmitoyl-CoA

Palmitoyl-CoA and certain long-chain acyl-CoA derivative metabolites (14-18 carbons in length) have been demonstrated to greatly potentiate the effect of cADPR on Ca^{2+} release in sea urchin egg homogenates [112]. The half-maximal concentration of cADPR was decreased more than fivefold by pre-treatment of the homogenate with 7μM palmitoyl-CoA, although the maximum Ca^{2+} release response to cADPR was not enhanced. At higher concentrations of ~12μM palmitoyl-CoA induced calcium release on its own. Palmitoyl-CoA induced Ca^{2+} release was suppressed by drugs that prevent activation of the ryanodine channel such as ruthenium red, spermine and calmodulin antagonist N-(6-aminohexyl)-1-napthalenesulfonamide, but was not affected by heparin. Addition of 6μM palmitoyl-CoA did not produce any significant release of Ca^{2+} by itself, but it sensitised the system to subthreshold concentrations of ryanodine, caffeine and Sr^{2+}. In contrast, similar potentiation effects were not observed for IP_3 or NAADP-controlled Ca^{2+}-release systems indicating that palmitoyl-CoA probably acts selectively by activating the ryanodine channel. cADPR was able to desensitise the sea urchin egg homogenates to subsequent Ca^{2+} release by palmitoyl-CoA and vice versa. Furthermore,

palmitoyl-CoA was found to counteract the inhibitory effect of Mg^{2+} and spermine, which in physiological concentrations suppress cADPR-induced mechanisms. A possible detergent effect of palmitoyl-CoA was ruled out because the concentrations used were below that required for micell formation or detergent action.

Palmitoyl-CoA is a pivotal component of intermediary metabolism. Interestingly, palmitoyl-CoA is present in concentrations between 6.61-15mM in unfertilised sea urchin eggs and the level decreased after fertilisation [113], clearly in a concentration range in which it may have a direct effect on the Ca^{2+} release and modulate effect of other agents. These observations provide evidences that palmitoyl-CoA and related long-chain acyl-CoA derivatives such as myristoyl- and stearoyl-CoA, in sea urchin eggs and probably in numerous other somatic cells, may serve as important modulators of the sensitivity of cADPR-regulated Ca^{2+} release and in higher concentrations may serve as a signal for triggering Ca^{2+}-release by itself. Whether cytoplasmic concentrations of palmitoyl-CoA serves as endogenous modulators of the cADPR system *in vivo* remains to be determined.

1.4.8 *cADPR-Induced Ca^{2+}- release in Mammalian cells*

The finding that enzymes involved in the metabolism of cADPR (ADP-ribosyl cyclase and cADPR hydrolase (Section1.4.3) are common enzymes in mammalian systems and the demonstration that cADPR was present in a wide range of mammalian tissue extracts suggests that cADPR may be a general Ca^{2+}-mobilising agent in mammalian cells [114]. Furthermore, the demonstration that cADPR exerts its effect through a RyR-like calcium release channel, indicated that the most likely cells in which cADPR would be effective were those displaying ryanodine-sensitive Ca^{2+} release. The widespread occurrence of

RyR receptors offered a number of cellular systems for testing cADPR action. Several studies have demonstrated cADPR-induced Ca^{2+} release in mammalian systems. cADPR is membrane impermeable because of its highly charged nature, hence the majority of these studies have been performed on microsomes derived from these cells or in permeabilised cell suspensions.

A) Cardiac muscle

High densities of RyRs in muscle cells made cardiac muscle an obvious choice in which to investigate the effects of cADPR in mammalian tissues [40]. The first direct evidence that cADPR-induced mechanism was present in cardiac muscles but not in skeletal muscle sarcoplasmic reticulum was demonstrated by Mezaros and co-workers [94]. This effect was Ca^{2+}-dependent and was abolished by ryanodine. At submicromolar extravesicular [Ca^{2+}], it increased the rate of $^{45}Ca^{2+}$ efflux, but at free Ca^{2+} above 10^{-7}M, the stimulatory effect of cADPR was diminished. Compelling data that cADPR is an endogenous activator of the type 2 RyR came from reconstitution studies, where cADPR increased the open probability of single RyR2s after cardiac SR vesicles are fused into lipid bilayers, but has little effect on RyR1 incorporated by the fusion of skeletal SR vesicles. Although cADPR appears to be capable of regulating calcium release from cardiac SR in intact cardiac myocytes [115], another study of RyR2 properties in lipid bilayers suggests that the effects of cADPR are nonspecific and unphysiological as they are not apparent in the presence of physiological levels of ATP [116]. A further study suggested that cADPR has no effect at all on muscle RyRs [103]. These apparent contradictory data might suggest that other factors such as calmodulin (section 1.4.6) are involved in conferring cADPR sensitivity upon SR release channels in intact cells.

B) Pancreatic cells

cADPR but not IP_3 has been reported to stimulate Ca^{2+} release in a cell-free system of islet microsomes and to stimulate insulin release in digitonin-permeabilised islets of Langerhans [87]. This is supported by the fact that glucose is effective in inducing insulin secretion in the absence of any change in inositol lipid turnover and that responses to cADPR or IP_3 vary according to tissue or cell types. cADPR showed a Ca^{2+} release in a dose dependent manner with a threshold of 90nM and a maximal release at 500nM. The release mechanism desensitised in response to repeated additions to cADPR, showed cross-desensitisation with ryanodine at 100μM and was not affected by heparin. cADPR and Ca^{2+} both induced insulin secretion in permeabilised islets. The combined addition did not induce significantly more insulin secretion than addition of cADPR or Ca^{2+} alone. The mechanism by which cADPR stimulates production of glucose is not known.

C) Pituitary cells

cADPR has been shown to release Ca^{2+} in a dose-dependent manner from permeabilised GH_4C_1 cells at nanomolar concentrations [86]. The mechanism of cADPR release in these cells is independent of the IP_3R since it persistes after IP_3 sensitive stores are depleted and it is insensitive to heparin. In support of this, GH4C1 cells appear to contain ADP-ribosyl cyclase since incubation of β-NAD^+ with an extract from pituitary cells for 15min resulted in the formation of a Ca^{2+}-mobilising activity that cross-desensitises with authentic cADPR.

D) Dorsal root ganglion cells

The presence of a robust caffeine sensitive Ca^{2+}-release mechanism in dorsal root ganglion cells made this cell a perfect mammalian cell in which to test the generality of cADPR as a Ca^{2+}-mobilising agent from caffeine- and ryanodine sensitive stores.

Caffeine treatment of rat dorsal ganglion cells under whole-cell voltage clamp yields a stereotypic response of activating a series of oscillations of cationic currents across the plasma membrane [117]. These currents are sensitive to increases in intracellular free Ca^{2+} concentrations and can be considered a physiological index of the intracellular free Ca^{2+} levels. These oscillatory currents are believed to reflect pulsatile Ca^{2+} release from intracellular stores as they are abolished by intracellular application of EGTA and persist in the absence of extracellular Ca^{2+}. Intracellular applications of cADPR as low as 10nM generated the Ca^{2+}-dependent oscillatory currents. Ca^{2+} release was from the same pool as with caffeine since the effects of cADPR were abolished in cells where caffeine-sensitive pools were emptied by prior treatment of cells with caffeine in Ca^{2+}-free media. The Ca^{2+}-dependent current induced by cADPR was restored on reintroduction of Ca^{2+} into the extracellular solution. Effect of cADPR was enhanced by increasing the intracellular free calcium concentration, consistent with cADPR modulating a CICR mechanism on a caffeine-sensitive calcium pool. Interestingly, in these cells, the responses to caffeine and cADPR were not abolished by ruthenium red (a known inhibitor of caffeine and cADPR-induced Ca^{2+} release in sea urchin eggs and other cells [95]) at 50μM.

E) Brain microsomes

Brain microsomes were a good candidate for investigating cADPR-induced mechanisms as nanomolar levels were found in rat brain tissue. Brain tissue appear to have the highest activities of ADP-ribosyl cyclase and cADPR hydrolase activities in the mammalian tissues examined to date [59]. Cerebellar microsomes have both IP_3 and cADPR-sensitive Ca^{2+}-release mechanisms. There are several reports documenting cADPR-induced Ca^{2+} release from brain microsomes [64,90,94]. Maximum Ca^{2+} release occured at ~400nm cADPR, whereas maximal release by IP_3 was at 1μM, although IP_3 released nearly twice as much Ca^{2+}

F) T- cells

The discovery of caffeine-sensitive Ca^{2+} pools in Jurkat T-lymphocytes suggested that cADPR mechanism may be a physiological modulator of the caffeine and ryanodine sensitive Ca^{2+} stores [118],. Indeed, cADPR has been shown to release Ca^{2+} from intracellular stores of permeabilised Jurkat and HPB.ALL T-cells in a dose-dependent manner. Half maximal release was obtained at 2.25μM [95] This release was insensitive to heparin, but was inhibited by ruthenium red and other known selective inhibitor of cADPR-induced Ca^{2+}-release such as 8-NH_2-cADPR and 8-Br-cADPR. Ryanodine prevented cADPR-induced Ca^{2+} release in Jurkat T-cells. cADPR has been shown to increase the binding affinity of [^{3}H]ryanodine to its receptor at lease 5-fold (K_d ~4-nM) in Mouse T-lymphoma cells [119]. Furthermore cADPR was detected endogenously in Jurkat and HPB.ALL T-cells and cGMP-induced Ca^{2+} release in these cells were inhibited by ruthenium red indicating that cGMP may be involved in the synthesis of cADPR [95].

1.4.9 *Physiological Roles for cADPR*

A) Fertilisation

Much of the current knowledge about the mechanism of action of cADPR, metabolism and role is derived from studies in sea urchin eggs as discussed in section 1.4.5. Microinjection of cADPR into intact eggs can induce a large Ca^{2+} transient, trigger the cortical reaction, and parthenogenically activate the eggs to undergo multiple cycles of nuclear envelope breakdown and DNA synthesis [84]. This effect is independent of external calcium [73]. The first of the multiple Ca^{2+} transients that occur during fertilisation reactions in the sea urchin eggs is triggered by surface interactions between the fertilising sperm and the egg and then sweeps across the egg as a propagating wave. Two studies demonstrate a redundancy in the mechanism of Ca^{2+} mobilisation at fertilisation [34,42]. It was shown that ryanodine receptors and IP_3 receptors both needed to be blocked by the pharmacological inhibitors ruthenium red and heparin before the wave was abolished. The first direct demonstration that the cADPR pathway is involved in fertilisation comes from the use of a novel specific antagonist of the cADPR-binding site, 8-amino-cADPR [120]. Co-injection of heparin and 8-amino-cADPR was required to block the fertilisation response. Inhibition of either was not sufficient to block response. Collectively, these studies provide direct evidence that the cADPR signalling pathway is activated at fertilisation in the sea urchin egg. Whether cADPR plays a permissive role, where it acts as a coagonist for Ca^{2+} mobilisation, or a true second messenger role, where its levels rise on fertilisation, remains to be determined.

B) Insulin secretion

The finding that drugs that inhibit glucose-induced insulin secretion also impair the ability of glucose to stimulate the production of a cADPR-like activity in islets suggests a key

role for cADPR signalling pathway in stimulus-secretion coupling in the pancreatic β-cells [87] (see section 1.4.7B). Pancreatic islet cells have recently been shown to express BST-1, a CD38-like surface molecule having both ADP-ribosyl cyclase and cADPR hydrolase acitivities. This suggests the involvement of multiple enzymes in the regulation of cADPR concentrations in pancreatic islet cells [121]. How glucose stimulates cADPR synthesis remains to be resolved. One possibility is that cGMP might be a coupling factor. cGMP has been proposed as a mediator of insulin secretion from rat islets since glucose causes an increase in cGMP levels in islets and since agents that elevate cGMP in islets such as ascorbic acid and sodium nitroprusside, enhance insulin secretion. Further, LY83583, an inhibitor of guanylyl cyclase, abolishes glucose-induced insulin secretion [122]. Nitric oxide an activator of soluble guanylyl cyclase, can also enhance insulin secretion from pancreatic β cells as well as increase islet cGMP levels [123]. Whether cGMP/nitric oxide-enhanced insulin secretion is mediated by increasing cADPR synthesis needs to be investigated.

C) Smooth muscle

Previous studies has shown that agonist-induced Ca^{2+} mobilisation in longitudinal muscle cells is mediated by Ca^{2+} influx, which triggers Ca^{2+} release from IP_3-insensitive, ryanodine-sensitive Ca^{2+} stores [124]. In contrast, Ca^{2+} mobilisation in adjacent intestinal circular muscle cells is mediated by IP_3-dependent Ca^{2+} release.

The study by Kuwemerle and co-workers suggests a functional role of cADPR as a Ca^{2+}-mobilising messenger in intestinal longtidunal muscle cells. Authentic cADPR was shown to bind with high-affinity to permeabilised longitudinal muscle cells (IC_{50} 1.9nM), release Ca^{2+} from nonmitochondrial Ca^{2+} stores (EC_{50} 3.8nM), increase cytosolic

Ca^{2+}(EC_{50} 2.0nM), and induce contraction in a concentration-dependent fashion. The pharmacology of cADPR- and ryanodine-induced $^{45}Ca^{2+}$ fluxes appear to be similar: they were blocked by ruthenium red and dantrolene and augmented by caffeine, but not affected by heparin. cADPR release was also blocked by the competitive inhibitor 8-amino cADPR. In contrast, cADPR did not bind to permeabilised circular muscle cells or induce Ca^{2+} release and contraction. cADPR binding and cADPR-induced Ca^{2+} release were dependent on the concentration of Ca^{2+}. cADPR was capable of stimulating Ca^{2+} release at subthreshold concentration of Ca^{2+} (25-100nM). Furthermore, longitudinal muscle extracts incubated with β-NAD^+ produced a time-dependent increase in Ca^{2+} mobilising activity. This activity was increased by pre-treating extracts with CCK-8 in a concentration-dependent manner. The Ca^{2+} mobilising agent was identified as cADPR by blockade of response with 8-amino-cADPR and ruthenium red. The increase induced by CCK-8 was suppressed by the CCK-A antagonist, L364,718, nifedipine, and guanosine-5′-thiophosphate.

These studies provide evidence that cADPR could act as an agonist-stimulated Ca^{2+}-mobilising messenger in intestinal longitudinal muscle cells on a par with IP_3 in intestinal circular muscle cells [125]. The Ca^{2+} requirement suggests that cADPR acts to modulate Ca^{2+}-induced Ca^{2+} release rather than initiate Ca^{2+} release.

1.5 *Nicotinic acid adenine dinucleotide phosphate (NAADP)*

Alkaline treatment of NADP generated a derivative which mobilised Ca^{2+} from sea urchin egg homogenates [44]. The active derivative was recently purified and shown by HPLC to be chromatographically distinct from NADP and NADPH. Structural analysis by NMR and MS identified this metabolite as NAADP (see Fig 1.10). The release from

NAADP showed half-maximal effective concentration of 30nM and was specific as NADP and nicotinic acid adenine dinucleotide were ineffective even at 10-40 fold higher concentrations. NAADP-induced Ca^{2+} release was desensitised to further addition of NAADP. The conversion of NADP to NAADP involves deamidation of the amide group. The possibility that this reaction can be catalysed by a cellular enzyme was investigated by Aarhus and co-workers [126]. ADP-ribosyl cyclase and CD38 were tested as candidates. It was discovered that both these enzymes catalyse the conversion of NADP to NAADP. The conversion required an acidic pH and the presence of nicotinamide indicating a base-exchange reaction. At neutral pH, the cyclase converts NADP to cyclic ADP-ribose 2′-phosphate which does not mobilise Ca^{2+} in sea urchin eggs, although has been shown to mobilise Ca^{2+} in other systems such as rat brain microsomes [127] and Jurkat T-cells. In contrast, CD38 converts NADP to ADP-ribose 2′-phosphate. In view of the above ADP-ribosyl cyclase and CD38 appear to be crucial enzymes in Ca^{2+} signalling.

NAADP Ca^{2+} stores are distinct from those of IP_3 and cADPR as identified by Percoll densitiy fractionation. There is no cross-desensitisation between NAADP- and IP_3/cADPR-induced Ca^{2+} mechanisms. Furthermore, NAADP-induced mechanism is not affected by known agonsits of IP_3 and cADPR. The microsomal Ca^{2+}-re-uptake inhibitor, thapsigargin, while funcitonally removing IP_3 and cADPR-sensitive pools, leaves the NAADP-sensitive Ca^{2+} pool intact. However, the non-additive release of NAADP-induced release and that by IP_3 and cADPR suggests either direct or indirect communication between the different Ca^{2+} pools [83,128]

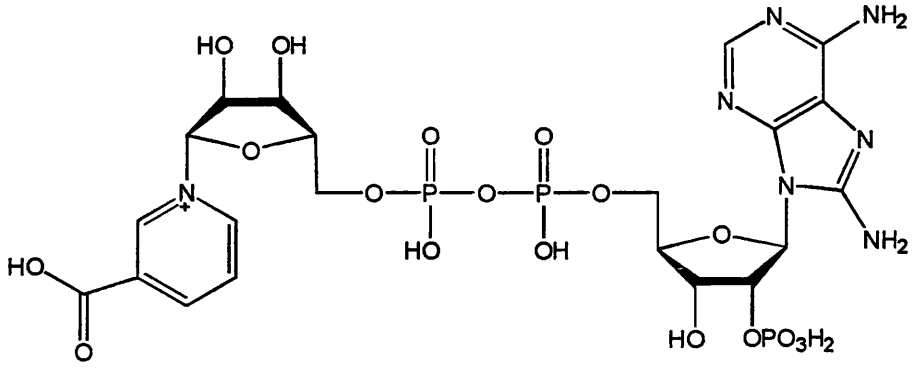

Figure 1.10: Structure of NAADP

1.6 Adenophostins.

Adenophostins A and B (Fig 1.11) are potent IP_3 receptor agonists which bind to the IP_3 receptor and induce Ca^{2+} release from IP_3-sensitive Ca^{2+} stores. They were discovered during the search for activities inhibiting the binding of $[^3H]$-$InsP_3$ to rat cerebellar membranes. Adenophostins A and B were isolated from the cultured broth of *Penicillum brevicompactum* SANK1191 and SANK12177 [18,19]. The compounds have been fully characterised using various techniques such as UV and NMR spectroscopy, chemical and enzymatic degradation together with elemental analysis and high resolution mass spectroscopy. They are adenosine-2′-phosphates with glucose unit at C3′ position of the adenosine. The glucose unit possesses phosphate groups at positions C3″ and C4″. Adenophostins have been shown to be 100 fold more potent than IP_3.

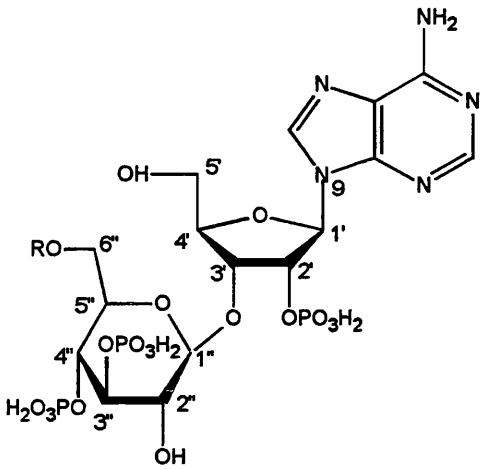

Figure 1.11 Structure of Adenophostins

1.7 *Aims of the Project*

Structural analogues of biologically active compounds have in many instances proven to be useful reagents or probes of studying biological processes. Synthetic analogues of cADPR are needed to probe structure activity relationships (SAR). Hence, our first aim was to test whether a chemo-enzymatic route which was designed could be generally applicable for synthesis of structural analogues of cADPR. This method involves the chemical synthesis of NAD^+ analogues followed by enzymatic cylisation into the corresponding cADPR analogue by ADP-ribosyl cyclase provided that the enzyme is sufficiently non-discriminatory. The loose substrate specificity of the *Aplysia* cyclase has been demonstrated in this work.

The second aim was to design, prepare and characterise structurally modified analogues of cADPR. The structure of cADPR provides a wealth of opportunity to design structurally modified compounds. Three types of modifications can be envisaged: (a)

modification to one or both ribose moieties (b) modification to the purine ring and (c) modification to the pyrophosphate linkage. This work has focused on the synthesis, characterisation and use of AMP analogues as tools for introducing modification to the purine ring and the adenine ribose moiety of NAD^+ (chapters 2&3) and as a result produce structural analogues of cADPR (chapter 4). The analogues synthesised will be used as tools in defining the key recognition elements of cADPR which contributes to its potent activity and ultimately used to design potent antagonists (chapter 5).

The role of the ribose hydroxyl groups on the Ca^{2+} releasing potential of cADPR were to be investigated by synthesis of hydroxyl deleted analogues of cADPR and also by substituting other functional groups in place of the ribose hydroxyl groups (chapters 4 & 5). Substitution of the hydrogen atom at the 8-position of the purine ring with amino or bromo group converted the molecule from an agonist to an antagonist when tested in the sea urchin egg system, hence we have looked at the effects of these analogues on cADPR induced mechanism in Jurkat T-cells. Several other 8-substituted analogues were prepared and characterised for use in studying the important feature that are responsible for transforming the activity of the 8-substituted molecule from an agonist to an antagonist. The structural analogues synthesised were tested in the non-mammalian sea urchin egg system and in the mammalian Jurkat T-cells in order to identify any differences in the structural requirements for the cADPR-sensitive Ca^{2+} release mechanism in these systems.

CHAPTER 2: SYNTHESIS OF ADENINE NUCLEOSIDES AND NUCLEOTIDES

Adenosine and adenosine 5′-monophosphate play a pivotal role in the synthesis of modified nucleosides and nucleotides of biological and biochemical importance [132-134]. The term nucleoside applies to carbohydrate derivatives of N-heterocyclic compounds whether the attachment is through nitrogen, carbon. A vast number of nucleosides have been isolated from natural sources and they exhibit a wide range of biological activities. Adenosine (**1**) consists of a purine base and a ribose moiety (Fig.2.1). Nucleotides are phosphate esters of nucleosides. In the simplest form, as in adenosine 5′-monophosphate, the hydroxyl groups of the pentose is esterified by a single phosphate monoester. Nucleoside 5′-monophosphates are quite stable in alkali in which they exist as the dianion [134], but are hydrolysed in acidic and neutral solution. The nucleotide monophosphate loses one proton at pH 1 and a second proton at around pH 7. Adenosine undergoes many reactions of its constituent base and sugar [135-137], however there are some reactions which are of particular importance in nucleoside chemistry. Several analogues of AMP have been synthesised as precursors in the preparation of cADPR analogues of interesting biological properties.

Chemistry of Nucleosides

2.1.1 *Acylation and Alkylation*

Nucleosides undergo esterification and etherification reactions. They can be fully acylated on the sugar hydroxyl groups, or on any amino group(s) of the heterocyclic ring by treatment with an acylating agent. These reactions are useful for introducing

protecting groups on the ribose hydroxyl groups and amino group(s). The chosen protecting group should be stable during synthesis and easily removed afterwards. Added protecting groups not only guarding against side reactions during synthesis, but also increases the lipophilicity of fully and partially protected nucleotides. Trialkylsilyl ethers are very useful when base-stable hydroxyl blocking groups are required. Base labile acyl groups such as acetyl (Ac) and benzoyl (B_2) groups are often used for 2′ and 3′-hydroxyl group protection. Acyl groups can be removed by ammonolysis at the end of the synthesis.

Alkylation of nucleosides with diazomethane or with alkyl-halides in the presence of alkali or silver oxide results in the alkylation of the ribose hydroxyl groups and alkylation of the heterocyclic moiety. For example, phenyldiazomethane has been used in the preparation of 2′ and 3′-O-benzyl derivatives of adenosine, inosine and guanosine in the presence of stannous chloride as catalyst [138].

2.1.2 *Reactions of the Heterocyclic Base Moiety of Adenosine*

A number of reactions of the nitrogen heterocyclic ring portion of adenosine may be carried out. Electrophilic substitution at carbon and nitrogen, nucleophilic subtitution of the amine group by nitrous acid (converts adenosine to inosine) [139] and other nucleophilic substitution reactions which require fuctionalisation of the purine, if no readily displaceable groups are present followed by nucleophilic displacement by other nucleophiles containing the desired substituent.

Studies on electrophilic substitution at the carbon of purines have been measured by deuterium incorporation, which occurs readily at the position 8 of nucleosides and

nucleotides of guanine and adenine [140]. Several experiments have suggested that electrophilic substitution involves initial protonation at N-7, followed by proton abstraction from C-8 by hydroxide (or deuteroxide).

2.2 8-Bromoadenosine and its Nucleotide

Introduction of a bromo group into the 8-position of the heterocyclic ring of various purine nucleosides and nucleotides has provided intermediates that are invaluable for the preparation of many 8-substituted derivatives. This is due to the ease at which the bromo group can be displaced with a suitable nucleophile. Initial attempts at the synthesis of 8-bromoadenosine (**3**) were made by treating 2′,3′,5′-tri-*O*-acetyl adenosine with bromine in sodium acetate-glacial acetic acid giving the product in 59% yield [141]. This method was not suitable for more labile deoxynucleosides, as acidic conditions were required. This prompted a study of the use of neutral apolar conditions. 2′3′5′-Tri-*O*-acetyl adenosine was treated with *N*-bromoacetamide in chloroform to produce the 8-bromo-derivative [141]. The acetyl groups were removed upon treatment with methanolic ammonia to give the 8-substituted purine nucleoside. Treatment of adenosine with *N*-bromosuccinimide in DMF as solvent also produced 8-bromoadenosine in reasonable yield [142]. Bromination of purine nucleosides in aqueous solution has been adopted as standard practice. Appropriate use of buffers can minimise the possibility of glycosidic cleavage [143,144].

Bromination of adenosine and AMP (Fig 2.1) was achieved by use of bromine in aqueous acetate buffer. The reaction proceeded well at room temperature and excess bromine can be removed by extraction into chloroform or by addition of sodium bisulphite. Introduction of bromine into position 8 of adenosine and AMP caused a slight shift in the

absorption maximum in the UV spectrum from 259 to 264nm. The bulky bromine atom restricts rotation about the glycosidic bond. X-ray diffaction studies by Tavale and

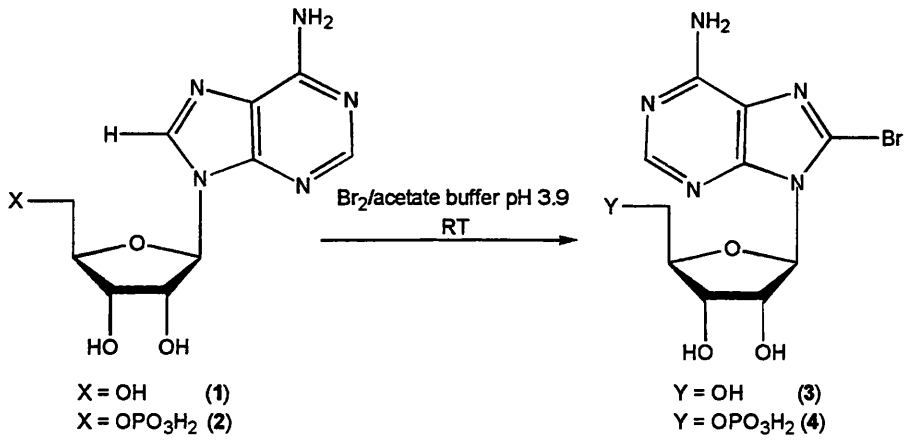

X = OH (1)
X = OPO_3H_2 (2)

Y = OH (3)
Y = OPO_3H_2 (4)

Figure 2.1 Bromination of adenosine and AMP

Sobell indicated the *syn*-conformation for 8-bromoadenosine compared to *anti* in adenosine in their crystal structures [145]. This also appears to be the preferred conformation of 8-bromopurine nucleotides in solution and thus confers interesting biological properties on the purine nucleotide analogues. ^{1}H-NMR spectrum of 8-bromo-AMP (Fig 2.2) showed all the protons of the nucleotide. The important feature of which the H2′ resonates at higher frequency (δ 5.1) compared to the H2′ (δ ~ 4.6) proton in AMP.

2.2.1 *8-Methyladenosine* (5)

8-Substituted adenosines have been used as probes of the influence of substitution on conformation around the glycosyl bonds, since 8-substituents tend to force the usual *anti* form of adenosine to adopt the *syn*-conformation as a result of steric effects [146]. Alkyl

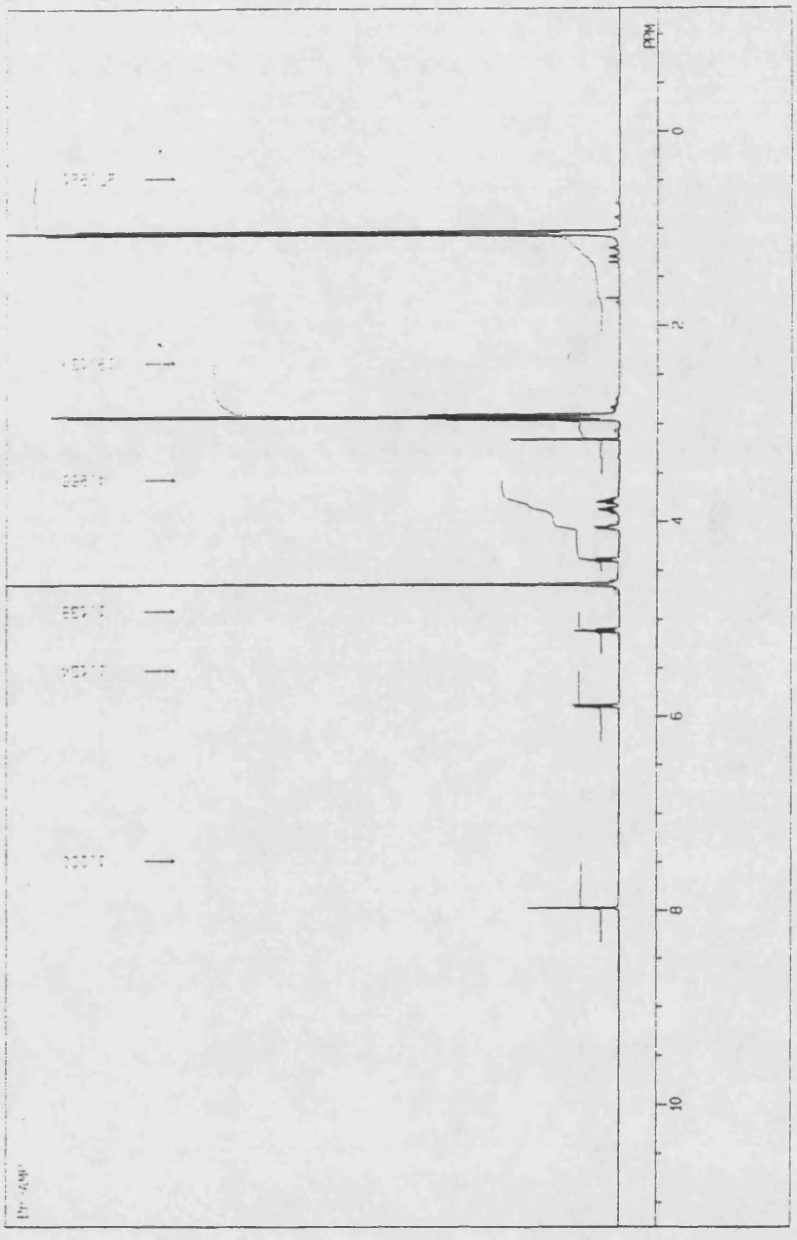

Figure 2.2: ^{1}H-NMR (400MHz, D_2O) spectrum of 8-bromo-adenosine 5′-monophosphate as its triethylammonium salt.

groups have the least electronic effect on the adenine nucleus. Hence, this has generated interest for their use in the investigation of enzymes utilising adenosine derivatives such as adenosine deaminase and adenosine kinase. The synthesis of 8-methyl-adenosine (**5** - Fig 2.3) was achieved using palladium-catalysed cross coupling reaction with trimethyl aluminium [147].

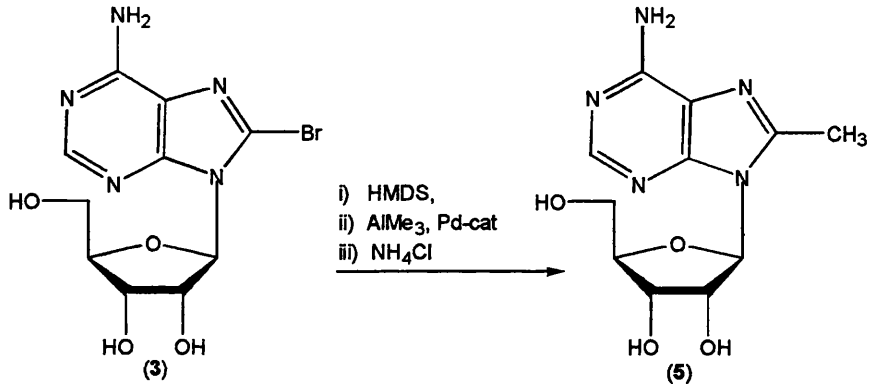

Figure 2.3: Synthesis of 8-Methyladenosine (5) from 8-Bromoadenosine (3)

8-Bromoadenosine smoothly cross-coupled with trimethyl aluminium in the presence of palladium catalyst to yield 8-methyladenosine. It was necessary to protect the ribose hydroxyl groups and the amino group on the purine ring to prevent side reactions. This was achieved by silylation using hexamethydisilazane in the presence of a catalytic amount of ammonium sulphate. The lipophilicity of the starting material was also improved by the protecting groups as shown by TLC in dichloromethane:methanol (9:1) in which protected 8-bromoadenosine had an R_f of 0.57 compared to 0.36 for the unprotected derivative. Protection was carried out *in situ* as it was not necessary to isolate protected product. The cross-coupling reaction was performed with extreme care

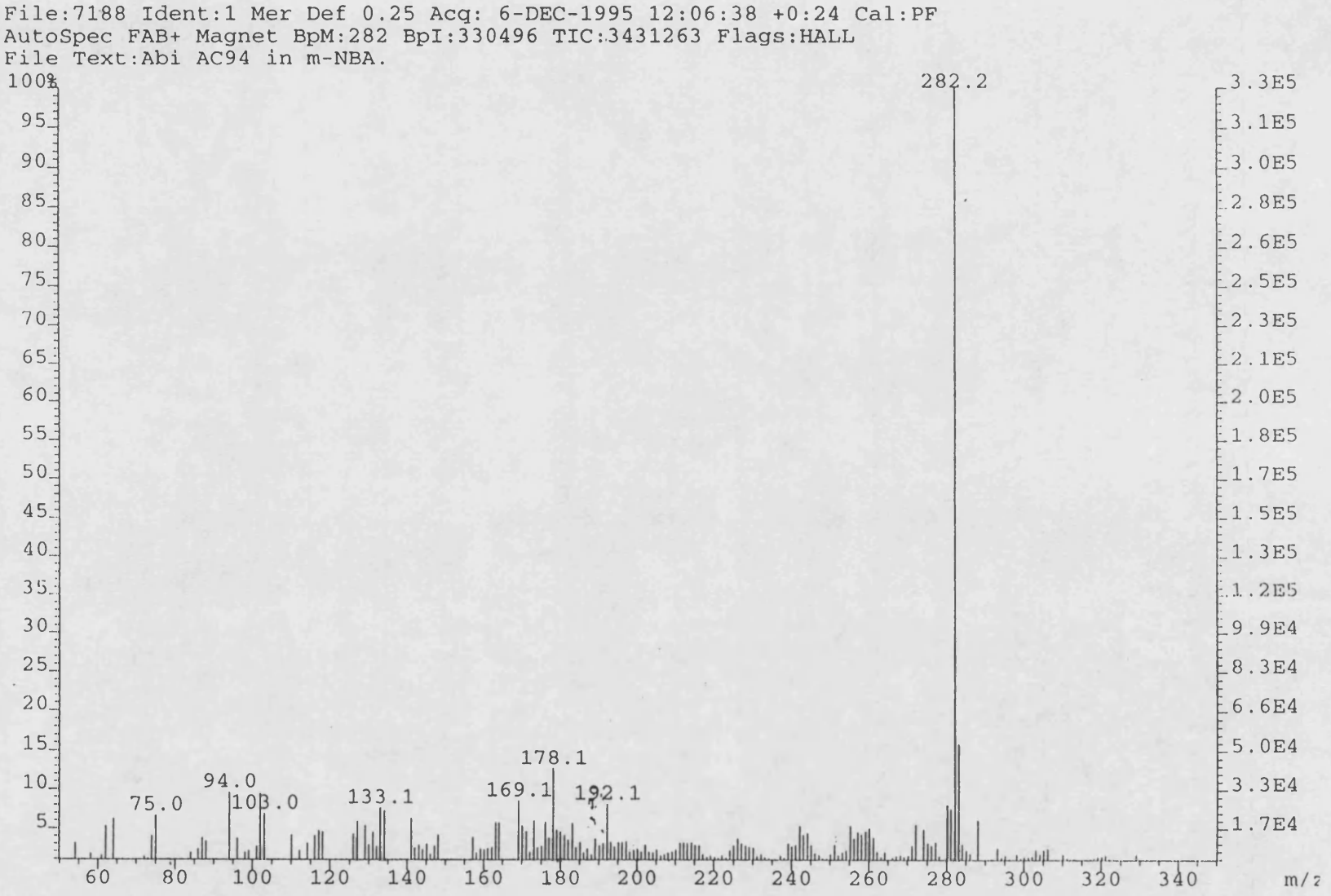

Figure 2.4: +ve Ion FAB mass spectrum of 8-methyladenosine (5)

under anhydrous conditions as trimethylaluminium is very reactive to small traces of water. De-protection of 8-methyladenosine was carried out under acidic condition by refluxing in methanol with a small amount of ammonium chloride. The crude product was purified by silica gel column chromatography to obtain pure 8-methyladenosine. The ^{1}H-NMR chemical shifts exhibited by the pure product was as reported previously[147]. It showed the absence of trimethyl esters indicating that the product was fully deprotected. A new peak at δ 2.46 equivalent to 3 protons confirmed that a CH_3 group had been added. FAB-MS showed a +ve *m/z* peak at [282 $(M + H)^+$ - Fig 2.4] and –ve ion peak at 434 $(M + NBA)^-$. The accurate mass was calculated as 282.120743 for $(M + H)^+$ and confirmed by +ve ion FAB-MS. These spectrosopic data confirmed the authenticity of the 8-methyladenosine synthesised.

2.2.2 *8-Methylaminoadenosine 5′-monophosphate* (6)

Nucleophilic displacement of the bromine atom of 8-bromoadenosine with methylamine[148] was carried out in an excess of methylamine solution in methanol under reflux to obtain 8-NHMe-AMP (**6** - Fig 2.5). A shift in the UV absorption maximum from 264nm to 278nm accompanied the displacement reaction. The crude sample was purified by ion-exchange chromatography to obtain the pure product in 65% yield. 8-Methylamino-AMP (**6**) is known to exist in the *anti* conformation as with 8-amino-AMP and AMP[148]. The H2′ chemical shift in AMP, 8-NH_2-AMP (**9**) and 8-NHMe-AMP is similar. A value of δ 4.6 was measured here with $J_{H(1')-H(2')}$ 8.0 Hz and $J_{H(2')-H(3')}$ measured as 5.8 Hz. These values are similar to those reported previously[148]. The H(2′) proton is sensitive to deshielding effects originating from the adenine ring depending on the glycosyl torsion angle. In the *syn* conformation, as in 8-Br-AMP, H(2′) resonates at a

higher frequency, δ 5.1 compared to 4.6 in 8-NHMe-AMP, with a $J_{H(1')-H(2')}$ value of 6.1 Hz. A new peak at δ 2.8 represents the three methyl protons on methylamine. This supported the fact that a displacement reaction had taken place. ^{31}P-NMR showed a singlet at δ 3.2 indicating the presence of a monophosphate. Mass analysis by electrospray showed *m/z* of the -ve ion as 375.4 $(M-H)^-$ which agrees with the molecular mass of 376 for 8-NHMe-AMP Fig. 2.6).

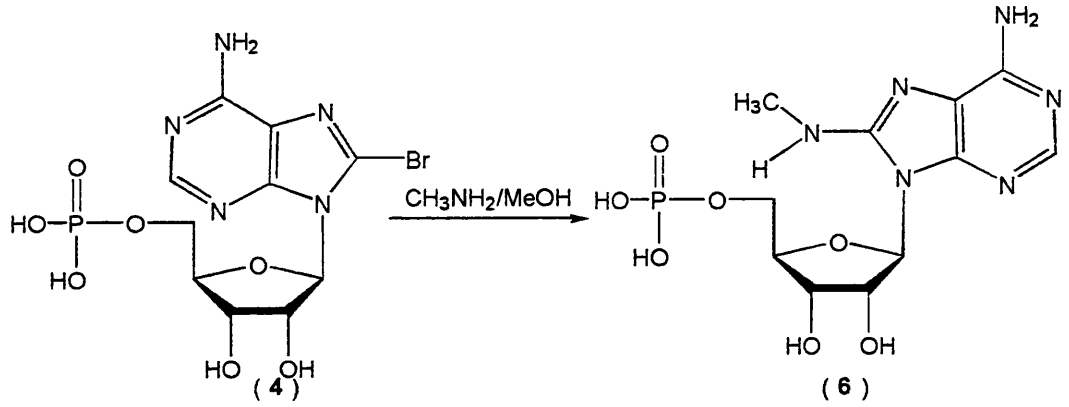

Figure 2.5: Synthesis of 8-methylaminoadenosine 5'-monophosphate (6)

2.2.3 *8-Dimethylaminoadenosine 5'-monophosphate* (7)

Nucleophilic displacement of the 8-bromo substituent of (**4**) using an excess of dimethylamine in methanol under reflux generated 8-NMe_2-AMP (**7** -Fig 2.7). A shift in UV absorption maxima from 264 to 274nm accompanied the displacement reaction. The ^{1}H-NMR spectrum was comparable to that reported previously[148]. The presence of a new peak at δ 2.8, equivalent to 6 protons, confirmed the substitution by the dimethylamino group. The H(2') chemical shift in 8-dimethylamino-AMP is similar to that of 8-Br-AMP. It has been established that 8-NMe_2 exists in the *syn* conformer as in

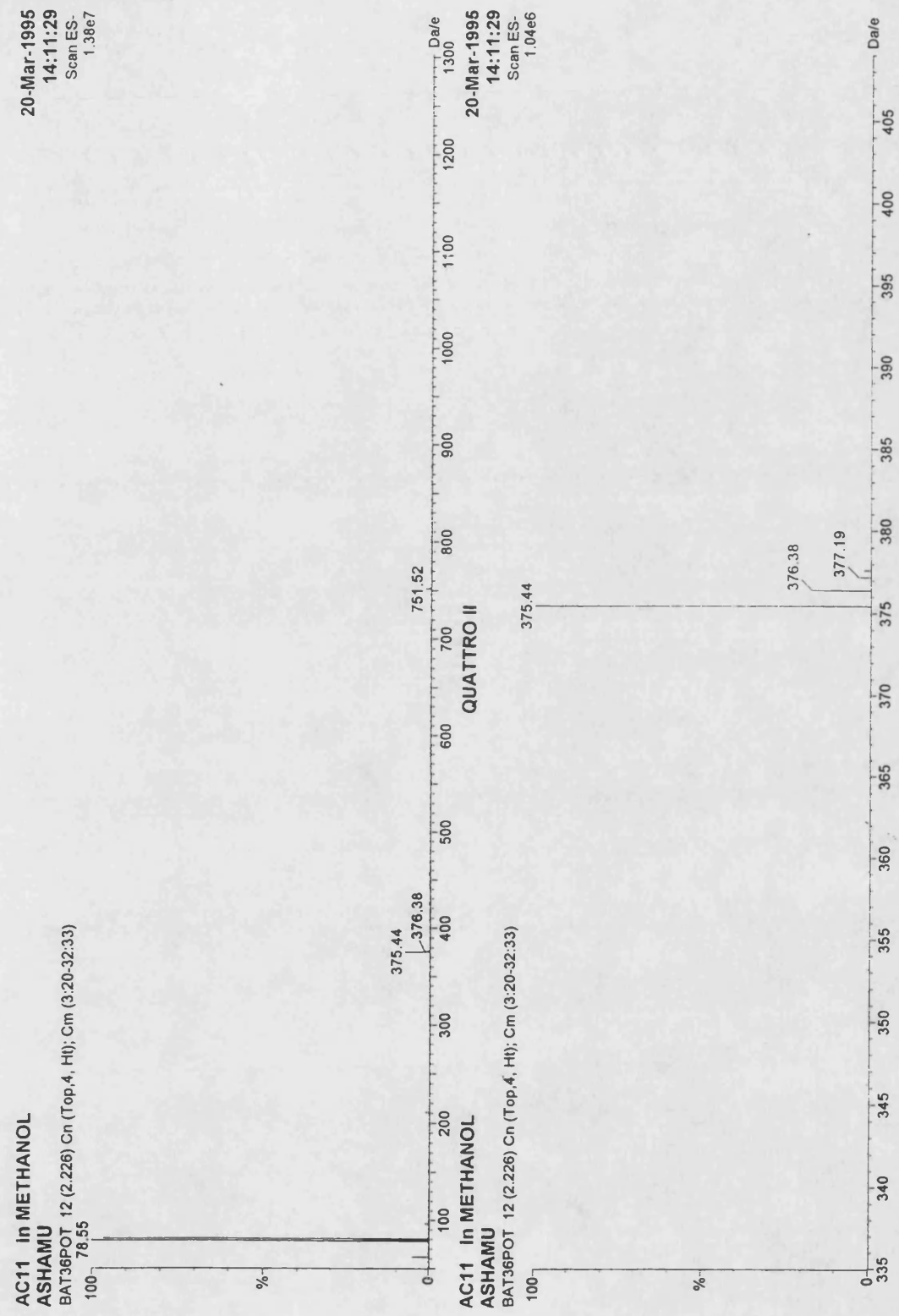

Figure 2.6: Electrospray mass spectrum of 8-methylamino-adenosine 5′-monophosphate

8-Br-AMP[148]. H2′ resonated at δ 5.1, a higher frequency compared to that for H2′ in AMP, with a $J_{(H1'-H2')}$ value of 6.7. This difference is due to the deshielding effect from the adenine ring in the *syn* conformer. ^{31}P-NMR spectrum showed a singlet at δ +2.2 indicating a monophosphate. Mass analysis was carried out using FAB-MS. *m/z* values of 391 $(M + H)^+$ and 389 $(M - H)^-$ were consistent with the molecular mass of 390 for 8-dimethylamino-AMP.

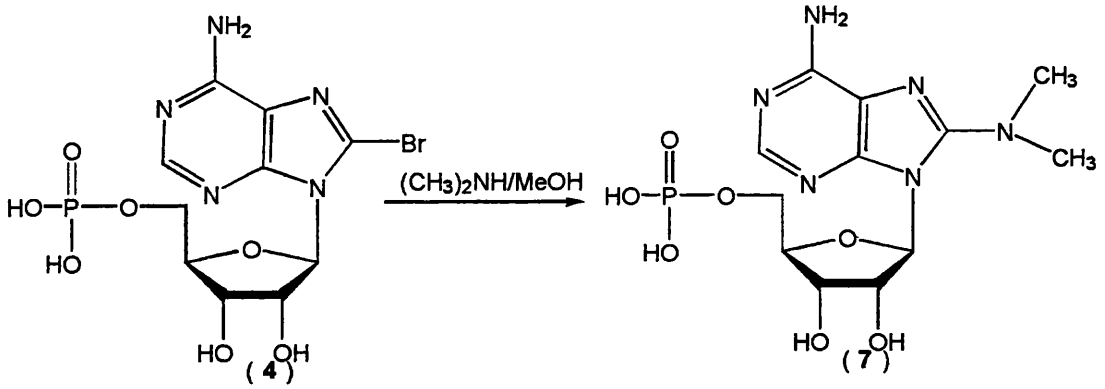

Figure 2.7: Synthesis of 8-dimethylaminoadenosine 5′-monophosphate (7)

2.2.4 *8-Aminoadenosine 5′-monophosphate* (9)

It is known that displacement of the bromo substituent of 8-Br-AMP with an amino group cannot be achieved by nucleophilic displacement with methanolic ammonia [149]. Hence 8-NH_2-AMP (**9**) was synthesised using the method used by Cartwright *et al* [150]. This was achieved by reduction of 8-azido-AMP (**8** -Fig 28) with dithiothreitol in TEAB (pH 8.3) under reduced light. A shift in the UV absorption maximum from 282 to 274nm accompanied the reaction as previously reported[150]. The crude sample was purified by ion-exchange chromatography to afford pure 8-amino-AMP in 65.3% yield. The ^{1}H NMR spectrum was as previously reported[148]. The H2′ chemical shift (δ 4.6) is

similar to that of AMP. This similarity in chemical shift suggests an *anti* conformation as with AMP. The mass spectrum was not recorded due to limitation of sample.

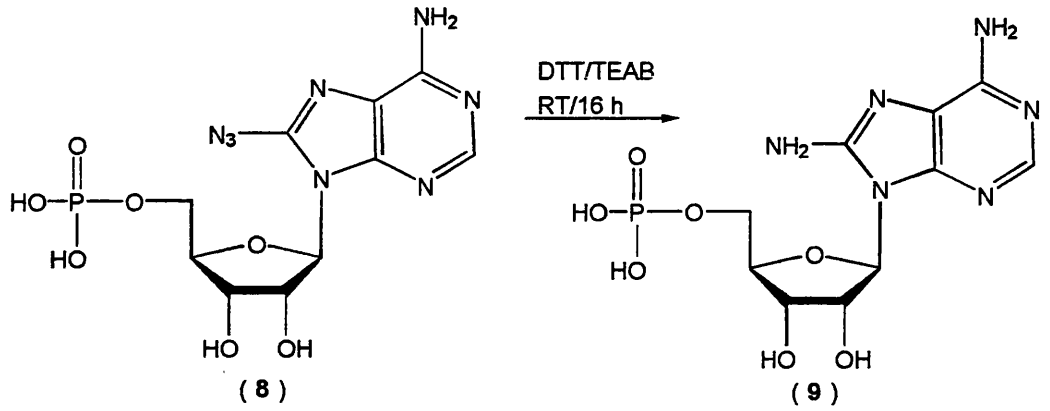

Figure 2.8: Synthesis of 8-amino-adenosine 5′-monophosphate (9)

2.2.5 *8-Piperidyladenosine 5′-monophosphate* (10)

Substitution of the bromo substituent of 8-Br-AMP with a piperidyl group was achieved by treating 8-Br-AMP with piperidine at 50°C (Fig 2.9). Nucleophilic substitution by piperidine resulted in a change in UV absorption maximum from 264 to 275nm. The ^{1}H-NMR spectrum of its product showed the presence of protons corresponding to the piperidyl protons at δ 3.2 (4 protons) and 1.6 (6 protons).. A chemical shift value of δ 5.1 was measured for H(2′), with a J(H1′-H2′) value of 6.4 Hz and these are similar to the values obtained for H2′ in 8-Br-AMP. This suggests that the nucleotide is in the *syn* conformation as in 8-Br-AMP, which may be a result of the steric bulk of the piperidyl group.. ^{31}P-NMR showed a singlet at δ +1.97 which is consistent with a monophosphate. *m/z* values measured by FAB-MS (-ve ion) of 860 $(2M)^-$ and 429$(M - H)^-$ also showed the presence of a dimeric structure as well as confirming the molecular mass of 430 for 8-piperidyl-AMP.

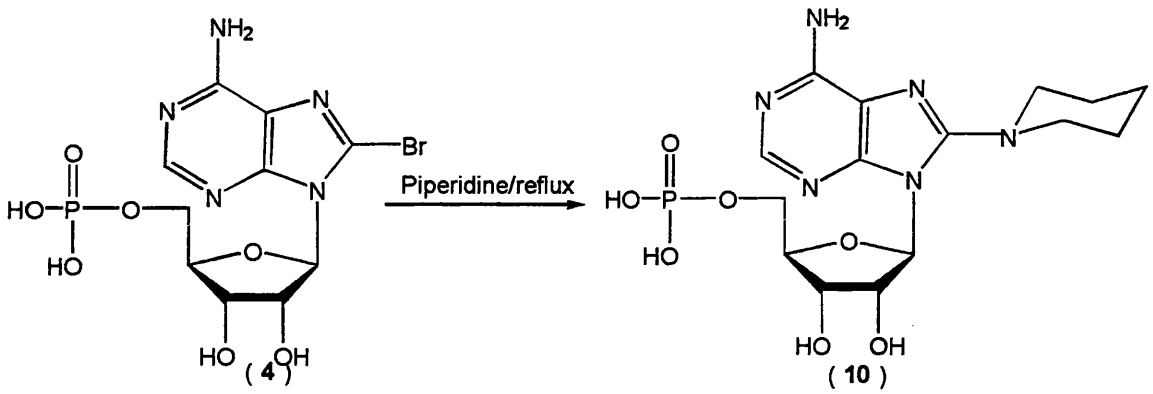

Figure 2.9: Synthesis of 8-piperidyladenosine 5′-monophosphate (10)

2.2.6 *8-Methoxyadenosine 5′-monophosphate* (11)

Nucleophilic substitution of 8-Br-AMP with methoxide anion was achieved using a similar procedure used for the synthesis of 8-methoxyadenosine 8-Br-adenosine[149] to yield 8-methoxy-AMP (**11**). 8-Br-AMP was treated with approximately 5 equivalents of sodium methoxide in methanol under reflux overnight. The UV absorption maximum changed from 264 to 260nm upon displacement of the bromo group with the methoxide group. The presence of a new singlet at δ 4.0 equivalent to 3 protons supported the presence of the methoxy protons. The protons resonated at a high frequency compared to methyl protons attached to carbon due to the deshielding effect of the oxygen atom in the methoxy group. The chemical shift measured for H2′ was δ 4.8 with $J_{(H1'-H2')}$ value of 5.5 suggest that 8-methoxy-AMP may be in the *syn* conformation. The ^{31}P-NMR spectrum showed a singlet at δ 3.7 indicating the presence of a monophosphate.

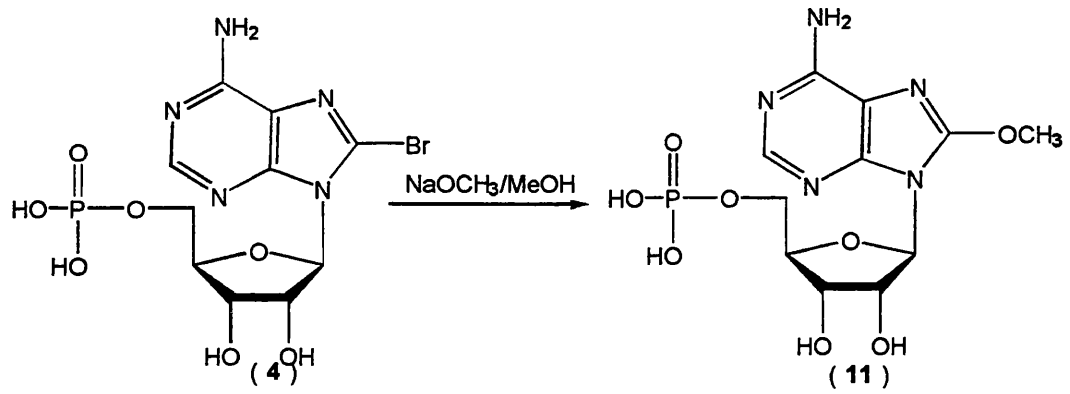

Figure 2.10: Synthesis of 8-methoxyadenosine 5′-monophosphate (11)

2.2.7 *8-Oxyadenosine 5′-monophosphate* (13)

Treatment of 8-Br-AMP with sodium acetate in acetic acid anhydride under reflux generated the 8-acetyl ester of 8-hydroxy-AMP. The ester formed at position ⁻8 of the purine ring was hydrolysed to 8-hydroxylAMP. A shift in UV absorption maximum from 264 to 270nm was observed with the formation of 8-Hydroxy-AMP. ^{1}H NMR spectroscopy identified all the ribose and H_A2 adenine protons. The proton chemical shift for H2′ at δ 4.9 with $J_{(H1'-H2')}$ of 5.5 is consistent with the predominant *syn* conformation of 8-hydroxy-AMP. 8-"hydroxy"-AMP (**12**) is known to exist predominantly in the keto tautomer in the physiological range 5 < pH <9 (**13** -Fig 2.10) [149,151], hence there is a proton on N-7. The phosphorus peak for the monophosphate was observed at δ –0.4 in the ^{31}P-NMR.

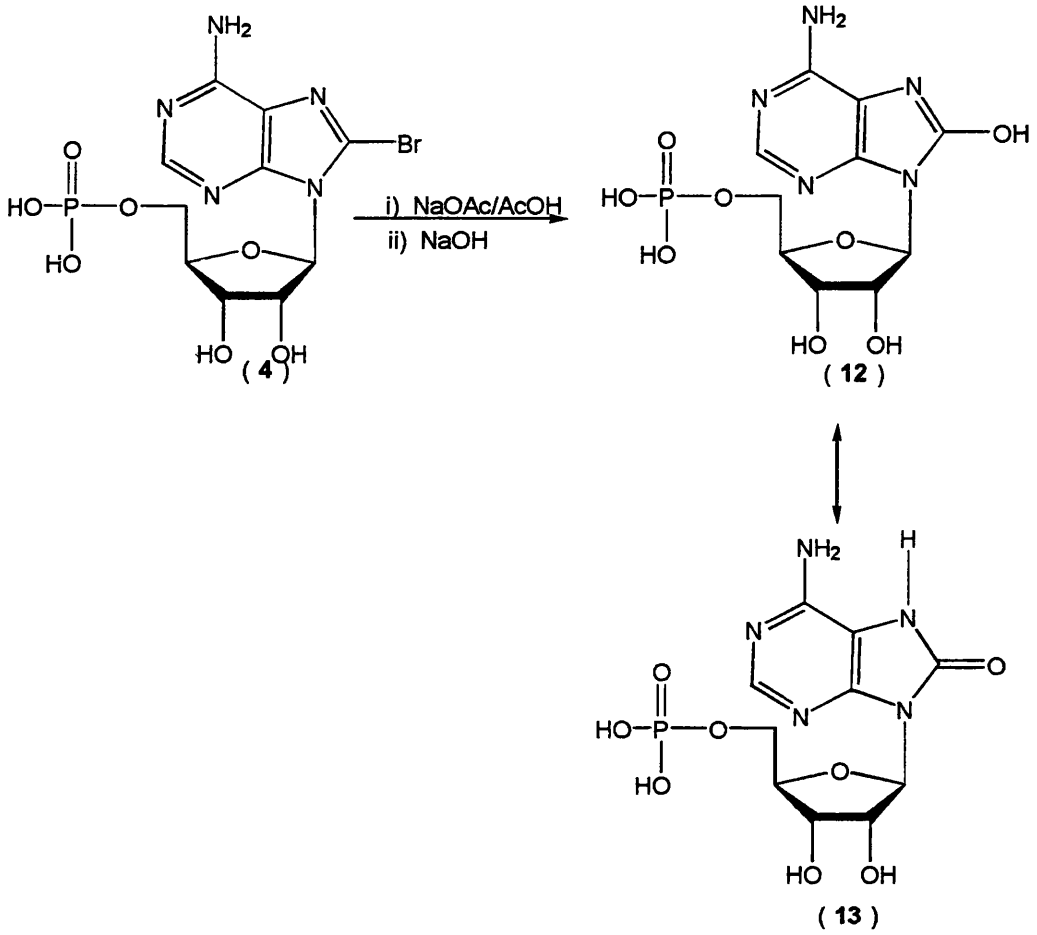

Fig 2.11: Synthesis of 8-oxy-adenosine 5′-monophosphate (13)

2.3 Phosphorylation of Adenosine Analogues

Nucleotides are phosphate esters of the nucleoside. They are commonly prepared by phosphorylation of the nucleoside. Phosphorylation of adenosine to its 5′-monophosphate ester involves use of a phosphorylating agent. It usually involves nucleophilic attack of oxygen on an activated phosphorus atom. Hence a phosphorus atom and three oxygens are transferred to the hydroxyl group of the nucleoside. As phosphoric acid is tribasic, measures have been taken to protect one or more of the phosphoryl hydroxyl groups to achieve selective phosphorylation. Khorana showed that

a monoalkyl phosphate reacts with DCC in pyridine to give an activated intermediate, which reacts to give an activated cyclic triphosphate [152]. The phosphate-DCC intermediate, or other pyrophosphate intermediates may then react with an alcohol to give a new dialkyl phosphate. The early procedures for phosphorylation of nucleosides involved a phosphate bearing benzyl esters, e.g use of dibenzyl phosphochloridate and *p*-nitrophenyl esters. Hydrogenolysis was required in the former case for removal of the blocking groups and strong alkali or enzymic method for the latter case. A problem encountered when DCC is used to prepare phosphodiesters is that *N*-acylureas are frequently formed as by-products. This problem can be overcomed if the phosphomonoester is activated with an arenesulfonyl chloride ($ArSO_2Cl$)[153]. Arenesulfonyl chlorides have been used extensively to condense phosphomono- and diesters with hydroxyl groups in nucleosides. β-Cyanoethyl phosphate was introduced by Tener as a phosphorylating agent [154]. This group can be conveniently removed by dilute alkali or ammonia by an α,β-elimination of acrylonitrile from the phosphate. This reagent has been found to be useful especially in preparation of nucleotides that may be sensitive to other deblocking methods [155].

The search for new phosphorylating agents grew simultaneously with the need for new phosphorylated nucleosides. Yoshikawa and co-workers found that phosphoryl chloride with a very small amount of water added was highly effective in the phosphorylation of isopropylidene nucleosides [156]. In their developmental studies, they found that trialkyl phosphate was a good solvent for phosphorylation requiring only a slight excess of $POCl_3$. More importantly, it was found that a wide range of unprotected nucleosides was selectively phosphorylated at the 5′-position by $POCl_3$ in trialkyl phosphate solvent,

particularly trimethyl or triethyl-phosphate. This method is now widely accepted and is elegant in its simplicity. Only very small amounts of 2′ or 3′ nucleotides are formed. Trialkyl phosphate is not only an excellent solvent, but it has recently been shown that reaction of guanosine with triethyl phosphate at 50°C for 15 min produced a guanosine – triethyl-phosphate complex in which the triethyl-phosphate is co-ordinated to guanosine of the high-anti form [157]. This complex showed excellent selectivity and high reactivity toward phosphorus oxychloride. The rate of selective phosphorylation was markedly improved by preheating the mixture of guanosine and triethyl-phosphate, followed by addition of the phosphorus oxychloride to the mixture at 0°C. We have adopted this method in the phosphorylation of adenosine analogues.

2.3.1 8-Bromoadenosine 5′-monophosphate (4)

8-Bromoadenosine (**3**) was selectively phosphorylated at the 5′ position in good yield using $POCl_3$ in triethyl-phosphate to yield the corresponding monophosphates (**4** Fig. 2.11). The reaction was quenched with pyridine :water to neutralise the acid produced as the product is labile to acid attack. The problem encountered with this method was the presence of inorganic impurity which could not be removed by ion exchange chromatography as this carries the same amount of charge as the mononucleotide

It is important to remove the inorganic phosphate impurity as this will interfere with the next stage of synthesis (i.e. synthesis of NAD^+ analogues) leading to formation of side products. The nucleotide was freed from inorganic phosphate impurities by adsorption onto a charcoal column[135] (Fig 2.12). The inorganic impurity elutes off straight off the

column and the pure nucleotide can be washed off the charcoal with ethanol:water:ammonia (25:24:1).

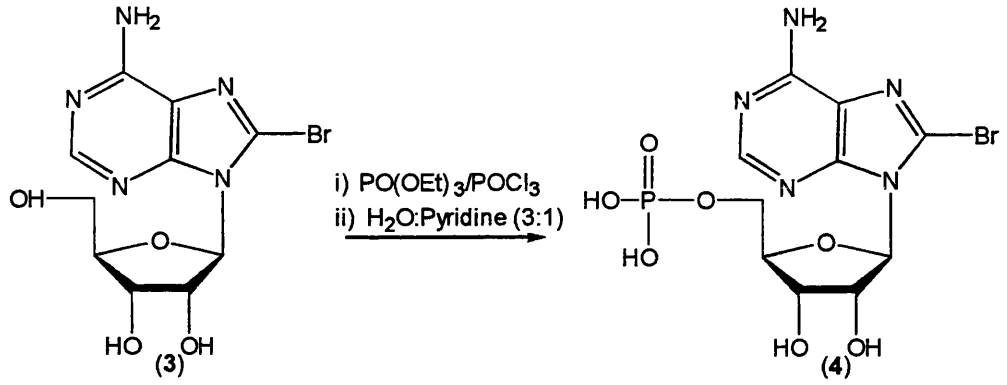

Figure 2.12: Phosphorylation of 8-bromoadenosine

2.3.2 8-Methyladenosine 5'-monophosphate (14)

8-Methyladenosine 5'-monophosphate was synthesised by selective phosphorylation of previously synthesised 8-methyladenosine (**5**- Fig 2.12) at the 5'-hydroxyl group, using $POCl_3$ in triethyl-phosphate. The crude product was purified by ion-exchange chromatography and the inorganic phosphate impurity was removed by passing the nucleotide solution through a charcoal column (Fig 2.13). The pure product was obtained in 60% yield. The ^{31}P-NMR spectrum showed the presence of the organic monophosphate at δp +4.0, which confirmed that phosphorylation was achieved. The ^{1}H-NMR spectrum exhibited all the protons of the nucleotide in question.

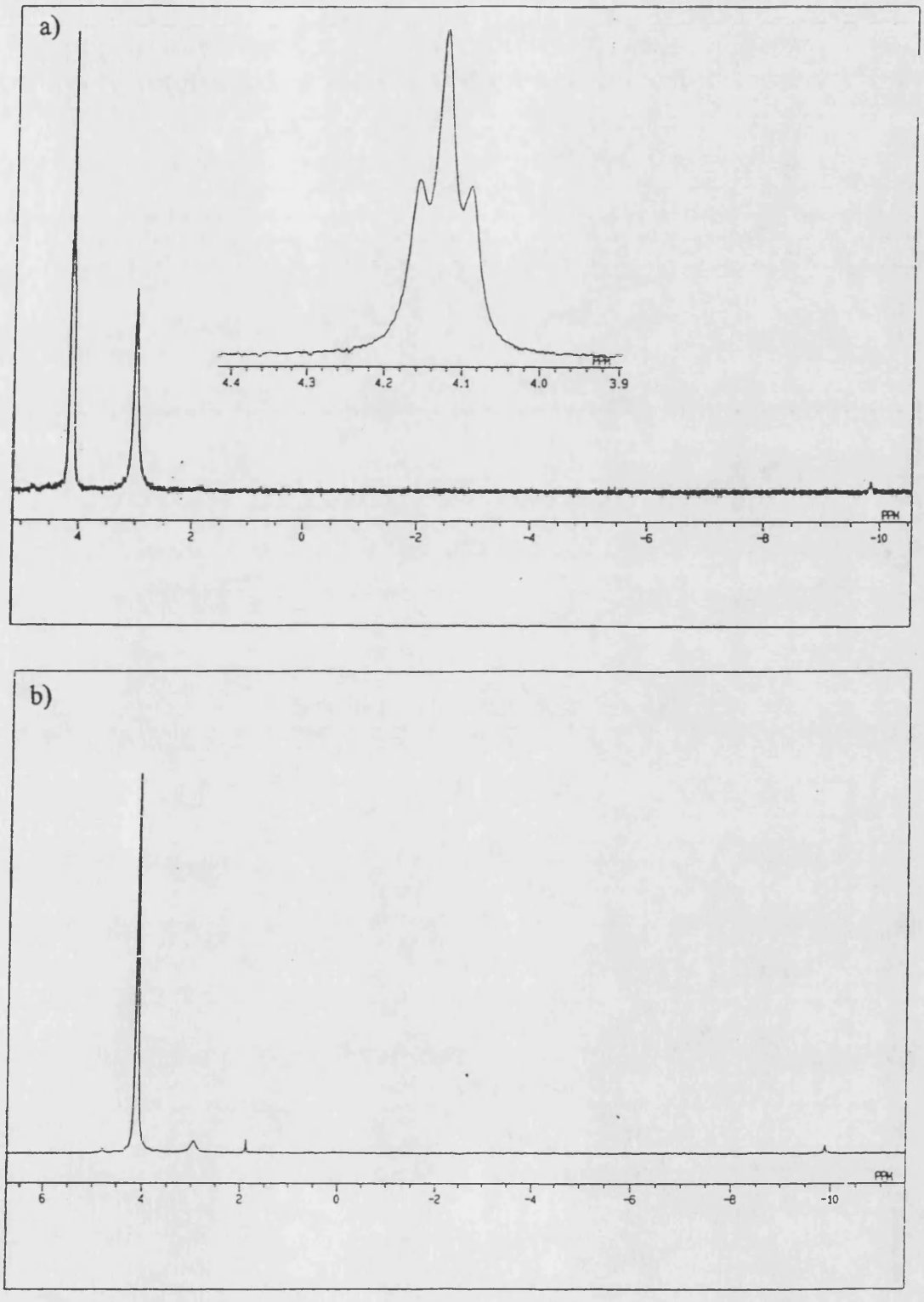

Figure 2.13: ^{31}**P-NMR (162MHz, D_2O) spectrum of 8-CH_3-AMP (14): illustrating the use of charcoal to remove inorganic phosphate impurity. a) ^{1}H-coupled spectrum before charcoal treatment b) ^{1}H-decoupled spectrum after charcoal treatment.**

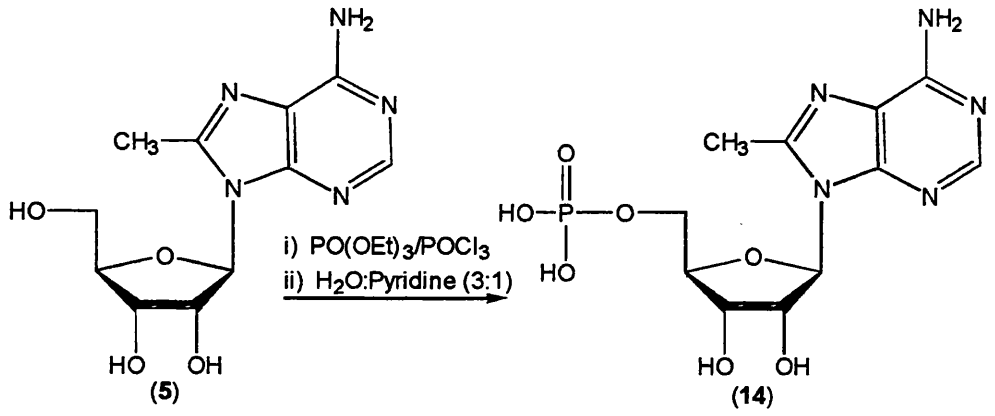

Figure 2.14: Synthesis of 8-methyladenosine 5′-monophosphate

2.3.3 3′-O-Methyladenosine 5′-monophosphate (16)

3′-*O*-Methyl-adenosine 5′-monophosphate was prepared to introduce a small change in the cADPR molecule, for the study of the role of the ribose 3′-OH group in cADPR release mechanism. The commercially available 3′-*O*-Me-adenosine (**15**) was selectively phosphorylated at the 5′-position using $POCl_3$ as the phosphorylating agent in triethyl-phosphate (Fig. 2.15). The product was purified by ion-exchange chromatography followed by treatment on a charcoal column to remove inorganic phosphate impurities.

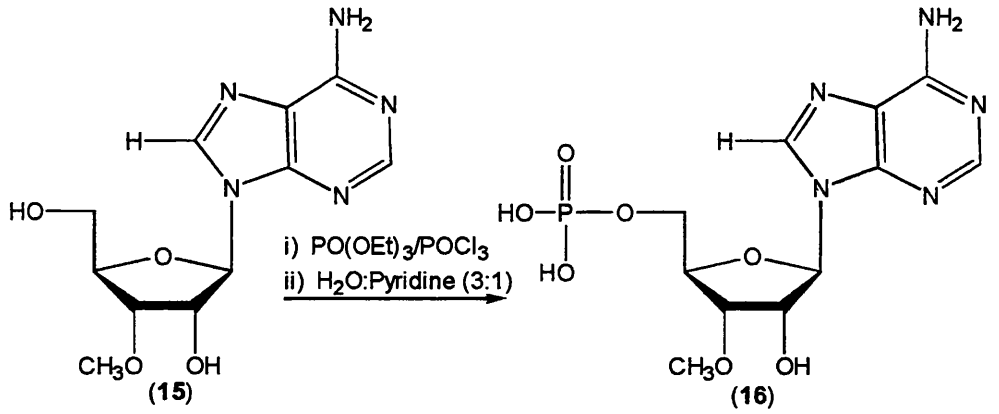

Figure 2.15: Synthesis of 3′-*O*-methyl-adenosine 5′-monophosphate (16)

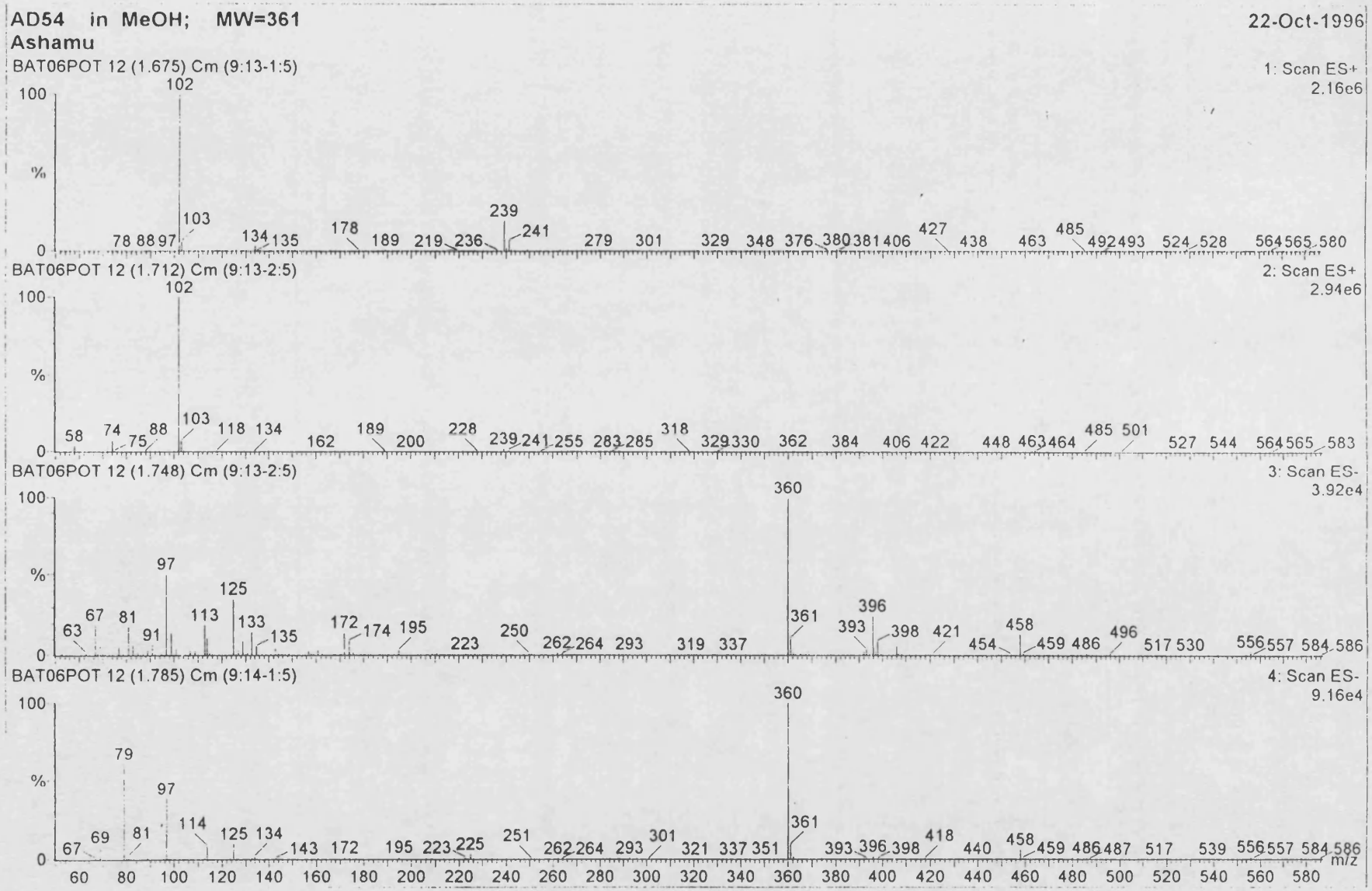

Figure 2.16: Electrospray mass spectrum of 3′*O*-methyl-adenosine 5′-monophosphate

The ^{31}P-NMR spectrum showed the presence of organic monophosphate at δ +2.3 and the ^{1}H-NMR spectrum exhibited all the nucleotide protons with the ribose methyl protons resonating at δ 3.4 equivalent to 3 protons. Mass analysis was carried out using ES-MS. m/z value of 360 $(M - H)^-$ is consistent with the molecular mass of 361 for 3′-*O*-methyl-adenosine 5′-monophosphate.

2.4 Purification and Analysis of Nucleosides and Nucleotides

The acidic and water-soluble nature of nucleotides governs the techniques used for their purification and analysis. Paper and thin-layer chromatography are useful techniques for the analysis of simple mixtures, but are not always satisfactory for the analysis of complex mixtures due to poor resolving power. Thin-layer chromatography has been employed for qualitative analysis of nucleosides in this work and purification was carried out using silica-gel column chromatography. HPLC has proven invaluable for analysis of nucleotides in view of the excellent resolution offered with this technique. We have employed the use of ion-exchange HPLC for qualitative analysis of nucleotide mixtures. In all cases, the purity of the final products were verified by HPLC analysis. A representative HPLC trace is shown in Fig. 2.17. Ion-exchange chromatography has been used for routine purification of nucleotides. Other available methods include reverse-phase HPLC and gas-liquid chromatography although the latter is not very popular owing to volatility problems. This problem may be overcome to a certain extent by derivatisation.

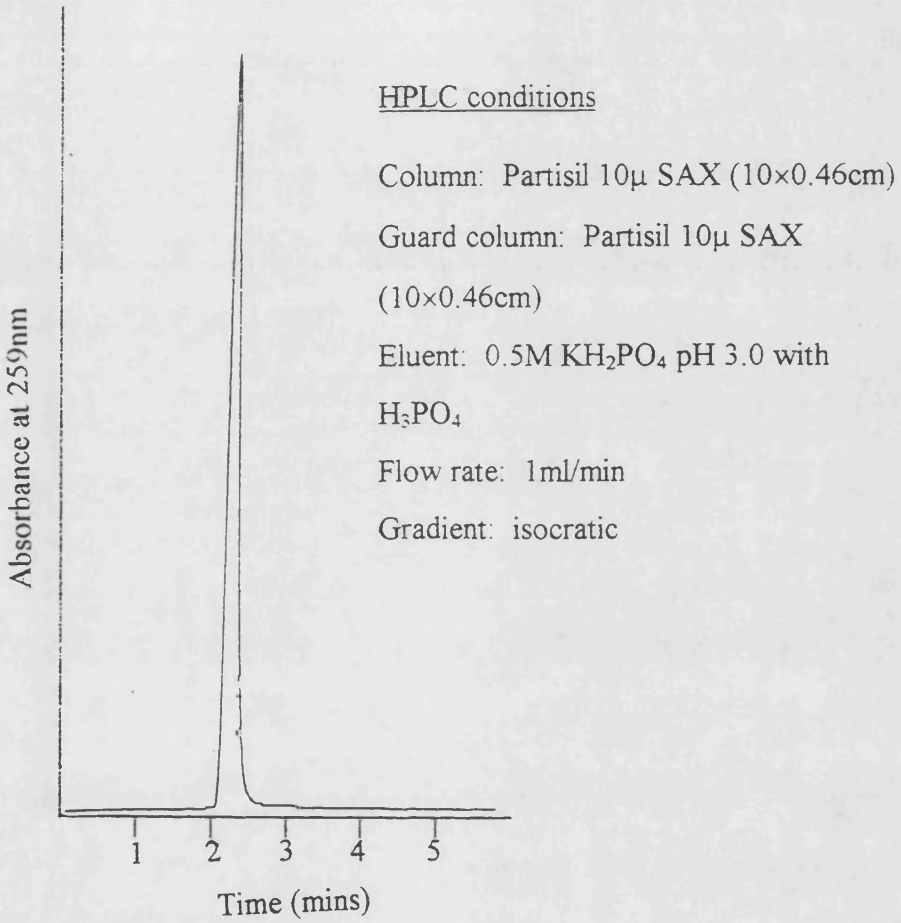

Figure 2.17: HPLC analysis of 3′-*O*-methyl-adenosine 5′-monophosphate

Mass spectrometric analysis of phosphorus-containing compounds has been well reviewed [158,159]. The problem encountered with nucleotides is that of low volatility. FAB-MS has emerged as an important technique for the analysis of nucleotides as it offers many advantages over field desorption mass spectrometry particularly with respect to sample manipulation and the ease of obtaining reproducible data. Improvements in liquid chromatography-MS, for example use of electrospray techniques has found use for analysis of nucleosides and nucleotides. FAB-MS and Electrospray-MS techniques have been employed for routine analysis of nucleotides in this work. FAB-MS and ES in the –ve ion mode is the most structurally informative due to great stability of the phosphate monanion in the $(M - H)^-$ species.

Nuclear magnetic resonance is very well established and described in texts for the identification of nucleotides. ^1H and ^{31}P-NMR spectroscopy have been employed routinely for structural analysis of nucleotides.

CHAPTER 3: SYNTHESIS OF NAD^+ AND ITS ANALOGUES

The use of NAD^+ as a common substrate for a large number of enzymes has generated widespread interest in the use of this coenzyme to investigate the mechanisms of enzyme catalysis. NAD^+ analogues have been extremely useful as biochemical probes to increase the understanding of the mechanism of action of dehydrogenases. Chemical and enzymatic procedures have been used extensively to prepare analogues of NAD^+ containing alterations in all major portions of the coenzyme molecule One hundred and eighty one analogues have been listed in a review[160] and various methods for the preparation of NAD^+ and its analogues have been described in texts [161]. NAD^+ analogues were synthesised in this work for use as intermediates in the synthesis of cADPR analogues (see chapter 4).

3.1 Chemical Synthesis of NAD^+ and its Analogues

NAD^+ is a dinucleotide anhydride consisting of nicotinamide 5′-mononucleotide (NMN) and adenosine 5′-monophosphate (AMP) moieties. Hence, in general NAD^+ and its analogues have been prepared through chemical condensation of nucleoside 5′-monophosphate making use of a condensing agent, as these compounds themselves are not suitable for condensation reactions and must therefore be activated. A pyrophosphate bond is formed in the condensation process. Introduction of an additional substituent polarises the bond between the ligand and the central phosphorus atom of the nucleotide which allows for the cleavage of the polarised bond by a second phosphoric acid ester, forming a more stable nucleotide anhydride (Fig 3.1).

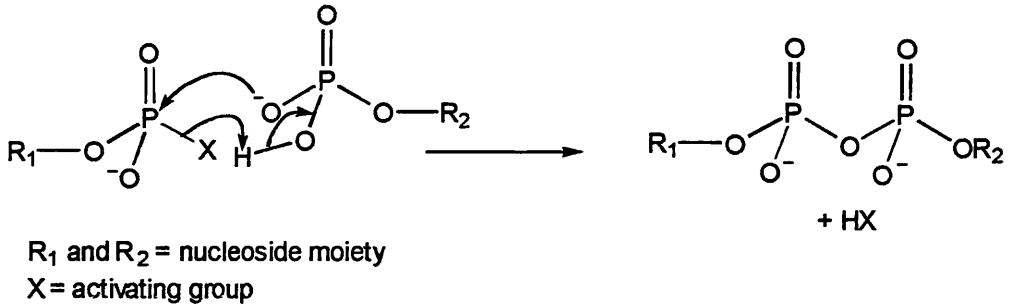

Figure 3.1: Formation of a pyrophosphate bond illustrating use of an activating group.

Amino-, imino-, isourea- and acid substituents are used for the activation of nucleoside monophosphates and in most cases the resulting activated phosphoric acid ester derivatives are unstable and are easily hydrolysed in aqueous solution. Phosphoramidates and isourea esters are relatively more stable due to the nitrogen electrons that decrease the polarisation. This stabilising effect is lost in acidic solution as protonation of the amide group results in an increase of polarisation which causes cleavage of the amide bond in the presence of a second phosphoric acid ester to form the desired diphosphate (Fig 3.2) [162].

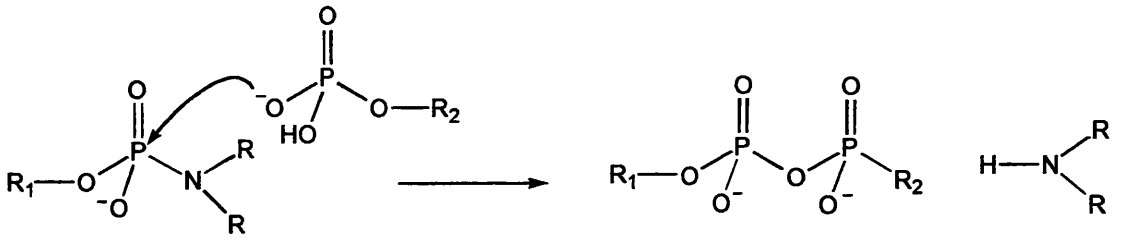

Figure 3.2: Use of phosphoramidates in pyrophosphate bond formation.

Imidazoles have been used frequently for the activation of phosphoric acid esters. Protonation is unecessary in this heterocyclic compound because of the aromatic character (Fig. 3.3), the imidazole is cleaved and the anhydride bond is formed in the presence of a

second nucleotide [163] Acidic substituents are also suitable to form polarized bonds. The group transfer potential of phosphoric acid anhydrides is well known for example, in aqueous solution, adenosine tri-phosphate (ATP) forms a mixture of various oligonucleotides.

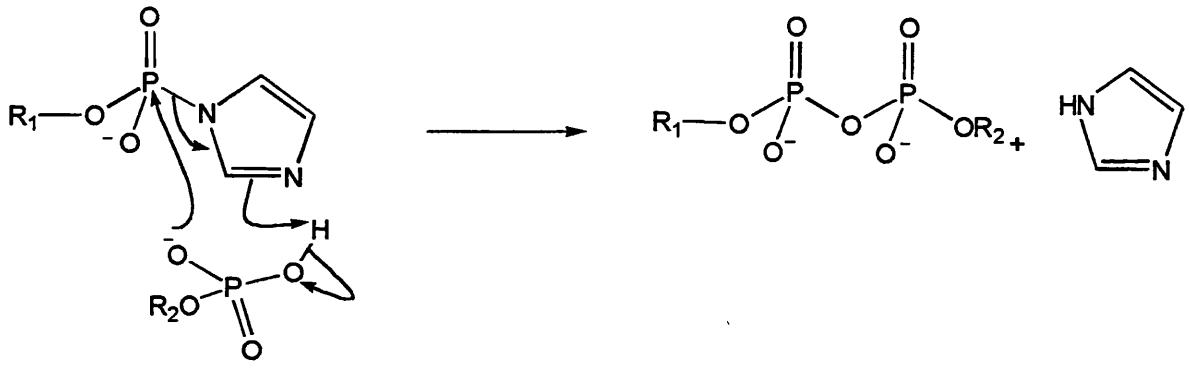

Figure 3.3: Imidazoles as activating groups in pyrophosphate formation.

This type of reaction is known as anion exchange (Fig. 3.4) [164]. Mixed anhydrides react similarly with trifluoroacetoxy residues being one of the most suitable groups [165]. Carbodiimides and nucleoside 5′-monophosphates react to form an isourea ester with the isourea ligand as the activating group. Isourea derivatives, as explained above, are often stable in aqueous solutions and are hydrolysed slowly except in acidic solution where hydrolysis occurs at a faster rate.

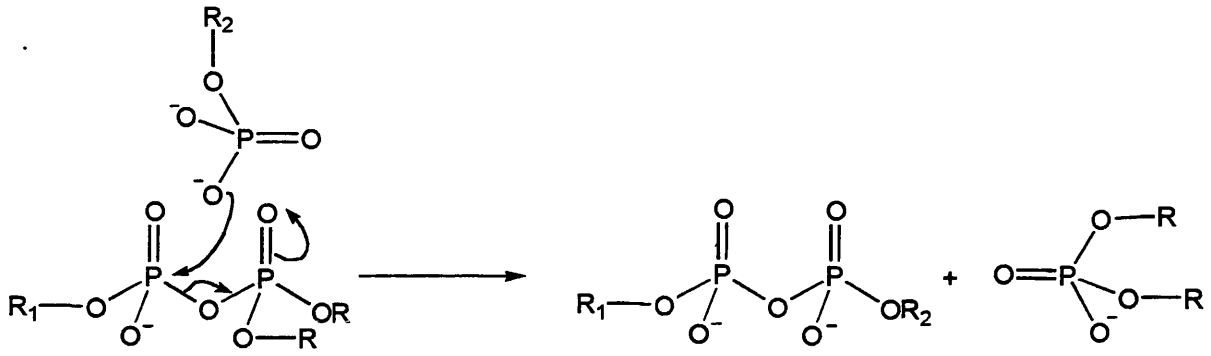

Figure 3.4: Formation of a pyrophosphate bond by an anion exchange method.

Addition of another nucleophilic ligand leads to simultaneous formation of urea (Fig. 3.5). The first successful synthesis of NAD^+ was described by Hughes and co-workers using a carbodiimide - N,N-dicyclohexylcarbodiimide (DCC) as the condensing agent [166].

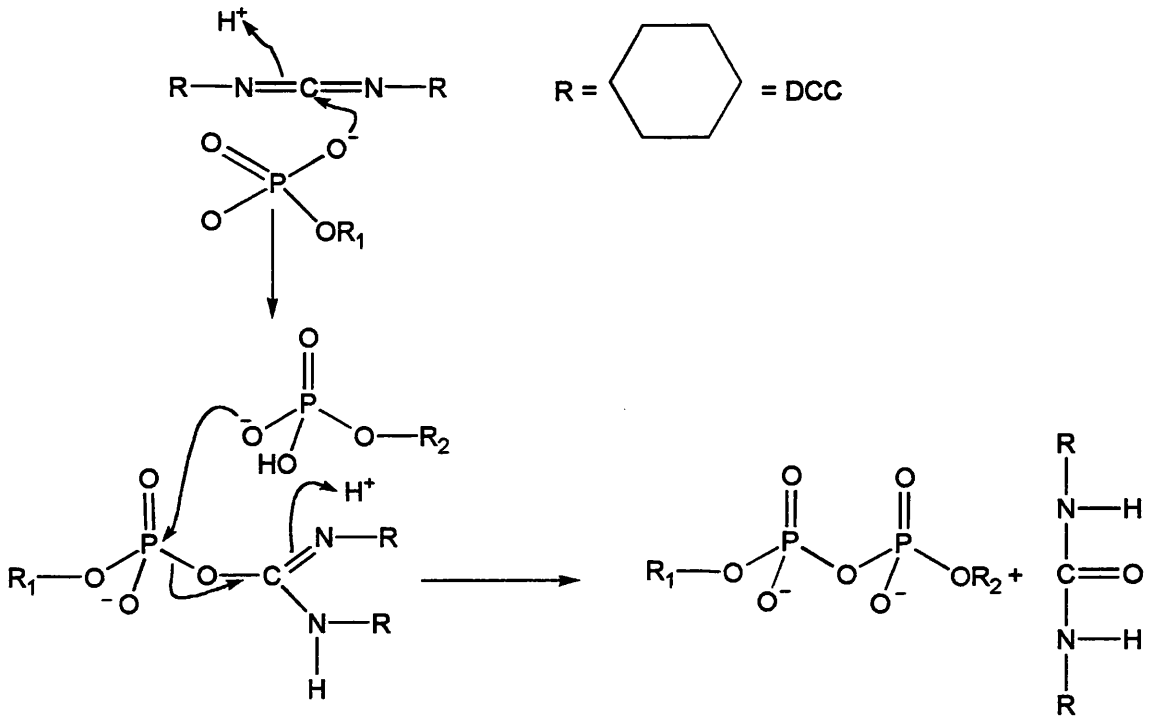

Figure 3.5: Carbodiimides in pyrophosphate synthesis

AMP and NMN were condensed with DCC in 75% aqueous pyridine as solvent. The two nucleotides were observed to react differently. AMP reacts with DCC to form the isourea derivative, however NMN isourea ester was only formed in small amounts possibly because of the betaine structure of NMN (inner salt). The unsymmetrical NAD^+ was isolated as the main product with 70% yield, with the formation of only small amounts of the symmetrical dinucleotide. This type of reaction has since been used by several investigators to prepare NAD^+ analogues. Variable yields have been reported, for example, $2'_A$-deoxy-NAD^+ was synthesised in 16% yield [167], nicotinamide formycin dinucleotide (NFD^+) was synthesised in 11.6% yield [168]

The experimental difficulty for the synthesis of NAD^+ and its analogues is not due to the formation of the anhydride bond but due to problems caused by the solubility of nicotinamide mononucleotide. The positively charged pyridine ring of the nucleotide results in an excellent solubility in polar solvents such as water. It is easily dissolved in dimethylsulfoxide (DMSO), but the solvent slowly oxidises the ribose hydroxyl groups to ketones This side reaction is enhanced by carbodiimides. NMN is not readily soluble in common solvents such as *N,N*-dimethylformamide (DMF), pyridine or *o*-chlorophenol. Attempts to overcome this problem involve the use of water soluble carbodiimides. 1-Ethyl-3-(3-dimethyl-amino-propyl)-carbodiimide (EDC) - a water soluble carbodiimide - has been used as a condensing agent with reasonable yields [120]

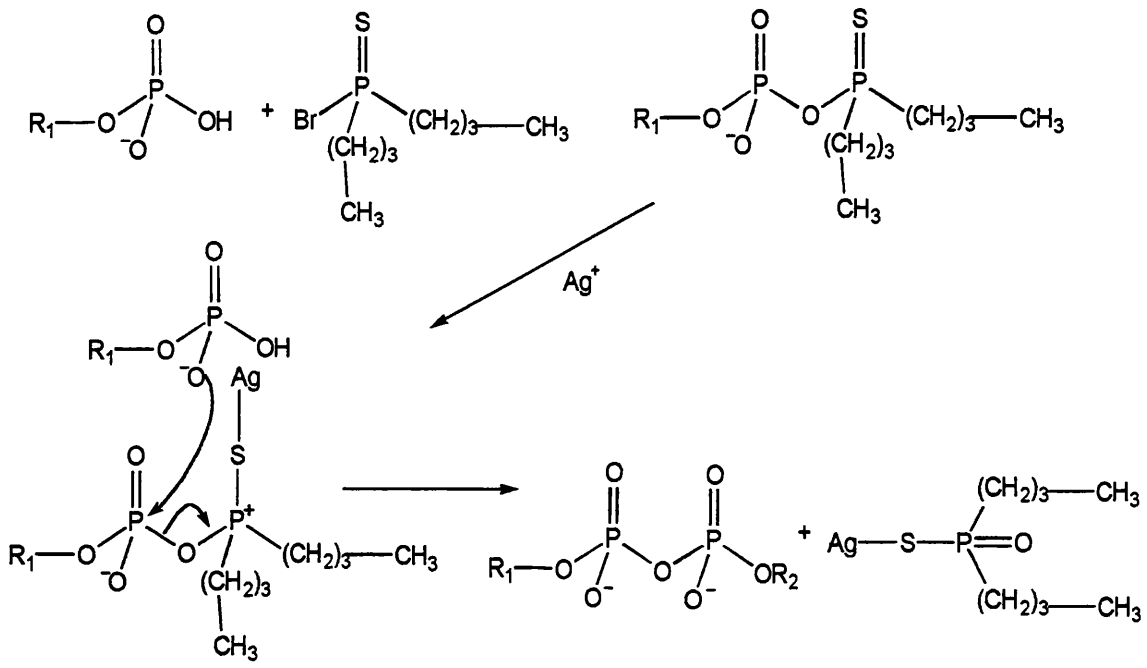

Figure 3.6: Use of Di-*n*-butylphosphinothoic bromide as an activating group in pyrophosphate syntheis.

A further attempt to resolve solubility problems involves reaction of di-*n*-butylphosphinothoic bromide with 5′-nucleotide (Fig. 3.6) to give mixed anhydrides which are sufficiently stable and are soluble in DMF. Addition of silver (Ag^+) activates the thiohypophosphites thus formed, and an anhydride bond is formed by the nucleophilic attack of a phosphoric acid ester The silver salt of di-*n*-butylphosphinothoic acid is simultaneously released. NMN reacts with activated adenosine derivative to form NAD^+ in yields exceeding 80% using this procedure [169] This kind of yield has been obtained by the ion-exchange method [170]. Michelson treated AMP with diphenyl phosphochloridate in anhydrous pyridine to obtain the ADP-β-diphenyl ester which is unstable and could be cleaved by NMN to give NAD^+ (Fig. 3.7).

Moffatt and Khorana have activated nucleotides via amidation [171]. The morpholidate of AMP was prepared by the reaction of AMP with morpholine and DCC as the condensing agent to form *N,N*-dicyclohexyl-4-morpholinocarboxamidine (Fig 3.8). A variety of monophosphomorpholidates could be prepared by this general method. The morpholidates are quite reactive and react with an equimolar quantity of the second nucleotide to give NAD^+ (or its analogue), with the cleavage of the morpholidate. Typical yields for diphosphates are about 50%. This was increased up to 70% when originally used solvents, *o*-chlorophenol and pyridine, were replaced by *o*-chlorophenol only.

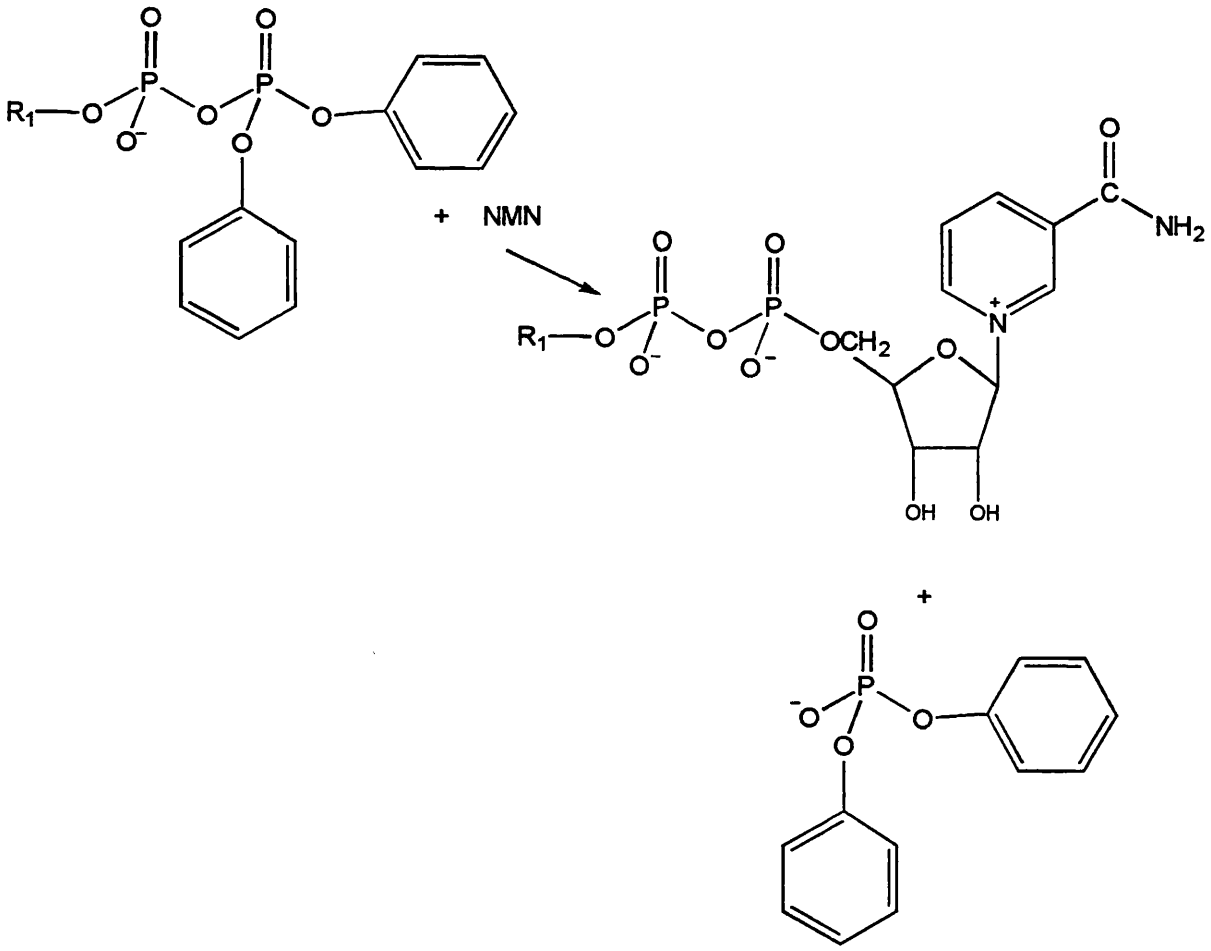

Figure 3.7: Diphenyl phosphochloridate method of pyrophosphate synthesis.

This method has an advantage over the method used by Hughes, Kenner and Todd as no symmetrical side products are formed, because only one of the nucleotides is activated. Separation of NAD^+ from the reaction mixture is achieved by ion-exchange chromatography, using anion exchangers.

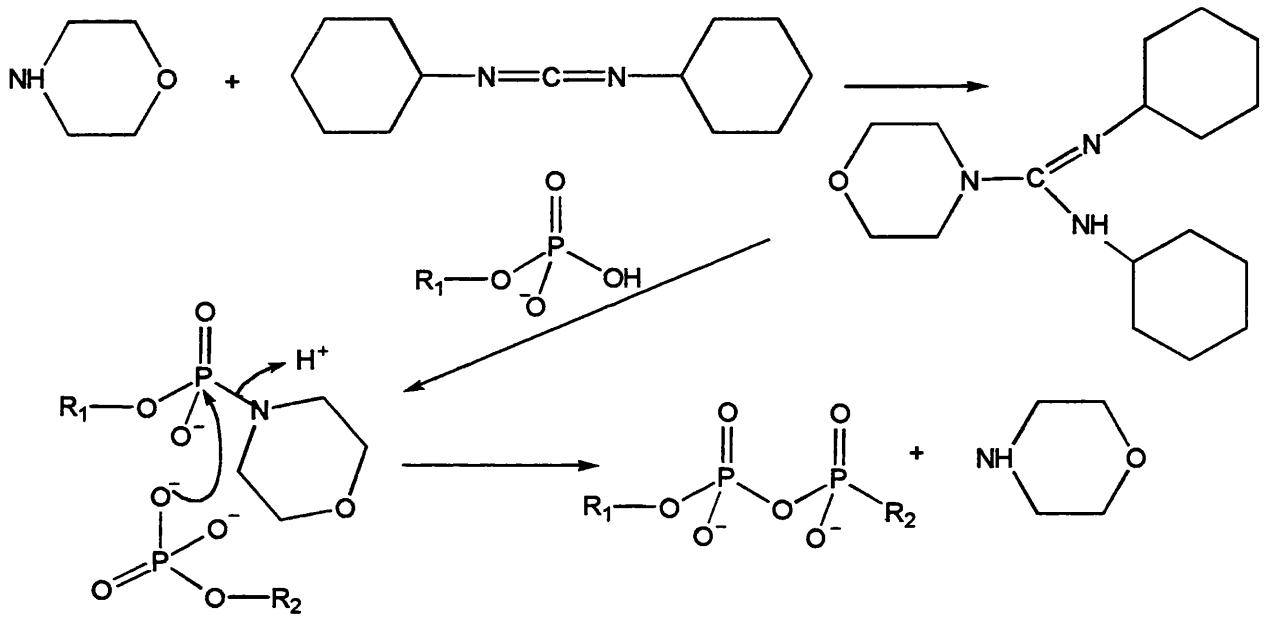

Figure 3.8: Morpholidates in pyrophosphate synthesis

3.2 Enzymatic Preparation of NAD^+

In biological systems NMN is formed from nicotinamide and 5'-phosphoribosyl-1-pyrophosphate by a nicotinamide phosphoribosyltransferase catalysed reaction, [172] NMN and other pyridine mononucleotide reacts with ATP or other purine riboside triphosphates in the presence of NAD^+ pyrophosphorylase to give NAD^+ and inorganic pyrophosphate [173,174]. For preparative purposes, this reaction can be shifted completely to the side of NAD^+ formation by the addition of inorganic pyrophosphate [174]. This enzymatic route is very

limited by the specificity of the enzyme [175] and as a consequence, this method has been applied predominantly for reactions of nicotinamide mononucleotide with nucleoside triphosphates containing nonpolar heterocyclic bases other than adenine. Adenine-substituted analogues of NAD^+ have been prepared with this procedure [168,175,176].

The major enzymatic route used for the preparation of pyridine nucleotide coenzyme analogues involves the transglycosidase activity of mammalian NAD^+ glycohydrolases. This enzyme-catalysed transglycosidation reaction is frequently referred to as the pyridine base-exchange reaction. It involves an exchange reaction between the nicotinamide moiety of NAD^+ and added nicotinamide or analogue [177]. This method is however not applicable for this work as the nicotinamide ring is removed during the enzymatic cyclisation of NAD^+ to cADPR, hence will not lead to the formation of cADPR analogues.

3.3 Nomenclature of NAD^+ analogues

In the nomeclature used in this thesis for NAD^+ and NAD^+ analogues as shown in Figure 3.9, H_N1', -2′, -3′, -4′, -5′ refer to protons on the nicotinamide ribose, H_N2, -4, -5, -6 refer to protons on the nicotinamide ring, H_A1', -2′, -3′, -4′, -5′ refer to protons on the adenine ribose, H_A2 and HA8 are protons on the adenine ring.

3.4 Results and Discussion

NAD^+ is the biological precursor for ADPR, hence several analogues were prepared for use as intermediates in the synthesis of cADPR analogues. The carbodiimide method described in Fig 3.6 has been employed for routine synthesis of NAD^+ analogues in this work. This method was found to be reasonable and convenient as it is a one-step synthesis. Moreover,

the method is generally applicable for the synthesis of dinucleotides. DCC was used as the coupling agent. Attempts at using the water soluble carbodiimide, EDC, were not succcessful.

3.4.1 *2′$_A$ and 3′$_A$-Modified NAD$^+$ Analogues*

A) 2′$_A$ and 3′$_A$-Hydroxyl deleted analogues of NAD$^+$

2′$_A$ and 3′$_A$-Deoxy analogues of nicotinamide adenine dinucleotide have been used to investigate the role of the hydroxyl groups at positions 2′$_A$ and 3′$_A$ for coenzyme binding to dehydrogenases [176]. 2′$_A$ and 3′$_A$-deoxy NAD$^+$ were synthesised with modifications to the method used by Fawcett and Kaplan [178]. 2′$_A$-deoxy-AMP (**17**) and 3′$_A$-deoxy-AMP (**18**) were coupled to NMN (**19**) using DCC as coupling agent to yield the corresponding 2′$_A$ and 3′$_A$-deoxy-NAD$^+$ analogues (**21, 22** - Fig 3.9). Pure samples were obtained from ion-exchange purification of the crude reaction mixture. ^{1}H-NMR analysis of the 2′$_A$-deoxy analogue showed the presence of the protons expected (Figure 3.10). The two H$_A$2′ protons appeared as a multiplet and resonated at a lower frequency of δ 2.8 and 2.5 compared to δ 4.8 in NAD$^+$ [161]. This is due to loss of deshielding effect from the 2′$_A$-OH in 2′$_A$-deoxy-NAD$^+$. ^{31}P-NMR showed an AB system in the region of -10 ppm with J_{pp} of 20 Hz. This shows that the sample contained an unsymmetrical pyrophosphate as expected from the structure of 2′$_A$-deoxy-NAD$^+$. Moreover, FAB-MS showed a peak corresponding to the protonated molecule $[M + H]^+$ at *m/z* 648 and an *m/z* value of 647 for $[M]^-$ was consistent with the deletion of an oxygen atom from NAD of molecular weight 663. *m/z* of 524 corresponds to the fragment $[M - H - \text{nicotinamide}]^-$. ^{1}H and ^{31}P-NMR spectra for 3′$_A$-deoxy-NAD$^+$ were similar to those of 2′$_A$-deoxy-NAD$^+$. The main differences observed were in the proton chemical shifts of the 2′$_A$ and 3′$_A$ protons as would be expected.

The H_A2' resonated at δ 4.7 similar to the chemical shift for H_A2' in NAD^+ however the H_A3' protons resonated at a lower frequency as a multiplet at δ 2.3 and 2.1 which is consistent with loss of deshielding from the $3'_A$-OH that is present in NAD^+. ^{31}P-NMR showed an AB system in the δ -10 region with a J_{PP} value of 20 Hz. This supports the formation of an unsymmetrical pyrophosphate, as present in the structure of $3'_A$-deoxy-NAD^+. FAB-MS exhibited similar peaks to that observed for $2'_A$-deoxy NAD^+. *m/z* value 648 for $[M + H]^+$ for the +ve ion and 647 $[M]^-$, 524 $[M - H -$ nicotinamide$]^-$ in the -ve ion mode.

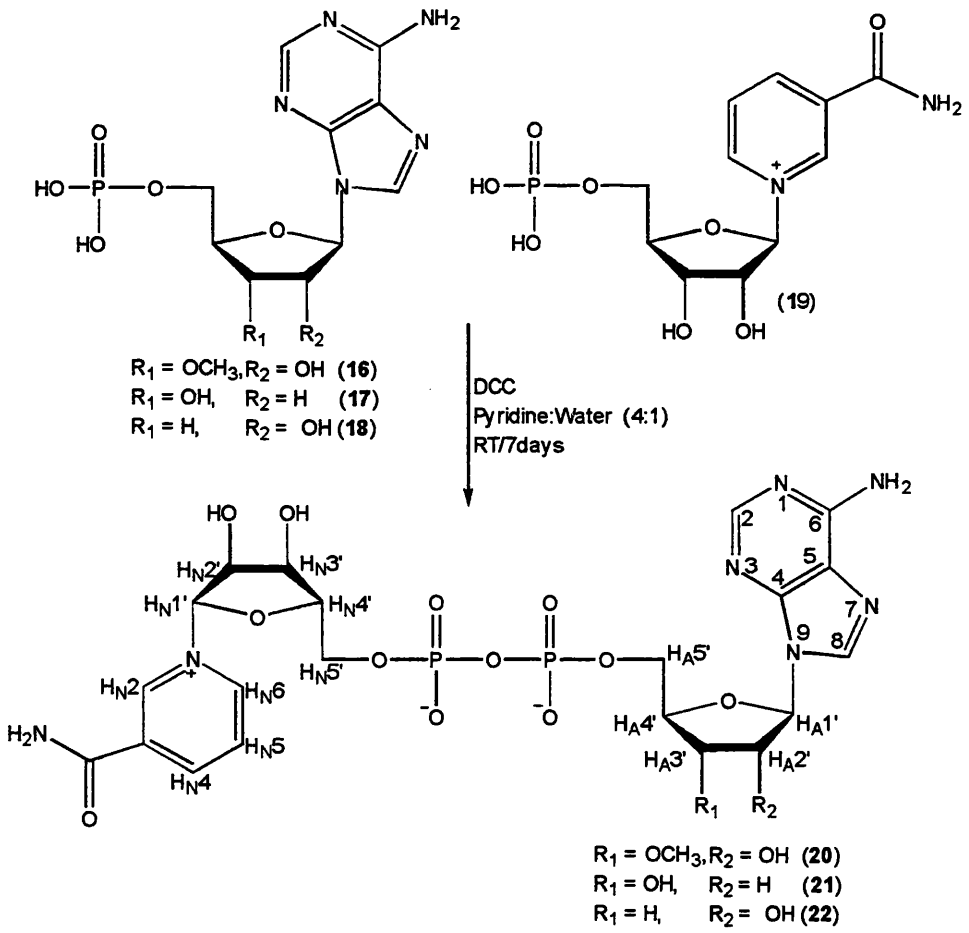

Figure 3.9: Synthesis of $2'_A$ and $3'_A$-Modified NAD^+ Analogues.

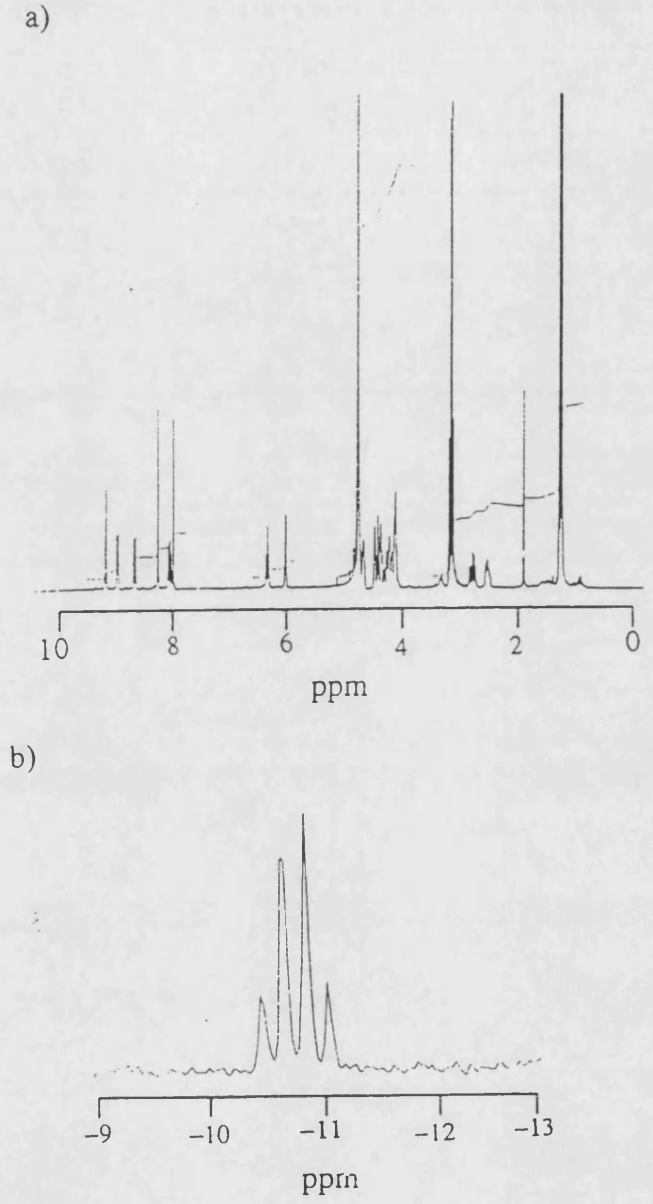

Figure 3.10: a) ^{1}H-NMR (400MHz, D_2O)spectrum and b) ^{31}P-NMR (109MHz, D_2O) spectrum of 2′$_A$-deoxy-NAD$^+$ as its triethylammonium salt.

B $3'_A$-*O*-Methyl-NAD^+

Interest in the synthesis of $3'_A$-*O*-methyl-NAD^+ (**20**) arose with the need to synthesise a precursor for the synthesis of cADPR analogues with modification at the $3'_A$-position. We have already discussed that NAD^+ analogues are precursors for the synthesis of cADPR analogues. The $3'_A$-OH in NAD is replaced by $3'_A$-O-Me hence the name $3'_A$-*O*-methyl-NAD^+. This substituent is larger in size compared to the –OH group and although it can accept a hydrogen bond, it cannot donate a hydrogen bond. It is also more hydrophobic.

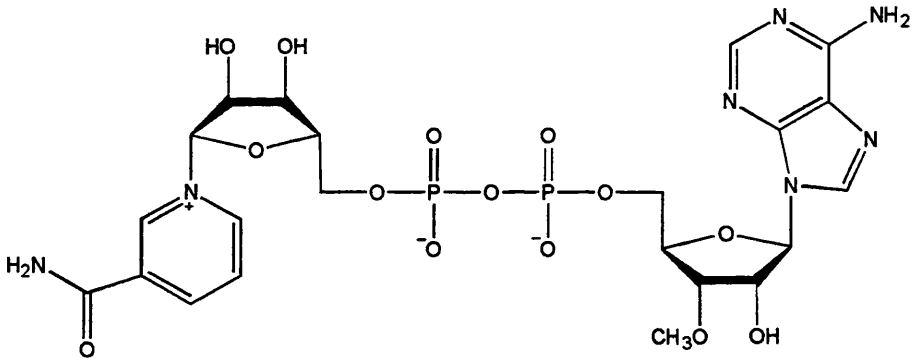

Figure 3.11: Structure of $3'_A$-*O*-methyl-NAD^+ (20)

$3'_A$-*O*-Methyl-NAD^+ (**20** Fig. 3.11)) was prepared by coupling of $3'_A$-*O*-methyl-AMP (**16**) with NMN (**19**) using DCC as the coupling agent (see Fig. 3.9). Purification of $3'_A$-*O*-methyl-NAD^+ proved difficult by ion-exchange chromatography as the sample eluted with residual NMN. Most of the residual NMN was removed by treating the mixture of $3'_A$-*O*-methyl-NAD^+ and NMN with alkaline phosphatase. This enzyme is known to cleave monophosphates and not pyrophosphates. Cleavage of the monophosphate of NMN by the alkaline phosphatase produced the nicotinamide mononucleoside which eluted straight off the ion-exchange column. The sample of $3'_A$-*O*-methyl-NAD^+ obtained, though not pure (83%

pure by HPLC analysis) was considerably improved in purity. This sample was used in this form for the next stage of synthesis.

^{31}P-NMR showed the presence of AB system at δ -10 region showing that the sample contained symmetrical pyrophosphate and ^{1}H-NMR showed the protons expected. The *O*-methyl protons resonated at high frequency of δ 3.5.

3.4.2 *8-Modified Analogues of NAD$^+$*

A) Nicotinamide-8-Bromoadenine Dinucleotide (8-Br-NAD$^+$)

8-Bromo-NAD$^+$ has found use in the synthesis of ligands for affinity chromatography employed in selective purification of dehydrogenases. 8-Bromo-NAD$^+$ (**24**) was synthesised by direct bromination of NAD$^+$ (**23**-see Fig. 3.12) as this reaction is cost effective and gives better yield compared chemical coupling of the two mononucleotide subunits (8-Br-AMP and NMN) using DCC[145]. This reaction involved electrophilic substitution at the 8-position of the adenine ring of NAD$^+$. A shift in the UV absorption maximum from 259-264nm was observed on conversion of NAD$^+$ to 8-Br-NAD$^+$. ^{1}H-NMR of the pure sample obtained after purification, showed the disappearance of H_A8 proton upon substitution with a bromo group and proton chemical shifts resembled those reported previously. ^{31}P-NMR showed that the pyrophosphate was intact as there was an AB system in the region of δ –11 with a J_{PP} value of 21.2 Hz. Electrospray mass spectroscopy of 8-Br-NAD$^+$ showed isotopic pattern of *m/z* 740/742 $(M - H)^-$, 618/620 $[M - H - \text{nicotinamide}]^-$ due to isotopic abundance of ^{79}Br and ^{81}Br (1:1) in the molecule. This is consistent with molecular weight of 741/743 for 8-Br-NAD$^+$.

B) Nicotinamide-8-Piperidyladenine Dinucleotide (8-pip-NAD$^+$)

An attempt was made to synthesise 8-Piperidyl-NAD$^+$ by nucleophilic displacement of 8-bromo-NAD$^+$ with the piperidyl group by treating 8-Br-NAD$^+$ with piperidine. This reaction was carefully monitored by HPLC as prolonged exposure of NAD$^+$-type compounds to base lead to decomposition of the material. This is a result of nucleophilic displacement of the nicotinamide ring from the NAD$^+$ compound to yield the ADP-ribose analogue. It was difficult to purify 8-pip-NAD$^+$ synthesised by this pathway by ion-exchange chromatography as it co-eluted from the column with 8-Br-NAD$^+$. We therefore prepared 8-pip-NAD$^+$ **(28)** by coupling 8-piperidyl-AMP **(10)** to NMN using DCC (Fig 3.13). Pure 8-piperidyl-NAD$^+$ was obtained by ion-exchange purification of the crude mixture.

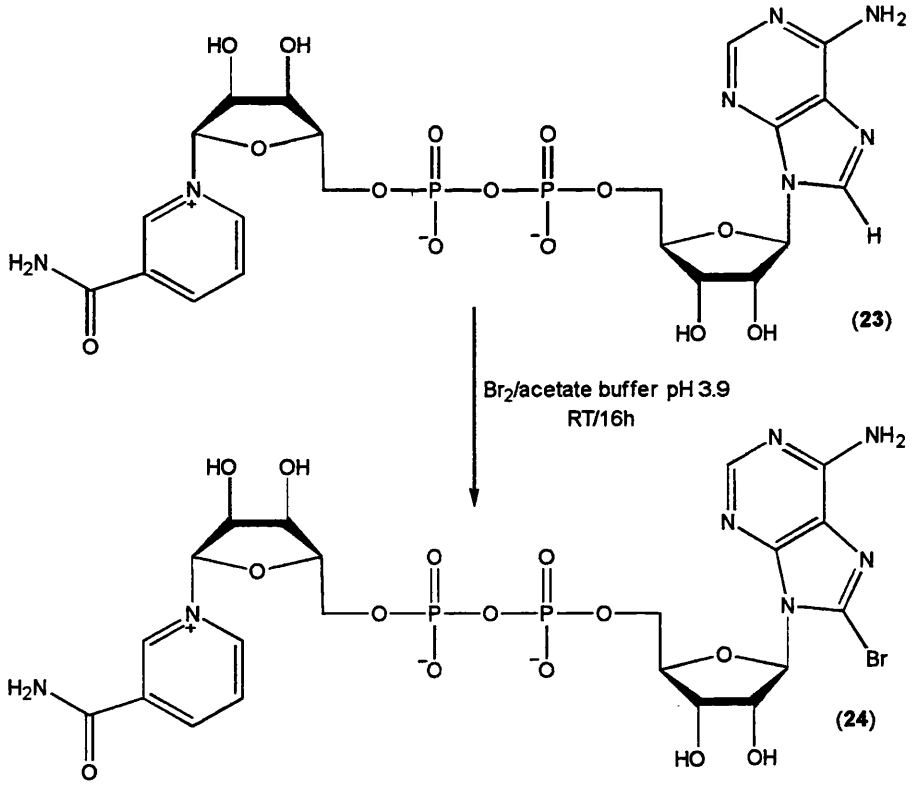

Figure 3.12: Bromination of NAD$^+$

^{1}H-NMR chemical shifts revealed the presence of 10 piperidyl protons at δ 3.2 (4 protons nearer to the piperidyl nitrogen) and δ 1.6 (6 protons further away from the piperidyl nitrogen). All the protons of 8-pip-NAD$^+$ were represented in the ^{1}H-NMR. ^{31}P-NMR showed the presence of a pyrophosphate in the molecule as there was an AB system at δ –11 region with a J_{PP} value of 20.8 Hz. ES-MS showed -ve ion *m/z* peaks at 746[M]$^-$, 745[M – H]$^-$ in low abundance, 623 [M – H – nicotinamide]$^-$. The mass spectroscopic data supports a molecular of 746 for 8-pip-NAD$^+$.

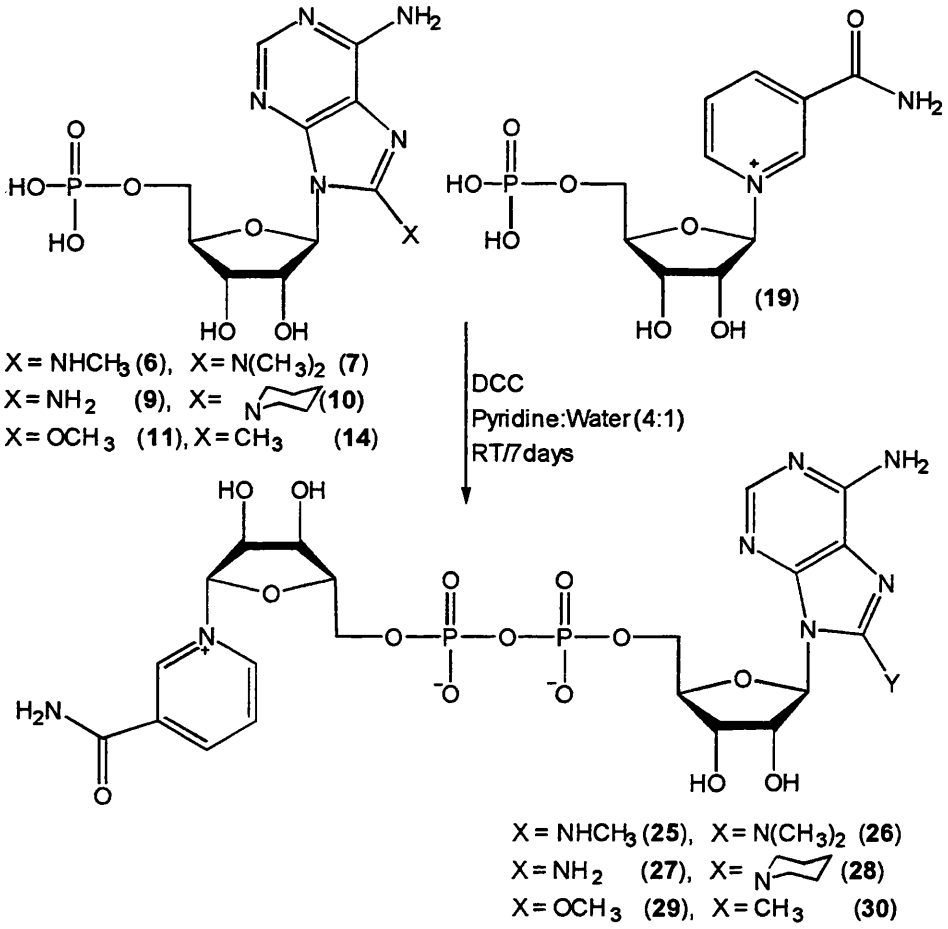

Figure 3.13: Synthesis of 8-substituted analogues of NAD$^+$

C) Nicotinamide-8-Methyladenine Dinucleotide (8-Me-NAD^+)

8-Methyl-NAD^+ (**30**) was prepared from 8-methyl-AMP (**14**) and NMN as described in the experimental section. ^{1}H-NMR analysis of the pure product obtained from ion-exchange purification of the crude mixture showed all the protons expected in the molecule. The three 8-methyl protons resonated at δ 2.5. ^{31}P-NMR of the product showed an AB system in the region of δ -11 with a J_{PP} value of 20.5 Hz. This is consistent with the presence of a pyrophosphate in the molecule. Electrospray mass spectroscopy showed peak of *m/z* value of 676 $[M - H]^-$ in high relative abundance, consistent with the molecular mass of 677 for 8-Me-NAD^+.

D) Nicotinamide-8-Methylaminoadenine Dinucleotide (8-NHMe-NAD^+)

8-Methylamino-NADH, the reduced form of 8-methylamino-NAD^+, but not 8-methylamino-NAD^+ has been synthesised for studying the solution conformation of 8-substituted analogues of NADH [180]. 8-Methylamino-NAD^+ (**25** –Fig. 3.13 & 3.15) was synthesised by chemical coupling of 8-methylamino-AMP (**6**) and NMN (see Fig 3.13). The pure product obtained after ion-exchange purification was established as 8-methylamino-NAD^+ by ^{1}H and ^{31}P-NMR and FAB-MS. ^{31}P-NMR in this case showed a singlet at δ -11.7. Usually a singlet in this region signifies the presence of a symmetrical pyrophosphate, however the sample could not have contained a symmetrical pyrophosphate as both the nicotinamide and adenine protons were present in the ^{1}H-NMR spectrum. The sample could not be mixtures of monophosphate from NMN and 8-methylamino AMP (starting materials) as there was no peak in the monophosphate region of the ^{31}P-NMR. The ^{31}P-NMR spectrum of this compound is therefore unusual in pattern. The three methylamino protons resonated at δ 2.8 in the ^{1}H-NMR spectrum. FAB-MS exhibited a *m/z* value of 693 corresponding to $[M + H]^+$

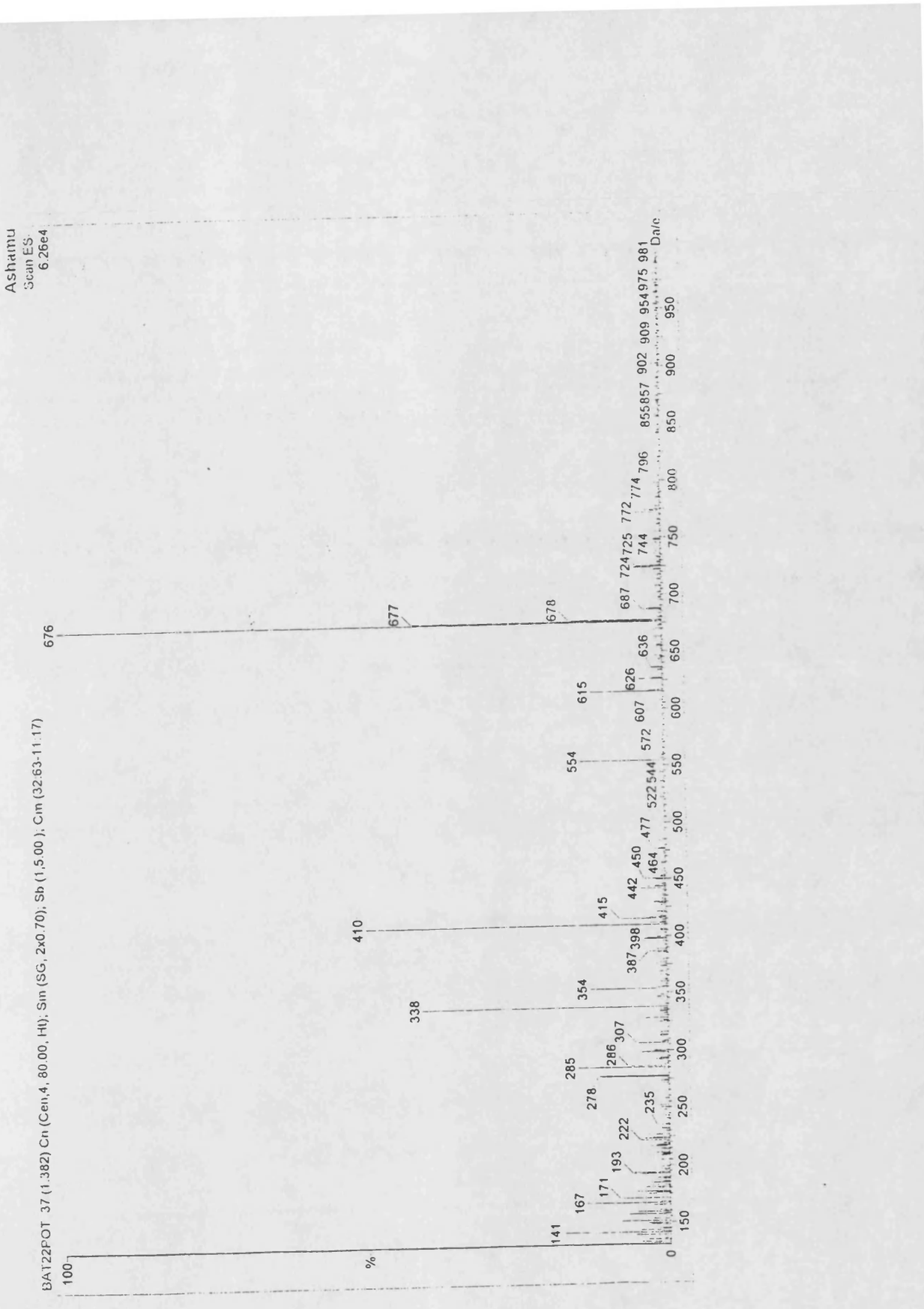

Figure 3.14: Electrospray mass spectrum of 8-methyl-NAD$^+$

in the +ve ion mode. This is consistent with a molecular mass of 692 for 8-NHMe-NAD$^+$. No fragements were seen in the -ve ion mode.

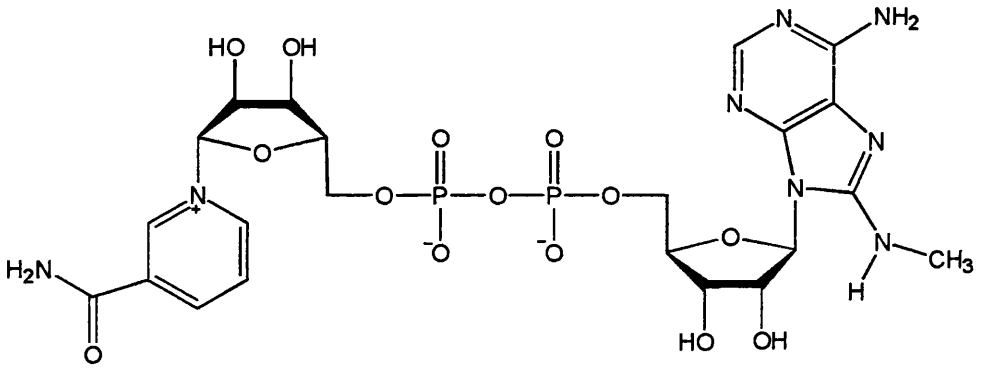

Figure 3.15: Structure of nicotinamide 8-methylaminoadenine-dinucleotide.

E) Nicotinamide-8-Dimethylaminoadenine Dinucleotide (8-NMe_2-NAD^+)

8-Dimethylamino-NADH, but not 8-dimethylamino-NAD$^+$ has been synthesised for studying the conformation of 8-substituted NAD$^+$ derivatives in solution [181]. 8-Dimethylamino-NAD$^+$ **(26)** was synthesised from 8-dimethylamino-AMP (7) and NMN (Fig 3.13). The pure product was identified by NMR spectroscopy and FAB-MS. ^{31}P-NMR exhibited an AB system in the region of δ -11 with a J_{PP} value of 21 Hz. This supports the presence of a pyrophosphate in the molecule. ^{1}H-NMR showed all the protons with the 6 dimethylamino protons resonating as a singlet at δ3.1, as they are all chemically equivalent (see Fig 3.16). FAB-MS of sample showed peaks with *m/z* of 707 $[M + H]^+$ in the +ve-ion mode and 706 $[M]^-$, 582 $[M - H -$ nicotinamide$]^-$ in the -ve-ion mode in high relative abundance. This supports a molecular weight of 706 for 8-NMe_2-NAD^+.

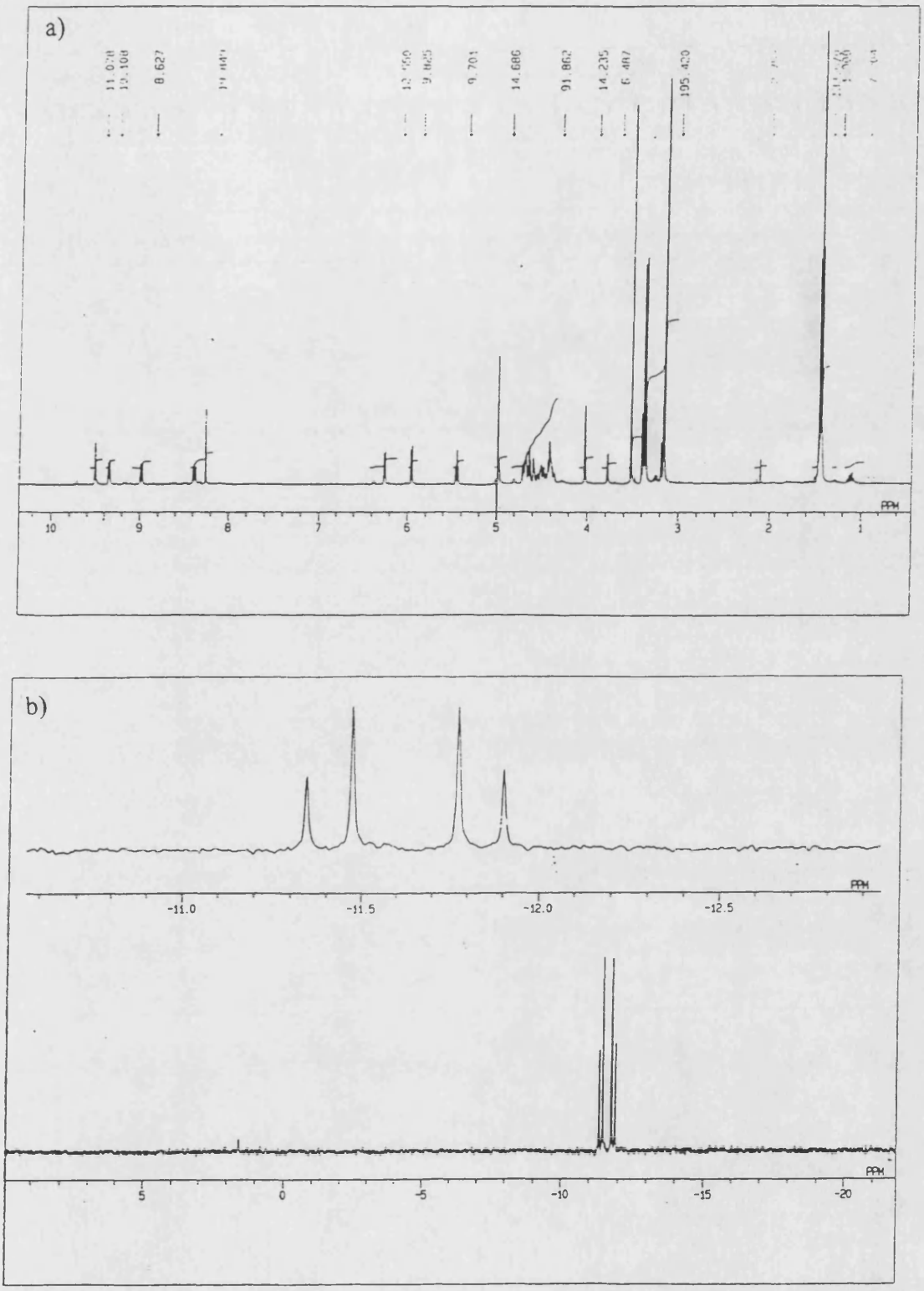

Figure 3.16: a) ^{1}H-NMR (400MHz, D_2O)spectrum and b) ^{31}P-NMR (162MHz, D_2O) spectrum of 8-dimethylamino-NAD^{+} as its triethylammonium salt.

F) Nicotinamide-8-Aminoadenine Dinucleotide (8-NH_2-NAD^+)

8-Amino-NAD^+ (Fig. 3.17) was synthesised by modification of the method by Walseth *et al.* in which a water soluble carbodiimide was used to couple 8-amino-AMP (**9**) to NMN [120]. We have used DCC in coupling the mononucleotide subunits of 8-amino-NAD^+ to obtain the product in question (Fig 3.13). ^{31}P-NMR of product showed an AB system in the region of δ −11 with a J_{PP} value of 19.4 Hz. Electrospray mass spectrometry showed *m/z* value of 677[M – H]$^-$ and 555 [M – H – nicotinamide]$^-$ for the -ve-ion. This supports a molecular weight of 678 for 8-amino-NAD^+.

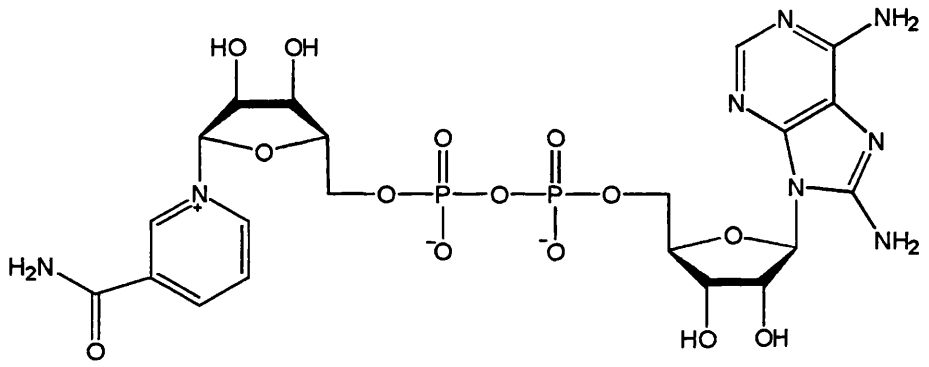

Figure 3.17: Structure of 8-amino-NAD^+

G) Nicotinamide-8-Oxyadenine Dinucleotide (8-Oxy-NAD^+)

Coupling of 8-Oxy-AMP (**13** -see chapter 2) to NMN (**19**) using DCC gave the dinucleotide, 8-Oxy-NAD^+ (**31** -Fig 3.18). This product was identified by the presence of an AB system in the ^{31}P-NMR spectrum at δ ~ −11 with a J_{PP} value of 21 Hz. ^{1}H-NMR spectrum identified the protons on 8-Oxy-NAD^+ and electrospray mass spectrometry showed *m/z* peaks of 678 [M – H]$^-$ in high abundance consistent with a molecular weight of 679 for 8-Oxy-NAD^+.

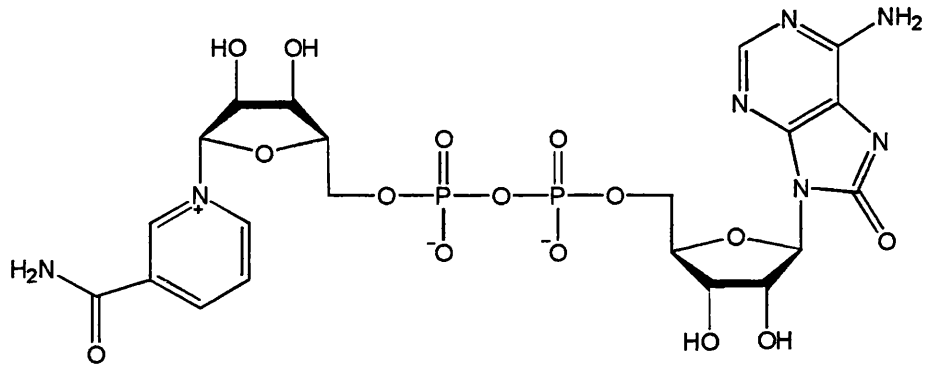

Figure 3.18: Structure of 8-Oxy-NAD$^+$

H) Nicotinamide-8-Methoxyadenine Dinucleotide (8-OCH_3-NAD^+)

Synthesis of 8-methoxy-NAD^+ (**29**) was achieved by chemical coupling of 8-methoxy-AMP (**12**) with NMN using DCC as the coupling agent. The product obtained was identified by spectroscopic analysis. ^{31}P-NMR spectrum showed the presence of an AB system at $\delta \sim$ 11ppm with a J_{PP} value of 20.9 Hz confirming that a pyrophosphate was present in the molecule. ^{1}H-NMR spectrum identified the protons with the methoxy protons at $\delta \sim$ 4.0ppm. Electrospray mass spectrometry in the +ve-ion and -ve ion mode showed peaks at *m/z* value of 694 $[M + H]^+$ and 692 $[M - H]^-$ in high abundance. This agrees with a molecular weight of 693 for 8-OCH_3-NAD^+.

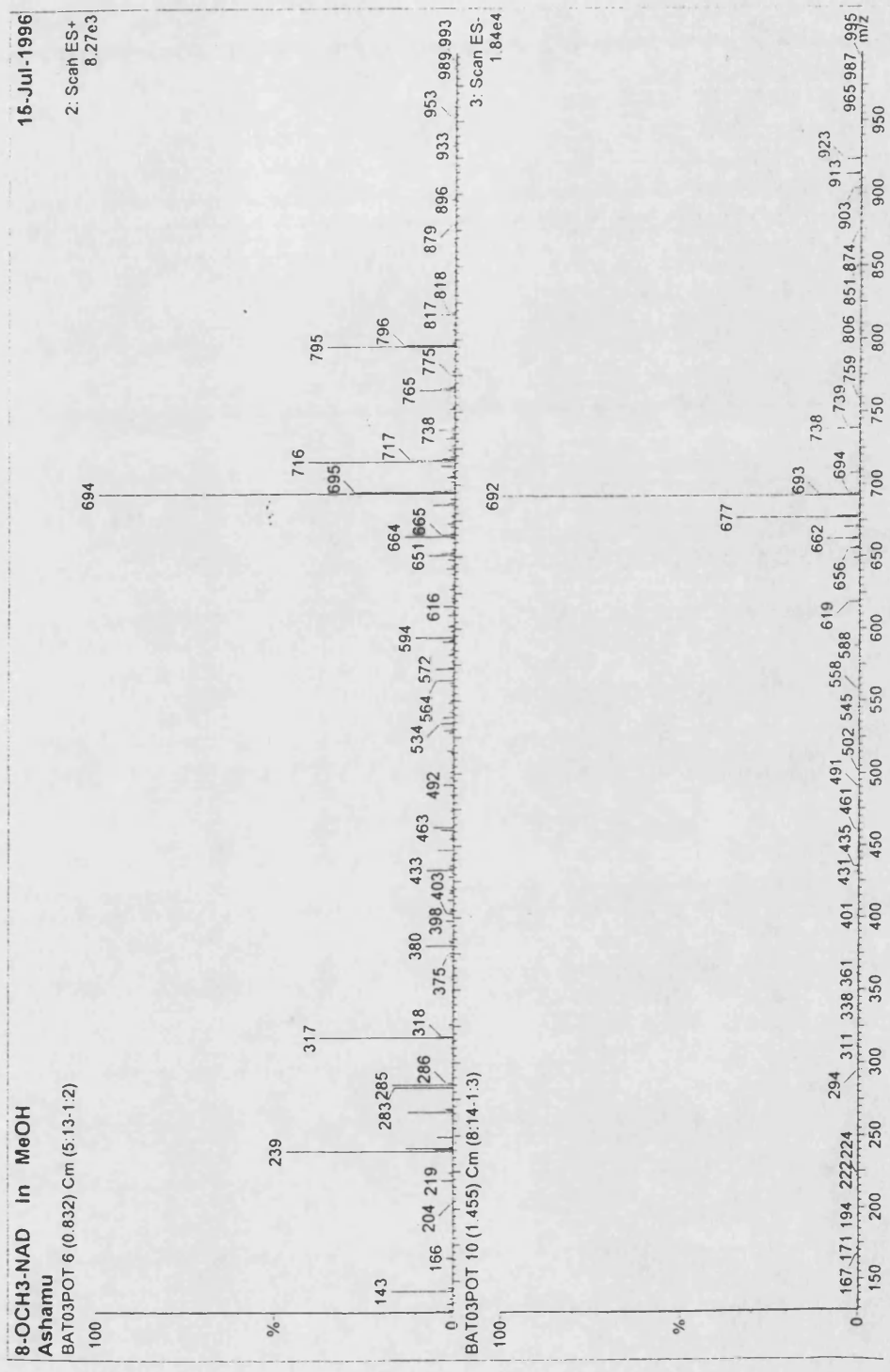

Figure 3.19: Electrospray mass spectrum of 8-methoxy-NAD$^+$

I) Nicotinamide-8-Aza-9-deazaadenine Dinucleotide (NFD^+)

Nicotinamide-8-aza-9-deaza-adenine dinucleotide (**33**- Fig. 3.20), a formycin analogue of NAD^+ is a known fluorescent analogue. It has been prepared by a similar method to that used by Ward and co-workers [168], by chemical coupling of formycin 5'-monophosphate (**32**) to NMN (Fig 3.20). The UV absorption spectra was similar to that previously reported. ^1H and ^{31}P-NMR was not reported by Ward *et al*[168]. ^1H-NMR and ^{31}P-NMR spectroscopy identified the product as NFD^+. ^{31}P-NMR showed an AB system at $\delta \sim -11$ with a J_{PP} value of 21.6 Hz. ES-MS showed a -ve ion peak with *m/z* value of 662 $[M - H]^-$ consistent with a molecular weight of 663 for NFD^+.

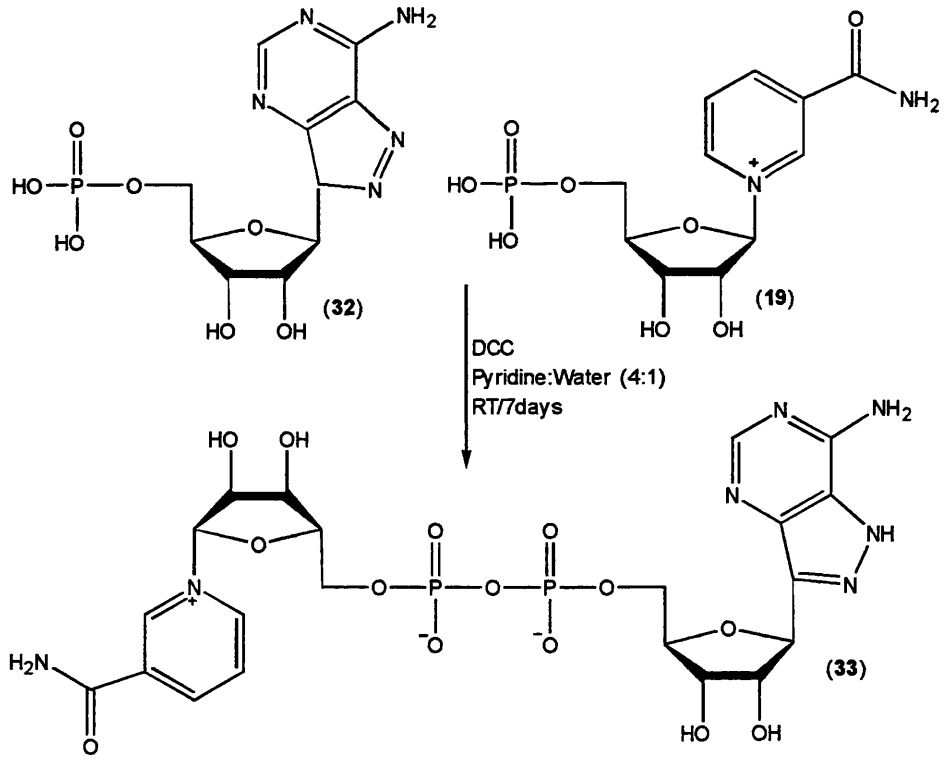

Figure 3.20: Synthesis of nicotinamide-8-aza-9-deazaadenine dinucleotide [NFD^+ (33)].

3.4.3 *Characterisation of NAD^+ analogues*

A) Mass Spectroscopy -FAB-MS and Electrospray

Due to the high polarity and hence low volatility of NAD^+ analogues, FAB-MS and electrospray mass spectroscopy have been chosen for mass analysis of this type of compounds. Under electron-Impact MS conditions NAD^+ thermally decomposed prior to ionisation by release of nucleobases nicotinamide and adenine [161]. NAD^+ was one of the first compounds used to demonstrate the efficiency of the FAB technique for mass spectrometric analysis of thermally sensitive, highly polar substances. Electrospray mass spectrometry is known to provide inherent gentle ionisation given rise to intact ions from thermally labile biological molecules. NAD^+ analogues have proven to be good candidates for this technique. The choice of method used between FAB-MS and Electrospray depended on availability at the time that mass analysis was required.

B) Nuclear Magnetic Resonance

^{31}P-NMR was used to follow the reaction by emergence of an AB system in the pyrophosphate region $\delta \sim -10$. ^{1}H and ^{31}P-NMR techniques were used to obtain structural information about the analogues prepared. These methods were also used along with HPLC techniques to judge purity of the sample as unexpected peaks in the spectra would indicate that other impurities were present. The quality of materials obtained after purification can be seen from the ^{1}H and ^{31}P-NMR spectra Fig. 3.10 & 3.16.

C) UV spectroscopy

The presence of chromophores on the nicotinamide and the adenine moiety of NAD^+ and analogues provide a useful property of this molecule. UV spectroscopic patterns and absorption maxima have been used to characterise this compounds. A general red shift was observed in the absorption maximum was observed upon subtitution at the 8-position of the purine ring. Optical density measurements with molar extinction determination were useful in accurate quantification of this compounds. NAD^+ compounds were produced as the triethylammo-nnium salts and were glasses. Moreover, the small quantity of sample involved would have made sample measurement by weight highly inaccurate. Elemental analysis could not be carried out as the samples obtained were glasses.

3.4.4 *Analysis of NAD^+ analogues*

A) Qualitative Analysis

i) *Chromatographic techniques*

NAD^+ analogues are highly charged water-soluble molecules. The purification method employed for routine use was ion-exchange chromatography on an anion exhange column. High perfomance liquid techniques were employed in the analysis of fractions collected from the anion exchange column. Samples were judged pure by ion-exchange HPLC analysis in combination with ^{31}P and ^{1}H-NMR analysis. The quality of the material prepared after purification can be seen from a typical HPLC trace for 8-oxy-NAD^+ (Fig. 3.21). A UV detector was used to detect samples eluting off the column. The chromophores of the nicotinamide and the adenine moiety are only detected as one as their absorption maxima are very similar, 262 and 260nm respectively in NAD^+.

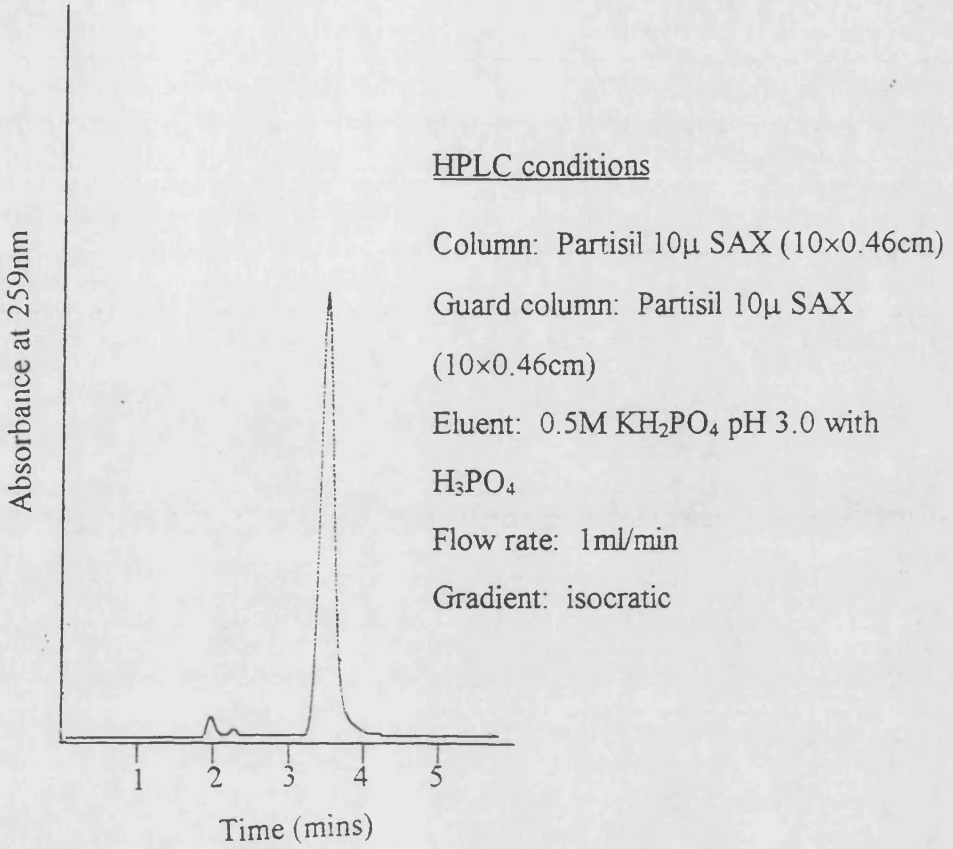

Figure 3.21: HPLC analysis of 8′-oxy-NAD^+

ii) *Co-enzyme Activity*

All the NAD^+ synthesised were screened for coenzyme activity [176] and the ability to form a complex with cyanide. NAD^+ is a natural coenzyme for alcohol and other dehydrogenase as mentioned previously. NAD^+ is reduced in the presence of ethanol and alcohol dehydrogenase to NADH. This conversion can be monitored by UV spectrophotometry in which a new peak at 340nm emerges upon formation of NADH. Conversion of these NAD^+ analogues into the reduced form NADH by incubation with yeast alcohol dehydrogenase in the presence of 5% ethanol in 0.1M Tris buffer pH 9 was monitored by UV analysis. A new peak at 340nm was recorded for all the analogues indicating that they have intrinsic coenzyme activity(see Figure 3.22). The relative rate of turnover was however not measured.

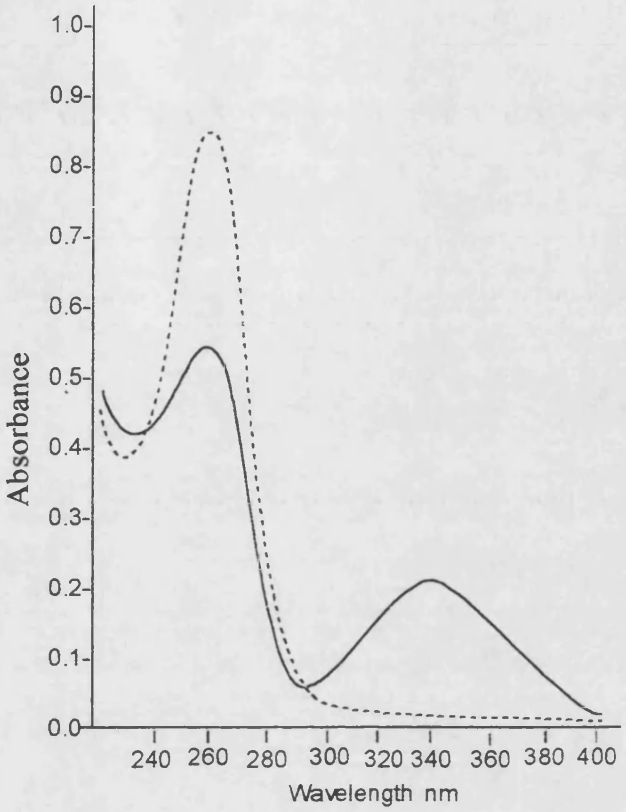

Figure 3.22: Schematic representation of the UV absorption spectrum of 2′$_A$-deoxy-NAD$^+$ (—) and change in the spectrum (----) after treatment of 2′$_A$-deoxy-NAD$^+$ with alcohol dehydrogenase in 5% ethanol.

iii) *Complex formation with Cyanide*

ii) Nicotinamide substituted in the ring nitrogen as in NAD$^-$ reacts with cyanide to form a cyanide adduct. This new adduct can be monitored by the emergence of a new peak at 325nm on the UV spectra. Complex formation of NAD$^-$ analogues with cyanide was performed as described previously [180].The reaction was monitored by UV and the appearance of the new cyanide adduct was recorded at 325nm for all analogues. This test with the assay for coenzyme activity confirmed the formation of NAD$^-$ type compounds.

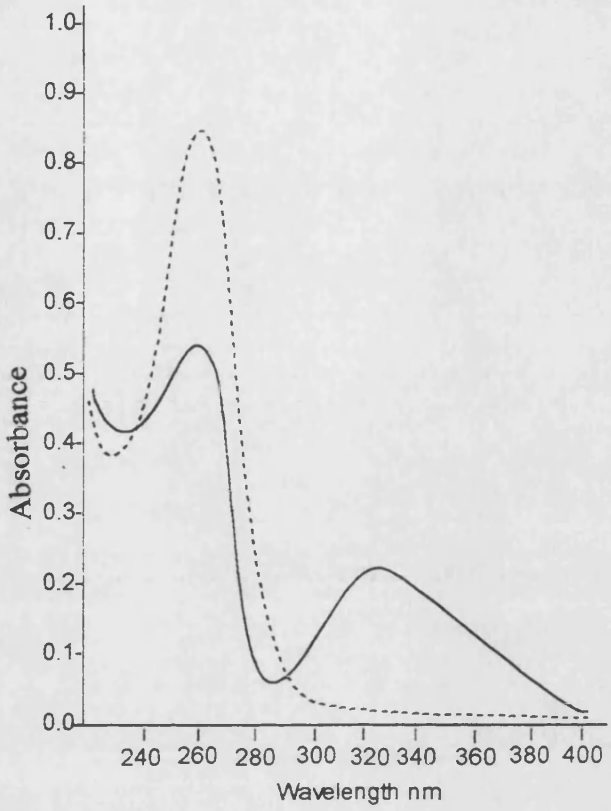

Figure 3.23: Schematic representation of the UV absorption spectrum of $2'_A$-deoxy-NAD^+ before treatment with KCN solution (—) and $2'_A$-deoxy-NAD^+ after treatment with KCN solution (—).

B) Quantitative Analysis

In most cases analogues were quantified by quantitative phosphate analysis [181] as described in the experimental section. The amount of phosphate in the sample can be calculated from the calibration curve obtained by analysis of a standard sample (KH_2PO_4) of known phosphate content. The extinction coefficient of each sample was calculated from the optical density of the known amount of sample in TEAB buffer at pH 8.3. In some cases were indicated in the experimental section, the extinction coefficient was obtained from literature values.

CHAPTER 4: SYNTHESIS OF ANALOGUES OF cADPR

4.1 Enzymatic Synthesis of cADPR

Enzymatic conversion of NAD^+ into cADPR was first achieved in 1987 [44] by the incubation of crude extracts of *Lytechinus pictus*, with NAD^+ for 3-7 hours at 17°C. Lee and co-workers used extracts from two species of sea urchin eggs (*Lytechinus pictus* and *Strongylocentrotus purpuratus*) for the preparation of cADPR, [then referred to as enzyme activated NAD^+ ($E\text{-}NAD^+$)] from NAD^+ [48]. The reaction was terminated at the end of the incubation period by the addition of an equal volume of acetone to precipitate the protein. The precipitated protein was removed by centrifugation, and the acetone was evaporated from the supernatant by a stream of nitrogen gas. This incubation was found to contain a multitude of metabolites, as the crude egg extracts contained too many other NAD^+ utilising enzymes. This caused difficulties in obtaining pure cADPR from the incubation mixture. Purification was achieved in two stages, first by a semi-preparative anion exchange column followed by purification of small volumes on an analytical reverse phase high performance liquid chromatography (HPLC) column. Partially purified ADP-ribosyl cyclase (the synthesising enzyme) was later prepared from dog brain extracts [46].

ADP-ribosyl cyclase has since been prepared from soluble extracts from the ovotestis of *Aplysia californica* [59] as there is an unusual abundance of this enzyme in this organism. Hence, enzymatic synthesis of cADPR was carried out by incubating partially purified

ADP-ribosyl cyclase with 2mM NAD^+ for 1-3 hours at 37°C (Fig 1.9). Separation of pure cADPR from the incubation mixture was achieved by preparative HPLC.

Another synthetic approache involved enzymatic cyclisation of N1-(5′-phosphoribosyl)-ATP catalysed by NAD^+ pyrophosphorylase (Fig 4.1). The yield via this method was about 4.7%. N1-(5′-Phosphoribosyl) ATP is predominantly in the protonated form at pH 7.5 so its β-N-glycosidic linkage resembles the NAD-like cation and thus , is accepted by NAD^+ pyrophosphorylase as a substrate to allow cyclisation into cADPR via a facile adenylyl transfer [182].

4.2 Chemical Synthesis of cADPR

Chemical synthesis of cADPR from NAD^+ has been reported by Yamada and co-workers[51]. Attempts at chemical synthesis of cADPR produced poor yields and the methods are unlikely to be useful for routine synthesis of cADPR analogues. Chemical cyclisation of β-NAD^+ by treatment with NaBr and triethylamine in DMSO at 70°C produced cADPR in 10% yield (Fig 4.2) Also traces of cADPR (<1%) have been noticed by treating N1-(5′-Phosphoribosyl) AMP with EDC in 1.5M Hepes buffer (pH 6.8) [182].

4.3 Analogues of cADPR

At the beginning of this work in May 1993, there was no known analogue of cADPR. However, over the years several analogues have been synthesised by other groups as well as from our group. The majority of modifications has been on the purine rings with only a few analogues possessing modifications in the ribose and pyrophosphate part of the

molecule in question. Below is a summary of other analogues that have appeared in publications, along with brief details on their biological activities. All the analogues have been synthesised by enzymatic cyclisation of an NAD^+ precursor using ADP-ribosyl cyclase.

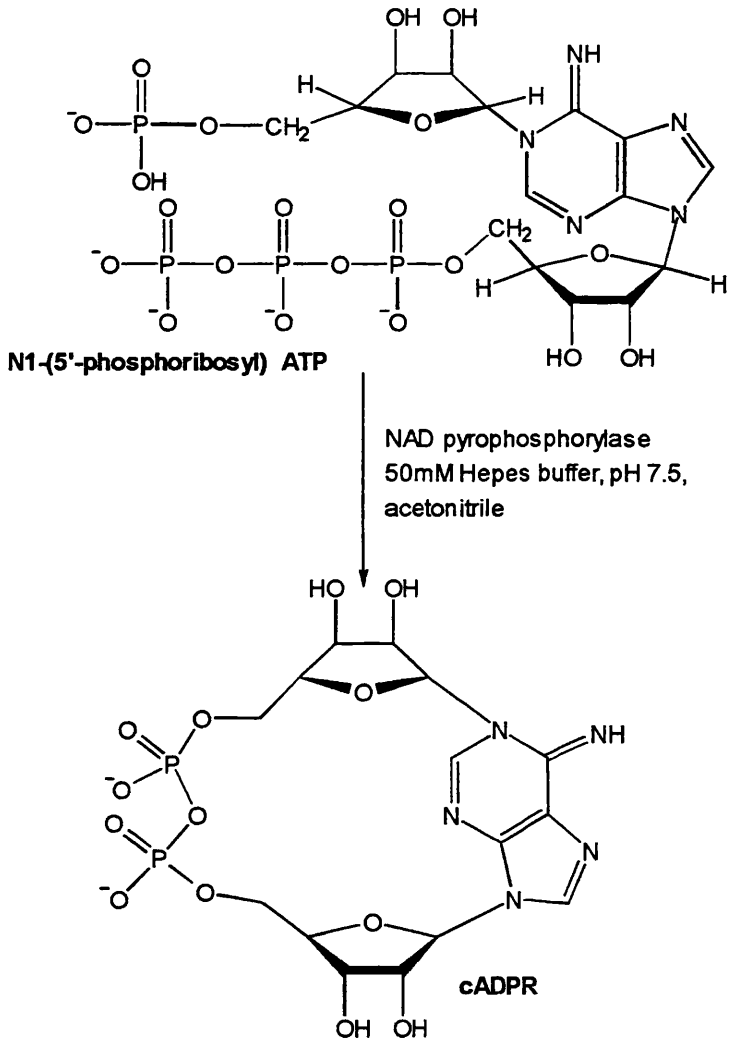

Figure 4.1: Synthesis of cADPR from N1-(5′-phosphoribosyl)-ATP

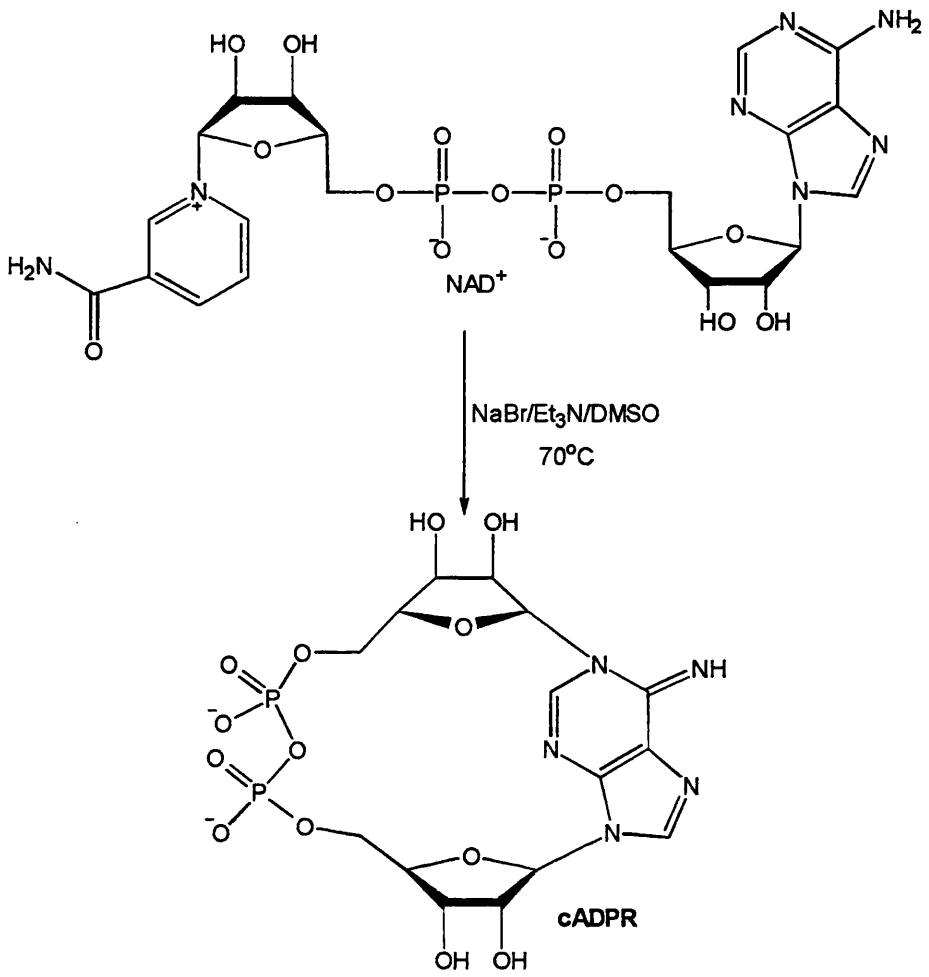

Figure 4.2: Chemical Cyclisation of β-NAD^+ into cADPR

4.3.1 *Antagonists of cADPR*

In August 1993, while this work was in progress, Walseth and co-workers reported the synthesis of 8-amino, 8-bromo and 8-azido-cADPR [120] (Fig 4.3). These analogues with small changes at the 8-position of the purine ring were shown to competitively inhibit cADPR-induced Ca^{2+} release in sea urchin eggs. The reason for this behaviour was not known, although the authors suggested that size of the group could be responsible for this activity. A change in size of the group from an hydrogen group to an amino-group (a difference of 15 atomic units) resulted in minimal change in the binding affinity compared to cADPR, but the analogue could not activate the release mechanism. However, further

increase in size to azido (42 atomic units) and bromo group (79 atomic units) resulted in substantial decrease in antagonist activity which may well be due to reduction in binding affinity of the analogues to the cADPR receptor due to steric hinderance. We have therefore decided to investigate the structural motif that is responsible for this activity by synthesis of analogues with different functional groups at position 8 of the adenine ring. Since then, we, in collaboration with a research group in Germany, have shown that exocyclic substitution at position 8 of the purine ring also produces analogues that inhibit cADPR-induced Ca^{2+} release in T-cells.

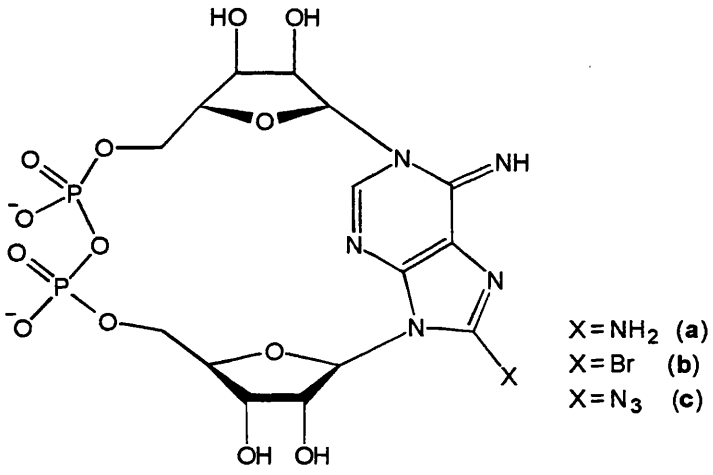

Figure 4.3: Structures of (a) 8-amino, (b) 8-bromo and (c) 8-azido-cADPR.

4.3.2 *Fluorescent analogues of cADPR*

Analogues in which the purine base adenine was replaced with other purine bases such as guanine, hypoxanthine, xanthine and an etheno-group have been synthesised [184,185]. Structural analysis of these analogues have shown that cyclisation is via N-7 linkage of the purine ring instead of N-1 as in cADPR (Figure 4.4). The UV spectral pattern of these analogues resembled those of N-7 alkylated purines. In contrast to cADPR, these analogues were found to be fluorescent. N7-Alkylated purines are known to be

fluorescent and show a pH-dependent spectral shift similar to those seen in the N7 substituted analogues synthesised. All the N7-substituted analogues are inactive (Fig 4.4). They do not induce Ca^{2+} release as they do not bind to the cADPR receptor. It is interesting that the same enzyme that catalyses the synthesis of cADPR from NAD^+ by linkage to the N1 position of adenine can also catalyse formation of the glycosidic link with the N7 position if for some reason the N1 position is electron deficient. Supporting evidence that ADP-ribosyl cyclase can cyclise the substrate at the N7 position comes from cyclisation of a NAD^+ analogue in which the N1 position is blocked, etheno-NAD^+ to yield cyclic 1, N^6-etheno-ADP-ribose [184,186]. The fact that the N1-linkage is preferred in the formation of cADPR would indicate that it is either chemically or sterically more reactive than N7. The keto group present at position 6 in all the fluorescent analogues (apart from etheno-analogue) is likely to render the N1 postion less reactive. The rate of formation of cADPR is faster than the rate of formation of these analogues. For example, the rate of formation of cADPR is 20 times faster than for cGDPR. The purine rings in these analogues are in the *anti*-configuration compared to *syn* in cADPR. They also exist in zwitterionic forms at neutral pH. Moreover the two ribose rings are linked via 4-bonds in cADPR, but the link is via two bonds in cGDPR, cIDPR, cXDPR and cHDPR (see Fig 4.4). This means that more bulk of the purine ring sticks out of the cyclic structure in the fluorescent analogue. The above may contribute to the inability of these analogues to bind to the receptor site.

A fluorimetric assay has been demonstrated in which these analogues can be used to study cyclisation and hydrolysis reactions. cGDPR is very resistant to hydrolysis [69].

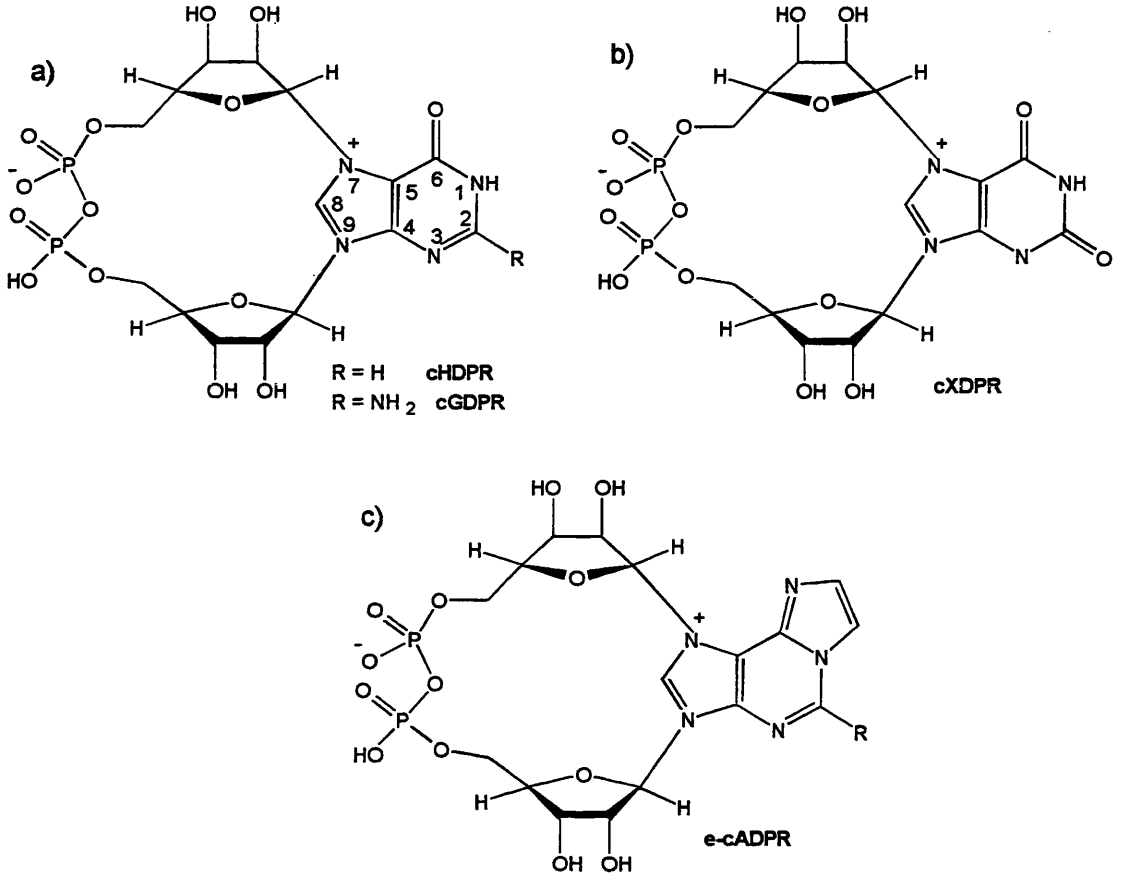

Fig 4.4: The proposed structures of the fluorescent analogues of cADPR[183]. cyclic Guanosine diphosphate ribose (cGDPR), cyclic Inosine diphosphate ribose (cIDPR), cyclic Xanthine diphosphate ribose (cXDPR), cyclic Hypoxanthine diphosphate ribose (cHDPR) and cyclic 1,N^6-etheno-ADPR (e-cADPR)..

4.3.3 *Poorly-Hydrolysable Analogues of cADPR*

Synthesis of another poorly hydrolysable, but active, analogue, cyclic aristeromycin diphosphate ribose (cArisDPR) has been reported [130]. This analogue has a similar Ca^{2+} release profile to cADPR in sea urchin homogenates, but was shown to have a $t_{1/2}$ value of 170min compared to 15min for cADPR. The adenosine ribose moiety in cArisDPR is replaced by a carbocyclic ring. Carbocyclic rings are known to confer more stability to the glycoside bond which is normally labile, however in this case the ribose ring is far removed from the site of hydrolysis. The authors suggest that this effect could be due to

conformational changes in the way cArisDPR binds to the receptor site of the hydrolase, making attack of a water molecule more difficult.

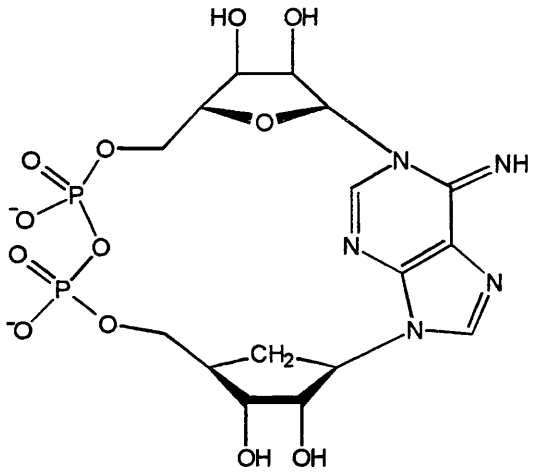

Figure 4.5: Cyclic aristeromycin diphosphate ribose (cArisDPR)

Synthesis of cyclic ATP-ribose, an analogue of cADPR in which the diphosphate is replace by a triphosphate has been reported [186]. This analogue is about 20 times more potent compared to cADPR in releasing Ca^{2+} in rat brain microsomes and was more stable compared to cADPR in buffers at different pH values. The effect of this analogue in sea urchin egg homogenate has not yet been reported. Replacement of the diphosphate bridge in cADPR with a triphosphate ring is likely to confer more flexibility to the molecule. This may account for increase in stability of this analogue. The stability of cATPR toward enzymatic cleavage was also investigated [186]. cATPR was more stable than cADPR when incubated with pig brain NADase at 37°C for 40 min. After 40 min, 80% of cADPR was hydrolysed whereas only 30% of cATPR was hydrolysed under the same conditions. Poorly hydrolysable and ultimately non-hydrolysable analogues will be

useful in exploring novel activities of cADPR. It should be easier to isolate and characterise cADPR-binding proteins using more stable analogues as affinity probes.

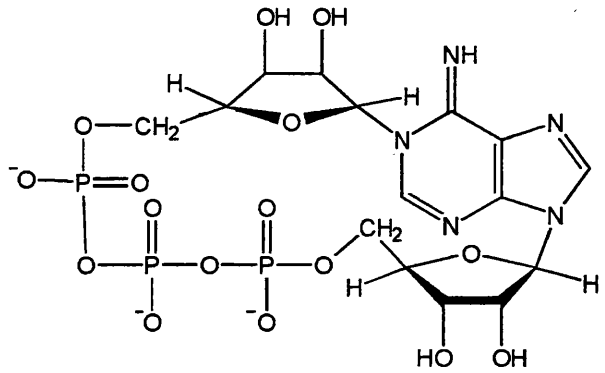

Figure 4.6: Cyclic adenosine triphosphate ribose

4.3.4 *2′$_A$-cADPRP, 3′$_A$-cADPRP and 2′$_A$,3′$_A$-cyclic-cADPRP*

We have synthesised 2′$_A$-cADPRP, 3′$_A$-cADPRP and 2′$_A$,3′$_A$-cADPRP, however while this work was in progress, synthesis of 2′$_A$-cADPRP was also reported by various research groups [126,127,131]. Synthesis is via enzymatic cyclisation of $NADP^+$ (see section 1.5) by ADP-ribosyl cyclase. 2′$_A$-cADPRP is inactive in sea urchin eggs but is more potent compared to cADPR in mobilising Ca^{2+} in rat brain microsomes [131] and in T-cells[187]. This is the first indication that there may be different structural requirements for cADPR-induced Ca^{2+} release in sea urchin compare to rat brain microsomes and T-cells. Vu and co-workers showed that $NADP^+$ is a better substrate compared to NAD^+ for the cyclase indicating that *in vivo* conversion of $NADP^+$ to 2′$_A$-cADPRP is likely [127]. The mechanism of Ca^{2+} release by 2′$_A$-cADPRP is similar to that of cADPR. 3′$_A$-cADPRP and 2′$_A$,3′$_A$-cyclic-cADPRP were synthesised from their corresponding NAD^+ analogues 3′$_A$-$NADP^+$ and 2′$_A$,3′$_A$-cyclic-$NADP^+$ and shown to be inactive in rat brain

microsomes [131]. However, the effects of $3'_A$-cADPRP and $2'_A,3'_A$-cyclic-cADPRP in sea urchin homogenates and T-cells have not yet been reported and we aimed to address this.

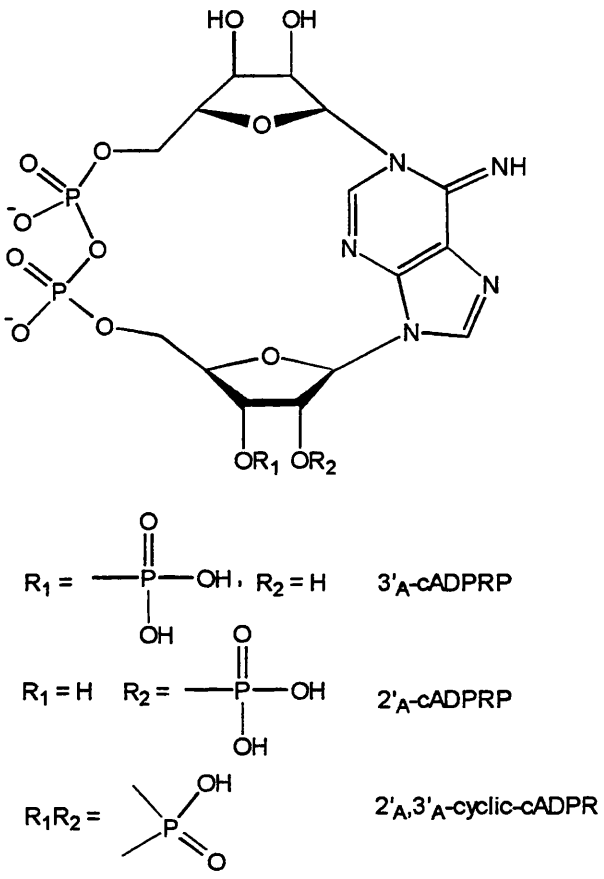

Figure 4.7: Structures of $2'_A$-cADPRP, $3'_A$-cADPRP and $2'_A,3'_A$-cADPRP

4.3.5 *Caged cADPR*

Caged cADPR was synthesised by reacting cADPR with 2-nitrophenethyldiazoethane[188]. The product obtained was inactive and could induce Ca^{2+} release from sea urcin egg homogenates only after photolysis. The availability of caged cADPR should eliminate problems encountered in investigating Ca^{2+} mobilisation induced by cADPR. For example, Ca^{2+} leakage during micro-injection could be mistaken

as Ca^{2+} release by cADPR. Ca^{2+} release by caged cADPR is induced by UV photolysis, eliminating the possible injection artefact. Moreover, increase in hydrophobicity due to the caging group could increase permeability of caged cADPR into cells.

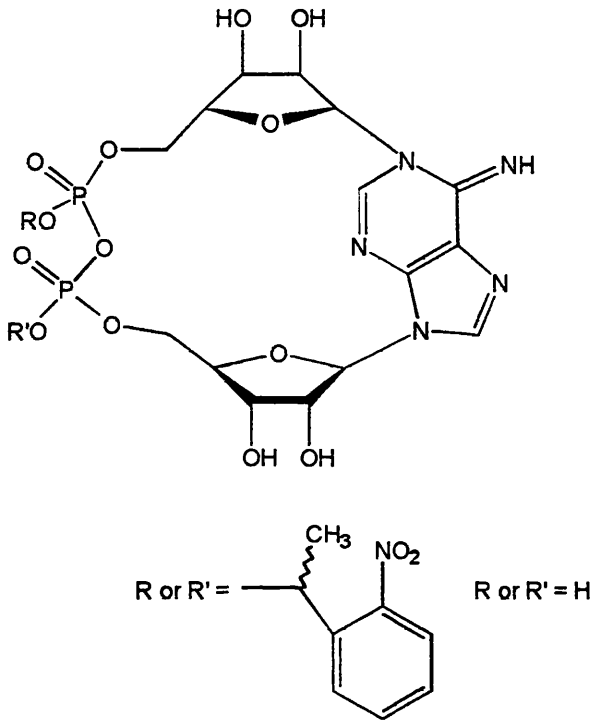

Figure 4.8: The proposed structure of mono-caged cADPR regioisomers.

4.4 Results and Discussion

4.4.1 *2′A and 3′A-Modified cADPR Analogues*

A) 2′A and 3′A-hydroxyl deleted analogues of cADPR

In order to study the role of the ribose hydroxyl groups, our first step was to synthesise 2′A and 3′A-deoxy analogues of cADPR. Biological testing of these compounds would give a clue toward the importance of the 2′A and 3′A ribose hydroxyl groups respectively in the Ca^{2+} releasing activity of cADPR. ADP-ribosyl cyclase catalysed the conversion

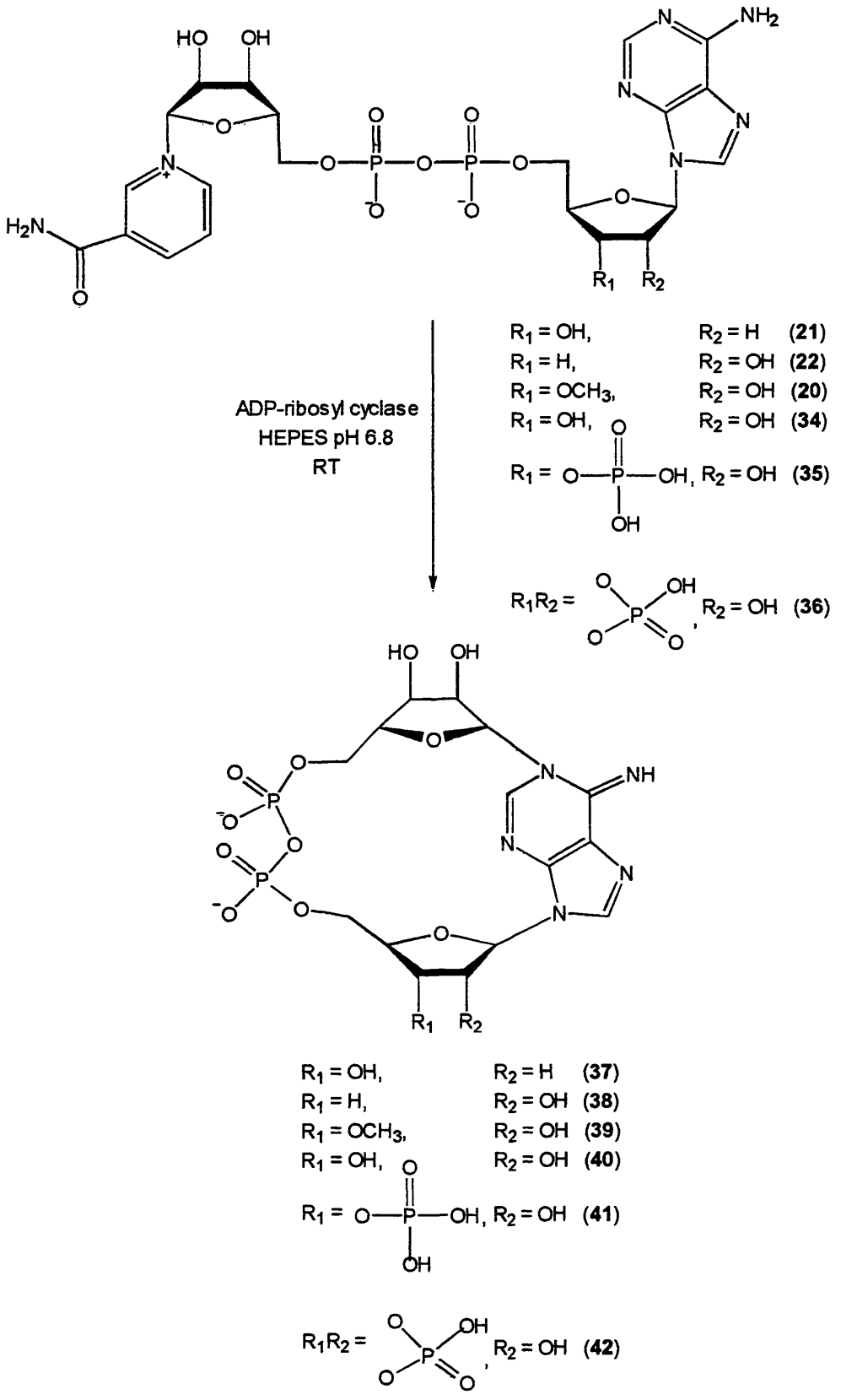

Figure 4.9: $2'_A$ and $3'_A$-Modified Analogues of cADPR

of 2′-deoxy (**21**) and 3′-deoxy-NAD^+ (**22**) to 2′-deoxy (**37**) and 3′-deoxy-cADPR (**38** - Fig 4.9) respectively. For comparison, cADPR (**40**) was also synthesised from NAD^+ (**34**). The products from the synthesis were as expected. HPLC analysis of the reaction mixture showed two new peaks after conversion to the cyclic product in all cases. The first peak corresponded to nicotinamide, followed by residual starting material and finally the cyclised product. In some cases, an extra peak corresponding to the hydrolytic product of the cADPR analogue (Fig 4.10) e.g. $2'_A$-deoxy-ADPR could be recorded on the chromatogram. This degradation product, produced by spontaneous breakdown of the material in an aqueous medium, can be easily removed by ion exchange purification. ^{1}H-NMR spectroscopy showed the disappearance of the nicotinamide protons [compare Fig. 3.10 (a) to Fig. 4.11 (a)]. ^{1}H and ^{31}P-NMR of cADPR were similar to those reported previously. Differences in proton chemical shifts and signal obtained from the ^{1}H-NMR spectum of $2'_A$-deoxy-cADPR and cADPR include the H_A1' signal which was downfield from H1′ and appeared as a triplet as it coupled to two H_A2' protons in the former, but in $3'_A$-deoxy and cADPR, H1′ appeared downfield from the H_A1' proton. A characteristic H_A2' proton at δ 5.2ppm was observed in cADPR, however in H_A2' protons resonated at a lower frequency - δ 3.2 and 2.4 ppm as a multiplet. H_A2' appeared as a multiplet at δ 5.2ppm in $3_A'$-deoxy-cADPR and the two H_A3' protons resonated at a lower frequency - δ 2.8 and 2.1ppm compared to δ 4.7 and 4.8 ppm in cADPR and $2_A'$-deoxy-cADPR respectively. This is consistent with the loss of the deshielding effect from the neighbouring hydroxyl group. AB Type signals in the ^{31}P-NMR spectra of cADPR, $2_A'$ and $3_A'$-deoxy-cADPR support the existence of the pyrophosphate group. There is a decrease of ca. 5Hz in J_{AB} values of cADPR and

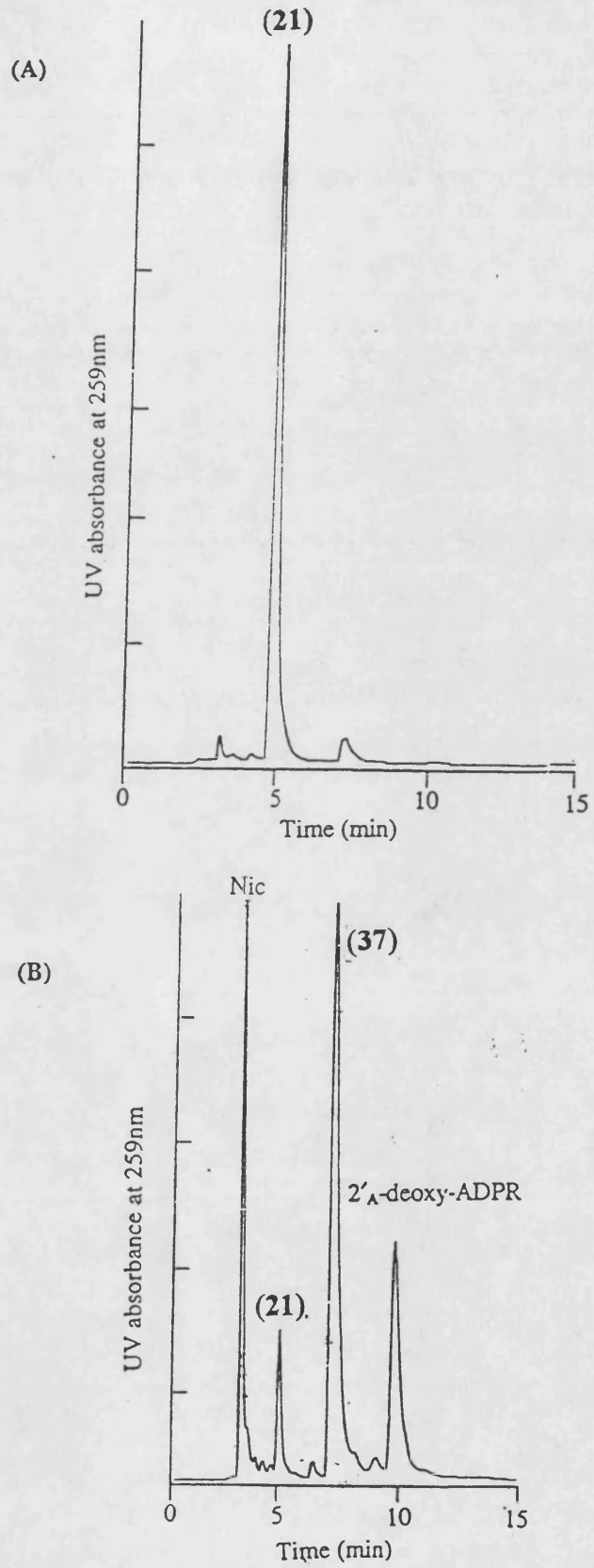

Figure 4.10: HPLC analysis of the cyclisation of $2'_A$-deoxy-NAD^+ (21). (A) HPLC analysis of $2'_A$-deoxy-NAD^+ as the starting material, (B) HPLC analysis of the products obtained 10mins after incubation of $2'_A$-deoxy-NAD^+ with crude ADP-ribosyl cyclase – nicotinamide (Nic), $2'_A$-deoxy-cADPR (37) and $2'_A$-deoxy-ADPR.

a)

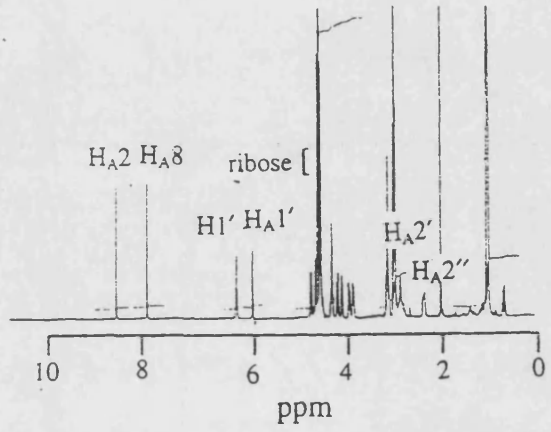

b)

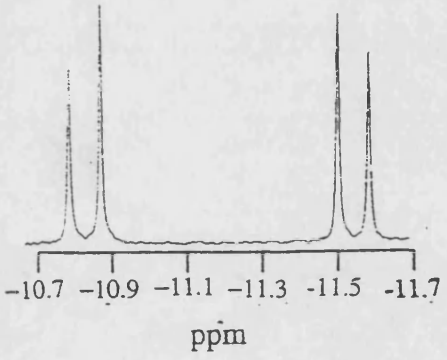

Figure 4.11: (a) ^{1}H-NMR (400MHz, D_2O) and (b) ^{31}P-NMR (162MHz, D_2O) spectra for 2′$_A$-deoxy-cADPR as its triethylammonium salt.

analogues from the corresponding NAD^+ precursor. FAB-MS of of $2_A'$ and $3_A'$-deoxy-cADPR showed a *m/z* peak of 524 for the negative ion $[M-H]^-$. *m/z* value of 1049 $[2M - H]^-$ were characteristic for both deoxy forms showing possible formation of dimeric structures. This was, interestingly, not observed in the mass spectrum of cADPR. All three compounds showed a UV absorption maximum at 259nm.

Relative rates of turnover and the affinity of the enzyme for the substrates were compared by kinetic studies. The kinetic parameters of the *Aplysia* cyclase for NAD^+, $2'_A$-deoxy-NAD^+ and $3'_A$-deoxy-NAD^+ were determined using an HPLC method. K_m and V_{max} values were obtained from the Lineweaver-Burk plot using the Enzpack3 computer programme. A representative plot is shown in Fig. 4.12 for $3'_A$-deoxy-NAD^+. K_m values obtained were 75.2μM, 0.7mM and 0.5mM for NAD^+, $2'_A$-deoxy-NAD^+ and $3'_A$-deoxy-NAD^+ respectively. V_{max} values obtained were 23.3, 47.9, 22.4μmol/mg/min. Hence the enzyme has a higher affinity for the natural substrate NAD^+. The affinity of the cyclase for NAD^+ is approximately 10 times better and 7 times higher compared to $2'_A$-deoxy-NAD^+ and $3'_A$-deoxy-NAD^+ respectively. While the specific activity of the enzyme for NAD^+ and $3'_A$-deoxy-NAD^+ appears similar, the turnover rate for $2_A'$-deoxy-NAD^+ appears to be twice that of NAD^+. This shows that, as expected, the relative turnover rate for NAD^+ (the natural substrate) is somewhat faster (though not significantly) compared to $2_A'$-deoxy-NAD^+ and $3_A'$-deoxy-NAD^+. This shows that the ribose hydroxyl groups are important although not crucial for binding to the active site of the cyclase. Removal of the ribose hydroxyl groups results in analogues with lesser affinity for the binding site of ADP-ribosyl cyclase. The K_m determination for NAD^+ as determined by Graeff and co-workers was 39μM [69]. This is of the same order as the

value obtained here, 75.2μM. Differences in the assay conditions used, such as buffers and buffer concentrations could be accountable for the difference in the K_m values obtained. Also, we have taken time points every minute over 6 mins and calculated initial velocity from the slope of a plot of relative area vs time. Graeff and co-workers took two time points, after 0 and after 3 min.

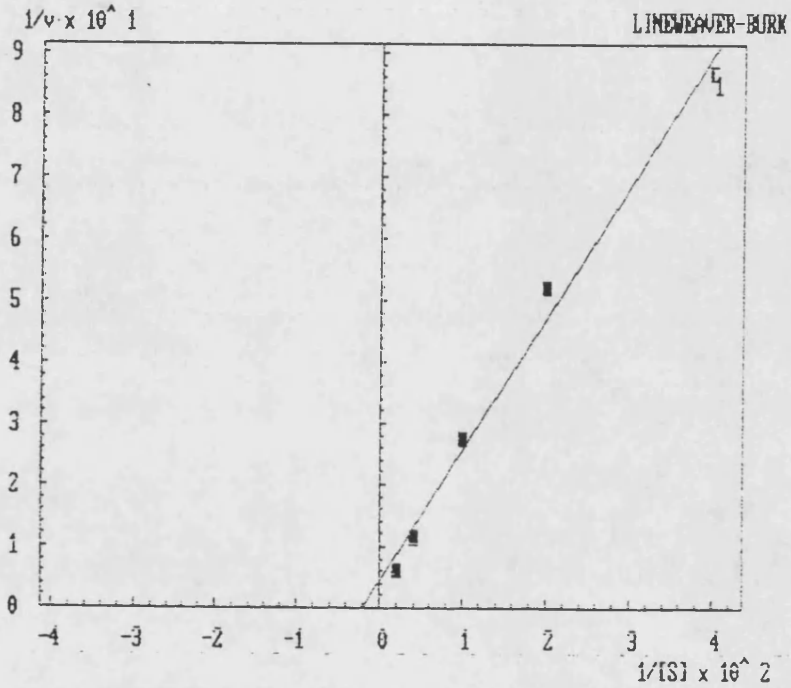

Figure 4.12: Lineweaver-Burk plot for 3′$_A$-deoxy-NAD$^+$. The *y* axis represents 1/V (μmol^{-1}mg-min) and the *x* axis represents 1/S (μmol^{-1}).

B) 3′$_A$-*O*-Methyl-cADPR

To further investigate the role of the 3′$_A$ ribose hydroxyl group, 3′$_A$-*O*-methyl-cADPR (**39**) was synthesised. In this molecule, a methyl group replaces the hydrogen group. The –OMe group, unlike the –OH group which can accept and donate an H-bond, can accept, but cannot donate a hydrogen bond, hence biological testing of this molecule will, in principle, be a pointer to the type of H-bonding interaction that is likely to occcur at the cADPR receptor site taking into account possible newly introduced steric constraints. Partially purified 3′$_A$-*OMe*-NAD$^+$ (**20**) obtained (see section 3.3.1B) was

cyclised by ADP-ribosyl cyclase to yield $3'_A$-*OMe*-cADPR (**39** -Fig 4.9). Pure cyclic product was obtained upon ion exchange purification as shown by HPLC analysis, ^1H and ^{31}P-NMR spectroscopy. ^1H-NMR spectroscopy identified all the purine protons and ribose protons. The signal for the ribose *O*-methyl protons appeared at δ 3.4ppm as expected. There were no signals corresponding to nicotinamide protons indicating that the nicotinamide ring has been lost. Replacement of the hydrogen of the hydroxyl group by a methyl group as in this compound appears to result in a slight hypsochromic effect on the wavelength. There was a shift in the absorption maxima from 259 to 256nm. -ve ion FAB-MS showed an *m/z* peak of 554$[M-H]^-$ corresponding to a molecular weight of 555 for this analogue.

C) $3'_A$-cADPRP

$3'_A$-cADPRP (**41**) contains a phosphate group at the $3_A'$ position (see Fig 4.9). It was synthesised to establish the effect of a charged phosphate group at this position relative to a neutral methyl group and furthermore to investigate the possiblity of an electrostatic interaction between the phosphate anion and the cADPR receptor site. It was prepared from the commercially available $3'_A$-$NADP^+$ (**35**), by cyclisation with ADP-ribosyl cyclase. This analogue was a substrate for the cyclase. HPLC analysis of the reaction mixture showed the production of nicotinamide. The cyclised product and the NAD^+ precursor co-eluted from the HPLC column with the same retention time of 15.9 min. However, it was easy to separate the desired product, $3'_A$-cADPRP, from the crude mixture on an anion exchange column using buffer at pH 7.6. ^{31}P-NMR spectroscopy showed that the monophosphate was intact and the signal was observed at δ 1.0ppm. The pyrophosphate was also intact as an AB system and was seen at δ ~ -11ppm

(Fig.4.13a). FAB-MS in both +ve and -ve ion modes along with accurate MS confirmed the molecular weight of the product as 621 consistent with an increase in mass by 80 atomic mass units compared to cADPR.

D) $2'_A,3'_A$-cyclic-cADPRP

To investigate the effect of having a phosphate bridge across the $2'_A$ and $3'_A$ position, $2'_A,3'_A$-cADPR was prepared. $2'_A,3'_A$-cyclic-cADPRP (**42**) were prepared from the commercially available $2'_A,3'_A$-cyclic-$NADP^+$ (**36** - Fig 4.9). ADP-ribosyl cyclase catalysed the conversion of $2'_A,3'_A$-cyclic-$NADP^+$ to the cyclised product with loss of nicotinamide. HPLC analysis of the reaction mixture showed the appearance a new peak corresponding to nicotinamide. The cyclised product and $2'_A,3'_A$-cyclic-$NADP^+$ eluted off the HPLC column with the same retention time under the conditions used for HPLC analysis. However, separation of the pure desired product from the crude mixture was achieved by purification on an anion exchange column using a buffer gradient at pH 7.6. Spectroscopic analysis showed that the product synthesised was authentic. ^{31}P-NMR spectroscopy showed the cyclic phosphate at δ +19 as a singlet and the pyrophosphate at δ ~-11ppm as an AB system (Fig. 4.13b). FAB-MS in both the +ve ion and the -ve ion mode with accurate mass analysis identified that the product has a molecular mass of 603 which is true of an increase in molecular weight by 62 compared to cADPR.

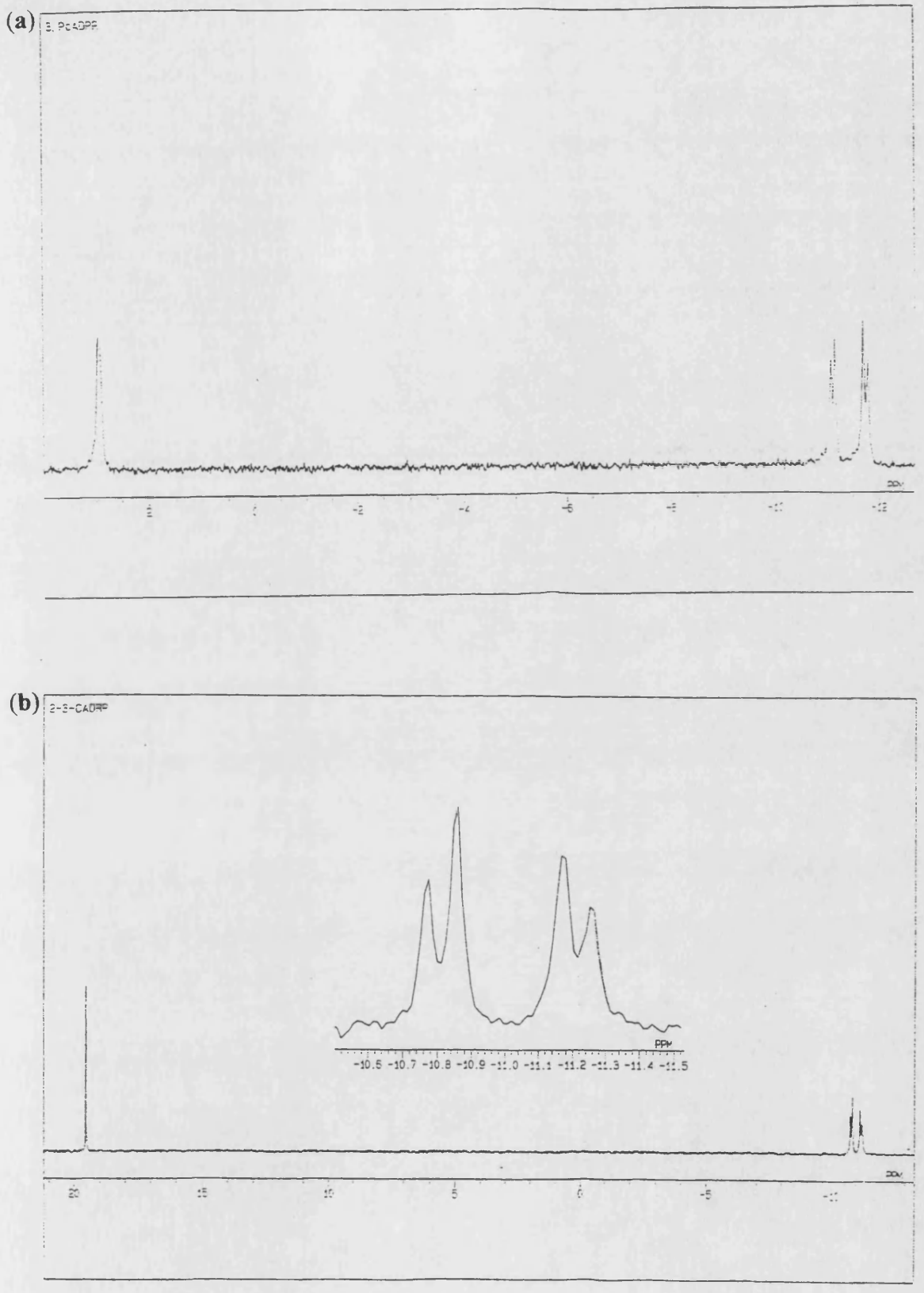

Figure 4.13: ^{31}P-NMR (162MHz, D_2O) spectra for (a) $3'_A$-cADPRP and (b) $2'_A,3'_A$-cADPRP

4.4.2 *8-Modified Analogues of cADPR*

8-Substituted analogues of cADPR were synthesised in order to study initially the effect of replacement of the hydrogen by groups such $-NH_2$ and $-CH_3$. While this work was in progress a paper appeared[120] that showed that replacement of the H_A8 with an amino, bromo or azido group converted the activity of the molecule from an agonist to an antagonist, of which 8-amino-cADPR was the most potent. The reason for this effect was however unclear. In order to attempt identifying the feature of the 8-substituent that is required for converting the cADPR molecule to an antagonist, several analogues of 8-substituted-cADPR analogues have been produced (Fig 4.10). The hydrophilic character of the amine substituent and molecular volume was varied by synthesising 8-NHMe **(44)**, 8-NMe_2 **(45)** and 8-piperidyl-cADPR(47). Replacement of the amine group was made by $-CH_3$ and an oxy group. The methyl group cannot form a H-bond, hence 8-CH_3-cADR would be useful in establishing whether H-bond interaction at position 8 of the purine ring is crucial for antagonist activity. Substitution with a $-OCH_3$ group **(46)** provides an analogue that can only accept a H-bond (the $-NH_2$ group can both accept and donate a H-bond). These analogues were all prepared from their 8-substituted NAD^+ precursors (Fig 3.11, 3.12). All the 8-substituted analogues of NAD^+ were substrates for the cyclase. The relative rates of conversion, though not investigated in detail here, appear to be similar in most cases apart from 8-CH_3-cADPR **(49)** which appears to be turned over faster and in greater yield than other analogues (see experimental section). In all cases, the formation of the product was followed by HPLC analysis. Two new peaks corresponding to nicotinamide and cyclised product were obtained in all cases. Purification by anion exchange chromatography afforded pure

product. Typically, the starting material eluted first, followed by the cyclised product and finally the linear form (ADPR analogue).

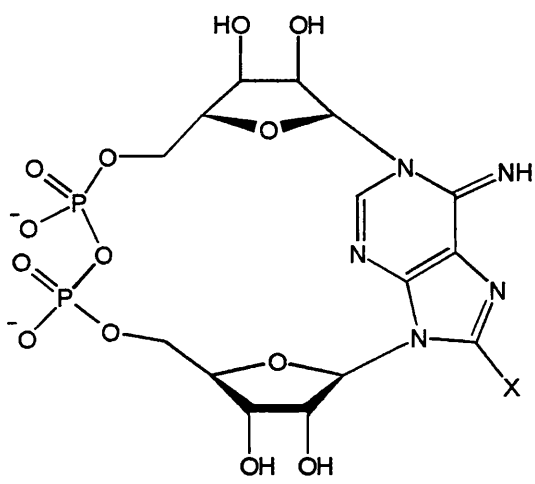

X= Br (**43**) X= NH_2 (**48**)
X= $NHCH_3$ (**44**) X= CH_3 (**49**)
X= $N(CH_3)_2$ (**45**)
X= OCH_3 (**46**)
X=  (**47**)

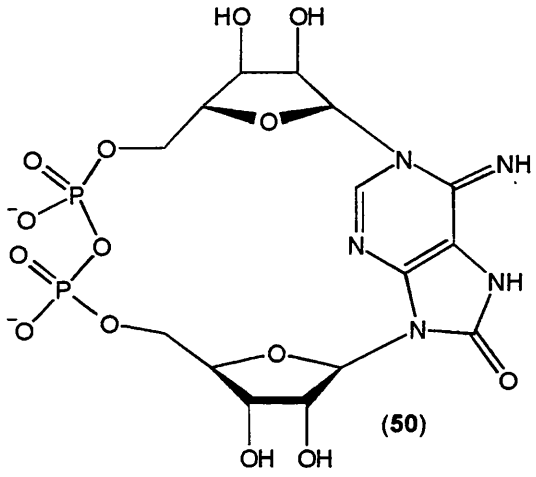

(**50**)

Figure 4.14: 8-Modified analogues of cADPR . Structures of 8-bromo-cADPR (**43**), 8-methylamino-cADPR (**44**), 8-dimethylamino-cADPR (**45**), 8-methoxy-cADPR (**46**), 8-piperidyl-cADPR(**47**), 8-amino-cADPR (**48**), 8-methyl-cADPR (**49**) and 8-oxy-cADPR(**50**). These were synthesised from 8-bromo-NAD^+ (**24**), 8-methylamino-NAD^+ (**25**), 8-dimethylamino-NAD^+ (**26**), 8-methoxy-NAD^+ (**27**), 8-piperidyl-NAD^+ (**28**), 8-amino-NAD^+ (**29**) 8-methyl-NAD^+ (**30**) and 8-oxy-NAD^+ (**31**) respectively (see Fig 3.11).

The cADPR analogue in water hydrolyses slowly in solution at room temperature to give the linear product. This can easily be removed by purification on the anion exchange column.

(a)

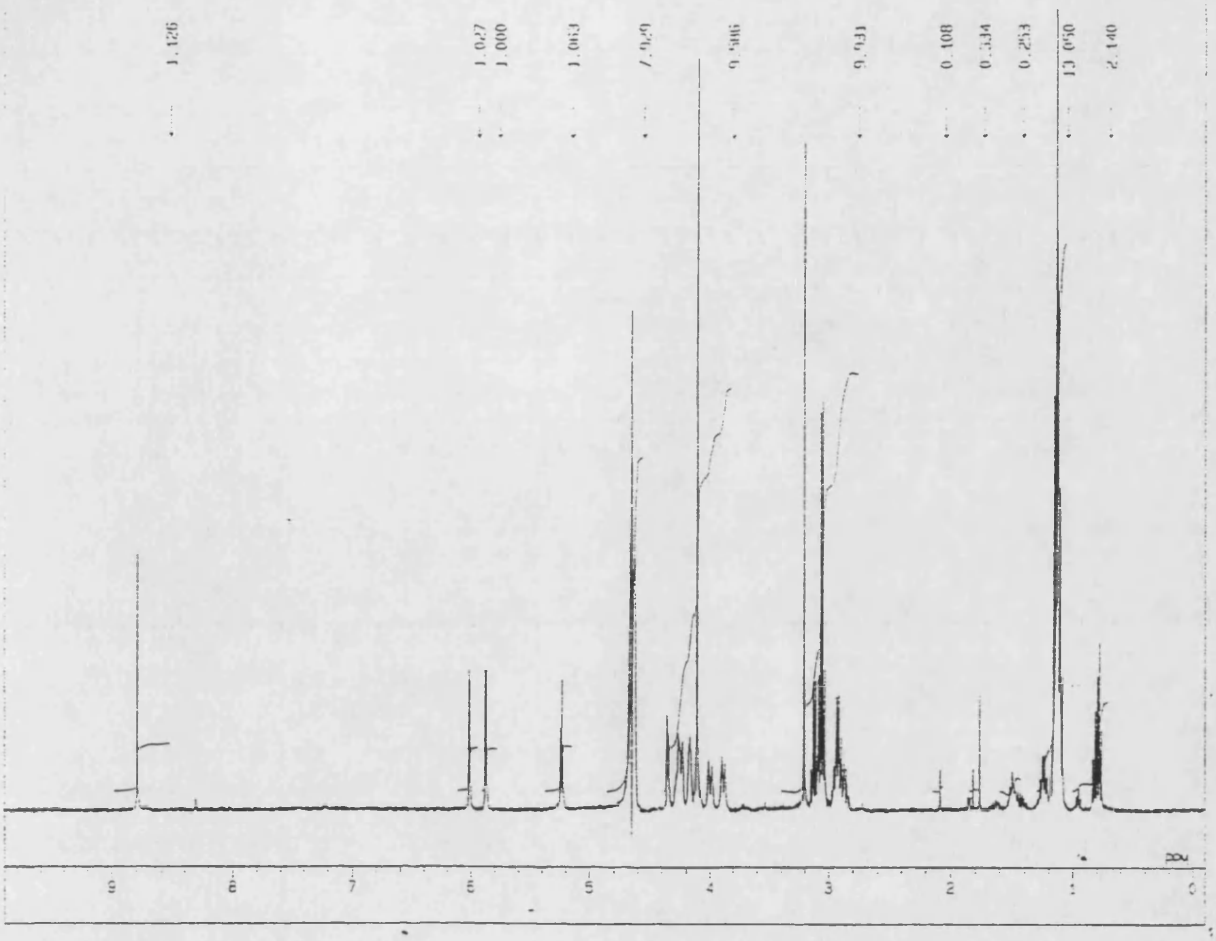

(b)

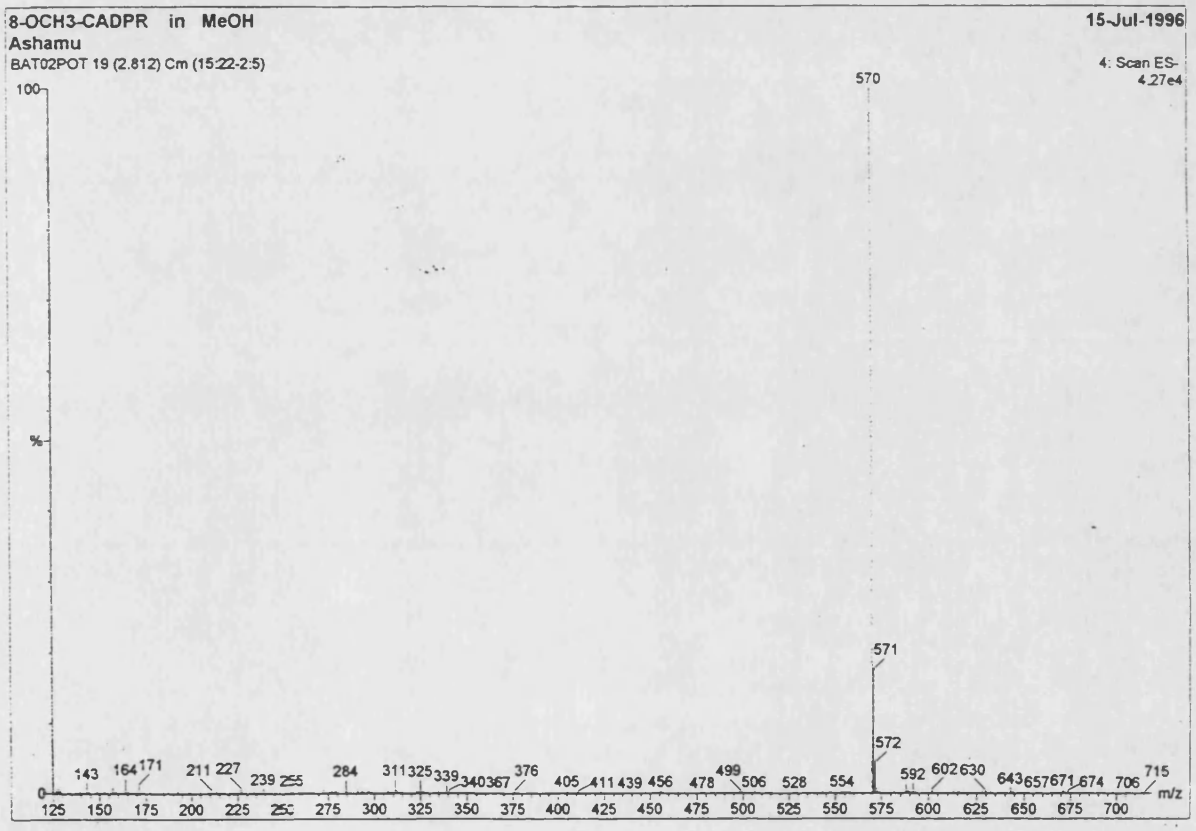

Figure 4.15: (a) ^{1}H-NMR (400MHz, D_2O) and (b) Electrospray mass spectra of 8-OCH_3-cADPR as its triethylammonium salt.

^{31}P-NMR spectroscopy showed the existence of a pyrophosphate in the molecule by an AB signal in most cases at δ ~11ppm. Interestingly, in the case of 8-OCH_3-cADPR the ^{31}P-NMR showed a signal in the pyrophosphate region as a singlet. However, it is clear from the ^{1}H-NMR data and mass spectroscopic data that 8-OCH_3-cADPR was synthesised.

All the above modifications were exocylic. 8-Aza-9-deaza-cADPR was synthesised to investigate the effect of modification in the purine ring on the Ca^{2+} release activity. The synthesis was via the NAD^+ precusor NFD^+ (**33** -Fig 3.13) prepared by chemical coupling of formycin 5′-monophosphate with NMN. NFD^+ was cyclised by ADP-ribosyl cyclase to 8-aza-9-deaza-cADPR (**50** -Fig 4.11). ^{31}P and ^{1}H-NMR analysis with mass spectroscopy supports the fact that cFDPR was synthesised. Furthermore, the UV absorption maximum at 295nm supports the presence of a pyrazolo ring.

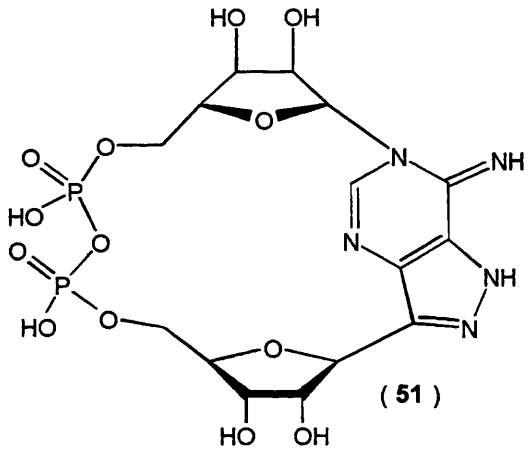

(**51**)

Figure 4.16: 8-aza-9-deaza-cADPR (cFDPR)

4.5 Characterisation of cADPR analogues

cADPR analogues, like NAD^+, are of low volatility and high polarity. Hence electrospray and FAB-MS were chosen for mass analysis. Electrospray mass spectroscopy appear to be most suitable for this type of compounds as it appeared from FAB-MS analysis that the analogues appear to decompose prior to ionisation leading to a low abundance of the molecular ion. ^1H and ^{31}P-NMR spectroscopy were employed for routine characterisation of analogues. 2D-^1H-^1H COSY experiments were also used

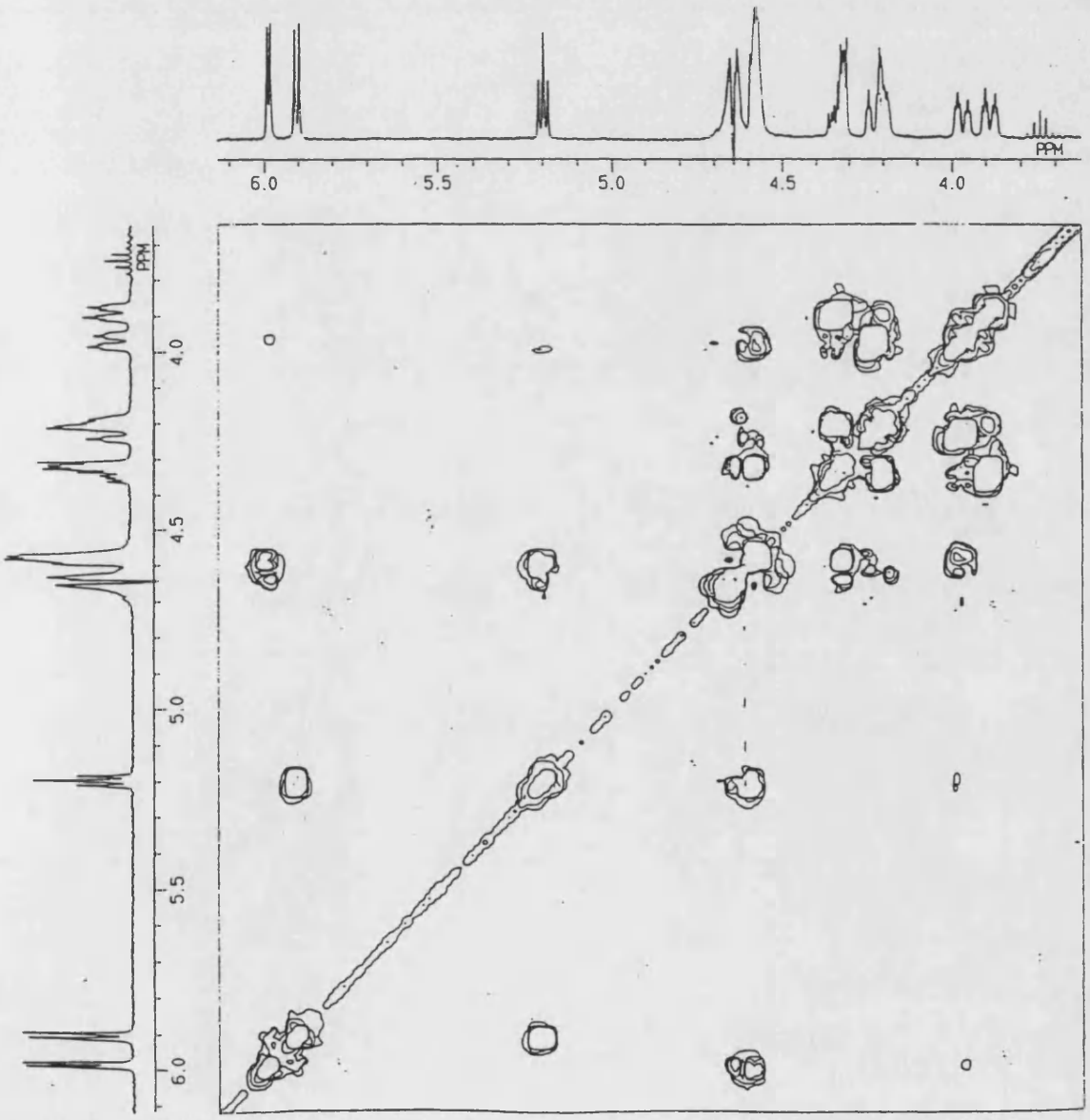

Figure 4.17: ^1H-^1H COSY of cADPR in D_2O.

to identify the ribose protons (Fig. 4.17). UV absorption spectroscopy was used to record the spectroscopic pattern of the analogues.

4.6 Purification, Qualitative and Quantitative Analysis of cADPR analogues

The analytical methods used for cADPR analogues were similar to those used for NAD^+ analogues (Chapter 3). Purification was carried out on an anion exchange chromatographic column at pH 7.6 where cADPR analogues in all cases are likely to have one extra negative charge compared to NAD^+ analogues making separation on a basis of charge possible. A representative chromatogram obtained from the ion-

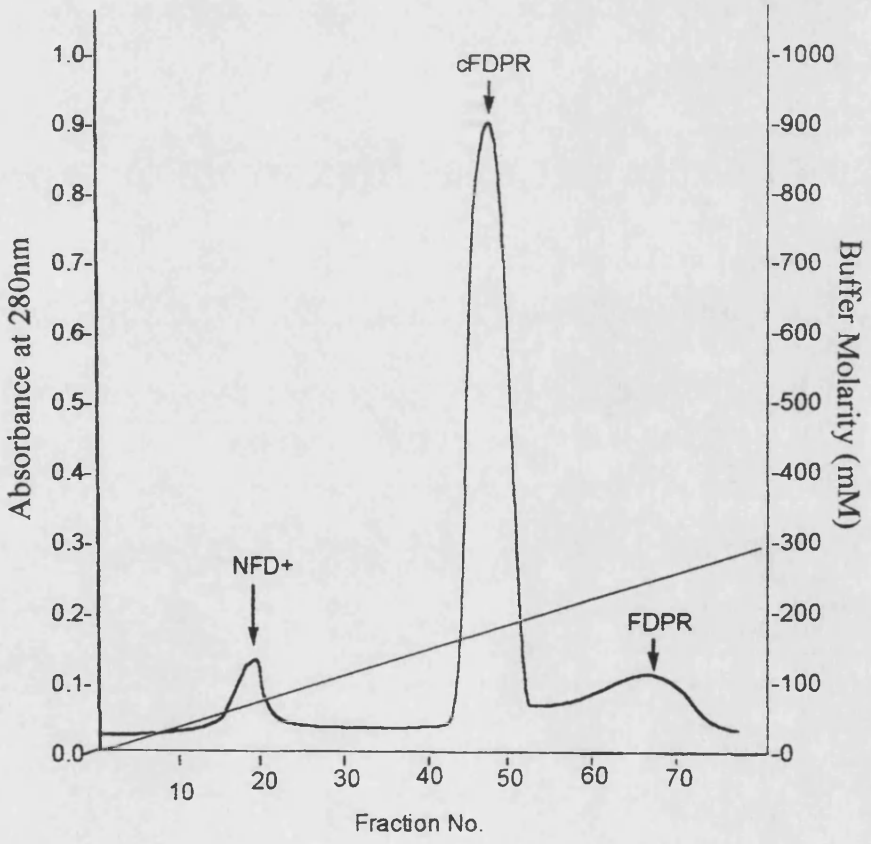

Figure 4.18: A schematic representation of the ion-exchange chromatogram obtained from the purification of cFDPR on a Sepharose Q column.

exchange purification of the product obtained form cyclisation of NFD^+ is illustrated in Fig. 4.18. The cyclic product can also be separated from the linear form, ADPR by this method even though they are likely to carry the same charge under the condition used for purification. The analysis of reaction products was carried out on an anion exchange HPLC column. Separation was also on the basis of charge and the size of the molecule is likely to play a role as well, as the cyclic product could also be separated from the linear form even though they are likely to carry the same amount of charge under the experimental conditions for HPLC analysis. The purity of the final products was judged by HPLC analysis and NMR spectroscopy .

Quantitative analysis was carried out by total phosphate analysis as described in experimental section [181]. This, in combination, with UV spectroscopy was used to obtain quantitative data on the analogues.

CHAPTER 5: BIOLOGICAL EVALUATION OF cADPR ANALOGUES

Several analogues of cADPR were synthesised with modification on the adenine ribose moiety as well as in position 8 of the adenine ring as discussed in chapter 4, were used to investigate the structure-activity relationships of cADPR. Analogues were tested in two systems, sea urchin egg homogenates and in permeabilised Jurkat T-cells as described in the experimental section. The biological activities of the analogues were compared to those of cADPR and the effect of each analogue on cADPR induced release were also investigated.

5.1: Results and Discussion

5.1.1 Biological evaluation of 2′$_A$ and 3′$_A$-Modified cADPR on Ca^{2+}-release in sea urchin eggs

A) 2′$_A$-deoxy-cADPR, 3′$_A$-deoxy-cADPR and 3′$_A$-*O*-Methyl-cADPR

Two hydroxyl deleted analogues, 2′$_A$ and 3′$_A$-deoxy-cADPR were used to study the effect of 2′$_A$ and 3′$_A$-hydroxyl group in the adenine moiety of cADPR on the Ca^{2+}-releasing potential of cADPR. These two analogues like cADPR were agonists but exhibited comparatively different activities as agonists for Ca^{2+} mobilisation in sea urchin egg homogenates. EC_{50} values were estimated to be 32nM, 58nM and 5μM for cADPR, 2′$_A$-deoxy-cADPR and 3′$_A$-deoxy-cADPR respectively. 2′$_A$-Deoxy-cADPR was similar in activity to cADPR, whereas, 3′$_A$-deoxy-cADPR was at least a hundred fold less potent, indicating that the 3′$_A$-hydroxyl group, but not the 2′$_A$-hydroxyl group is essential for calcium releasing activity. A dramatic difference is observed from the dose response curve of these two analogues(see Fig 5.1). There is a shift of the curve to the right with

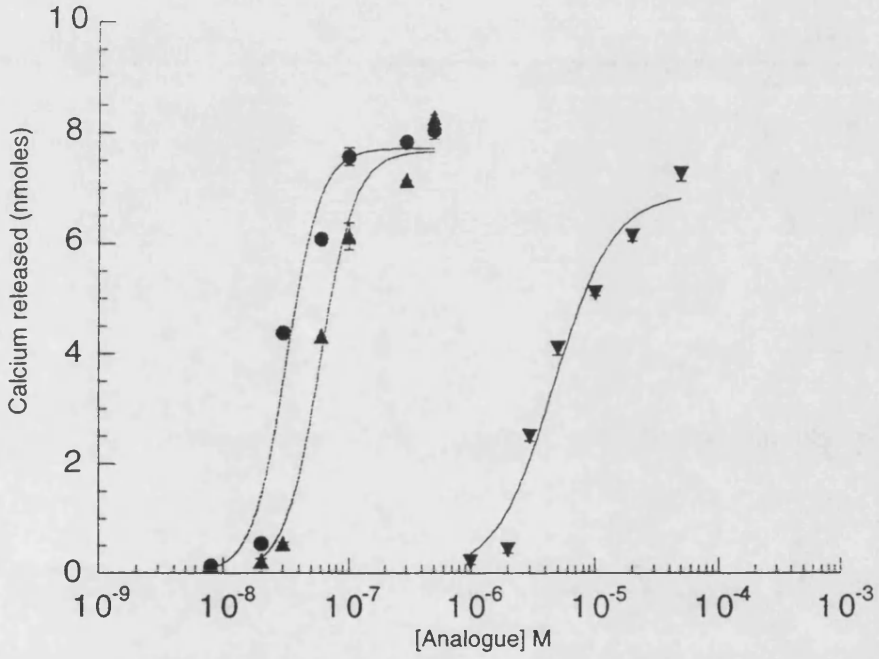

Figure 5.1: Concentration response curves for cADPR (●), $2'_A$-deoxy-cADPR (▲) and $3'_A$-deoxy-cADPR (■) from Ca^{2+} release studies in sea urchin homogenates.

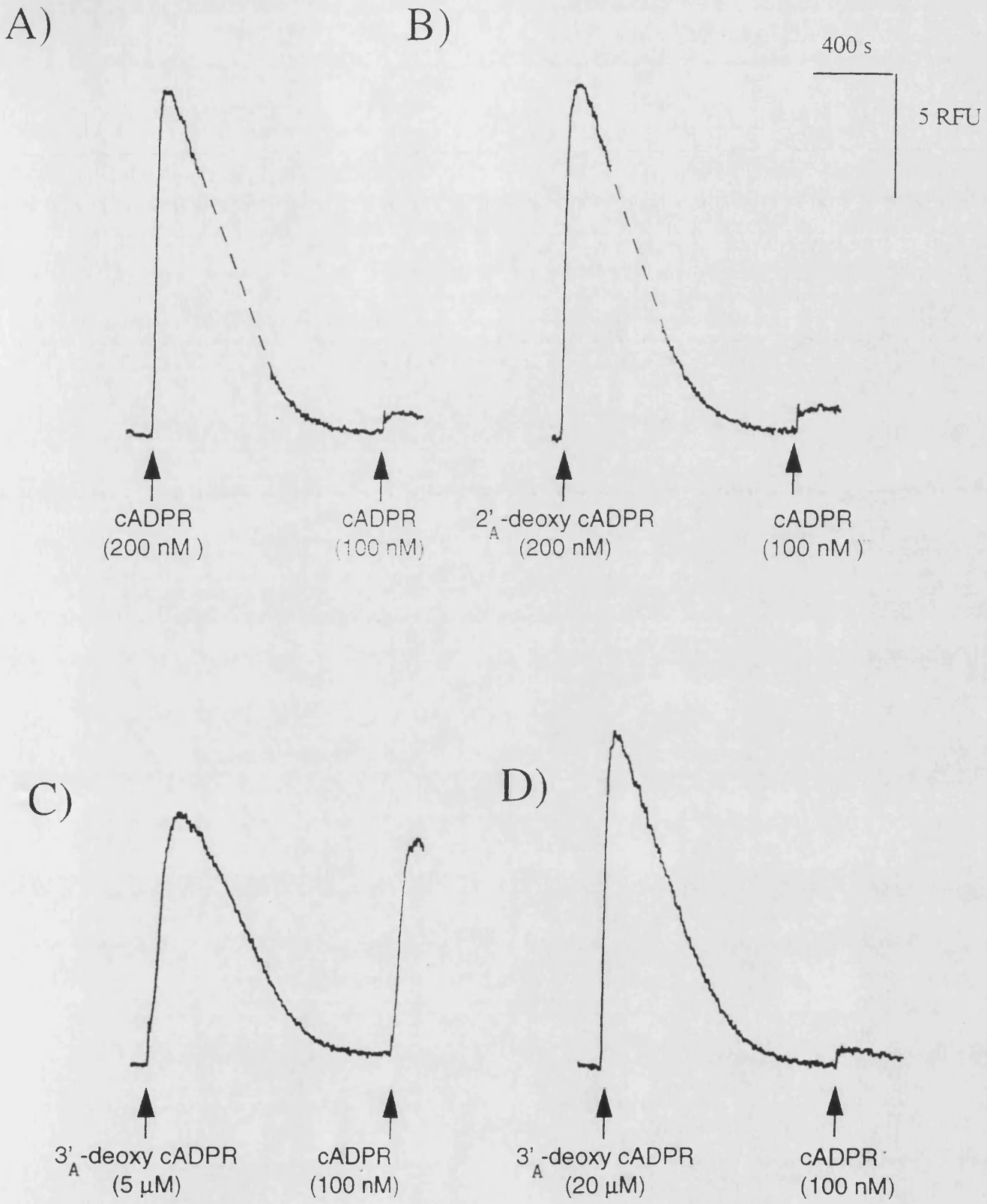

Figure 5.2: Desensitisation effect of $2'_A$-deoxy and $3'_A$-deoxy-cADPR on cADPR-induced Ca^{2+} release in sea urchin egg homogenates. (A) Release by cADPR (100nM), (B) effect of $2'_A$-deoxy-cADPR (200nM) on cADPR-induced release, (C and D) effect of 5µM and 20µM of $3'_A$-deoxy-cADPR respectively on cADPR-induced release.

release by $3'_A$-deoxy-cADPR (Fig 5.1). This shows that there is a loss of potency on the deletion of the $3'_A$-OH group, hence, a higher concentration of $3'_A$-deoxy-cADPR is required to release the same amount of Ca^{2+} as cADPR. That Ca^{2+} release from these analogues was from the same Ca^{2+} pool as cADPR was shown by desensitisation studies (see Fig 5.2). Ca^{2+} release by either analogue desensitised the homogenate to further release by cADPR. 200nM of $2'_A$-deoxy-cADPR was required to desensitise the cADPR-sensitive Ca^{2+} channel to a subsequent addition of 100nM cADPR, but 20μM of $3'_A$-deoxy-cADPR was required to produce the same desensitisation effect. This is consistent to a 100 fold lower potency exhibited by $3'_A$-deoxy-cADPR. It is currently unclear whether the inhibitory effect of these analogues on cADPR-induced release is due to desensitisation of cADPR-sensitive receptors or to store depletion. In a control experiment to test whether the differing activities between $2'_A$-deoxy-cADPR and $3'_A$-deoxy-cADPR was due to different rates of analogue breakdown by endogenous cADPR hydrolase, cADPR, $2'_A$-deoxy-cADPR and $3'_A$-deoxy-cADPR were each incubated in sea urchin homogenates. HPLC analysis of products over 10 h showed that neither $2'_A$-deoxy-cADPR nor $3'_A$-deoxy-cADPR were metabolsied faster than cADPR, suggesting that the reduced activity of $3'_A$-deoxy-cADPR is not due to an unusual hydrolytic breakdown under the experimental conditions (J. Sethi & V.Bailey personal communication).

The large difference in activity between the $2'_A$ and $3'_A$ hydroxyl deleted analogues prompted further study to the role of the $3'_A$-OH group. $3'_A$-OMe-cADPR was synthesised to investigate the importance of the $3'_A$ position further. The OMe group is larger than the OH group and unlike the OH group does not possess the ability to donate

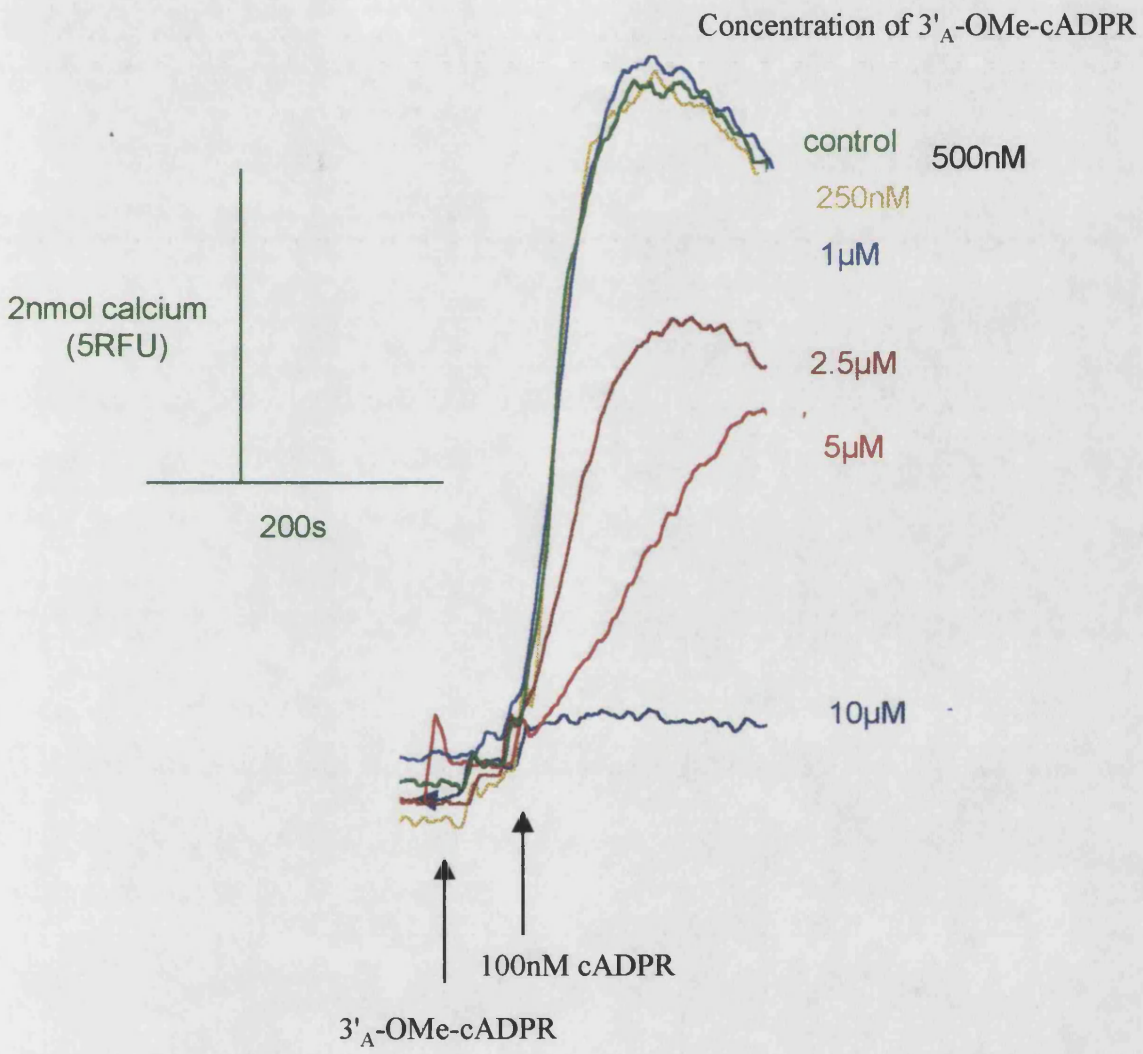

Figure 5.3: Inhibitory effect of 3'$_A$-*OMe*-cADPR on cADPR-induced Ca^{2+} release.

a proton in a potential hydrogen bond interaction with the receptor, although it can still act as an acceptor. Interestingly, $3'_A$-OMe-cADPR did not mobilise Ca^{2+} in the sea urchin egg homogenate system up to a concentration of 20μM. To investigate whether there was a possible interaction of $3'_A$-OMe-cADPR at the cADPR receptor, the effect of this analogue on cADPR induced release was investigated. It acted, surprisingly as an antagonist as it inhibited the cADPR induced release in a concentration dependent manner with an approximate IC_{50} value of 5μM (see Fig 5.3). The response to 100nM of cADPR was abolished with 10μM of $3'_A$-OMe-cADPR.

It appears from the above results that the oxygen atom is somehow important for interaction at the cADPR receptor site as $3'_A$-OMe-cADPR must interact with the receptor in order to inhibit cADPR-induced Ca^{2+} release in a dose dependent manner. $3'_A$ –doexy-cADPR (**38**), the poor agonist can neither donate nor accept a H-bond at the $3'_A$ position, hence it appears that the ability of an analogue to potentially accept a hydrogen bond as in $3'_A$-OMe-cADPR (**39**) may be important for receptor binding. Furthermore, the possibility of a hydrophobic interaction between $3'_A$-OMe-cADPR with the cADPR receptor may account for the antagonist activity of this analogue. These different possibilities need to be explored in order to understand the property which is important for antagonist activity. Nevertheless it is interesting that loss of the $3'_A$-OH group is crucial whereas the $2'_A$ is not as important for agonist activity and that mere substitution of the hydrogen atom of the $3'_A$-OH group of cADPR by a methyl group is sufficient to convert the ligand from an agonist to an antagonist. $3'_A$-OMe-cADPR, is the first antagonist not modified at the 8-position of the adenine ring and it provides a

new lead compound for the synthesis of novel potent inhibitors of cADPR-induced release.

B) 3′$_A$-cADPRP and 2′$_A$,3′$_A$-cADPRP.

The calcium release potentials of 3′$_A$-cADPRP (**41**) and 2′$_A$,3′$_A$-cyclic-cADPRP (**42**) (Fig.4.9) were investigated to study the effect of a phosphate group at the 2′$_A$ and 3′$_A$ positions and to investigate the possibility of an electrostatic attraction between the phosphate group and the cADPR receptor. These analogues were both inactive in releasing calcium in the sea urchin egg homogenate up to concentrations of 20μM and did not exhibit any effect on Ca^{2+} release by 100nM cADPR. This would infer that they are neither agonists nor antagonists. These results are consistent with previous preliminary study of the Ca^{2+} release potential of 3′$_A$-cADPRP and 2′$_A$,3′$_A$-cyclic-cADPRP in rat brain microsomes[131]. This action was found by the authors to contrast with the agonistic action of 2′$_A$-cADPRP (structure shown in Fig 4.7).

3′$_A$-cADPRP is similar in structure to cADPR except that it possesses a phosphate group at the 3′$_A$-hydroxyl. The 2′$_A$ and 3′$_A$-hydroxyls are both substituted in 2′$_A$, 3′$_A$-cADPR by a cyclic phosphate. Moreover, 3′$_A$-cADPR has around two extra negative charges and 2′$_A$, 3′$_A$-cADPR has one extra negative charge at physiological pH compared to cADPR. It is likely that a combination of these factors may result in electrostatic repulsion and steric hinderance of the molecules at the cADPR receptor site relative to cADPR, preventing binding to the receptor. 2′$_A$-cADPR, an analogue with a phosphate group substituted on the 2′$_A$-hydroxyl and with two extra negative charge at physiological pH compared to cADPR has been found to be active in rat brain

microsomes[131] and permeabilised T-cells [188], however, we found it to be inactive in mobilising Ca^{2+} in sea urchin egg microsomes, in support of a previous report by Aarhus and co-workers [126]. It appears from these studies that there may be subtle differences in the cADPR-sensitive Ca^{2+} release mechanism for the ryanodine receptor of sea urchin eggs and mammalian tissue. We have demonstrated that while replacement of the $3'_A$-OH with a hydrogen atom reduced the activity of the analogues, replacement of the H atom of $3'_A$-OH with a phosphate group completely abolished the activity of analogue. Moreover, replacement of the $2'_A$-OH with a hydrogen atom has little effect on the activity of cADPR, but activity is completely abolished by the attachment of a phosphate group at this position

5.1.2 Biological evaluation of $2'_A$ and $3'_A$-Modified cADPR on Ca^{2+}-release in Jurkat T-cells

A) $2'_A$-deoxy-cADPR, $3'_A$-deoxy-cADPR and $3'_A$-*O*-Methyl-cADPR

The effect of hydroxyl deletion at position $2'_A$ and $3'_A$ of the adenine ribose as in $2'_A$ and $3'_A$-deoxy-cADPR on Ca^{2+}-release in Jurkat T-cells show remarkably different profile compared to the effect seen in the sea urchin egg homogenate system. $2_A'$-deoxy-cADPR showed very poor activity as an agonist. Mamimum release was observed at ~100μM compared to 7μM in cADPR. There was no release observed with up to 100μM of $3'_A$-deoxy-cADPR (see Fig.5.4). It thus appears that unlike the sea urchin egg system, where only the $3'_A$-OH appears to be crucial for activity, both the $2'_A$ and $3'_A$ hydroxyls are necessary for effective Ca^{2+} release activity in Jurkat T-cells. To further investigate the role of the $3'_A$-hydroxyl group, the Ca^{2+} release potential of $3'_A$-OMe-

cADPR was investigated in Jurkat T-cells. $3'_A$-OMe- cADPR was an agonist comparable to cADPR (Dr Guse-personal communication) in this system in contrast to the antagonist activity exhibited in sea urchin egg homogenates. Hence replacement of the $3'_A$-OH group with an –OMe group has little effect on the activity of cADPR, but replacement with a hydrogen atom completely abolished its activity in this system. As previously explained (section 5.1.1), $3'_A$-doexy- cADPR can neither donate nor accept a hydrogen bond at the $3'_A$-position the –Ome group in $3'_A$-OMe- cADPR is larger compared to the hydroxyl group in cADPR and does not possess the ability to donate a proton ina potential H-bond interaction with the receptor, although it can still act as an acceptor. It thus appears that the ability of the functional group at position $3'_A$ to accept a hydrogen bond may be important for binding to the receptor, but activation of the ion channel may require donation of a hydrogen bond. These results further highlights that there may be differences in the cADPR-sensitive Ca^{2+} release mechanism for the ryanodine receptor of sea urchin eggs and the mammalian Jurkat T-cell.

B) $3'_A$-cADPRP and $2'_A,3'_A$-cyclic-cADPRP

The effect of a phosphate group in positions $2'_A$ and $3'_A$ of cADPR was investigated by studying the Ca^{2+} releasing potential of $3'_A$-cADPR and $2'_A,3'_A$-cyclic-cADPRP in Jurkat T-cells. These analogues were not active in mobilising Ca^{2+}. $2'_A$-cADPRP has been shown recently to be as potent as cADPR in Ca^{2+} releasing activity in permeabilised Jurkat T-cells. These results are consistent with those reported previously in another mammalian system (rat brain microsomes) [131]. It is interesting to note that substitution at the $2'_A$-OH with a phosphate group did not appear to affect the activity of cADPR despite the increase in the total negative charge and size of the molecule, but replacement

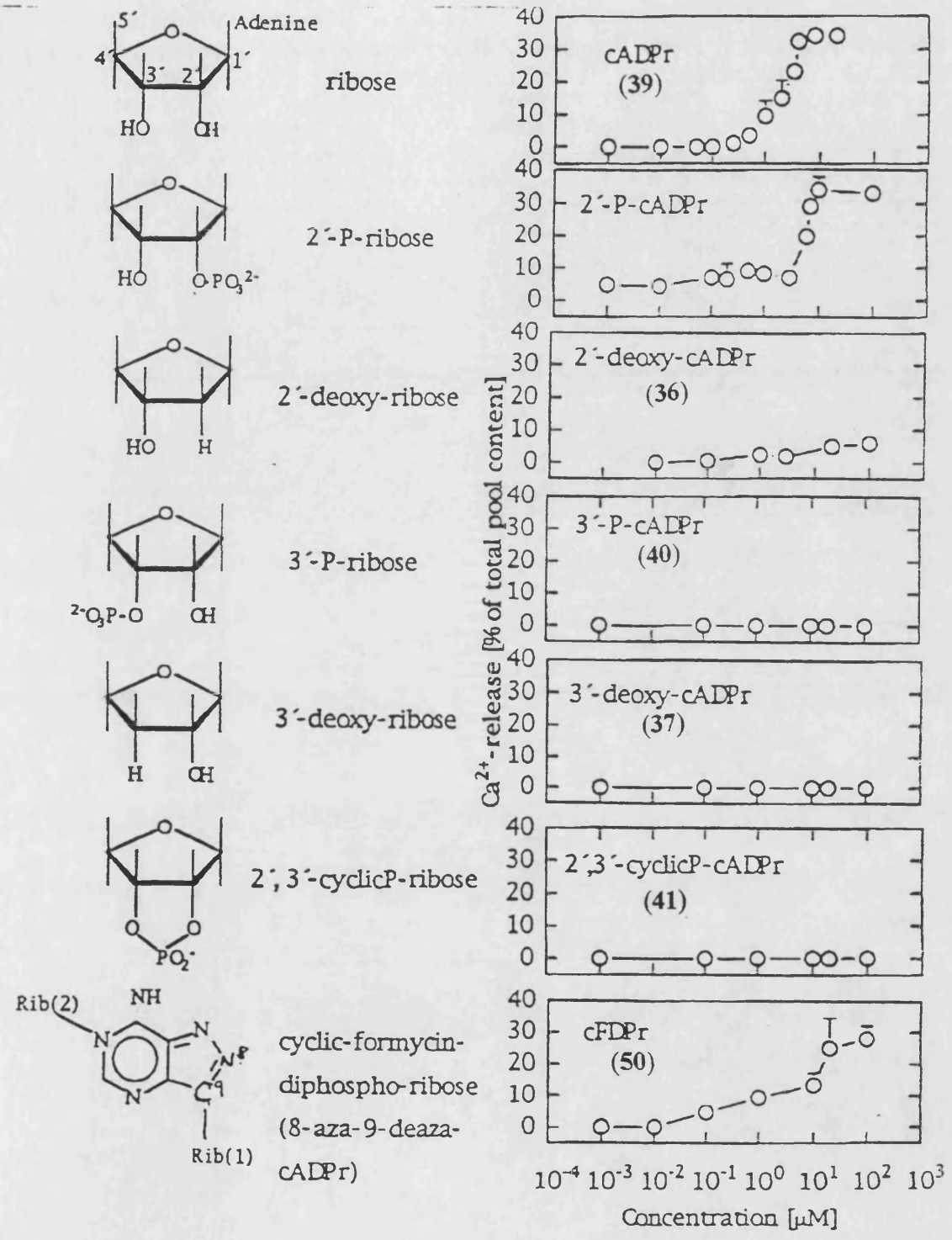

Figure 5.4: Concentration response curves for cADPR, $2'_A$ and $3'_A$-modified cADPR analogues and cFDPR (51), showing Ca^{2+} release activity in permeabilised Jurkat T-cells.

with a hydrogen atom resulted in considerable loss of activity. It is unclear at this stage whether loss of activity with $3'_A$-cADPRP and $2'_A$, $3'_A$-cyclic-cADPRP is due to the removal of the –OH proton by substitution or rather is the result of increase in steric volume by addition of a phosphate.

5.1.3 *Biological Evaluation of 8-Modified analogues of cADPR on Ca^{2+}-release in sea urchin eggs*

The first indication that an exocyclic substitution in position 8 of the adenine ring of cADPR might be important in designing antagonist of cADPR-induced Ca^{2+}release was demonstrated by Walseth & Lee [120]. This group found that substitution of H_A8 with an amino group converted the compound cADPR from an agonist to an antagonist. Two other analogues, 8-Br and 8-azido-cADPR were also found to be antagonists, but with lesser potency. The potency of 8-azido was in between that of 8-amino-cADPR and 8-azido-cADPR although IC_{50} values were not reported. It was suggested that the size of the substituent (expressed in atomic units) may be responsible for the difference in potency of the three 8-substituent analogues synthesised as antagonists. The larger size the substituent at this position the lower the potency, as an increase in size from 16 (-NH_2) to 42 (-N_3) to 79 (-Br) resulted in decrease in potency as an antagonist in this order. We have therefore synthesised various 8-substituted analogues of cADPR in order to further investigate this hypothesis.

8-Amino-cADPR was synthesised in our laboratory to enable us to carry out comparative studies. 8-Amino-cADPR was also found to act as antagonist in sea urchin egg homogenates with an IC_{50} value of 0.01μM. Replacement of the amino group with a methyl group as in 8-methyl-cADPR (**48**) gave an antagonist with an IC_{50} value of

0.53μM. The $-CH_3$ group is similar in atomic mass to $-NH_2$ and yet 8- Me-cADPR was 53 times less potent as an antagonist compared to 8-NH_2-cADPR. Substitution with an oxy group (with an atomic mass of 17) was attempted. The analogue obtained showed still weaker activity as an antagonist with an approximate IC_{50} of 2μM. Substitution with groups of varying sizes such as -NHMe, NMe_2 and -piperidyl as in 8-NHMe, 8-NMe_2 and 8-piperidyl-cADPR produced novel compounds which were investigated for antagonist activity (see table 5.1). 8-NHMe-cADPR was a weaker antagonist compared to 8-NH_2-cADPR with an IC_{50} of ~ 40μM, 8-NMe_2 was weaker than 8-NHMe-cADPR as an antagonist, but 8-piperidyl was not active at all as antagonist up to 50μM. This indicated that the potency of the substituent at the 8-position could be a function of size such as molecular volume. Other analogues such as 8-OCH_3-cADPR and 8-Br-cADPR were also synthesised for comparative study. These analogues were antagonist with IC_{50} values of 4.8 and 0.97μM respectively. It appears, therefore, in this preliminary study, that the ability of the molecule to hydrogen bond is not important for activity as an antagonist as 8-CH_3-cADPR is a better antagonist compared to analogues that can form hydrogen bonds such as 8-OCH_3-cADPR and 8-NHMe-cADPR.

The molecular volume of the substituents were measured using SYBYL molecular modelling software package. A qualitative correlation between the molecular volume of the substituent and IC_{50} value was observed. The larger the molecular volume of the substituent, the higher the IC_{50} value of the analogue. Only 8-Oxo-cADPR did not fit in. The volume measured for the substituent in 8-oxo-cADPR was less than that of 8-NH_2 and yet the molecule was 200 times less potent as an antagonist. It is well documented that 8-hydroxyl purine can tautomerise to the purinone and it has been shown that the

keto tautomer is more stable at physiological pH [150,152]. The existence of the keto tautomer will alter position 7 of the adenine ring. In the purinone tautomer N7 becomes protonated. This small change may be enough to affect the potency of this analogue as an antagonist, so that even though -OH has a lower molecular volume compared to -NH_2, the named molecule is not able to bind well to the receptor site, and hence is a weaker antagonist. Hence the following rank of order of activity was obtained in this study: 8-piperidyl-cADPR (inactive) < 8-NMe_2-cADPR < 8-NHMe-cADPR < 8-OCH_3-cADPR< 8-oxo-cADPR < 8-CH_3-cADPR < 8-NH_2-cADPR. 8-Amino-cADPR is the still the most potent antagonist to date.

8-substituted analogue of cADPR	Molecular Volume of substituent (Å^3)	Action on cADPR-induced Ca^{2+} release (100nM), antagonist (IC_{50})μM
8-NH_2-cADPR (**48**)	15.6	0.01
8-Br-cADPR (**43**)	19.1	0.97
8-NHMe-cADPR (**44**)	32.0	<40
8-NMe_2-cADPR (**45**)	47.0	>40
8-OCH_3-cADPR (**46**)	26.9	4.8
8-piperidyl-cADPR (**47**)	86.8	No effect
8-Me-cADPR (**49**)	16.5	0.53
8-Oxy-cADPR (**50**)	9.1	~2.0

Table 5.1: IC_{50} values of 8-substituted analogues of cADPR (from Ca^{2+} release studies in sea urchin egg homogenates) and the molecular volume of the substituent.

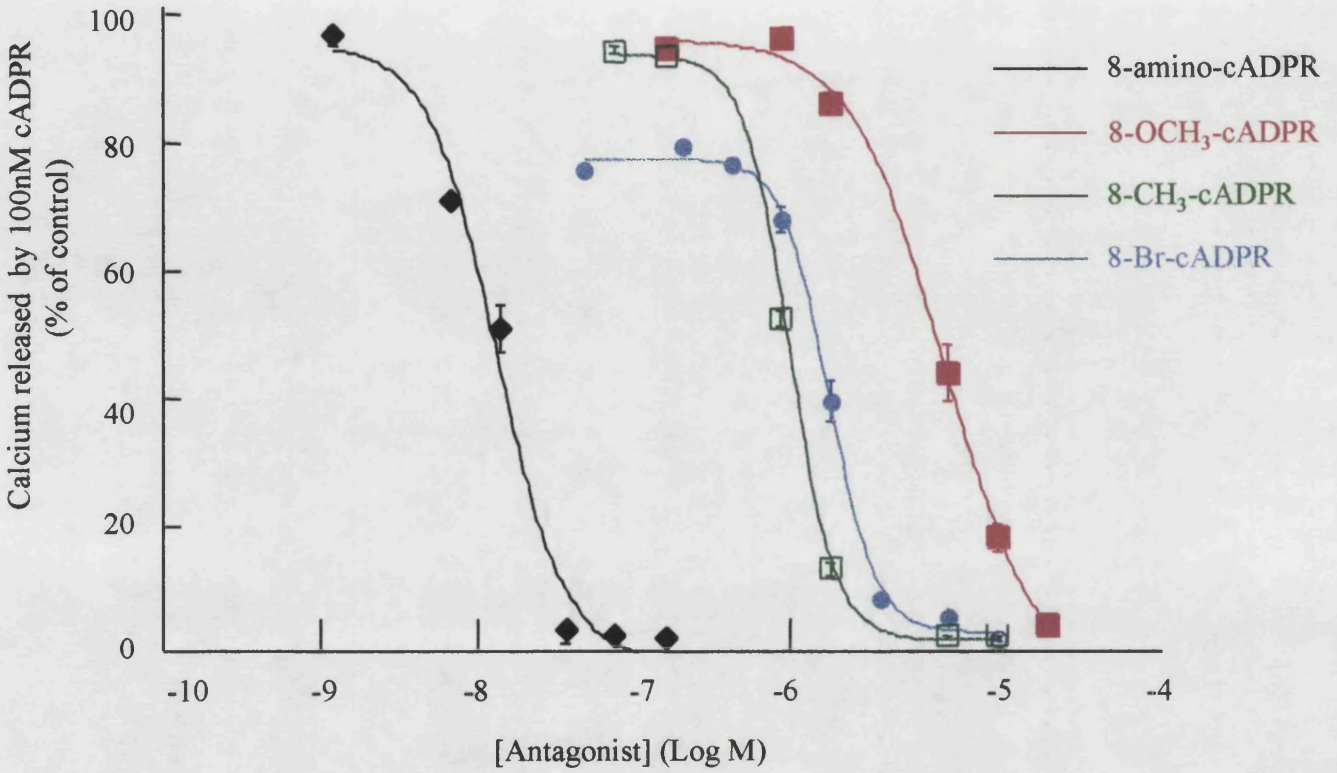

Figure 5.5: Graph showing inhibitory effect of some 8-substituted analogues of cADPR on cADPR induced Ca^{2+} release in sea urchin egg homogenates. *x* axis shows response obtained with 100nM cADPR and *y* axis is the log (dose of antagonist).

Modification in the purine ring as in 8-aza-9-deaza-cADPR (**51**), resulted in an analogue that is 10 times less potent as an agonist compared to cADPR (EC_{50} = 0.31μM). In this molecule the carbon atom of position 8 in the purine ring is replaced with a nitrogen atom and the nitrogen atom of position 9 of the purine ring is replaced with a carbon atom. Modification in the purine ring hence did not produce an antagonist compared to exocyclic modification as discussed above. Reduction in activity could be due to protonation at the N7 which may affect receptor binding. A small modification at this position as in 7-deaza-cADPR has been reported to result in partial agonist activity.[191]

5.1.4 *Biological evaluation of 8-Modified Analogues of cADPR on Ca^{2+}-release in Pemeabilised Jurkat T-cells.*

In order to design antagonists for cADPR-induced mechanisms in Jurkat T-cells, we decided to investigate whether 8-amino-cADPR and 8-bromo-cADPR (both prepared by the author) would have a similar effect to that seen in the sea urchin egg system. We found that these two analogues inhibited Ca^{2+} release mediated by cADPR. 8-Br-cADPR was less effective as an antagonist compared to 8-amino-cADPR[95]. We decided to investigate whether there is a link between the size of the 8-substituent and the potency of the antagonist as an aid to designing potent inhibitors of the cADPR-induced mechanism. The extension to mammalian cells is essential for the aim of defining a wider applicability for the cADPR signalling system.

Substitution of any group other than hydrogen into position 8 of the adenine ring resulted in analogues with antagonist activity in this system. Hence all the 8-substituted analogues synthesised (**43-50**) all inhibited cADPR-induced Ca^{2+}-release. 8-NH_2 (**48**), 8-CH_3 (**49**) and 8-NMe_2-cADPR (**45**) are potent inhibitors with low IC_{50} values (see

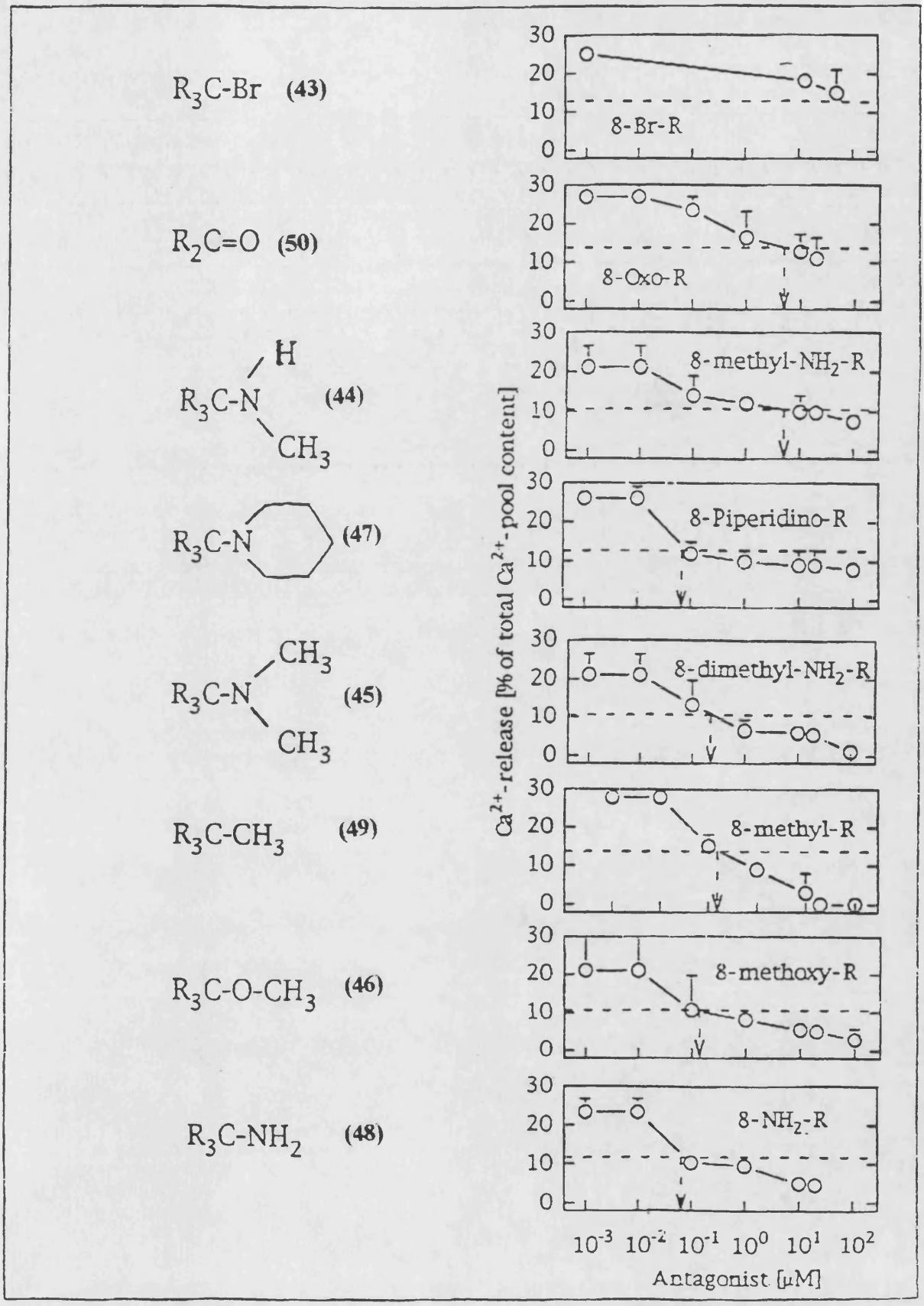

Figure 5.6: Concentration response curves illustration inhibitory effect of 8-substituted analogues of cADPR-induced Ca^{2+} release in permeabilised Jurkat T-cells.

Fig.5.6 and table 5.2) of 0.08μM, 0.2μM and 0.3μM respectively. 20μM of 8-CH_3-cADPR completely abolished cADPR induce release, suggesting that hydrogen bond interaction between the substituent and the receptor site is unlikely to be responsible for antagonist activity as the -CH_3 group in (**49**) cannot form a hydrogen bond. There is, however, a possibility of a hydrophobic interaction taking place. This is supported by the fact that 8-NHMe-cADPR, has a higher IC_{50} value of 8.0μM and shows less potent inhibition at 20μM compared to 8-NMe_2-cADPR. The -NMe_2 substituent being more hydrophobic than the -NHMe group. Moreover. 8-piperidyl-cADPR (**47**) exhibited a low IC_{50} value of 0.08μM comparable to 8- NH_2 -cADPR, though less potent inhibition at higher concentrations (see table 5.2). The remaining signal at 20μM (defined in the experimental section) of 8-piperidyl-cADPR was 9.0 compared to 4.7 for 20μM of 8-NH_2-cADPR. The piperidyl group, though large, is hydrophobic and flexible. Hence, it can change its conformation to fit the receptor site. 8-Br-cADPR showed poor inhibition, possibly due to the bulk of the bromo substituent and unlike the piperidyl group the bromo group is a large rigid structure and hence is potentially hindered from fitting tightly into the receptor site. 8-Oxo-cADPR showed poor inhibitor (IC_{50} = 8μM) even though the substituent is similar in size to -NH_2 and -CH_3 substituent. There are potential multiple alterations in this analogue compared to cADPR as the ntirogen in position 7 can become protonated. This change though small may be sufficient to affect the interaction of this analogue with the receptor. 8-OCH_3-cADPR showed good inhibition with an IC_{50} value of 0.2μM comparable to 8-CH_3-cADPR. Overall, it appears that the presence of a hydrophobic group in position 8 enhances antagonist activity of the analogue in permeabilised Jurkat T-cells.

Modification in the purine ring in analogue (**51**) did not affect the Ca^{2+} releasing property of the analogue (see Fig. 5.4). This analogue showed similar Ca^{2+} release profile compared to cADPR in Jurkat T-cells even though the 8-position is altered (although not outside the ring), the carbon at position 8 is replaced by nitrogen atom and the nitrogen at position 9 is altered to a carbon. These alterations appear to be unimportant for Ca^{2+} releasing activity.

8-substituted analogue of cADPR	Action on cADPR-induced Ca^{2+} release (7μM), antagonist (IC_{50})μM	Remaining signal at 20μM antagonist [% of total Ca^{2+} pool released]
8-NH_2-cADPR (**48**)	0.08	4.7
8-Br-cADPR (**43**)	>20	18
8-NHMe-cADPR (**44**)	8.0	9.7
8-NMe_2-cADPR (**45**)	0.3	5.5
8-OCH_3-cADPR (**46**)	0.2	4.7
8-piperidyl-cADPR (**47**)	0.08	9.0
8-Me-cADPR (**49**)	0.2	0
8-Oxy-cADPR (**50**)	8.0	11

Table 5.2: IC_{50} values of 8-substituted analogues of cADPR from Ca^{2+} release studies in permeabilised Jurkat T-cells.

5.2 Conclusion

The chemoenzymatic synthesis of cADPR analogues has proved to be a versatile approach [191]. We have demonstrated the broad substrate specificity of ADP-ribosyl cyclase for NAD^+ analogues with modification to the ribose hydroxyl group and for modification to position 8 of the purine ring. All of the NAD^+ analogues synthesised in this work were substrates for the cyclase.

Biological evaluation of analogues in the sea urchin homogenates (A) and Jurkat T-cells (B) have revealed some differences in the structural requirements for cADPR receptor in the systems concerned. The $2'_A$-OH and $3'_A$-OH both appear to be important for potent agonist activity in permeabilised Jurkat T-cells. In the sea urchin egg homogenate, only the $3'_A$-OH is crucial for effective Ca^{2+} release activity. Addition of a phosphate group at the $2'_A$-OH does not affect agonist activity in the permeabilised Jurkat T-cells, but this activity is abolished in the sea urchin egg homogenate. Substitution of the $3'_A$-OH with a phosphate group, however, resulted in loss of activity in both systems. Substitution on the $2'_A$ and $3'_A$ ribose hydroxyl groups with a cyclic phosphate also resulted in loss of activity in the biological systems studied. Substitution of the $3'_A$-OH with a methyl group resulted in a change in activity from an agonist to an antagonist in (A), but in (B) $3'_A$-OMe-cADPR had potent agonist activity. Hence, it appears that the ability of the -OH to donate a hydrogen bond may be important for potent Ca^{2+}-releasing activity in (B). Replacement of the hydrogen atom at the 8-position of the purine ring of cADPR with other groups produced a change in activity from an agonist to an antagonist. The potency of the antagonist appears to be dependent on the molecular volume of the substituent in position 8 in (A). The larger the molecular volume of the substituent, the

higher the IC_{50} of the antagonist (i.e. weaker antagonist effect). Substitution with a piperidyl group resulted in loss of antagonist activity as the molecule is bulky and therefore is likely to be sterically hindered from interacting with the cADPR receptor. All the 8-substituted analogues were also antagonists in (B) although there were differences in potency and rank order. This activity appear to be enhanced by increasing the hydrophobicity of the substituent, although there is also limitation to the size of the group as 8-Br-cADPR was a poor antagonist in this system.

These results represent the first steps towards establishing a wider structure-activity profile for cADPR and suggests that there may be structural differences in the cADPR-binding protein in the sea-urchin egg homogenate and in permeabilised Jurkat T-cells. Identification of the cADPR receptor in biological systems in question will help to verify our findings. Combined data from this work and results from a co-worker along with results from other groups are summarised below in Fig. 5.7.

5.3 Suggestions for further study.

1. Determine kinetic properties of cADPR hydrolase using various cADPR analogues as substrates.
2. Synthesis of fluorescent labelled analogues of cADPR.
3. Synthesis of membrane permeable analogues of cADPR
4. Synthesis of non-hydrolysable analogues of cADPR
5. Study on inhibition of the enzymes involved in the metabolism of cADPR
6. Preparation of analogues with modifications in the top ribose ring (i.e. the ribose ring that previously carried the nicotinamide ring in NAD^+.)

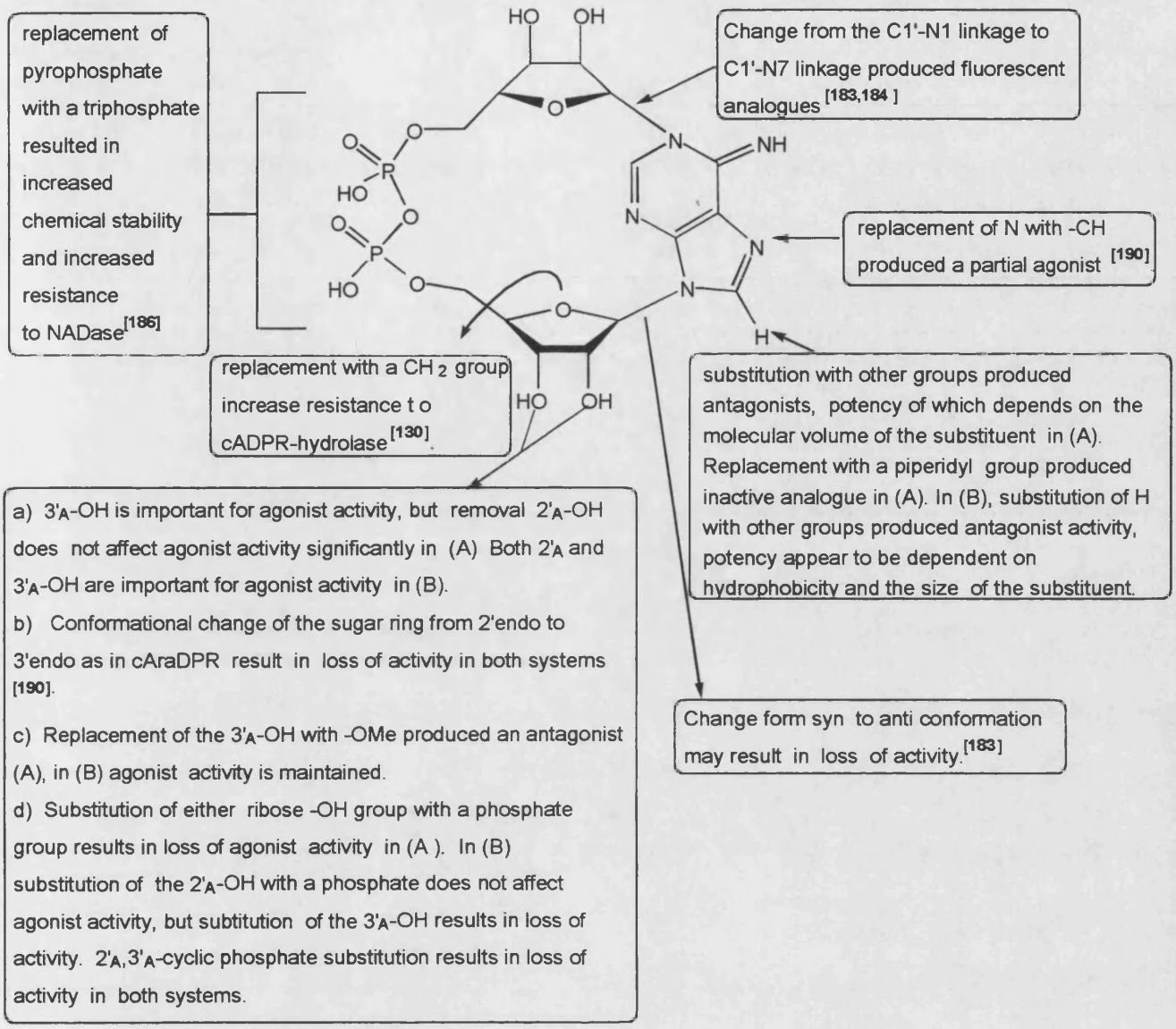

Figure 5.7: Structure-activity relationships of cyclic adenosine diphosphate ribose

CHAPTER 6: EXPERIMENTAL

6.1 General Procedures

Adenosine, Adenosine 5′-monophosphate, Nicotinamide-5′-mononucleotide (NMN), 2′-deoxyadenosine-5′-monophosphate (2′-deoxy-AMP), 3′-deoxy-adenosine-5′-monophosphate (3′-deoxy-AMP), 3′-*O*-methyl-adenosine (3′-*OMe*-adenosine), $3'_A$-nicotinamide adenine dinucleotide phosphate ($3'_A$-$NADP^+$), $2'_A,3'_A$-cyclic-nicotinamide adenine dinucleotide phosphate ($2'_A,3'_A$-$NADP^+$), 2-[4-(2-hydroxyethyl)piperazin-1-yl)ethanesulfonic acid (HEPES), N,N-dicyclohexylcarbodiimide (DCC), NAD^+, yeast alcohol dehydrogenase, alkaline phosphatase and tris(hydroxymethyl)aminoethane (Tris) were purchased from Sigma (London). Organic solvents were obtained from Aldrich. Pyridine was dried overnight with calcium hydride, re-distilled and stored over potassium hydroxide pellets. *Aplysia* ovotestis homogenate containing ADP-ribosyl cyclase was prepared as previously described [59]. The protein concentration of the *Aplysia cyclase* used in all cases was estimated as 10mg/ml using a Bio-rad protein estimation assay. Fluo-3 was purchased from Molecular Probes Inc. (Camb. BioSci.). All other reagents were from Aldrich (London). Ion exchange chromatography was performed on an LKB-Pharmacia medium pressure ion exchange chromatograph using a Sepharose Q fast flow column with gradients of triethylammonium bicarbonate buffer (TEAB) pH 7.6 as eluent. 1M TEAB was prepared by bubbling carbon dioxide gas into 1M triethylamine solution for ca. 6h. HPLC was performed on a Shimadzu LC-6A chromatograph with the UV detector operating at 259nm using a combination of a Partisil 10μ SAX guard column (10×0.46cm) and a Technicol (10×0.46cm) 10μ SAX HPLC column, or using a

Spherisorb 10μ SAX (25×0.46cm) column with an isocratic elution using phosphate buffer (KH_2PO_4), pH 3.0 at a flow rate of 1ml/min. ^1H NMR and ^{31}P NMR spectra were recorded on either Jeol JNM GX-270 FT NMR or Jeol EX-400 FT NMR spectrometers. Chemical shifts were measured in ppm relative to deuteriated water (D_2O) for ^1H NMR and to external 85% H_3PO_4 for ^{31}P NMR. ^{31}P-NMR were measured at 162MHz or 109MHz in D_2O. For the latter, δ values are positive when downfield from this reference. J values are given in Hertz (Hz). Mass spectra were recorded at the EPSRC Mass Spectrometry Service Center at the University of Swansea and at the University of Bath. Ultraviolet (UV) absorbance was measured with a Perkin-Elmer Lambda 3 UV/VIS spectrophotometer. Melting points were determined with a Reichert-Jung Thermo Galen Kogler block, using two glass plates and are uncorrected.

6.2 Synthesis of AMP Analogues

6.2.1 3′$_A$-O-Methyl-adenosine 5′-monophosphate (3′-OMe-AMP) 16

100mg (0.355mmol) of dry 3′-*OMe*-adenosine was placed in a dry round bottom flask. 2ml of triethyl-phosphate was added to the dry powder. The solution was heated for a few seconds to ensure formation of a complex with $PO(OEt)_3$. The flask was fitted with a $CaCl_2$ drying tube and was cooled to 0°C on an ice bath. 50μl (0.54mmol) of phosphorus oxychloride were added to the solution dropwise at 0°C and the reaction was left stirring for a total of 2 h at room temperature. HPLC analysis of an aliquot of the reaction mixture in water after two hours showed the presence of a new product at 2 min, with the starting material eluting at 1.5 min. The reaction was quenched by stirring in 4ml of pyridine:water (1:3) for 30 min. The solution changed from yellow to

colourless. The solvent was removed *in vacuo* and excess $PO(OEt)_3$ was extracted into cold petroleum ether 40-60° (3x10ml aliquots). The sample was dried *in vacuo*, the residue dissolved in 200ml of milliQ water and the product was purified by IE chromatography using a gradient of 0-400mM TEAB. The sample eluted off between 110-160mM TEAB, and inorganic phosphate impurity was removed by passing the solution through a charcoal column and eluting the product as described under phosphorylation of 8-bromo-adenosine, to afford 48% yield (0.17mmoles).

δ_H (D_2O, 400MHz): 8.3 (H8), 7.9 (H2, s), 5.9 (H1′, d, J 5.8), 4.75 (H2′, t, J 5.5, 5.8), 4.3 (H3′, t), 4.05 (H4′, m), 3.9 (H5′, 5′, m), 3.4 (3H, Me, s). δ_P (D_2O, 162MHz): 2.3, s, 1P (^{1}H-decoupled).

m/z (-ve ion ES): 360 [100%, $M - H)^-$]. λ_{max} 256nm (pH 8.3) ε_{259} 15,300.

6.2.2 Synthesis of 8-Bromo-adenosine 5′-monophosphate (8-Br-AMP) 4

8-Br-AMP can be synthesised from adenosine (A) and by direct bromination of AMP (B). The synthesis from adenosine is in two stages i) bromination of adenosine, ii) phosphorylation of 8-Br-adenosine.

A) Synthesis from Adenosine

i) *Bromination of adenosine*

2g (0.75mmol) of adenosine (**1**) was dissolved in 50ml of 1.0M acetate buffer pH 3.9 by gentle heating. 0.5ml of Br_2 was added and the solution was left stirring overnight. The

nucleoside had precipitated out of the solution after ca. 18 h at room temperature. TLC of the precipitated material in solvent system I chloroform:ethanol (3:2) and solvent system II dichloromethane:methanol (9:1) showed that the reaction was not complete. Therefore the nucleoside suspension was forced back into solution by heating and a further 0.5ml of Br_2 was added. This solution was left stirring for a further 30min after which the reaction was judged complete by TLC. For system I R_f adenosine (0.36), 8-Br-adenosine (0.6) and in system II, R_f adenosine (0.05), 8-Br-adenosine (0.26). 10 drops of 1.25M sodium hydrogen sulphite ($NaHSO_3$) was added to discharge the colour of the solution from dark red to light yellow colour. The sample was dried *in vacuo*, redissolved in 40ml of water and a further 10 drops of $NaHSO_3$ was added to discharge the colour further. Care was taken not to add too much $NaHSO_3$ as this can cause debromination of the product. The pH of the solution was adjusted to 7 with 5M sodium hydroxide and the solution was left in the refrigerator to recrystallize to afford an analytically pure material by HPLC. The solvent was decanted off and crystals was washed with water: acetone (1:1) solution. The pure product thus obtained was dried in a vacuum oven under reduced pressure at 60°C and sample was weighed (91% yield).

δ_H (D_2O, 270MHz): 8.1 (H2, s), 5.8 (H1′, d, J 7.0), 5.2 (H2′, dd, J 5.5, 7.0), 4.2 (H3′, dd), 4.0 (H4′), 3.9 (H5′, H5′). m.p. 207-209°C (lit.[158] >200°C)

ii) Phosphorylation of 8-Bromoadenosine.

8-Bromoadenosine was dried in a vacuum oven at 60°C for 2 h. 0.212g (0.61mmol) of dry 8-bromoadenosine (**3**) was dissolved in 4.0ml of dry triethyl-phosphate by heating

with a heat gun until solution became clear. The flask was fitted with a $CaCl_2$ drying tube and the solution cooled to 0°C in an ice bath. 200µl (2.16mmol) of phosphorus oxychloride ($POCl_3$) was added dropwise and the flask was left stirring for 3 h at rt. with the drying tube in place. HPLC analysis of the reaction mixture dissolved in water showed the presence of a phosphorylated material with the same retention time as an authentic sample of 8-Br-AMP, purchased from Sigma. HPLC analysis was performed on a Partisil SAX column (10×0.46cm) using an isocratic gradient of 0.05M KH_2PO_4 pH 3.0. Retention times: R_t 8-Br-adenosine (1.2min) 8-Br-AMP (1.8min). The reaction was quenched with 8ml of pyridine :water (1:3v/v) and left stirring for a further 30min The sample was dried *in vacuo* and ^{31}P NMR spectroscopy in D_2O with the pH adjusted to 8.0 with 1.0M TEAB buffer showed the presence of inorganic phosphate at δ -0.1 and 8-Br-AMP at δ 0.4ppm. The peak due to nucleotide was distinguished by proton coupled ^{31}P NMR spectroscopy in which the peak due to the inorganic phosphate remained a singlet and the peak due to 8-Br-AMP became a triplet with J value of 5.67Hz, on proton coupling.

Ion exchange purification of 8-Br-AMP removed contaminating 2′-phosphorylated nucleotide, but a large amount of inorganic phosphate was still present. Inorganic phosphate was removed by passing the nucleotide mixture dissolved in 50ml of water through a charcoal column. This column (25×4cm) was prepared by using ca. 1cm of celite as a bed on top of which 7cm of activated charcoal (Norit^B) were added. The nucleotide solution in water was poured unto the column and the eluent was collected. Water was used to flush inorganic phosphate off the column and a total of 75ml of eluent

was collected. The inorganic phosphate-free nucleotide was eluted off the column using 25:24:1 (v/v) ethanol:water:concentrated ammonia (2×500ml). The first fraction collected in water was stirred with 2g of charcoal in 50ml of water and filtered off through through a sintered column layered with celite. The filtrate was discarded and more nucleotide was eluted off with 100ml of 25:24:1 ethanol:water:conc ammonia. The two eluted fractions were combined and dried *in vacuo*. ^{31}P NMR spectroscopy showed the absence of inorganic phosphate impurities. Measurement of OD units before and after charcoal treatment showed 80% recovery of pure nucleotide.

δ_H (D_2O, 400MHz): 8.0 (H2, s), 5.8 (H1′, d, J 6.1), 5.1 (H2′, t, J 6.1), 4.4 (H3′, t, J 6Hz), 4.1 (H4′, m), 3.9 (H5′, m), 3.8 (H5′, m). δ_P (D_2O, 162MHz):+3.7, s, 1P (^1H-decoupled), 1P, t, J 5.67 (^1H-coupled). λ_{max} 264nm (pH 7.0) ε 15,100

B) By direct bromination of AMP

8-Br-AMP (**4**) was prepared by bromination of AMP (**2**) as the disodium salt [141]. AMP (1g, 2.88mmol) was dissolved in 50ml of 1M sodium acetate buffer pH 3.9. 0.5ml (0.02mol) of Br_2 was added dropwise to this solution while stirring and the solution was left stirring at room temperature for 30min. The progress of the reaction was followed by UV spectroscopy, where the spectrum showed a shift in λ_{max} from 259 to 264nm upon conversion of AMP to 8-Br-AMP. Excess bromine was extracted into 3×50ml aliquots of chloroform. The resulting pale yellow aqeous solution was dried at 30°C under reduced pressure to obtain a dry powder. The powder was dissolved in milliQ water and purified by ion-exchange chromatography using a gradient of 0-40% TEAB.

The pure sample eluted off between 170-210mM. The sample was dried *in vacuo* and quantified using an extinction coefficient of $15,100M^{-1}cm^{-1}$ at 264nm (Townsend). 8-Br-AMP (1.87mmol) was obtained in 68% yield.

δ_H (D_2O, 400MHz): 8.0 (H2, s), 5.8 (H1′, d, J 6.1), 5.1 (H2′, t, J 6.1), 4.4 (H3′, t, J 6Hz), 4.1 (H4′, m), 3.9 (H5′, m), 3.8 (H5′, m). δ_P (D_2O, 162MHz):+3.7, s, 1P (^{1}H-decoupled), 1P, t, J 5.67 (^{1}H-coupled). λ_{max} 264nm (pH 7.0) ε 15,100

6.2.3 8-Methyladenosine 5′-monophosphate (8-Me-AMP) 16

8-Me-AMP was synthesised in two steps A) synthesis of 8-methyladenosine (**5**) followed by B) phosphorylation of (**5**) to 8-methyladenosine 5′-monophosphate.

A) Synthesis of 8-Methyladenosine **5** [148]

1g (2.89mmol) of dry 8-bromoadenosine was dissolved in 20ml of hexamethyldisilazane and 8ml of dry dioxane in a three-necked flask. A catalytic amount of ammonium sulphate was added to the suspension and the mixture was left under reflux at 130°C for 2-3 h. TLC in dichloromethane:methanol (9:1) showed that protection was complete. 8-Br-adenosine (R_f 0.36), Product (R_f 0.57) was observed as a single spot. The sample was dissolved in 8ml anhydrous dry THF under an atmosphere of nitrogen. 0.1 equivalent of triphenylphosphine (76mg, 2.89mmol), 0.05 equivalent of palladium dichloride (26mg, 0.1445mmol) and 2 equivalents of trimethylaluminium (2.89ml, 5.78mmol) were added to the solution of sample in dry THF under N_2. The reaction was left under reflux and a gentle stream of N_2 for 2.5 h. The R_f of protected 8-Me-adenosine

on TLC developed in DCM:MeOH (9:1) was 0.39. The crude mixture was dried *in vacuo* to give a green residue. Deprotection of the crude product was carried out by dissolving the residue in 50ml of methanol and refluxing for 4 h with a small amount of ammonium chloride. The R_f of the deprotected 8-methyladenosine was 0.05. The crude sample was purified on a short silica gel column eluting first with 200ml of DCM:MeOH (9:1) followed by $CHCl_3$:EtOH (3:2). The sample was dried down on a rotary evaporator, the residue dissolved in water and the pH adjusted to 7 with 5M NaOH. The sample was allowed to recrystallized at 4°C overnight. The crystals obtained were very fine soft jellied, hence the suspension was centrifuged and water was decanted off. The crystals were dried overnight in a vacuum oven at 60°C to afford 48% (0.39mg, 1.4mmol) yield dry weight.

δ_H (D_2O, 270MHz): 8.0 (H2, s), 5.8 (H1′, d, J 7.3), 4.8 (H2′, dd, J 5.1, 7.3), 4.1 (H3′,dd), 4.0 (H4′, m), 3.7 (H5′, m), 3.5 (H5′, m).

m/z (+ve ion FAB) 282 [100%$(M + H)^+$], (-ve ion FAB): 434 (M + NBA).

FAB accurate mass 282.120743. Found 282.120229.

m.p. 208°C, (lit [192] 207-208°C)

B) Phosphorylation of 8-methyladenosine

170mg (0.6mmol) of dry **5** was placed in a dry round bottom flask. 4ml of triethyl-phosphate was added to the dry powder. 8-Methyladenosine dissolved readily in $PO(OEt)_3$. The solution was heated for a few seconds to ensure formation of a complex with $PO(OEt)_3$. The flask was fitted with a $CaCl_2$ drying tube and was cooled to 0°C on an ice bath. 100µl (1.08mmol) of phosphorus oxychloride were added to the solution dropwise at 0°C and the reaction was left stirring for a total of 3 h at room temperature. HPLC analysis of an aliquot of the reaction mixture in water after two hours showed the presence of a new product at 2 min, with starting material eluting at 1.5 min. The reaction was quenched by stirring in 8ml of pyridine:water (1:3) for 30 min. The solution changed from yellow to colourless. The solvent was removed *in vacuo* and excess $PO(OEt)_3$ was extracted into cold petroleum ether 40-60° (3×10ml aliquots). The sample was dried *in vacuo*, the residue dissolved in 350ml of milliQ water and the product was purified by IE chromatography using a gradient of 0-400mM TEAB. The sample eluted off between 110-160mM TEAB, and inorganic phosphate impurity was removed by passing the solution through a charcoal column and eluting the product as described under phosphorylation of 8-bromoadenosine to afford the product 60.3% yield (0.38mmole).

δ_H (D_2O, 400MHz): 7.9 (H2, s), 5.8(H1′, d, J 6.8), 4.8 (H2′, t, J 6.2), 4.3 (H3′, t, J 6.2), 4.1 (H4′, m), 3.9 (H5′, 5′, m), 2.46 (3H, Me, s). δ_P (D_2O, 162MHz): 4.0, s, 1P (^{1}H-decoupled), 1P, t, J 5.6 (^{1}H-coupled). λ_{max} 260nm (pH 8.3) ε 15,300.

6.2.4 8-Methylaminoadenosine 5'-monophosphate (8-NHMe-AMP) 6

To 270.8μmol of 8-Br-AMP (**4**) as the triethylammonium salt were added 10ml of anhydrous 2M methylamine in methanol. The solution was left stirring under reflux at 50°C using an oil bath for 3 h after which little conversion had taken place as monitored by HPLC system. The temperature of the reaction mixture was therefore increased to 60-70°C. Considerable conversion to 8-NHMe-AMP had occurred after 1 h. The reaction was left stirring at this temperature for a further hour, but no further conversion was noticed. The progress of the reaction was monitored by HPLC on a combination of Partisil 10μ SAX 3cm column with Partisil 10μ SAX column (10×0.46cm). R_t 8-Br-AMP 2.5min, 8-NHMe-AMP 2.3 min. A definite change in λ_{max} from 264-278nm followed conversion to the product. The crude sample was dried down *in vacuo*, the residue dissolved in milliQ water and the product purified by IE chromatography using a gradient of 0-350mM TEAB. Pure product eluted off between 200-300mM TEAB to yield 176.02μmoles (65%) of **6** as quantified by phosphate analysis.

δ_H (D_2O, 400MHz): 7.8 (H2, s), 5.8 (H1', d, J 8), 4.6 (H2', t, 5.8Hz), 4.26 (H3', t, J 5.5), 4.1 (H4', m), 3.9 (H5',m), 3.8 (H5', m), 2.8 (3H, -NMe, s). δ_P (D_2O, 162MHz): +3.2, s, 1P (^{1}H-decoupled). λ_{max} 278nm, pH 8.3 (ε 17,700$M^{-1}cm^{-1}$).

m/z (ES^-): 376.4 [20% $(M)^-$], 375.4 [100% $(M - H^-)$].

6.2.5 8-Dimethylamino-adenosine 5'-monophosphate (8-NMe_2-AMP) 7

10ml of anhydrous 2M dimethylamine solution in methanol were added to 146.93μmol of **4** in a round bottom flask. The solution was left stirring under reflux at 40°C overnight, after which the sample was dried down *in vacuo*. A change in λ_{max} from 264-274nm confirmed the change from 8-Br-AMP to 8-NMe_2-AMP. The crude sample was purified on an ion-exchange column using a TEAB gradient of 0-400mM. Pure sample eluted off between 140-210mM TEAB to afford 99.9μmoles (68%) of **7**. HPLC analysis on a Spherisorb column (25×0.46cm) R_t 4.9min.

δ_H (D_2O, 400MHz): 7.9 (H_A2, s), 5.6 (H_A1', d, J 6.7), 5.1 (H_A2', t, J 6.4), 4.3 (H_A3', t, J 5), 4 (H_A4', m), 3.9 (H_A5', 5', m), 2.8 (6H, -NMe_2, s). δ_P (D_2O, 162MHz): +2.2, s, 1P (^{1}H-decoupled). m/z (+ve ion FAB): 492 [70% $(M + TEA)^+$], 391 [90% $(M + H)^+$], 283 [20% $(ribose + NBA)^+$].

m/z (-ve ion FAB): 779 [30% $(2M–H)^-$], 389 [90% $(M–H)^-$], 231.9 [100% $(PO_3^{2-} + NBA)^-$]. λ_{max} 274nm, pH 8.3 (ε 10,900$M^{-1}cm^{-1}$).

6.2.6 8-Amino-adenosine 5'-monophosphate (8-NH_2-AMP) 9

25mg (59.2μmol) of the comercially available 8-azido-AMP (**8**) as the bis-ammonium salt was dissolved in 7.5ml of 50mM TEAB, pH 8.0 in a round bottom flask covered with foil to reduce light. 13.97mg (90.6μmol) of dithiothreitol were added to the

nucleotide solution, and the mixture was left stirring for 16h at room temperature [150]. The reaction was judged to be complete by a change in UV absorption maximum from 282 to 274nm. The crude sample was dried down *in vacuo* and the residue purified by ion-exchange chromatography using a gradient of 50-1000mM TEAB pH 7.6. Pure 8-NH_2-AMP eluted as the triethylammonium salt between 310-390mM TEAB with 65.3% (38.69μmols) yield using ε 16,000 at λ_{max} 274nm.

δ_H (D_2O, 400MHz): 7.8 (H2, s), 5.8 (H1′, d), 4.6 (H2′, dd), 4.3 (H3′), 4.2 (H4′, m), 4.1 (H5′, H5′). δ_P (D_2O, 162MHz): 0.35, s, 1P (^{1}H-decoupled).

6.2.7 8-Piperidyl-adenosine 5′-monophosphate (8-pip-AMP) 10

To 111.3μmol of dry (**4**) was added 0.4ml of dry distilled piperidine. The solution was left stirring at 50°C for 40 h. The reaction was monitored by HPLC analysis using a combination of Partisil 10μ SAX guard column (10×0.46cm) and a Technicol (10×0.46cm) 10μ SAX using an isocratic elution with KH_2PO_4, pH 3.0 with a flow rate of 1ml/min. 8-pip-AMP eluted at 5.1min followed by 8-Br-AMP at 6.8min. The sample was dried *in vacuo*, the residue dissolved in milliQ water and product purified by ion-exchange chromatography using a gradient of 0-300mM TEAB. Pure 8-pip-AMP eluted between 30-65mM TEAB (65% yield). The sample was quantified by phosphate analysis[182] and the extinction coefficient was determined therefrom.

δ_H (D_2O, 400MHz): 7.9 (H2,s), 5.6 (H1′, d, J 6.4), 5.1 (H2′, t, J 6), 4.34 (H3′, t, J 6), 4.0 (H4′, m), 3.9 (H5′, 5″, m), 3.2 (4H, piperidyl, m), 1.6 (6H, piperidyl, m). δ_P (D_2O, 162MHz): +1.97, s, 1P (^{1}H-decoupled).

m/z (–ve ion FAB): 860 [15% $(2M)^-$], 429 [85% $(M - H)^-$], 262 (45%), 232 [100% $(PO_3^{2-} + NBA)^-$].

λ_{max} 275nm (pH 8.3) ε 11,660$M^{-1}cm^{-1}$.

6.2.8 8-Methoxy-adenosine 5′-monophosphate 8-(OCH_3)-AMP (11)

0.229mmol of 8-Br-AMP (**4**) were treated with a total of 20ml of 0.5M sodium methoxide in methanol under reflux overnight. The reaction was monitored by HPLC analysis and by measuring a change in λ_{max} from 264 to 260nm. The pH of the solution was adjusted to 7 with glacial acetic acid and the solvent was removed *in vacuo*. The residue was redissolved in milli Q water and purified by IE chromatography using a TEA gradient from 50-350mM. The pure sample eluted off between 210-250mM TEAB followed by 8-Br-AMP between 280-320mM TEAB. Pure 8-OCH_3 was obtained in 79% yield.

δ_H (D_2O, 400MHz): 7.8 (H2, s), 5.7(H1′, d, J 5.5), 4.8 (H2′, t, J 5.8, 5.5), 4.25 (H3′, t, J 4.2, 5.7), 4.2 (H4′, m), 4.0 (3H,O-CH_3, s), 3.8 (H5′,m) 3.7(H5′, m). δ_P (D_2O, 162MHz): 3.7, s, 1P (^{1}H-decoupled).

λ_{max} 260nm (pH 8.3) ε 13,500.

6.2.9 8-Oxy-adenosine 5'-monophosphate 8-oxy-AMP 13

128mg (301.9μmol) of **4** was dried by repeated co-evaporation with pyridine. 50mg of anhydrous sodium acetate and 4.4ml of acetic anhydride were added to **4**. The homogenous solution was refluxed at 150-165°C for 2 h and then left stirring for 24 h at room temperature after which 2ml of methanol were added to the solution. The sample was dried down *in vacuo* and the residue dissolved in 11ml of NaOH which was stirred for 24 h at rt. The resulting solution was neutralised by adding ca. 6ml of 1M HCl, and the pH was adjusted to 8.0 with ammonia. The change in UV absorption from 264-271nm confirmed that 8-oxy-AMP had been synthesised [143]. HPLC retention: 8-Br-AMP (2.5 min), 8-oxy-AMP (3.7min) using a guard column of Partisil 10μ SAX (3cm) in combination with a Partisil column of 10μ SAX (10×0.46cm). The sample was purified on an IE column using a gradient between 0-400mM TEAB. Pure product eluted off between 300-360mM TEAB in 51.4% yield (0.155mmol). λ_{max} 270nm. The sample was quantified by using ε 10,545$M^{-1}cm^{-1}$ at 260nm.

δ_H (D_2O, 400MHz): 8.0 (H2, s), 5.6 (H1', d, J 5.5), 4.9 (H2', dd, 5.0, 5.5), 4.2 (H3', dd, J 4.6, 5.5), 3.9 (H4', m), 3.7 (H5', H5'). δ_P (D_2O, 162MHz): -0.4, s, 1P (^1H-decoupled).

6.3 THE SYNTHESIS OF NAD^+ ANALOGUES

All NAD^+ analogues with the exception of 8-Br-NAD^+ were prepared essentially by coupling the two mononucleotide units - AMP analogue and nicotinamide mononucleotide, by a method similar to that described by Hughes *et al* [167] using dicyclohexylcarbodiimide as the coupling agent.

NMN and the appropriate AMP analogue were dissolved in water in a round bottom flask, dry pyridine was added to make a 4:1 pyridine:water mixture and excess DCC was subsequently added to the nucleotide mixture. The solution was left stirring at room temperature for 7days. The resulting mixture was poured into 100ml of cold distilled water to quench it and left at 4°C for 2 h to precipitate the DCU formed in the reaction. DCU was filtered off through a sintered glass funnel and the filtrate was extracted with 3×50ml aliquots of chloroform to remove other water insoluble organic impurities. The aqueous layer contained the desired product and was collected, dried down *in vacuo*, the residue dissolved in milliQ to sufficiently lower the conductivity of the solution before ion-exchange purification. The purity of the sample was determined primarily by the presence of an AB system in the ^{31}P-NMR spectrum; ^{1}H NMR, HPLC analysis, MS, quantitative phosphate analysis and UV data were used as analytical techniques to fully characterize the sample. In all cases, unreacted starting materials were recovered and could be coupled again to obtain more material if required.

6.3.1 2′$_A$-Deoxy-nicotinamide adenine dinucleotide (2′$_A$-deoxy-NAD$^+$) **21**

50mg, 149.6μmol of NMN (**19**) and 80mg, 241.5μmol 2′$_A$-deoxy AMP (**17**) were dissolved in 12.5ml of 75%^{V}/v pyridine/water. 2g (9.7mmol) of N,N-dicyclohexylcarbodiimide (DCC) was added to the mixture and the solution was left stirring at room temperature for 7 days. The reaction was quenched by pouring the mixture into 150ml of cold water and the suspension was left at 0°C for 2 h to allow the DCU to precipitate. DCU was filtered off through a sintered glass funnel, and the filtrate was extracted with 3×50ml aliquots of chloroform. The aqueous layer was evaporated to dryness *in vacuo*, the residue was re-dissolved in milli Q water and purified on a Sepharose Q ion exchange column, using a gradient of 0-500mM TEAB buffer, pH 7.6. 2′$_A$-Deoxy-NAD$^+$ eluted as the triethylammonium (TEA) salt between 160-180mM TEAB, in 19% yield and was quantified by measuring UV absorbance at 259nm, using an extinction coefficient of 17,800M^{-1}cm^{-1}.

δ_H (D_2O, 270MHz): 9.3 (H_N2,s), 9,1 (H_N6, d, J 6.2), 8.78 (H_N4, d, J 8), 8.3 (H_A8,s), 8.1 (H_N5, t, J 7), 8.0 (H_A2, s), 6.36 (H_A1′, t, J 7), 6.02 (H_N1′, d, J 5.5), 4.7-4.2 (9 ribose protons - H_A3′, -4′, -5′, -5′ and H_N2′, -3′, -4′ -5′, -5′), δ 2.8 (H_A2′, m), δ 2.5 (H_A2′, m).

δ_P (D_2O, 109MHz): -11.08, -10.72 (2P, J_{PP} 20).

m/z (+ve ion FAB) 648 $(M + H)^+$, *m/z* (-ve ion FAB) 647 M^-, 524 $[M - H - \text{nicotinamide})]^-$.

λ_{max}(pH 8.3)/259nm.

6.3.2 3′$_A$-Deoxy-nicotinamide adenine dinucleotide (3′$_A$-deoxy-NAD$^+$) **22**

15.7mg, 47.4μmol of NMN and 25mg, 75.4μmol of 3′$_A$-deoxy-AMP (**18**) were dissolved in 6ml of 75% aqueous pyridine. DCC (0.63g, 3.05mmol) was added to the solution, which was left stirring at room temperature for 7 days. The reaction was poured into 50ml of cold distilled water and the mixture was left to stand for 2 h at 0°C, after which the precipitate formed was filtered off. Water-insoluble impurities were extracted by shaking the filtrate with 3×50ml aliquots of chloroform. The aqueous layer was dried *in vacuo*, the residue was re-dissolved in milli Q water and purified by ion-exchange chromatography, using a buffer gradient of 0-300mM TEAB, pH 7.6. 3′$_A$-Deoxy-NAD$^+$ eluted between 165-185mM TEAB, in 25% yield, and was quantified by measuring UV absorbance at 259nm using an extinction coefficient of 17,800M^{-1}cm^{-1}.

δ_H (D_2O, 270MHz): 9.2 (H_N2, s), 9.0 (H_N6, d, J 6.2), 8.7 (H_N4, d, J 7.7), 8.2 (H_A8, s), 8.1 (H_N5, t, J 7.5), 8.0 (H_A2, s) 6.0 (H_N1′, d, J 6.0), 5.9 (H_A1′, d, J 3), 4.7-4.0 (9H), 2.3 (H_A3′, m), δ 2.1 (H_A3′, m). δ_P (D_2O, 109MHz): -10.26, -10.74 (2P, J_{PP} 20).

m/z (+ve ion FAB) 648 (M + H)$^+$, *m/z* (-ve ion FAB) 647 M$^-$, 524 [M - H - nicotinamide)]$^-$.

λ_{max}(pH 8.3)/259nm.

6.3.3 3′$_A$-O-Methyl-nicotinamide adenine dinucleotide (3′$_A$-OMe-NAD$^+$) **20**

149μmol of NMN and 170μmol of 3′$_A$-OMe-AMP (**16**) were dissolved in 8ml of 75% aqueous pyridine. DCC (2.0g, 9.5mmol) was added to the solution, which was left stirring at room temperature for 7 days. The reaction was poured into 50ml of cold distilled water and the mixture was left to stand for 2 h at 0°C, after which the precipitate formed was filtered off. Water-insoluble impurities were extracted by shaking the filtrate with 3×50ml aliquots of chloroform. The aqueous layer was dried *in vacuo*, the residue was re-dissolved in milli Q water and purified by ion-exchange chromatography, using a buffer gradient of 0-120mM TEAB, pH 7.6. 3′$_A$-OMe-NAD$^+$ co-eluted with NMN between 40-55mM. There was no improvement in purity by using a shallower gradient of TEAB from 0-70mM. An attempt was made to remove NMN from the desired product by treating the mixture with alkaline phosphatase for 4 h. Care was taken not to leave the solution for too long to avoid degradation of 3$_A$′-OMe-NAD$^+$. After 4 h most of the NMN obtained was converted to nicotinamide mononucleoside which eluted straight off an ion-exchange column upon purification. The sample of 3′-OMe-NAD$^+$ thus obtained was 83% pure by HPLC. This material was used directly to obtain the cyclised product as further attempts to purify the material would have resulted in more loss of material.

δ_H (D_2O, 270MHz): 9.4 (H_N2, s), 9.2 (H_N6, d, J 6.1), 8.7 (H_N4, d J 7.3), 8.5 (H_A8, s), 8.35 (H_A2, s), 8.2 (H_N5, t), 6.15 (H_N1′, d, J 6.5), 5.9 (H_A1′, d, J 5.2), δ 4.8 (H_A2′, J 5.2,

5.5), 4.4.6-4.0 (9H), δ 3.5 (3H, s, -OMe). δ_P (D_2O, 109MHz): -11.5, -11.8 (2P, J_{PP} 19.8).

λ_{max}(pH 8.3)/256nm.

6.3.4 Nicotinamide-8-Bromoadenine dinucleotide (8-Br-NAD$^+$) **24**

200mg (0.3mmol) of β-NAD$^+$ (**23**) as free acid were dissolved in 5ml of acetate buffer pH 3.9. 0.2ml of bromine was added dropwise while stirring rapidly. The reaction was left for 30min after which a 1.25M solution of $NaHSO_3$ was added dropwise to discharge the bromine colour. The sample was dried *in vacuo*, the residue dissolved in milliQ water and the product purified by IE chromatography using a gradient of 0-350mM TEAB. Pure 8-Br-NAD$^+$ eluted between 45-70mM TEAB 61% (184.12μmol) yield. HLPC retention times on technicol column (10x0.46cm) Rt: β-NAD$^+$ (2.0min), 8-Br-NAD$^+$ (2.4min).

δ_H (D_2O, 270MHz): 9.1 (H_N2, s), 8.9 (H_N6, d, J 6.2), 8.6 (H_N4, d, J 8.2Hz), 8.0 (H_N5, t, J 7), 7.8 (H_A2, s), 5.8 (H_N1', d, J 4.8), 5.7 (H_A1', d, J 5.5), 5.0 (H_A2', t, J 5.8), 4.4-4.0 (9H - ribose). δ_P (D_2O, 109MHz): -11.54, -11.92, 2P, AB, J 21.2 (^{1}H-decoupled).

m/z (ES^-): 741.9 [50% $(M)^-$], 637.9 [40% $(M + H_2O$ + nicotinamide$)^-$], 619.9 [100% $(M-$nicotinamide$)^-$].

λ_{max} 264nm (pH 8.3), ε 15,500$M^{-1}cm^{-1}$.

6.3.5 *Nicotinamide-8-Methylaminoadenine dinucleotide(8-NHMe-NAD$^+$)* 25

174.03μmol of 8-methylamino-AMP **6** was coupled to NMN as described above using 2g of DCC. The reaction was worked up after 7days and the crude product was purified by IE chromatography using gradient of 0-350mM TEAB. Residual NMN eluted off first, followed by, 8-NHMe-AMP between 70-100mM TEAB in 16.4% yield. Unreacted 5 eluted off between 170-220mM TEAB. HPLC retention times Rt (min) on a Spherisorb 10μ SAX (25x0.46cm) column with a 3cm Partisil guard column: β-NMN 3.9min, Product (**24**) 4.8min, 8-NHMe-AMP 4.2min.

δ_H (D_2O, 400MHz): 9.1 (H_N2, s), 9.0 (H_N6, d, J 5.8), 8.6 (H_N4, d, J 7.9), 8.0 (H_N5, t. J 7Hz), 7.9 (H_A2, s), 5.9 (H_N1', d, J 4.58), 5.7 (H_A1', d, J 7), 4.5-4.0 (10H - ribose), 2.8 (3H, NMe, s). δ_P (D_2O, 162MHz): -11.7, 2P, s (^{1}H-decoupled).

m/z (+ve ion FAB): 693 [60% $(M + H)^+$], 593 [60% M + NBA - (8-MeNH-adenosine - $CH_2O)^+$], 102 (100%).

λ_{max} 273nm (pH 8.3), ε 13,000$M^{-1}cm^{-1}$.

6.3.6 *Nicotinamide-8-Dimethylamineadenine dinucleotide (8-Me$_2$NH-NAD$^+$)* 26

161μmol of 8-dimethylamino-AMP **7** was coupled to 149.6μmol of β-NMN with 2g of DCC in 12.5ml of pyridine:water (4:1). The reaction mixture was worked up after seven days and the crude product was purified using a gradient of 0-25% TEAB. The desired product sample eluted off with NMN between 70-90mM TEAB, 8-Me_2NH-AMP eluted

off pure between 150-205mM TEAB. The first fraction containing product was re-purified using a gradient of 0-200mM TEAB and pure product eluted between 75-90mM TEAB in 11.5% (17.15μmol) yield. HPLC R_t on Paritsil 10μ SAX (3x0.46cm) in combination with a Spherisorb 10μ SAX column (25x0.46cm): 8-(Me_2NH-NAD^+) 5.5min.

δ_H (D_2O, 400MHz): 9.5 (H_N2, s), 9.3 (H_N6, d, J 6.3), 8.9 (H_N4. d. J 8.0), 8.4 (H_N5, t, J 7), 8.2 (H_A2, s), 6.3 (H_N1', d, 5.4), 5.9 (H_A1', d, J 6.3), 5.4 (H_A2', t, J 6.3), 5.0-4.4 (9H - ribose), 3.1 (3H, NMe_2, s). δ_P (D_2O, 162MHz): -11.42, -11.82, 2P, AB. J 21 (^{1}H-decoupled). *m/z* (+ve ion FAB): 707 [70% $(M + H)^+$], 255 (60%), 120 (100%).

m/z (-ve ion FAB): 706 [70% $(M)^-$, 583.2 [100% $(M - H - \text{nicotinamide})^-$], 469.1 (60%).

λ_{max} 273nm (pH 8.3), ε 16,100$M^{-1}cm^{-1}$.

6.3.7 *Nicotinamide-8-Aminoadenine dinucleotide (8-NH_2-NAD^+)* 27

14mg, 38.69μmol of 8-NH_2-AMP **9** and 8.08mg, 24.18μmol of NMN were dissolved in 1.25ml of distilled water, 5ml of pyridine was added and 0.32g of DCC was added. The solution was left stirring at RT for 7 days and worked up as described above. The crude product was purified using a gradient of 0-150mM TEAB. Pure product eluted between 70-90mM TEAB and was obtained in 16% yield.

δ_H (D_2O, 400MHz): 9.3 (H_N2, s), 9.3 (H_N6, d, J 6.6), 8.75 (H_N4, d, J 6.6), 8.2 (H_N5, t, J 6.6), 8.0 (H_A2,s), 6.1 (H_N1', d, J 4.7), 5.86 (H_A1', d, J 7H), 4.9-4.2 (10H - ribose). δ_P (D_2O, 162MHz): -11.83, -11.97, AB, 2P, J 19.4. (^{1}H-decoupled).

m/z (ES^-): 677 [10% $(M-H)^-$], 555.2 [50% $(M-H-nicotinamide)^-$], 152 [50% $(8\text{-}NH_2\text{-}adenine)^-$], 89.5 (100%).

λ_{max} (pH 8.3) 274nm

6.3.8 *Nicotinamide-8-Piperidyladenine dinucleotide (8-pip-NAD$^+$)* **28**

An attempt was made to synthesise 8-pip-NAD^+ by nucleophilic deplacement of bromide from 8-Br-NAD^+ (**24**) by piperidine. 62.6μmol of 8-Br-NAD^+ were reacted with 0.4ml of piperidine at 50°C for 2.5 h. HPLC analysis showed the presence of a new product. Rt 8-Br-NAD^+ (2.4min), β-NAD^+ (2.0min), 8-pip-NAD^+ (4.9min) on a Technicol 10μ SAX column (10x0.46cm).This was identified as 8-pip-NAD^+ by ^{1}H-NMR, however attempts to separate product from residual 8-Br-NAD^+ were found to be futile. Hence, we decided to couple 8-pip-AMP to NMN in an attempt to obtain pure 8-pip-NAD^+. 107.8μmol of **10** were dissolved in 2.5ml of water and 10ml of anhydrous pyridine. 45.03mg of β-NMN were added followed by 1.8g of DCC. The sample was left stirring for 7 days at room temperature, and worked up. ^{31}P NMR of crude sample showed a singlet at δ 0.5 (singlet - 8-pip-AMP), 0 (singlet β-NMN), -11.5 (AB, 2P, Product), -11.75 (singlet, symmetrical pyrophosphate AMP-AMP). The crude sample was purified

initially using a gradient of 0-500mM TEAB, however, β-NMN eluted off with 8-pip-NAD^+, symmetrical pyrophosphate eluted off between 170-210mM and 8-pip-AMP eluted between 220-280mM TEAB. Fractions containing product were pooled and the product was re-purified using a gradient of 0-200mM TEAB. Pure product eluted between 80-90mM TEAB in 7% yield.

δ_H (D_2O, 400MHz): 9.1 (H_N2, s), 8.9 (H_N6, d, J 6.1), 8.6 (H_N4, d, J 7), 8.1 (H_N5, dd, J 6.4, 7.9), 7.9 (H_A2, s), 5.8 (H_N1', d, J 5.5), 5.5 (H_A1', d, J 6.1), 5.0 (H_A2', dd, J 6.4, 6.1), 4.5-4.0 (9H - ribose), 3.2 (4H, piperidyl, m), 1.6 (6H, piperidyl, m). δ_P (D_2O, 162MHz): -11.44, -11.84, 2P, AB J 20.8 (^{1}H-decoupled).

m/z (ES^-): 747 [20%], 746 [50% (M^-)], 624 (M–nicotinamide), 623 [50% (M–H - nicotinamide)$^{-1}$, 237 [100% (nicotinamide + ribose)$^-$], 97.2 (100%).

λ_{max} 274nm (pH8.3), ε 12,800$M^{-1}cm^{-1}$.

6.3.9 *Nicotinamide-8-Methoxyadenine dinucleotide (8-OCH_3-NAD^+)* 29

166.6μmol of **11** were coupled to 50mg (149.6μmol) of NMN as described in **6.1**. The sample was worked up after 7 days followed by purification of the crude product using a gradient of 0-130mM TEAB on an ion exchange GP250 column. NMN eluted off between 4-5mM, 8-OCH_3-NAD^+, 5-6mM, 8-OCH_3-AMP 11-11.5mM TEAB. Pure 8-OCH_3-NAD^+ was obtained in 16% (25.3μmol) yield. HPLC R_t on a Partisil guard

column (3×0.46cm) in combination with a (10×0.46cm) Partisil 10μ SAX column 8-(OCH_3)NAD^+ 2.4min

.

δ_H (D_2O, 400MHz): 9.1 (H_N2,s), 9.0 (H_N6, d, J 6.1), 8.6(H_N4, d, J 7.9), 8.1 (H_N5, t, J 6.4, 7.61), 7.9 (H_A2, s), 5.85 (H_N1', d, J 4.9), 5.7 (H_A1', d, J 5.2), 4.8 (H_A2', t, J 5.2, 5.8), 4.6 - 4.0 (9H- ribose), 4.0 (3H, O-CH_3, s). δ_P (D_2O, 162MHz): -11.38, -11.51, -11.8, -11.97, 2P, AB, J 20.9 (^{1}H-decoupled).

m/z (ES^+): 694 [100%, $M+H)^+$], 795 [40%, $M+TEA)^+$], 239 (50%), 317 (40%). (ES^-): 692 [100%, $M-H)^-$], 677 [40% $(M-H-CH_3)^-$].

λ_{max} 259 (pH 8.3), ε 13,000$M^{-1}cm^{-1}$.

6.3.10 *Nicotinamide-8-Methyladenine dinucleotide (8-Me-NAD^+)* 30.

139.2μmol of **14** as the triethylammonium salt was coupled to 149.6μmol of β-NMN (**19**) in 12.5ml of pyridine:water (4:1) and 2g of DCC as described above. The reaction mixture was worked up after 7 days followed by ion exchange purification of the crude product on GP250 IE chromatograph using a gradient of 0-150mM TEAB. Unreacted NMN eluted off between 35-40mM, 8-Me-NAD^+ at 45-50mM, and unreacted 8-Me-AMP at 100-120mM TEAB. Pure product was obtained with 12.4% yield (17.23μmol). HPLC R_t: 8-Me-NAD^+ (2.46min).

δ_H (D_2O, 400MHz): 9.3 (H_N2, s), 8.9 (H_N6, d, J 6.1), 8.6 (H_N4, d, J 6.3), 8.0 (H_N5, t, 7), 7.9 (H_A2, s), 5.8 (H_N1', d, J 5.2), 5.7 (H_A1', d, J 6.4), 4.7 (H_A2', t, 6.2), 4.6-4.2 (9H - ribose), 2.5 (3H, Me, s). δ_P (D_2O, 162MHz): -10.96, -11.34, 2P, AB, J 20.5 (^{1}H-decoupled).

m/z (ES^-): 676 [100% $(M-H)^-$], 410 [50% $(NMN + HPO_3^{2-})^-$], 338 [45% (M–H + TEA- (8-Me-adenosine diphosphate - O-)$^-$].

λ_{max} 259nm (pH 8.3), ε 13,755$M^{-1}cm^{-1}$.

6.3.11 *Nicotinamide-8-Oxyadenine dinucleotide (8-oxy-NAD$^+$)* 31

155.28μmol of **13** were coupled to 50mg (149.6μmol) of NMN in the usual manner. The sample was worked up after 7 days followed by purification of the crude product using a gradient of 0-150mM TEAB on an ion exchange GP250 column. NMN eluted off between 3-4mM, 8-oxy-NAD^+, 8-9mM, 8-oxy-AMP 13-20mM TEAB. Pure 8-oxy-NAD^+ was obtained in 8.8% (13.1μmol) yield. HPLC Rt on (3x0.46cm) Partisil guard column in combination with a (10x0.46cm) Partisil 10μ SAX column 8-oxy-NAD^+ 3.4min.

δ_H (D_2O, 400MHz): 9.1 (H_N2,s), 8.9 (H_N6, d, J 6.0), 8.5(H_N4, d, J 6.5), 8.1 (H_N5, t, J 5.1), 7.7 (H_A2, s), 5.85 (H_N1', d, J 4.5), 5.5 (H_A1', d, J 5.6), 4.9 (H_A2', t, J 5.3), 4.4 - 4.0 (9H- ribose). δ_P (D_2O, 162MHz): -11.44, -11.92, 2P, AB, J 21 (^{1}H-decoupled).

m/z (ES^-): 678 [100% $(M-H)^-$], 339 (90%), 277 (60%).

λ_{max} 266 (pH 8.3), ε 13,100$M^{-1}cm^{-1}$.

6.3.12 *8-Aza-9-deaza-nicotinamide adenine dinucleotied* (NFD^+) 33

75mg (205.36μmol) of formycin 5′-monophosphate A (**32**) as the monoammonium salt was coupled to 50mg (149.6μmol) of NMN in 12.5ml Pyridine : water (4:1). 2g of DCC was added and the mixture was left stirring at RT for 8 days. The reaction was worked up as already described above and products were purified using a TEAB gradient between 0-150mM TEAB. The residual NMN eluted first between 50-60mM TEAB followed by NFD^+ at 80-90mM, and formycin 5′- monophosphate at 120-130mM TEAB. Pure product was obtained in 9.3% (13.9μmol) yield. HPLC retention time: (column as above) 2.2min (NFD^+).

δ_H (D_2O, 270MHz): 9.2 (H_N2, s), 9.05 (H_N6, d, J 5.3), 8.6 (H_N4, d, J 8), 8.05 (H_N5, t), 8.0 (H_A2, s), 6.0 (H_N1', d, J 5.3), 5.2 H_A1', d, J 7.1), 5.0-4.0 (10H). δ_P (D_2O, 162MHz): -11.78, -12.48, 2P, AB J 21.6 (^1H-decoupled).

m/z (ES^-): 662 [30% $(M-H)^-$], 278 (50%), 209 (95%), 164 (100%).

λ_{max} 275nm (pH 8.3) ε_{275} 4,600$M^{-1}cm^{-1}$.

6.4 Qualitative Analysis of NAD^+ analogues.

The authenticity of the NAD^+ analogues thus synthesized was confirmed by testing for coenzyme activity [176] and the ability to form a complex with cyanide [180]. 1μmol of NAD^+ or analogue was diluted to 25ml in 5%v/v ethanol in 0.1M Tris buffer pH 8.8. 3.75ml of the nucleotide solution was measured into a curvette. The UV spectrum was recorded at this stage as the blank (i.e without alchohol dehydrogenase). 3μl of a 7.8units/μl solution of alcohol dehydrogenase was added into the solution in the curvette. The UV spectrum was scanned after two minutes. A new peak at around 340nm that was not present in the blank was observed for all analogues. As a further control, the UV spectrum of the enzyme in the 5% Ethanol in 0.1M Tris buffer was scanned. There was no peak observed at 340nm.

NAD^+ and analogues were treated with potassium cyanide to see whether they complex with cyanide. 2.75ml of 0.1M KCN solution in distilled water was measured in a curvette. 0.25ml of 0.2mM of the NAD^+ or NAD^+ analogue was added to the cyanide solution in the curvette. A new peak at around 325nm was observed which represents the complex formed with cycanide. In two control experiment, UV absorption spectra of the cyanide solution alone and another with just the dinucleotide, there was no peak at 325nm.

6.5 Synthesis of Analogues of Cyclic-Adenosine Diphosphate Ribose.

6.5.1 *Cyclic adenosine diphosphate ribose* (cADPR) 40.

2.5ml of 1.5mM solution of NAD^+ in 25mM HEPES, pH 6.8 was incubated with 10µl of crude ADP-ribosyl cyclase for 10 min at room temperature. The sample was analyzed before and after enzymatic incubation by HPLC using a Partisil 10µ SAX guard column (10×0.46cm) in combination with a Technicol (10×0.46cm) SAX column and isocratic elution with 0.05M phosphate buffer pH 3. After 10 min, the incubation mixture was diluted with 100ml of milli Q water and the products were purified by ion exchange chromatography using a gradient of 0-300mM TEAB, pH 7.6. The purity of the product obtained was verified by HPLC analysis as described above. cADPR was obtained in 60% yield and was quantified by measuring UV absorbance at 254nm using an extinction coefficient of $14{,}300M^{-1}cm^{-1}$ [55].

R_t - (incubation mixture after 10min): 4.7min (nicotinamide), 7.8min (cADPR), 10.3min (NAD^+). δ_H (D_2O, 400MHz): 8.9 (H_A2,s), 8.2 (H_A8, s), 6.0 (H1′, d, J 3.8), 5.85 (H_A1', d, J 7), 5.2 (H_A2', t, J 7) 4.7 (H_A3'), 4.6 (H2′, H4′), 4.4 (H3′, H_A5'), 4.3 (H5′), 4.2 (H_A4 ′), 4.0 (H5′), 3.8 (H_A5'). δ_P (D_2O, 162MHz): −11.36, -11.84 (2P, J_{PP} 14.9).

m/z (+ve ion FAB) 541 M^+. *m/z* (-ve ion FAB) 540 $(M - H)^-$.

6.5.2 *$2'_A$-Deoxy-cyclic adenosine diphosphate ribose ($2'_A$-deoxy-cADPR)* 37

Enzymatic cyclisation of $2'_A$-deoxy-NAD^+ (21) was carried out as described above for NAD^+. HPLC analysis was on a Spherisorb SAX column using isocratic elution with

phosphate buffer. Ion exchange purification of the product was carried out using a gradient of 0-300mM TEAB.pH 7.6 Nicotinamide eluted straight off the column followed by $2'_A$-deoxy-cADPR between 190-240mM TEAB, in 61% yield, and lastly $2'_A$-deoxy-ADPR. Pure $2'_A$-deoxy-cADPR was quantified by measuring UV absorbance at 254nm using an extinction coefficient of $14{,}300M^{-1}cm^{-1}$.

R_t - (incubation mixture): 3.1min (nicotinamide), 4.9min ($2'_A$-deoxy-NAD^+), 7.2min ($2'_A$-deoxy-cADPR), 10.2min $2'_A$-deoxy-ADPR. δ_H (D_2O, 400MHz): 8.9 (H_A2, s), 8.2 (H_A8, s), 6.4 (H_A1', t, J 7), 6.1 (H1', d, 5.5), 4.8 (H_A3'), 4.7 (H2', t), 4.6 (H4'), 4.4 (H3', H_A5'), 4.3 (H_A5'), 4.2 (H_A4'), 4.0(H5'), 3.9(H_A5'), 3.2 (H_A2', m), 2.4 (H_A2', m). δ_P (D_2O, 162MHz): -11.37, -11.68 (2P, J_{PP} 15.8) (Fig 6).

m/z (+ve ion FAB) 1051 $(2M + H)^+$ dimer, 627 $(M + TEA)^+$. *m/z* (-ve ion FAB) 524 $(M - H)^-$ 1049 $(2M - H)^-$.

λ_{max}(pH 8.3)/259 nm.

6.5.3 $3'_A$-Deoxy-cyclic adenosine diphosphate ribose ($3'_A$-deoxy-cADPR) **38**.

Enzymatic cyclisation of $3'_A$-deoxy-NAD^+ (**22**), purification and the analytical procedures used were as described for NAD^+ above. $3'_A$-deoxy-cADPR eluted from the ion exchange column between 165-185mM in 50% yield, and was quantified by measuring UV absorbance at 254nm using an extinction coefficient of $14{,}300M^{-1}cm^{-1}$.

R_t - (incubation mixture after 10min) - 4.85min (nicotinamide), 11.3min (3′$_A$-deoxy-cADPR), 18.3min (3′$_A$-deoxy-NAD$^+$). δ_H (D_2O, 400MHz): 8.7 (H_A2, s), 8.4 (H_A8, s), 6.0 (H1′, d, J 6), 5.9 (H_A1′, d, J 3), 5.2 (H_A2′, m) 4.7 (H2′), 4.5 (H4′, H5′), 4.4 (H3′), 4.2 (H_A5′, H_A4′), 4.0 (H5′), 3.8 (H_A5′), 2.8 (H_A3′), 2.1 (H_A3′). δ_H (D_2O, 400MHz): -11.56, -12.44 (2P, J_{PP}=15.13).

m/z (+ve ion FAB) 526 $(M + H)^+$, 627 $(M + TEA)^+$ *m/z* (-ve ion FAB) 524 $(M - H)^-$, 1049 $(2M - H)^-$.

λ_{max}(pH 8.3)/259 nm.

6.5.4 ***3′$_A$-O-Methyl-cyclic adenosine diphosphate ribose (3′$_A$-OMe-cADPR)*** **39**

2×2.5μmol of 3′-OMe-NAD$^+$ (**20**) were each dissolved to 2ml in 25mM HEPES-NaOH buffer pH6.8. 20μl of *Aplysia* cyclase (10mg/ml protein concentration) were added to each solution. The mixtures were left to incubate for 20min after which the solutions were combined and diluted with 100ml milliQ water and the products purified by ion exchange chromatography using a gradient of 0-200mM TEAB. Residual product 3′-OMe-NAD$^+$ eluted between 60-70mM, followed by 3′$_A$-OMe-cADPR between 140-150mM TEAB. Pure product was obtained in 40% (2.0μmols) yield quantified using by measuring UV absorbance at 254nm using an extinction coefficient of 14,300$M^{-1}cm^{-1}$. HPLC retention times were measured on 3x0.46cm guard column in combination with a 10x0.46cm Partisil 10μ SAX column.

R_t - (incubation mixture after 20min): 1.7 min (nicotinamide), 2.5 min ($3'_A$-OMe-NAD^+),4.4 min. δ_H (D_2O, 400MHz): 8.9 (H_A2, s), 8.3 (H_A8, s), 6.0 (H1′, d, J 3.6), 5.9 (H_A1', d, J 5.5), 5.3 (H_A2', dd, J 5.5, 5.2) 4.7-3.8 (9H - ribose protons H2′, 3′, 4′, 5′, 5′, H_A3', -4′, -5′, -5′). δ_P (D_2O, 162MHz): -10.55, -11.55, 2P (^{1}H-decoupled).

m/z (+ve ion-FAB): 376.3 (75%), 239.2 (25%), 297.2 (20%). *m/z* (-ve ion FAB) 554[20%. M – H)$^-$], 494 (90%) 478 (70%), 341.

λ_{max} 256nm (pH 8.3), ε_{254} 14,300$M^{-1}cm^{-1}$.

6.5.5 *$3'_A$-Phospho-cyclic adenosine diphosphate ribose ($3'_A$-cADPRP)* 41`

2×3μmol of $3_A'$-$NADP^+$ (**35**) were each dissolved to 2ml in 25mM HEPES-NaOH buffer pH6.8. 20μl of *Aplysia* cyclase (10mg/ml protein concentration) was added to each solution. The mixtures were left to incubate for 20min after which the solutions were combined and diluted with 100ml milliQ water and the products purified by ion exchange chromatography using a gradient of 0-500mM TEAB. Pure $3_A'$-cADPRP eluted off between 120-145mM TEAB. Pure product was obtained in 54% (3.2μmols) yield. HPLC retention times were measured on 3x0.46cm guard column in combination with a 10x0.46cm Partisil 10μ SAX column:

R_t -(incubation mixture after 20 min) : 2.1 min (nicotinamide), 15.9 min ($3'_A$-P-NAD^+), 15.9 min ($3'_A$-P-cADPR). δ_H (D_2O, 400MHz): 8.9 (H_A2, s), 8.3 (H_A8, s), 6.0 (H1′, d, J

3.7), 5.98 (H_A1', d, J 7.3), 5.3 (H_A2', dd, J 5.0, 7.0) 4.6-3.9 (9H - ribose protons H2', 3', 4', 5', 5', H_A3', -4', -5', -5'). δ_P (D_2O, 162MHz): +1.0, (1P,s), -11.0, -11.75, 2P J_{PP}=22.6Hz (^1H-decoupled).

m/z (+ve ion FAB): 723.1 [40%, M + TEA)$^+$], 622 [40%, M + H)$^+$], 301.2 (40%). *m/z* (-ve ion FAB): 620.1[30%. M – H)$^-$], 341 (40%) 188 (100%).

FAB-accurate mass (-ve ion) 621.021317 (18.6%, M)$^-$], 620.019562 (91.3%, M – H)$^-$].

λ_{max} 256nm (pH 8.3)

6.5.6 *$2'_A,3'_A$-cyclic-phospho-cyclic adenosine diphosphate ribose ($2'_A,3'_A$-cyclic-cADPRP)* 42

2×3μmol of $2'_A,3'_A$-cyclic-NADP$^+$ (**36**) were each dissolved to 2ml in 25mM HEPES-NaOH buffer pH6.8. 20μl of *Aplysia* cyclase (10mg/ml protein concentration) was added to each solution. The mixtures were left to incubate for 20min after which the solutions were combined and diluted with 100ml milliQ water and the products purified by ion exchange chromatography using a gradient of 0-400mM TEAB. Residual product $2'_A,3'_A$-cyclic-NADP$^+$ eluted between 180-190mM, followed by $2'_A,3'_A$-cyclic-cADPRP between 260-290mM TEAB. Pure product was obtained in 45% (2.7μmols) yield, quantified by measuring UV absorbance at 259nm using an extinction coefficient of

14,300$M^{-1}cm^{-1}$. HPLC retention times were measured on 3×0.46cm guard column in combination with a 10×0.46cm Partisil 10μ SAX column.

R_t - (incubation mixture after 20min) 2.1 min (nicotinamide), 9.0 min ($2'_A,3'_A$-cyclic-NADP), 8.3 min ($2'_A,3'_A$-cyclic-cADPRP). δ_H (D_2O, 400MHz): 8.7 (H_A2, s), 8.1 (H_A8, s), 6.2 (H1', s), 5.9 (H_A1', d), 5.3 (H_A2', dd, J 8.0, 6.4), 5.5 (HA3', dd, J 4.3, 5.8), 4.6-3.9 (8H - ribose protons H2', 3', 4', 5', 5', H_A4', - -5', -5'). δ_P (D_2O, 162MHz): +19.0, (1P,s), -10.8, -11.2, 2P J_{PP} 13.8Hz (^1H-decoupled).

m/z (+ve ion FAB): 604 [70%, $M + H)^+$], 490 (20%). (-ve ion FAB): 602.1[100%. $M - H)^-$]. FAB-accurate mass (-ve ion) 603.011932 (19.6%, $M)^-$], 620.0008835 (100%, $M - H)^-$].

λ_{max} 256nm (pH 8.3)

6.5.7 *8-Bromo-cyclic-adenosine diphosphate ribose* (8-Br-cADPR) 43

2×2.24mg of **24** were dissolved in 2.5ml with 25mM HEPES-NaoH buffer pH 6.8, 10μl of *Aplysia* cyclase (protein concentration of 10μg/ml) was added to the solution which was shaken. The incubation mixture was left for 10min at room temperature and the course of reaction was followed by HPLC analysis. The mixtures were pooled, dissolved in milliQ water and the crude products were purified immediately by ion exchange purification using a gradient of 0-30% TEAB, pure 8-Br-cADPR eluted off between

185-220mM TEAB in 60% yield. HPLC retention times was measured on Partisil 10μ SAX column (10x0.46cm):

R_t - (incubation mixture after 10min) 1.5min (nicotinamide), 2.4min (8-Br NAD^+), 3.9min (8-Br-cADPR). δ_H (D_2O, 400MHz): 8.8 (H_A2', s), 6.3 (H1', d, J 6.1), 6.0 (H_A1', d, J 2), 5.6 (H_A2', t, J 5), 4.2-5.0 (9H - ribose). δ_P (D_2O, 162MHz): -10.83, -11.05, 2P, AB, J 13.2 (^{1}H-decoupled).

m/z (Electrospray): 619.9 (M), 96.9 ($H_2PO_4^-$), 80.9 ($H_2PO_3^-$), 78.9 (PO_3^{2-}).

λ_{max} 264nm ε 15,730$M^{-1}cm^{-1}$[120].

6.5.8 ***8-Methylamino-cyclic-adenosine diphosphate ribose (8-NHMe-cADPR)*** **44**

2x2.5mg of **25** were each diluted to 2.5ml in HEPES-NaOH pH 6.8. 15μl of crude *Aplysia* cyclase (protein concentration of 10mg/ml) was added to each solution and mixed in. The reaction mixture was diluted with milliQ water after 10min and the product subsequently purified using a TEAB gradient of 0-25% TEAB. Pure sample eluted off between in 42% (3μmol) yield. HPLC retention times were measured on a combination of 3x0.46cm guard column and a Spherisorb 25x0.46cm column.

R_t - (incubation mixture after 10min): 3.6min (nicotinamide), 4.7min (8-NHMe-NAD^+), 7.8min (8-NHMe-cADPR). δ_H (D_2O, 400MHz): 8.6 (H_A2, s), 5.9 (H1', d, J 4), 5.7

(H_A1', d, J 5.5), 5.4 (H_A2', t, J 5), 4.4-3.8 (9H), 2.8 (3H, -NMe, s). δ_P (D_2O, 162MHz): -10.87, -11.58, 2P, AB, J 14.9 (^{1}H-decoupled).

m/z (ES^-): 569 [100% $(M-H)^-$], 164 [50% (8-NMe-adenine)$^-$, 79 (100%$^-$).

λ_{max} 279nm(pH 8.3) ε_{279} 11,050$M^{-1}cm^{-1}$.

6.5.9 8-Dimethylamino-cyclic-adenosine diphosphate ribose (8-NMe_2-cADPR) 45

2×2.98mg of **26** were each dissolved each in 2.5ml of HEPES-NaOH buffer pH 6.8. 15µl of *Aplysia* cyclase (protein concentration of 10µg/ml) was added to each solution which was left to incubated for 10min at room temperature. The mixtures were combined and the crude product was purified by using a TEAB gradient of 50-250mM. Residual 8-Me_2NH-NAD^+ eluted off between 100-110mM followed by 8-NMe_2-cADPR between 120-140mM and lastly 8-ADPR between 160-170mM TEAB. Pure 8-NMe_2-cADPR was obtained in 61.6% (5.2µmol) yield. HPLC retention time was measured on a combination of 3x0.46cm guard column and 25×0.46cm Spherisorb 10µ SAX column.

R_t - (incubation mixture after 10min): 3.7min (nicotinamide), 5.8min (8-NMe_2-NAD^+), 9.7min (8-NMe_2-cADPR). δ_H (D_2O, 400MHz): 9.1 (H_A2, s), 6.3 (H1', d, J 4), 6.2 (H_A1', d, J 6.4), 5.6 (H_A2', dd, J 5.8, 5.5), 5.0-4.2 (9H), 3.2 (6H, -NMe_2, s). δ_P (D_2O, 162MHz): -5.66, -6.42, 2P, AB, J 15.4 (^{1}H-decoupled).

m/z (ES^-): 583 [100% $(M-H)^-$], 161 (20%).

λ_{max} 282nm ε_{282} 11,800$M^{-1}cm^{-1}$.

6.5.10 *8-Methoxy-cyclic-adenosine diphosphate ribose (8-OCH_3-cADPR)* 46

3×4μmol of 8-OCH_3-NAD^+ (**29**) were each dissolved to 2ml in 25mM HEPES- NaOH buffer pH 6.8 and incubated with 20μl of *Aplysia* cyclase for 20min after which the crude mixtures were pooled, diluted with milliQ water to 100ml and purified using a gradient of 50-250mM TEAB. 8-OCH_3-NAD^+ eluted off between 60-65mM TEAB, followed by 8-OCH_3-cADPR between 70-75mM. Pure product was obtained in 53% yield (6.4μmols). HPLC analysis was measured using a 3cm guard column in combination with a Partisil 10μ SAX (10×0.46cm):

R_t - (incubation mixture after 20min): 1.9min (nicotinamide), 2.4min (8-OCH_3-NAD^+), 4.0min (8-OCH_3-cADPR). δ_H (D_2O, 400MHz): 8.8 (H_A2, s), 6.0 (H1′, d, J 4.0), 5.9 (H_A1', d, J 5.9), 5.2 (H_A2', t, J 5.4, 4.9) 4.65 (H2′, H_A3'), 4.6 (H4′), 4.35 (H3′), 4.25 (H_A4', H5′), 4.2 (H_A5'), 4.1 (3H, O-CH_3, s) 4.0 (H5′,), 3.9 (H_A5',). δ_P (D_2O, 162MHz): -10.9, 2P, s, (^{1}H-decoupled).

m/z (ES^-): 570 [100%, $(M-H)^-$], 571 [20%, M^-].

λ_{max} 259nm (pH 8.3), ε_{259} 10,300$M^{-1}cm^{-1}$.

6.5.11 *8-Piperidyl-cyclic-adenosine diphosphate ribose (8-pip-cADPR)* **47**

3.75mg of **28** were diluted to 3.3ml in 25mM HEPES buffer pH 6.8, 10µl of crude *Aplysia* cylase (protein concentration of 10µg/ml) was added to the solution which was shaken well. Incubation mixture was left for 15min after which it was diluted with milliQ water and the product purified using a gradient to 0-350mM TEAB on an ion exchange column. Residual 8-pip-NAD^+ eluted off between 60-110mM, followed by 8-pip-cADPR between 135-165mM, and 8-pip-ADPR at 210-240mM TEAB. Pure product was obtained in 49.5% (2.5µmol) yield. HPLC retention times on 3x0.46cm guard colum with a partisil 10µ SAX column (10×0.46cm):

R_t - (incubation mixture after 15min): 2.1min (nicotinamide), 6.3min (8-pip-NAD^+), 16.2min (8-pip-cADPR). δ_H (D_2O, 400MHz): 8.9 (H_A2, s), 6.1 (H1′, d, J 4.0), 5.9 (H_A1', d, 5.8), 5.4 (H_A2', t, J 4.2), 4.5-4.0 (9H - ribose), 3.2 (4H, piperidyl, m), 1.7 (6H, piperidyl, m). δ_P (D_2O, 162MHz): -10.92, -11.76, 2P, AB, J 15.9 (^{1}H-decoupled).

m/z (ES^-): 624 [20% $(M)^-$, 623 [100% $(M-H)^-$], 291 (ribose diphosphate-O-), 96.8 80.79 (50%), 78.6 (70%).

λ_{max} 282nm (pH 8.3) ε_{282} 12,000$M^{-1}cm^{-1}$.

6.5.12 *8-Amino-cyclic-adenosine diphosphate ribose (8-NH_2-cADPR)* 48

1.5mM solution of 8-NH2-NAD+ (**27**) in 1ml of 25mM HEPES-NaOH pH 6.8 was incubated with 10µl of *Aplysia* enzyme at RT for 10min. The sample was analysed before and after incubation by HPLC on a Spherisorb 10µ SAX (25×0.46cm) column. The crude products were purified using a TEAB gradient of 50-500mM TEAB, and pure 8-NH_2-cADPR eluted off between 145-170mM TEAB in 48% (0.72µmol) yield.

R_t - (incubation mixture after 10min): 2.8min (nicotinamide), 4.1min (8-NH_2-NAD^+), 6.4min (8-NH_2-cADPR).δ_H (D_2O, 400MHz): 9.0 (H_A2, s), 6.4 (H1′, d, J 5.0), 6.1 (H_A1', d, J 7.6), 5.0-4.2 (9H - ribose). δ_P (D_2O, 162MHz): -13.35, -14.05, 2P, AB, J 17.5 (^1H-decoupled).

m/z (ES^-): 555.2 [100% $(M-H)^-$], 353 (50%), 176.4 (40%).

λmax 274, ε_{274} 15,730$M^{-1}cm^{-1}$ [120].

6.5.13 *8-Methyl-cyclic-adenosine diphosphate ribose (8-Me-cADPR)* 49

3×3µmol of **30** were each dissolved to 2ml in 2.5mM HEPES-NaOH buffer pH6.8. 20µl of *Aplysia* cyclase (10mg/ml protein concentration) was added to each solution. The mixtures were left to incubate for 10min after which the solutions were combined and diluted with 100ml milliQ water and the products purified by ion exchange chromatography using a gradient of 50-250mM TEAB. Residual product 8-Me-NAD^+ eluted between 60-70mM, followed by 8-Me-cADPR between 80-90mM TEAB. Pure

product was obtained in 83.6% (7.5μmols) yield. HPLC retention times were measured on 3x0.46cm guard column in combination with a 10×0.46cm Partisil 10μ SAX column.

R_t - (incubation mixture after 10min): 1.96min (nicotinamide), 2.4min (8-Me-NAD^+), 4.2min (8-Me-cADPR) δ_H (D_2O, 400MHz): 8.8 (H_A2, s), 6.0 (H1′, d, J 4), 5.85 (H_A1', d, J 5.5), 5.3 (H_A2', t, J 5.5), 4.6-4.0 (9H - ribose), 2.5 (3H, Me, s). δ_P (D_2O, 162MHz): -8.3, -9.1, 2P, AB, J 16.1 (^{1}H-decoupled).

m/z (ES^-): 555 [20% $(M)^-$], 554 [60%$(M-H)^-$], 276 [40% $(M+H-(8\text{-Me-adenosine})^-$], 97 (60%), 81, 79 (100%).

λ_{max} 260 pH 8.3 ε_{260} 10,000$M^{-1}cm^{-1}$.

6.5.14 *8-Oxy-cyclic-adenosine diphosphate ribose (8-oxy-cADPR)* **50**

3×3μmols of **31** were each treated with 20μl of the crude *Aplysia* cyclase (protein concentration of 10μg/ml) for 20min as described above. Mixtures were combined and diluted with 100ml of milliQ water followed by purification using a TEAB gradient of 50-250mM TEAB sample eluted off between 220-250mM with 48.7% (4.4μmol) yield. HPLC retention times were measured on 3×0.46cm guard column with a 10×0.46cm column.

R_t - (incubation mixture after 20min): 1.96min (nicotinamide), 2.5min (8-oxy-NAD^+), 5.95min (8-oxy-cADPR). δ_H (D_2O, 400MHz): 8.8 (H_A2, s), 6.0 (H1′, d, J 4), 5.8 (H_A1', d, J 5.6), 5.2 (H_A2', t, J 5.3), 4.6-3.9 (9H - ribose). δ_P (D_2O, 162MHz): -10.85, -11.3, 2P, AB, J 16.1 (^{1}H-decoupled).

m/z (ES^-): 556 [20% $(M-H)^-$], 277 [30% $(M + 2H$ - 8-oxy-adenosine$)^-$], 97 (90%), 81, 79 (100%).

λ_{max} 279nm pH 8.3 ε_{279} 9,800$M^{-1}cm^{-1}$.

6.5.15 8-Aza-9-deaza-cyclic adenosine diphosphate ribose (cFDPR) 51

3×2μmol of **33** were each dissolved to 2ml in 25mM HEPES- NaOH buffer pH 6.8 and incubated with 20μl of *Aplysia* cyclase for 20min after which the mixture was diluted with milliQ water to 100ml and products were purified using a gradient of 0-300mM TEAB. The pure product eluted between 170-190mM TEAB with 40% yield. HPLC analysis of the incubation mixture was measured on a 3cm guard column in combination with a Partisil 10μ SAX (10×0.46cm) column.

R_t - (incubation mixture after 20min): 1.96min (nicotinamide), 2.2min (NFD^+), 5.95min (cFDPR). δ_H (D_2O, 400MHz): 8.2 (H_A2, s), 6.0 (H1′, d, J 5.3), 5.2 (H_A1', d, J 7.1), 5.0 (H_A2', t) 4.65 (H2′, t, H_A3'), 4.6 (H4′), 4.35 (H3′), 4.255 (H_A4', H5′), 4.2 (H_A5'), 4.0 (H5″), (H_A5'). δ_P (D_2O, 162MHz): -11.65, -11.95, 2P, AB, J 15.7 (^{1}H-decoupled).

m/z (ES^-): [540 (70% $M-H)^-$], 269 (100%).

λ_{max} 275nm (pH 8.3), ε_{275} 10,300$M^{-1}cm^{-1}$.

6.6 K_m and V_{max} Determination for NAD^+, $2_A'$ and $3_A'$-Deoxy-NAD^+

The kinetics of enzymatic conversion of the above analogues in their cyclic products were investigated using an HPLC method. The conversion was followed by measuring the area under the peak for nicotinamide, which is a product formed during conversion. Substrate concentrations between 25-500μM in 25mM HEPES buffer pH 6.8 were used. The total volume in the reaction vessel (an Eppendorff) was kept at 500μl for each reaction. The incubation mixture was prepared to have 250μl of sample with 225μl of buffer and 25μl of enzyme to make a total of 500μl. A final enzyme concentration of 5μg/ml was used in the assay for NAD^+, and 2.5μg/ml for $2_A'$deoxy NAD^+ and $3_A'$-deoxy-NAD^+. Each reaction was analysed every minute over 6 minutes. The relative area for nicotinamide was measured and a graph of area of nicotinamide vs time was plotted at each concentration of substrate used. The reaction was carried out in duplicates. Initial velocity was calculated from the slope of this curve and an average initial velocity obtained from the two sets of data. A double reciprocal plot (Lineweaver-burke plot) was plotted of 1/V (*y* axis) vs 1/S (*x*-axis) using the Enzpak3 computer programme (a representative graph plot is shown in Fig. 4.12. K_m and V_{max} were obtained from this plot. K_m values obtained were 75.2μM, 0.7mM and 0.5mM and V_{max}

values were 23.3, 47.9, 22.4μg/mg/min for NAD^+, $2'_A$-deoxy-NAD^+ and $3'_A$-deoxy-NAD^+ respectively.

6.7 Protein Estimation of ADP-ribosyl cyclase

The Biorad protein estimation assay was used to estimate the amount of protein in the crude *Aplysia* cyclase. Bovine albumin of known protein concentration was used as a standard. Final concentrations of standard were made from 1.56μg.ml to 25μg/ml. Serial dilution of test samples of 1 in 25, 1in 50, 1in 100 and 1 in 200 were made. 200μl of test samples (1.56, 3.125, 6.25, 12.5, 15, 20 and 25μg/ml) and test solutions of different dilution factor were measured into wells in a microtitre plate in duplicate. Solutions were made in 150mM PBS buffer. 50μl of the Biorad reagent was added to each sample and left for 15mins to allow for colour to develop. UV absorption was measured and analysed on a Biolink 2.10. A standard curve was obtained of absorbance vs. protein concentration for bovine albumin. The protein concentration corresponding to the absorbance measured for the test samples were obtained from the standard plot. Dilutions 1in 25 and 1in 50 were over the UV range of the standard curve. Therefore results obtained form the 1 in 100 and 1 in 200 dilution were used for the assay. The mean of the two sets of data for each concentration was obtained and estimated value obtained was 10mg protein per ml.

6.8 Quantitative Phosphate Analysis

All phosphorus containing compounds were quantified by using a modificatio of the Briggs test for phosphate analysis [182]. KH_2PO_4 was used as a standard. Standard stock

solution containig 1nmol/μl was made from KH_2PO_4. 50, 100, 150 and 200nmols of standard phosphate solution were used. Each solution was made to 400μl in Pyrex test tubes. Test stock solutions were prepared to contain an estimated value of 2000nmols of phosphate in 5mls. 125, 250 and 375μl of the test solution were used and each solution were made to 400μl. Milli Q water was used throughout test for dilutions and experiment was carried out in triplicates. A blank was also prepared with 400μl of milli Q. The blank, standard and sample solutions were dried in an oven at 175°C for 1 h. After 1 h the samples were allowed to cool down and 3 drops of concentrated sulphuric acid was added to the sample in each test tube and heated for 1.5 h to free the phosphates. Briggs solutions were prepared meanwhile as thus: Solution 1 was 2.5g of ammonium molybdate dissolved in 20ml of water. 8ml of concentrated H_2SO_4 was added to ammonium molybdate solution. Solution 2, 0.1g of quinol was dissolved in 20ml of water and one drop on acid added. Solution 3, 4.0g of sodium sulphite was dissolved in 20ml of water. After 1.5 h samples were taken out of the oven and cooled down. 200μl of milli Q water was added to each test tube to dissolve the phosphate in solution. 400μl of solution 1, 200μl of solution 2 and 200μl of solution 3 were added to each solution. Solutions were heated in the test tube for 10 s using a heat gun. Each solution was dissolve to 5ml in a 5ml volumetric flask and left for 30mins for the blue colour to develop. UV absorbance was measured against blank at 340nm. A standard graph of absorbance vs amount of phosphate was plotted. The amount of phosphate in the test samples were obtained from the standard curve and the total amount of sample in

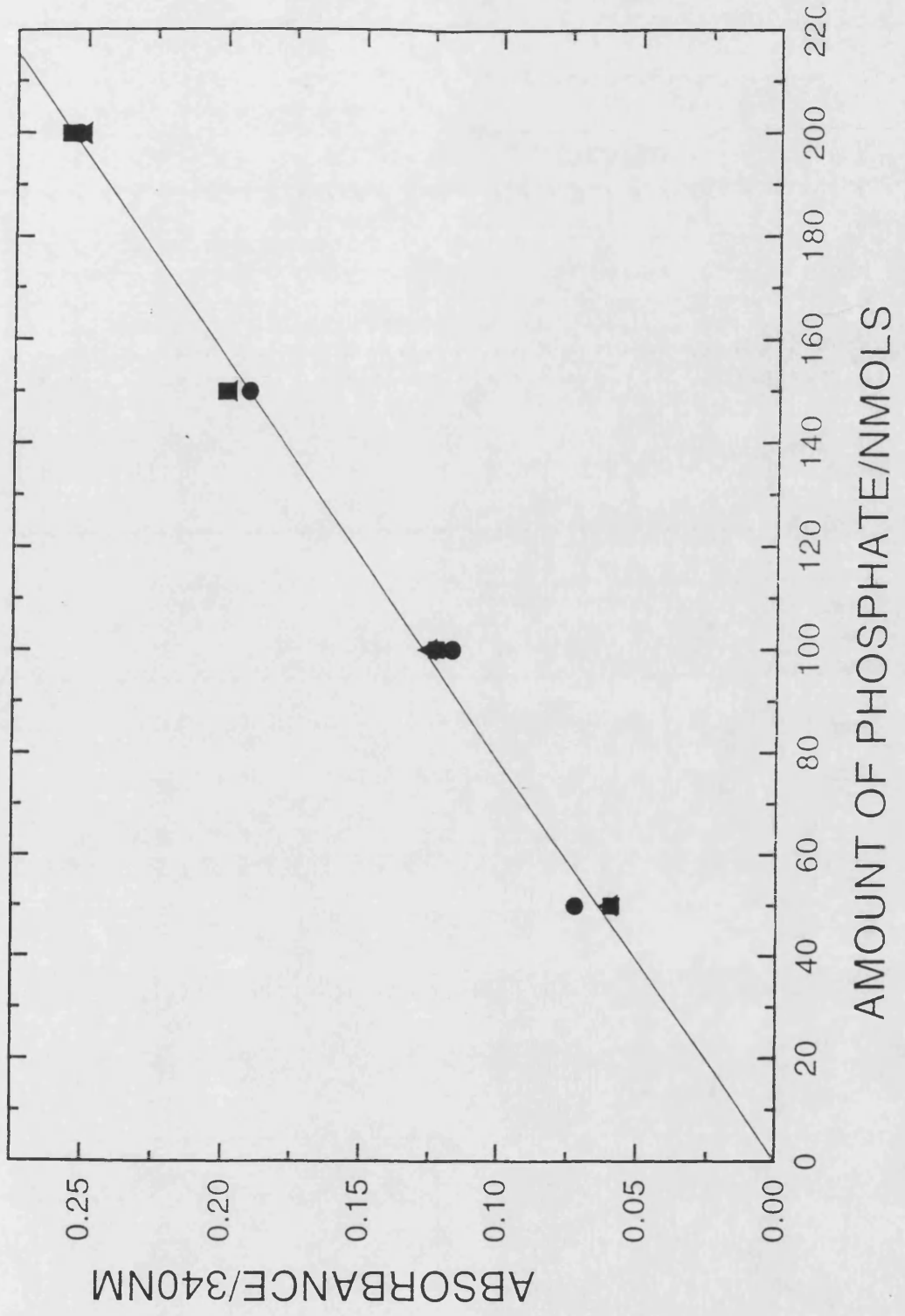

Figure 6.1: A representative standard plot of absorbance (*y* axis) nm vs amount of phosphate (*x* axis) nmols used in Briggs test. The plot is obtained using KH_2PO_4 as the standard sample.

the original solution was worked out by taking dilution factors into consideration and taking a mean value from a total of nine sets of data. The molar extinction coefficient was calculated from the absorbance measured from a known concentration of sample.

6.9 Ca^{2+} Release Assays for cADPR and cADPR Analogues

Ca^{2+} mobilisation from sea urchin egg microsomes by synthetic analogues was evaluated fluorimetrically using 2.5% egg homogenate containing the Ca^{2+} probe Fluo-3 (3μM). The homogenates were prepared from *L. Pictus* eggs and diluted as previously described[78]. Ca^{2+} release assay in Jurkat T-cells was carried out as reported previously[95].

REFERENCES

1 Ringer, S. (1883) *J. Physiol. (London)*, 1883, **4**, 29-42.

2 Sutherland, E. W. and Rall, T.W. (1958) *J. Biol. Chem.*, **232**, 1065-1076.

3 Cori,G. and Cori, C. (1945) *J. Biol. Chem.*, **158**, 321-332.

4 Rall. T.W., Sutherland, E.W. and Wosilait, W.D. (1956) *J. Biol. Chem.*, **218**, 483-495.

5 Lipkin, D., Markham, R. and Cook, W.H. (1959) *J. Am. Chem. Soc.*, **81**, 6075-80.

6 Ashman, D.F., Lipton, R., Melicow, M.M. and Price, T.D. (1963) *Biochem. Biophys. Res. Commun.*, **11**, 330-334.

7 Baevo, J.A., Hardman, J.G. and Sutherland, E.W. (1971) *J. Biol. Chem.*, **246**, 3842-3846.

8 Fesenko, E.E., Kolesnikov, S.S. and Lyubarsky, A.L. (1985) *Nature*, **313**, 315-325.

9 Berridge, M.J. and Irvine, R.F. (1989) *Nature*, **341**, 197-205.

10 Hokin, M.R. and Hokin, L.E. (1953) *J. Biol. Chem.*, **203**, 967-977.

11 Michell, R.H. (1975) *Biochem. Biophys. Acta*, **415**, 81-147.

12 Berridge, M.J. (1983) *Biochem.* J., **212**, 849-858.

13 Streb, H., Irvine, R.F., Berridge, M.J. and Shultz, I.(1983) *Nature*, **306**, 67-69.

14 Wilson, D.B., Connolly, T.M., Bross, T.E., Magarus, P.N., Sherman, W.R., Tyler, A.W., Rubin, L.J. and Brown, J.E. (1985) *J. Biol. Chem.*, **260**, 13496-13501.

15 Changya, L., Gallacher, D.V., Irvine, R.F. and Petersen, O.H. (1989) *FEBS Lett.*, **251**, 43-48.

16 Inoue, M., Kishimoto, A., Takai, Y and Nishizuka, Y. (1977) J. *Biol. Chem.*, 252, 7601-7616.

17 Nishizuka, Y. (1984) *Nature*. **308**, 693-698.

18 Takahashi, S., Kinoshita, T.and Takahashi, M. (1994) *J. Antibiotics* **47**, 95-100.

19 Takahashi, M., Tanzawa, K. and Takahashi, S. (1994) *J. Biol. Chem.*, **269**, 369-372.

20 Berridge, M.J. and Galione, A. (1988) *FASEB J*, **2**, 3074

21 Cornell-Bell, A.H., Finkbeiner, S., Cooper, M.S. and Smith, S.J. (1990) *Science*, **247**, 470.

22 Saluja, A.R., Powers, R.E., Sterr, M. (1989) *Biochem. Biophys. Res. Comm.* **164**, 8-13

23 McCann, J.D., Bhalli, R.C., Welsh, M.J. (1989) *Am. J. Physiol.*, **257**, L166-L124.

24 Chows, C., Jondel, M.J. (1990) *J. Biol. Chem.* **265**, 902-907.

25 Matozaki, T., Goke, B., Tsunode, Y., Rodriguez, M., Martinez, J., Williams, J.A. (1990) *J. Biol. Chem.* **265**, 6247-54.

26 Endo, M. (1977) *Physiol. Rev.* **57**, 71-108.

27 Fabiato, A. (1983) *Am. J. Physiol.* **245**, C1-C14.

28 Malgroli, A., Fresce, R., Meldolesi, J. (1990) 265, 3005-3008.

29 Lipscombe, D., Madison, D.V., Poenie, M., Reuter, H., Tsien, R.W., Tsiem, R.Y. (1988) *Proc. Natl. Acad. Sci.* (USA)

30 Thayer, S.A., Hirring, L.D., Miller, R.J., (1988) *Mol. Pharmacol.* **34**, 664-673.

31 Dupont, G., Berridge, M.J., Goldbeter, A. (1990) *Cell Regulation* **1**, 853-861.

32 Burgoyne, R.D., Cheek, T.R., Morgan, A., O'Sullivan, A.J., Moreton, R.B., Berridge, M.J., Mata, A.M., Colyer, J.,Lee, A.G., East, J.M. (1989) *Nature*. **343**, 72.

33 Galione, A. (1992) *Trends. Pharmacol. Sci.* 304-306.

34 Galione, A., McDougall, A., Busa, W.B., Willmott, N., Gillot, I., Whitaker, M. (1993) *Science*. **261**, 348-352.

35 Berridge, M.J. (1993) *Nature*, **361**, 315-325.

36 Coronado, R., Morrissette, J., Sukhareva, M. and Vaughan, D.M. (1994) *Am. J. Physiol.*, **266**, C1485-C1504.

37 Meissner, G. (1994) *Annu. Rev. Physiol.* 56, 485-508.

38 Ogawa, Y. (1994) *Crit. Rew. Biochem. Mol. Biol.*, **29**, 229-274.

39 Rousseau, E., and Meissner, G. (1989) *Am. J. Physiol.* **256**, H2-H33.

40 Fleischer, S., and Innui, M.(1989) *Ann. Rev. Biophys. Chem.* **18,** 333-364.

41 Galione, A., Lee, H.C., Busa, W.B. *Science.* (1991) **253**, 1143-1146.

42 Lee, H.C. (1993) *J. Biol. Chem.* **268**, 293-299.

43 Buck, W.R., Hoffmann, E.E., Rakow, T.L. and Shen, S.S. (1994) *Dev. Biol.*, **163**, 1-10.

44 Clapper, D.L., Walseth, T.F., Dargie, P.J. and Lee, H.C. (1987) *J. Biol. Chem.* **262**, 9561-68.

45 Clapper, D.L. and Lee, H.C. (1985) J. *Biol. Chem.*, **260**, 13947-13954.

46 Lee, H.C. (1991) *J. Biol. Chem.*, **266**, 2276-2281.

47 Epel, D. (1964) *Biochem. Biophys. Res. Commun.*, 17, 69-73.

48 Lee, H.C., Walseth, T.F., Bratt, G.T., Hayes, R.N. and Clapper, D.L (1989) *J. Biol. Chem.*, **264**, 1608-1615.

49 Kim, H., Jacobson, E.L. and Jacobson, M.K. (1993) *Biochem. Biophys. Res. Commun.* **194**, 1143-1147.

50 Lee & Levitt (1994) *Nature. Struct. Biol.* **1**, 143.

51 Yamada, S., Gu, Q.-M., and Sih, C.J. (1994) *J. Am. Chem. Soc.* **116**, 10787-10788.

52 Wada, T., Inegada, K., Arimoto, K., Tokita, K., Nishina, H., Takaheshi, K., Katada, T. and Sekin, M. (1995) *Nucleosides & Nucleotides* **14**(6), 1301-15.

53 Lee, H.C. (1994b) *Cell. Signalling.* **6**, 591-600.

54 Saenger, W., Reddy, B.S., Muhlegger, D. and Weimann, G. (1977) *Nature* **267**, 225-229.

55 Rusinko, N. and Lee, H.C. (1989) *J. Biol. Chem.*, **264**, 11725-11731.

56 Lee, H.C., Galione, A.and Walseth, T.F. (1994) *Vitam. Horm. (N.Y)* **48**, 199-254.

57 Glick, D.L., Hellmich, M.R., Beushausen, S., Tempst, P., Bayley, H. and Strumwasser, F. (1991) *Cell Reg.*, **2**. 211-218.

58 Hellmich, M.R. and Strumwasser, F. (1991) *Cell Reg.*, **2**, 193-202.

59 Lee, H.C. and Aarhus, R. (1991) *Cell Reg.*, **2**,. 203-209.

60 Koguma, T., Takasawa, S, Tohgo, A., Karasawa, T., Furuya, Y., Yonekura, H. and Okamoto, H. (1994) *Biochim. Biophys. Acta.*, **1223**, 160-162.

61 Kim, H., Jacobson, E.L. and Jacobson, M.K. (1993) *Science*, **261**, 1330-1333.

62 Lee, H.C., Zocchi, E., Guida, L., Franco, L., Benatti, U. and De Flora, A. (1993) *Biochem. Biophys. Res. Commun.*, **191**, 639-645.

63 Lee, H.C. and Aarhus, R. (1993) *Biochim. et Biophys. Acta.*, **1164**, 68-74.

64 Takasawa, S., Tohgo, A., Noguchi, N., Koguma, T., Nata, K., Sugimoto, T., Yonekura, H. and Okamoto, H. (1993) *J. Biol. Chem.*, **268**, 26052-26054.

65 Malavasi, F., Funaro, A., Roggero, S., Horenstein, A., Calosso, L. Metha, K. (1994) *Immunol. Today*, **15**, 95-97.

66 Howard, M., Grimaldi, J.C., Bazan, J., Santos-Argumedo, L., Parkhouse, R.M.E., Walseth, T.F. and Lee, H.C. (1993) *Science*, **262**, 1056-1059.

67 Zocchi, E., Franco, L., Guida, L., Benatti, U., Bargellesi, A., Malavasi, F., Lee, H.C. and De Flora, A. (1993) *Biochem. Biophys. Res. Commun.*, **196**, 1459-1465.

68 Harada, N., Santos-Argumedo, L., Chang, R., Grimaldi, J.C., Lund, F.E., Brannan, C.I., Copeland, N.G., Jemloms, N.A., Heath, A.W., Parkhouse, R.M.E. and Howard, M.(1993) *J. Immunol.*, **151**, 3111-3118.

69 Graeff, R.M., Walseth, T.F., Fryxell, K., Branton, W.D. and Lee, H.C. (1994) *J. Biol. Chem.*, **269**, 30260-30267.

70 Inegada, K., Takahashi, K., Tokita, K., Nishina, H., KanaHo, Y.M., Kakimoto, I., Kontani, K., Hoshino, S. and Katada, T. (1995) *J. Biochem.*, **117**, 125-131.

71 Galione, A., White, A., Willmott, N., Turner, **M., Potter, B.V.** and Watson, S.P. (1993) *Nature*, **365**, 456-459.

72 Kurland, I.J., EL-Maghrabi, M.R., Correia, J.J. and Pilkis, S.J. (1992) *J. Biol. Chem.* **267**, 4416-4423

73 Whitaker, M.J. and Swann, K. (1993) *Development (Cambridge, UK)*, **117**, 1-12.

74 Whalley, T., McDougall, A., Crossley, I., Swann, K. and Whitaker, M. (1992) *Mol. Biol. Cell*, **3**, 373-383.

75 Goy, M.F. (1991) *Trends Neurosci.*, **14**, 293-299.

76 Schulz, S., Chinkers, M. and Garberes, D.L. (1989) *FASEB J.*, **3**, 2026-2035.

77 Lowenstein, C.J. and Snyder, S.H. (1992) *Cell*, **70**, 705-707.

78 Willmott, N., Walseth, T.F., Lee, H.C., White, A.M., Sethi, J. and Galione, A. (1995) *J. Biol. Chem.* **271**, 3699-3705.

79 Schmidt, H.H.H.W, Lohmann, S.M. and Walter, U. (1993) *Biochim. Biophys.* Acta, **1178**, 153-175.

80 Publicover, N.G., Hammond, E.M. and Sanders, K.M. (1993) *Proc. Natl. Acad. Sci.*, **90**, 2087-2091.

81 Poenie, M., Alderston, J., Tsien, R.Y. and Steinhardt, R.A. (1985) *Nature*, **315**, 147-149.

82 Shmidt, H.H.H.W., Patton, C. and Epel, D. (1982) *Dev. Biol.*, **58**, 185-196.

83 Genazzi, A.A. and Galione, A.(1996) *Biochem. J.*, **315**, 721-725.

84 Dargie, P.J., Agre, M.C. and Lee, H.C. (1990) *Cell Reg.*, **1**, 279-290.

85 Galione, A. and Sethi, J. (1996) *in Biochemistry of Smooth Muscle Contraction,* chapter 23 (Michael Barany, ed), pp. 295-305, Academic Press.

86 Koshiyama, H., Lee, H.C. and Tashijian, A.H., Jr. (1991) *J. Biol. Chem.*, **266**, 16985-16988.

87 Takesawa, S., Nata, K., Yonekura, H. and Okamoto, H. (1993) *Science*, **259**, 370-373.

88 Takeshima, H., Nishimura, S., Nishi, M., Ikea, M. and Sugimoto, T. (1993) *FEBS Lett.*, **322**, 105-110.

89 White, A., Watson, S.P. and Galione, A. (1993) *FEBS Lett.*, **318**, 21-24.

90 Berridge, M.J. and Dupont, G. (1994) *Curr. Opin. Cell Biol.* **6**, 267-274.

91 Bezprozvanny, I., Watras, J. and Ehrlich, B.E. (1991) *Nature*, **351**, 751-754.

92 Finch, E.A., Turner, T.J. and Goldin, S.M. (1991) *Science*, 252, 443-446.

93 Iino, M. and Endo, M. (1992) *Nature*, **360**, 76-78.

94 Meszaros, L.G., Bak, J. and Chu, A. (1993) *Nature*, **364**, 76-79.

95 Guse, A.H., da Silva, C.P., Emmrich, F., Ashamu, G.A., Potter, B.V.L. and Mayr, G.W. (1995) *J. Immunol.*, **155**, 3353-3359.

96 Sharp, A.H., McPherson, P.S., Dawson, T.M., Aoki, C, Campbell, K.P. and Snyder, S.H. (19930 *J. Neurosci.*, **13**, 3051-3063.

97 Meldolesi, J., Madeddu, L. and Pozzan, T. (1990) *Biochim. Biophys. Acta.*, **1055**, 130-140.

98 Miyazaki, S., Yuzaki, M., Nakada, K., Shirakawa, H., Nakanishi, S., Nakade, S. and Mikoshiba, K. (1992) *Science*, **257**, 251-255.

99 Kume, S., Muto, A., Aruga, J., Nakagawa, T., Michikawa, T., Furuichi, T., Nakade, S., Okano, J. and Mikioshiba, K. (1993) *Cell*, **73**, 555-570.

100 Chen, Q. and van Breeman, C. (1992) *Adv. Second Mess. Phosphorylation Res.* **26**, 335-350.

101 Shen, S.S. and Buck, W.R. (1993) *Dev. Biol.*, **157**, 157-169.

102 Morissette, J., Heisermann, G.,Cleary, J., Ruoho, A. and Coronado, R. (1993) *FEBS Lett.*, **330**, 270-274.

103 Fruen, B.R., Mickelson, J.R., Shomer, N.H., Velez, P. and Louis, C.F. (1994) *FEBS Lett.* **352**, 123-126.

104 Walseth, T.F., Aarhus, R., Kerr, J.A. and Lee, H.C. (1993) *J. Biol. Chem.* **268**, 26686-26691.

105 Lee, H.C., Graeff, R., Gurnack, M.E. and Walseth, T.F. (1994) *Nature*, **370**, 307-

106 Wagenknecht, T., Berkowitz, J., Grassucci, R., Timerman, A.P. and Fleischer, S. (1994) *Biophys. J.*, **67**, 2286-2295.

107 Graeff, R.M., Podein, R.J., Aarhus, R. and Lee, H.C. (1995) *Biochem. Biophys. Res. Commun.*, **206**, 786-791.

108 Guse, A.H., da Silva, C.P., Weber, K., Ashamu, G.A., Potter, B.V.L. and Mayr, G.W. (1996). *J. Biol. Chem.*, **271**, 23946-23953.

109 Chini, E.N., Beers, K.W., Chini, C.C.S. and Dousa, T.P. (1995) *Am. J. Physiol. (Cell Physiology)*, **269** C1042-C1047.

110 Koenig, H., Goldstone, A. and Liu, C.Y. (1983) *Nature*, **305**, 530-534.

111 Kusunoki, S. and Yasumasu, I. (1976) *Biochim. Biophys. Acta.*, 68, 881-885.

112 Chini, E.N. and Dousa, T.P. (1996) *Am. J. Physiol.*, C530-C537.

113 Mita, M. and Uasumasu, I. (1983) *J. Exp. Zool.*, 228, 71-77.

114 Walseth, T.F., Aarhus, R., Zeleznikar, R. J., Jr. And Lee, H.C. (1991) *Biochim. Biophys. Acta* **1094**, 113-120.

115 Rakovic, S., Galione, A., Ashamu, G.A., Potter, B.V.L. and Terrar, D.A. (1996) *Curr. Biol.*, **6**, 989-996.

116 Sitsapesan, R., McGarry, S.J. and Williams, A.J. (1994) *Circ. Res.*, **75**, 596-600.

117 Currie, K., Swann, K., Galione, A. and Scott, R. (1992) *Mol. Biol. Cell*, **3**, 1415-1422.

118 Guse, A.H., Grainer, E., Emmrich, F., Brand, K. (1993) *J. Biol. Chem.*, **263**, 7129-7133.

119 Bourguignon, L.Y.W., Chu, A., Jin, H. and Brandt, N.R. (1995) *J. Biol. Chem.*, **270**, 17917-17922.

120 Walseth, T.F. and Lee, H.C. (1993) *Biochim. Biophys. Acta* **1178**, 235-242.

121 Kajimoto, Y., Miyagawa, J., Ishihar, K., Okuyama, Y., Fujitani, Y., Itoh, M., Yoshida, H., Kaisho, T., Matsuko, T., Watada, H., Hanafusa, T., Yamasaki, Y., Kamada, T., Matsuzawa, Y. and Hirano, T. (1996) *Biochem. Biophys. Res. Commun.*, **219**, 941-946.

122 Laychock, S.G. (1981) *Endrocrinology* **108**, 1197-1205.

123 Schmidt, H.H.H.W., Warner, T.D., Ishii, K., Sheung, H. and Murad, F. (1992) *Science*, **255**, 721-723.

124 Kuemmerle, J.F., Murthy, K.S. and Makhlouf, G.M. (1995) *J. Biol. Chem.*, **270**, 25488-25494.

125 Murthy, K.S., Grider J.R. and Makhlouf, G.M. (1991) *Am. J. Physiol.* 261, G937-G944.

126 Aarhus, R., Graeff, R.M., Dickey, D.., Walseth, T.F. and Lee, H.C. (1995) *J. Biol. Chem.*, 30327-333.

127 Vu, C., Lu, P-J., Chen, C -S. and Jacobson, M.K. (1996) *J. Biol. Chem.*, **271**, 4744-4754.

128 Perez-Terzic, C.M., Chini, E.N., Shen, S.S., Dousa, T.P. and Clapham, D.E. (1995) *Biochem. J.*, **312**, 955-959.

129 McCarren,, M., Potter, B.V.L.and Miller, R. (1989) *Neuron*, **2**.461.

130 Bailey, V.C., Fortt, S.M., Summerhill, R.J., Galione, A. and Potter, B.V.L. (1996) *FEBS Lett.*, **379**, 227-230.

131 Zhang, F.-J., Yamada, S., Gu, Q.-M. and Sih. C.J. (1996) *Bioorg. Med. Chem. Lett.*, **6**, 1203-1208.

132 Daly, J.W., Phillis, J.W., Kuroda, Y., Shimizu, H., Ui, M. (1983) *Physiology and Pharmacology of Adenosine Derivatives*, Raven Press, New York.

133 Suhadolnik, R.J. (1979) *Nucleosides as Biological Probes. Wiley.*

134 Blackburn, G.M and Gait, M.J. (1990) *Nucleic Acids in Chemistry and Biolgy. Oxford University Press.*

135 Townsend, L.B. *Chemistry of Nucleosides and Nucleotides vol 1&2. Plenum Press, NewYork & London.*

136 Michelson, A.M. (1963) *The Chemistry of Nucleosides and Nucleotides, Academic Press.*

137 Scheit, K.H. (1980) *Nucleotide Analogues, Synthesis and Biological Function, Wiley, New York.*

138 Christensen, L.F. and Broom, A.D. (1972) *J. Org. Chem.*, **37**, 3398-3401.

139 Levene, P.A. and Jacobs, W.A. (1910*) Beridite*. 3150.

140 Elridge, J.A, Jones, J.A., O'Brien, C. and Evans, E.A. *Chem. Commun.* (1971) 394.

141 Holmes, R.E. and Robins. (1964) *J. Am. Chem. Soc.*, **86**, 1242-1245

142 Srivastava, P.C. and Nagpal, K.L. (1970) *Experientia*, **26**, 220.

143 Ikehara, M. and Uesugi, M. (1969) *Chem. Pharm. Bull.*, **17**, 348-354.

144 Lee, C.Y. and Kaplan, N.O. (1975) *Arch. Biochem. Biophys.* **168**, 665-676.

145 Tavale, S.S. and Sobell, M. (1970) *J. Mol. Biol.*, **48**, 109-123.

146 Ueda, T., Nomoto, Y. and Matsuda, A. (1984) *Chem. Pharm. Bull.*, **33**, 3263-3270.

147 Hirota, K., Kitade, Y., Kanbe, Y. and Maki, Yoshifunmi. (1992) *J. Org. Chem.* 57, 5268-5270.

148 Evans, F.E. and Kaplan, N.O. (1976) *J. Biol. Chem.* **251**, 6791-6797.

149 Holmes, R.E. and Robins, R.K. (1965) *J. Am. Chem. Soc.* **87**, 1772-1776.

150 Cartwright, I.L., Hutchinson, D.W. and Armstrong, V.W. (1976) *Nucleic Acids Res.*, **3**, 2331-2339.

151 Folayan, J.O. and Hutchinson, D.W. (1977) *Biochim. et Biophys. Acta.*, **474**, 329-333.

152 Weiman, G. and Khorana, H.G. (1962) *J. Am. Chem. Soc.*, **84**, 4329-4341.

153 Zarytova V.F. and Knorre, D.G. (1984) *Nucleic Acids Res.*, **12**, 2091-2110.

154 Tener, G.M. (1961) *J. Am. Chem. Soc.* **83**, 159-168.

155 Montgomery, J.A. and Thomas, H.J. (1961) *J. Org. Chem.* **26**, 1926-1929.

156 Yoshikawa, M., Kato, T. and Takenishi, T. (1967) *Tetrahedron Lett.*, 5065-5068.

157 Ikemoto, T., Haze, A. Hatano, H, Kitamoto, Y., Ishida, M. and Nara, K. (1995) *Chem. Pharm. Bull.* **43**, 210-215.

158 Chapman, J.R. (1983) in "*Organophosphorus Chemistry*" (Hutchinson, D.W. and Miller, J.A. eds.), 14, pp 278-304. Royal Society of Chemistry, London.

159 Edmonds, C.G., Vestal, M.L. and McCeoskey, J.A. (1985) *Nucleic Acid Res.* **13**, 8197-8206.

160 Everse, J., Anderson, B.and You, K.-S. (1982) *The Pyridine Nucleotide Coenzymes. Academic Press* (London) Ltd.

163 Woenckhaus, C. and Jeck, R. (1987). Preparation and properties of NAD^+ and $NADP^+$ analogs. In "Coenzymes and Cofactors" (Dolphin, R. and Avramovic eds.), Vol **2**, Part A, pp 499-568.

164 Chambers, R.W., Moffatt, J.G. (1958) *J. Am. Chem. Soc.*, **80**, 3752-3756.

165 Schaller, H., Staab, H.A. and Cramer, F. (1961) *Chem. Ber.*, **94**, 1621-1633.

166 Michelson, A.M. (1964) *Biochim et Biophys. Acta.* **223**, 569-576.

167 DeLuca, C. and Kaplan, N.O. (1956) *J. Biol. Chem.*, **223**, 569-576.

168 Hughes, N.A., Kenner, G.W. and Todd, A.R. (1957) *J. Chem. Soc.* **735**, 3733-3738.

169 Apps, D.K. (1971) *FEBS Lett.*, **15**, 277-279.

170 Ward, D.C., Horn, T.and Reich, E.J. (1972) *J. Biol. Chem.*, **247**, 4014-4020.

171 Hata, T., Furasama, K.K. and Sekine, M.J. (1975) *J. Chem. Soc., Chem. Commun.* 196-197.

172 Michelson, A.M. (1964) *Biochim. Biophys. Acta.*, **91**, 1-13.

173 Moffatt, J.G. and Khorana, H.G. (1961) *J. Am. Chem. Soc.*, **83**, 649-658.

174 Pinder, S., Clark, J.B.and Greenbaum, A.L. (1971). *Methods Enzymol.* 18B, 20-46.

175 Imsande, J. and Handler, P. (1961) *The Enzymes.* **5**, 284.

176 Kornberg, A. (1950) *J. Biol. Chem.*, **182**, 779-793.

177 Atkinson, M.A., Jackson, J.F. Morton, R.K. and Murray. (1962) *Nature*, **196**, 35-36.

178 Suhadolnik, R.J., Lennon, M.B., Uematsu, T., Monahan, J.E. and Baur, R. (1977) *J. Biol. Chem.*, **252**, 4125-4133.

179 Zatman, L.J., Kaplan, N.O. and Colowick, S.P. (1953) *J. Biol. Chem.*, **200**, 197-212.

180 Fawcett, C.P. and Kaplan, N.O. (1961) *J. Biol. Chem.*, **237**, 1709-1715.

181 Lappi, D.A., Evans, F.E. and Kaplan, N.O. (1980) *Biochemistry*, **19**, 3841-3845.

182 Colowick, S.P., Kaplan, N.O. and Ciotti, M.M. (1951) *J. Biol. Chem.* (1951) **191**, 447-459.

183 Briggs, A. (1992) *J. Biol. Chem.*, **53**, 13-16.

184 Gu, Q.-M. and Sih, C.J. (1994) *J. Am. Chem. Soc.*, **116**, 10787-10788.

185 Graeff, R.M., Walseth, T.F., Hill, G.K. and Lee, H.C. (1996) *Biochemistry*, **35**, 379-386.

186 Zhang, F.-J. and Sih, C.J. (1995) *Tett. Lett.*, **36**, 9289-9292.

187 Zhang, F.-J. and Sih, C.J. (1995) *Bioorg. Med. Chem. Lett.*, **5**, 1701-1706.

188 Zhang, F.-J., Yamada, S., Gu, Q.-M. and Sih, C.J. (1996) *Bioorg. Med. Chem. Lett.*, **6**, 1203-1208.

189Guse, A.H., da Silva, C.P., Weber, K., Armah, C.N., Ashamu, G.A., Schulze, C., Potter, B.V.L., Mayr, G.W. and Hilz, H. (1997) *Eur. J. Biochem.* **245**, 411-417.

190Aarhus, R., Gee, K. and Lee, H.C. (1995) *J. Biol. Chem.* **270**, 7745-7749.

191Bailey, V.C., Sethi, J.K., Fortt, S.M., Galione, A. and Potter, B.V.L. (1997) *Chem. Biol.* **4**, 51-61.

192 Bailey, V.C. PhD Thesis, University of Bath, 1997.

193 Ashamu, G.A., Galione, A. and Potter, B.V.L. (1995) *J. Chem. Soc. Chem. Commun.* 1359-1360 *Corrigendum* (1995) 1929.

194 Memos, P., Van Aerschat, A.A., Weyns, N.J., Herdwyn, (1992) P.A., *Tett. Lett.*, **33**, 2413-2416.